Assembly of the copper centres of nitrous oxide reductase in *Paracoccus denitrificans* and connections to copper detoxification/trafficking

Sophie P. Bennett

A Thesis submitted to the University of East Anglia in accordance with the requirements of the degree of Doctor of Philosophy

School of Chemistry

2018

Declaration

I declare that the work contained in this thesis, submitted by me for the degree of Doctor of Philosophy, is my own original work, except where due reference is made to other authors, and has not been previously submitted by me for a degree at this or any other university.

Sophie Bennett

September 2018

Acknowledgements

My first and foremost thank you to my supervisor Prof Nick Le Brun, for the support and mentoring you have provided during this exciting and challenging research experience. Many thanks to Dr Andrew Gates and Prof David Richardson, for your supervision and for providing the discussions that helped guide this research. I wish to thank the Norwich Research Park Doctoral Training Partnership, funded by the BBSRC, for funding over the past 4 years.

To those who have helped with experiments. I'm gratefuly to Dr Mark Alston for mapping the RNA-Sequencing data, performing the differential expression and generating the volcano plots. Thanks also to Dr Dimitri Svistunenko for the EPR measurements and to Dr Manuel Soriano Laguna for providing essential plasmids.

As for those that helped on a daily basis. A big thanks to Jason and Justin, for your advice and for showing me how to use equipment over the years. Thanks to the many fantastic members of Lab 2.30 who made this experience a sociable and fun one. A special mention to Amy, a great friend and housemate who supported both me and my Alan Partridge obsession, and to Mike, for all the laughs.

Finally, to old friends and new; Jack and everyone at home; Abby; Holly and Kayla; Jonny, Sian and the rest of the bunch, thank you all for the support and entertainment over the years. To Sharon and Paul, thank you for letting me hide up in your cozy office while I wrote the majority of this. The warmest of thanks to my parents – and yes, my bacteria are doing fine! One last thanks to the best friend I made along this journey, Max, for your patience and encouragement throughout.

Abstract

The α-proteobacterium *Paracoccus denitrificans* uses nitrate as an alternative electron acceptor under anaerobic conditions to survive, reducing it stepwise to nitrogen gas in the process known as denitrification. Agricultural practices have presented large amounts of anthropogenic nitrogen to soil microbes over the past century, which has led to a significant rise in the emission of nitrous oxide (N_2O), a potent ozone depleting and greenhouse gas. The last step yields N_2 from N_2O and is catalysed by N_2OR, a homo dimeric multi-copper enzyme with 2 copper cofactor centres: the Cu_A electron entry site, and the Cu_Z site, a unique 4Cu-2S cluster. Understanding how the copper metal centres of N_2OR are assembled, and the effect of copper on organisms that require this metal, is an essential pre-requisite for efforts towards mitigating N_2O emissions.

Here we present an investigation of the role of two accessory genes in the *nos* gene cluster, *nosL* and *nosX*, in *P. denitrificans*. Phenotype analysis of gene deletion mutants demonstrates the two genes are necessary for whole cell N_2O reduction. Spectrosopic characterisation of N_2OR from each background demonstrates the role of NosX is not to assemble the Cu centres, while NosL is involved in this process. Further studies of NosL heterologously expressed in *E. coli* demonstrate the capacity of NosL to specifically bind Cu(I) with a high affinity, suggesting a role for NosL as a copper binding protein involved in the copper centre biogenesis of N_2OR.

An additional study of the *P. denitrificans* transcriptome in the presence of Cu excess, using RNA-Sequencing, is discussed, covering the most differentially expressed transcripts from aerobic and anaeroic datasets. Importantly, there is no complete system dedicated to copper detoxification and common to prokaryotes and eukaryotes, in *P. denitrificans*. We have identified, however, 2 new genes involved in Cu trafficking in this bacterium.

Table of Contents

Abbreviations

A	Absorbance
aa	Amino acids
amp	Ampicillin
AOA	Ammonia oxidising archae
AOB	Ammonia oxidising bacteria
BCS	Bathocuproinedisulfonic acid
CcO	Cytochrome *c* oxidase
CD	Circular dichroism
Cu	Copper
Da	Dalton
DE	Differential expression
DEAE	Diethylaminoethyl
DT	Sodium dithionite
Δε	Difference extinction coefficient ($M^{-1}cm^{-1}$)
ε	Extinction coefficient ($M^{-1}cm^{-1}$)
EDTA	Ethylenediaminetetraacetic acid
EPR	Electron paramagnetic resonance
EXAFS	Extended X-ray absorption fine structure
Fe-S	Iron sulfur
GC	Gas chromatography
gen	Gentamycin
gN_2OR	Genomic nitrous oxide reductase
HEPES	4-(2-hydroxyethyl)-1-piperazineethanesulfonic acid
IPTG	Isoproyl β-D-1-thiogalactopyranoside
K_d	Dissociation constant
kan	Kanamycin
LB	Luria Bertani broth
LC-MS	Liquid chromatography mass spectrometry

LMCT	Ligand to metal charge transfer
LOL	Localisation of lipoproteins
MES	2-(*N*-morpholino)ethanesulfonic acid
MGD	molybdopterin guanine dinucleotide
MOPS	3-(*N*-morpholino)propanesulfonic acid
MS	Mass spectrometry
MV	Methyl viologen
N_2O	Nitrous oxide
N_2OR	Nitrous oxide reductase
N-cycle	Nitrogen cycle
NGS	*nos* gene cluster
PCR	Polymerase Chain Reaction
pN_2OR	Plasmid nitrous oxide reductase
Ppb	Parts per billion
Q Sepharose	Quaternary ammonium sepharose
SDS PAGE	Sodium dodecyl sulfate polyacrylamide gel electrophoresis
SOD	Superoxide Dismutase
spec	Spectinomycin
Strep-tag II	Streptavidin tag II
TPM	Transcripts per million
Tris	tris(hydroxymethyl)aminomethane
UV-Vis	Ultraviolet-Visible
VS	Vischniacs and Santer trace elements
WT	Wild type

CHAPTER 1

Introduction

1.1 Biogeochemical cycles

Nitrogen, carbon, sulfur and phosphorus are circulated through the abiotic and biotic components of the earth's biosphere as individual chemical cycles. These elements are transformed through simple redox reactions in order to maintain life on earth and recycle essential niutrients. An imbalance occuring in a cycle can contribute to, and elevate, global issues with resulting harmful consequences for the environment. Such an imbalance is apparant in both the carbon and nitrogen cycle where consequently, global temperatures are rising along with atmospheric CO_2 and N_2O levels; both gases are contributing to the growing issues of ozone depletion, global warming and general climate change [1, 2]. Maintaining a consistent quantity of each chemical component throughout the biogeochemical cycles is important for sustaining the earth's biosphere.

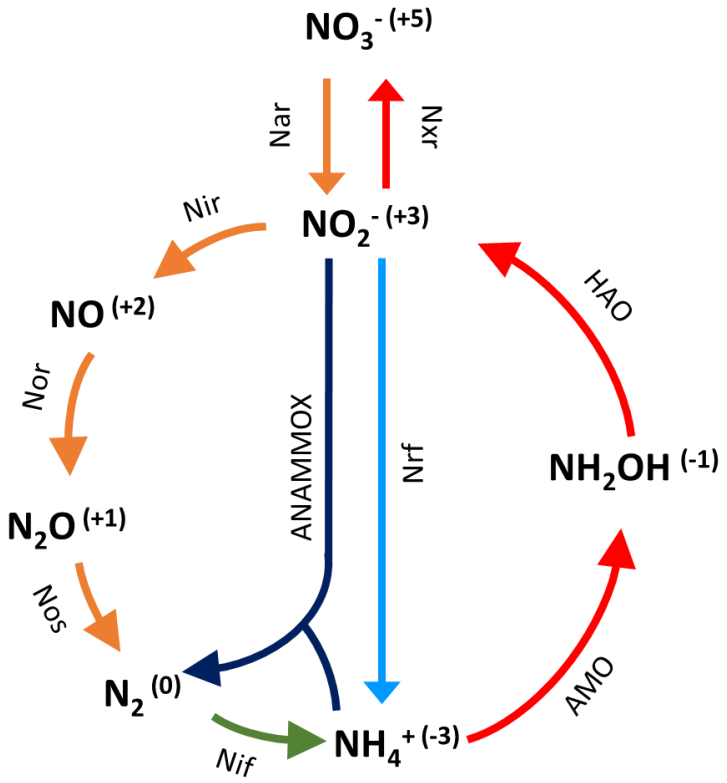

Figure 1.1: The Microbial Nitrogen Cycle, transforming nitrogen through 8 oxidation states (shown in brackets). Pathways included in this cycle are: nitrogen fixation (green), nitrification (red) denitrification (orange), dissimilatory nitrite reduction to ammonium (light blue) and anaerobic ammonium oxidation (dark blue). Each step in the cycle is catalysed by an enzyme which is noted next to the pathway.

The nitrogen cycle (N-cycle) represents the natural flow of nitrogen from the atmosphere and oceans into the biosphere and back again, cycling this element through several oxidation states, from +5 to -3. The N-Cycle supports life on earth by providing biological systems with nitrogen, an essential elements used in the synthesis of both DNA and amino acids [3]. Nitrogen gas (N_2) is extremely inert but it is made biologically available to plants and animals through the process of nitrogen fixation (Figure 1.1, green arrow). Nitrogen fixation is undertaken by microbes residing in plant root nodules which use iron and molybdenum based nitrogenase metallo-enzymes to catalyse the reduction of N_2 to ammonia under micro-anaerobic conditions [4] . Fixed nitrogen species in the form of ammonia are aerobically oxidised to hydroxylamine, nitrite and nitrate by ammonia- and nitrite- oxidising bacteria (AOB and NOB) (Figure 1.1, red arrow). Nitrate, the most oxidised form of nitrogen in the cycle, is reduced to nitrogen gas through the process of denitrification. Four distinct metallo-enzymes reduce this substrate stepwise under anaerobic conditions to replenish N_2 in denitrifying bacteria such as *Paracoccus denitrificans.* Further pathways discovered and involved in this cycle include dissimilatory nitrite reduction to ammonium (DNRA): a single step reduction of nitrite to ammonia, catalysed by the cytochrome *c* nitrite reductase, Nrf. Ammonium can also be anaerobically oxidised to produce N_2 via the intermediates hydrazine and nitric oxide through the process of anaerobic ammonium oxidation (ANAMMOX). This pathway is catalysed by a hydrazine synthase and a variant of a hydroxylamine oxidoreductase [5]. Historically, bacteria in the cycle were associated with the single step or pathway which they catalysed within the N-cycle. However, new metagenomic data has identified organisms which are complete nitrifiers and not simply AOB or NOB. These COMMAMOX (COMplete AMMonia OXidation) microorganisms, such a members of the *Nitrospirae* phylum, perform complete ammonia oxidation to nitrate [6]. Ammonia oxidising bacteria also produce N_2O (a substrate in the denitrification pathway) through a process termed nitrifier denitrification. The majority of cultivated AOB express a nitrite- and nitric oxide- reductase enzymes and therefore produce the two products, nitric oxide and nitrous oxide[6, 7]. These novel findings suggest the activity of some organisms are much more complex than first thought, in terms of the different pathways and substrates which they can catalyse. With the rise of metagenomics and the ability to analyse the genetics of environmental samples, there is more to be learnt about nitrogen cycling bacteria.

The microbial processes mentioned take place in the biosphere where, from a global perspective, a third of the biotic sources of nitrogen originate from terrestrial systems

and two thirds from the marine environment [3]. Alternate abiotic nitrogen sources arise from fossil fuel combustion, which increases nitrogen in the atmosphere, and lightening which fixes atmospheric nitrogen in the soil.

Incomplete microbial denitrification

The microbial denitrification pathway is a process carried out in soil and lake sediments under anaerobic conditions, where nitrate is reduced to nitrogen gas which in turn diffuses back into the atmosphere. Incomplete denitrification has become a substantial problem in the past century as emissions of nitrous oxide (N_2O), the penultimate gas in this pathway, continue to rise exponentially [8]. A recent study has also implicated mmonia oxidising bacteria in N_2O production due to their ability to carry out nitrifier denitrification in coastal ecosystems [7]. Abiotic N_2O formation from ammonium metabolism in ammonium oxidising archae (AOA), under low ammonium concentrations, has also been reported [9]. However, both AOA and AOB seem unable, at our current understanding, to remove N_2O. Therefore, we look to denitrifying bacteria, with the genetics to produce the enzyme to remove N_2O, as the main focus of this work.

Nitrous oxide in the atmosphere is currently at a level of 314 parts per billion (ppb) and is the third most abundant greenhouse gas behind methane and CO_2 [10]. Concerns are often raised about the implication of rising CO_2 and methane gas levels from fossil fuel combustion, primarily regarding their effect on global warming, yet the dramatic rise in atmospheric N_2O and its activity in the stratosphere is just as much of a threat. Nitrous oxide, like chlorofluorocarbon (CFC), is stable in the earth's troposphere but once transported out to the stratosphere, generates reactive chemicals [8]. Approximately 10% of the N_2O in the stratosphere is photochemically oxidised to chemicals described as NO_X, which include NO and NO_2. These chemicals in turn catalyse the destruction of stratospheric ozone through reactions described in Equation 1.1 to 1.3 [8].

$$NO + O_3 \longrightarrow NO_2 + O_2 \qquad \text{(Eq. 1.1)}$$

$$O + NO_2 \longrightarrow NO + O_2 \qquad \text{(Eq. 1.2)}$$

$$\text{Net: } O + O_3 \longrightarrow 2O_2 \qquad \text{(Eq. 1.3)}$$

With a lifetime in the atmosphere of 114 years before being destroyed by chemical reactions in the stratosphere, N_2O is contributing to global warming with a 300 times greater effect, like for like, than that of CO_2 and is therefore a primary target in controlling climate change [10].

The largest global producer of N_2O is the agricultural sector, with 40% of the total N_2O emissions emerging from microbial communities within soil [11]. The development of the Haber-Bosch process in 1908 enabled anthropogenic nitrogen sources to be applied to the soil, the introduction of which strongly correlates with the rise in atmospheric N_2O [12]. As a result of this human intervention, the amount of nitrogen in the N-cycle has now doubled with the relative magnitudes of anthropogenic and natural sources almost equal, at 210 Tg N y^{-1} and 203 Tg N y^{-1} [3], respectively. The absorption of ammonia based nitrogen fertiliser by plant crops is only 17% efficient [13], leaving the remaining fertilizer to either leach off into rivers, or to return to the atmosphere over time. The inefficient use of fertiliser is a possible explanation for the dominance of reduced nitrogen species on a global level, with an 85%:15% ratio of reduced:oxidised nitrogen species available [3]. Examples of the environmental impact of these excess nitrogen based nutrients on entering ecosystems include the accelerated growth of plants which consequently give rise to eutrophication of coastal regions where rivers meet [1], and acidification of the soil.

The distubance of the abiotic sector as a consequence of applying excessive fertiliser to the soil, with the rise in N_2O emissions, means we look to the process of denitrification (the pathway with the means to remove N_2O) as a major source of rising N_2O emissions [10, 14]. Typically, 1–5% of the fertiliser is biologically converted to N_2O and released by bacteria [13]. In Figure 1.1 the red route of nitrification involves the oxidation of hydroxylamine back to nitrite and nitrate, which effectively replenishes nitrate levels in the soil for denitrification and adds to nitrous oxide emissions at the end of the process [15]. Using animal waste as a fertiliser is also increasing the amount of nitrification taking place in the soil and once again, replenishing nitrate levels which can be reduced to N_2O [10]. A number of single components in the microbial nitrogen cycle is therefore disturbed by using

fertiliser on soil with a global impact, after what was initially an attempt to improve crop yield to feed the rising global population.

A greater understanding of how microbial communities within the soil produce and consume N_2O allows us to identify potential ways of reducing N_2O emissions. Nitrous oxide is reduced to nitrogen gas by denitrifying organisms such as the γ-proteobacterium *Pseudomonas stutzeri*, the β-proteobacterium *Achromobacter cyclcoclastes*, and the focus of this work, the α-proteobacterium *Paracoccus denitrificans.* The well studied enzyme responsible for this reduction is Nitrous Oxide Reductase (N_2OR). The polypeptide chain of N_2OR is encoded by the *nosZ* gene which sits among a gene cluster in denitrifying bacteria with regions up- and down- stream that encode accessory genes primarily involved in the maturation of N_2OR. Together these genes are known as the *nos* gene cluster (NGC) and are described in section 1.4.4. Phylogenetic analysis of the *nosZ* gene has revealed two distinct groups of bacteria that reduce N_2O, each with their own common ancestors, otherwise known as a clade. The conservation of genes in the NGC among the 2 equally proportioned clades is described in Figure 3.1[16]. The classic denitrifying bacteria are members of clade I and are able to produce and consume N_2O (as described in Figure 1.1, orange arrows). The atypical Clade II members do not produce N_2O through denitrification but act as N_2O sinks, removing N_2O to produce N_2. To determine how we might mitigate N_2O emissions from such clade I microbes, we must first understand why this pathway is used and the biochemical process through which N_2O is consumed and produced.

1.2 Respiratory adaption and control in *Paracoccus denitrificans*

Respiration is a fundamental process carried out by eukaryote and prokaryote organisms to provide the energy source needed to metabolise, grow and essentially survive. In eukaryotes, the mitochondrion houses 4 intra-membrane proteins which make up the electron transport chain. *P. denitrificans* is phylogenetically the closest extant relative of the mitochondrion, based on similarities not only between the Gram-negative cell membranes and those of the mitochondrion, but also similarities in their respiratory enzyme topology [17]. *P. denitrificans* is therefore an exemplary bacterium for investigating respiration.

In contrast to eukaryotes, which only survive under oxic conditions using oxygen as a terminal electron acceptor in order to drive adeniosine triphosphate (ATP) production, some prokaryotes are versatile and can use alternative electron acceptors such as sulfur, fumarate and nitrogen oxides. Respirational flexibility features in *Salmonella* species where sulfate or fumerate are used to generate ATP in the absence of oxygen. Other Gram-negative , such as the *Shewanella* genus, use Fe(III) to respire, specifically using multi-heme proteins which work as electron wires in the cell [18]. This flexibility offers an advantage to the microbe in a changing environment which ensures it adapts and survives. This is especially true in the case of *Salmonella tyhphi* where the advantage of being able to adapt to a lowering in available oxygen and therefore undergo anaerobic respiration plays a role in invasiveness in the gut [19]. As a facultative anaerobe, *P. denitrificans* also adapts to a lowering of oxygen in the cell by switching on alternative respiratory enzymes that make use of nitrogen oxides, allowing the bacterium to survive in an anaerobic environment. In other words, they carry out denitrification, as described in Figure 1.1. Four distinct metallo-enzymes catalyse this process: nitrate reductase (encoded by *nar* and *nap),* nitrite reductase*,* nitric oxide reductase (*nor)* and nitrous oxide reductase (*nos).* For the cell to switch its electron acceptor and survive, the process of change must be tightly regulated and controlled to ensure the correct respiratory system is made. To produce both fleets of oxic and anoxic respiratory enzymes would be energetically unfavourable and for this reason systems are in place to sense a loss of O_2, sense the alternative electron acceptor and modulate the expression the enzymes responsible for reducing the electron acceptor. The bacterium must maintain ATP production in order to continue survive and colonise. As it switched to an alternate electron acceptor is continues to make use of a present core electron transport enzyme, the cytochrome bc_1 complex, which supplies the electrons used in to reduce alternative species [20].

The transition from aerobic to anaerobic respiration

The level of gene expression in a microorganism can be raised or lowered in response environment signals within the cell. Some genes are constituively expressed, but the expression of others is controlled by regulatory proteins which sense a change in environment and respond by changing their behaviour with regard to DNA binding upstream of a transcription start site. A change to the internal environment of the cell, such as oxgyen tension in the cell, is sensed by regulatory proteins which ensure the

necessary genes are transcribed and protein translated, to deal with the new environment. Metals and small molecules such as nitric oxide, for example, are known as effectors which are indicators of the change in the environment; they bind to the regulatory protein and regulate its biological activity. Once a regulatory protein is bound to the DNA it behaves either as an activator or repressor of gene expression, controlling whether the transcription machinary can proceed and transcribe the downstream DNA. An activator protein binds to the DNA and promotes binding of the RNA polymerase to favour transcription. In contrast, a repressor will bind upstream of the transcription start site and inhibit RNA polymerase binding. Regulatory proteins often contain metal cofactors which sense the effector and respond with changes to the cofactor oxidation state or structure which consequently changes the protein conformation. An example of the iron-sulfur cluster bound *E. coli* FNR is described below. Controlled expression of respiratory systems using effectors to sense environmental changes is essential to ensure energy is not wasted, for example, in an oxic environment in *P. denitrificans* there is no need for both aerobic as well as anaerobic respiratory enzymes. Using energy to produce proteins which have no use in the cell is counterproductive. It is more favourable to concentrate on and use one system to produce ATP, than to use energy producing both if only one substrate is available.

In *P. dentrificans* transcriptional regulators belonging to the superfamily (FNR)-type transcription factors, sense environmental change and switch on the denitrification genes. Three factors have been identified in *P. denitrificans*: FnrP, NnrR and NarR, which sense O_2, nitric oxide and nitrate/nitrite, respectively [21].

Under anaerobic conditions, *E. coli* FNR binds a [4Fe-4S] cluster which enables the protein to dimerise and to bind tightly to an FNR binding DNA sequence, known as an FNR box. In the presence of O_2, the cluster is oxidised and undergoes a cluster conversion reaction to a [2Fe-2S] form, which dissociates into monomer and can no longer bind DNA. With its [4Fe-4S] cluster intact, FNR acts as a transcriptional activator therefore this is a regulator which inhibits expression of downstream genes in the presence of O_2 but activates transcription in an anoxic environment. Under micro-oxic conditions FnrP, an orthologue of *E. coli* FNR, binds to a DNA sequence upstream of nitrate reductase gene, *nar.* FnrP shares the same 4 conserved cysteine residues which bind a [4Fe-4S] cluster [22]. In a *fnrP* mutant, the expression of *nar* is reduced and is, therefore, a regulator for the first enzyme in the pathway, the cytoplasmic bound nitrate reductase [22].

FnrP regulates the expression of *nar, nir* and *nos* once the majority of O_2 has been removed and from then on, the anaerobic respiratory system starts working. It is the high affinity *cbb*$_3$ type oxidases that remove the final trace of O_2. At the same time, the nitrite sensitive transcriptional regulator NarR activates transcription of the nitrate/nitrite reductases [20].

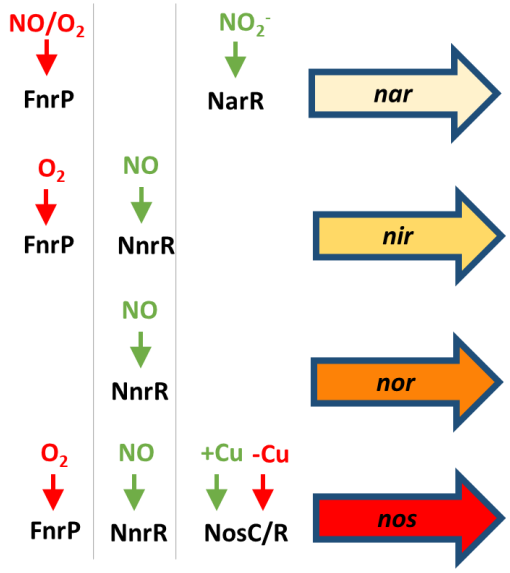

Figure 1.2: The transcriptional regulators of the four operons encoding the denitrification metalloenzymes. Substrates activating the regulators are described using green arrows and repressors are in red.

The product of each reduction reaction does not necessarily behave as an effector that regulates the expression of the next gene in the denitrification pathway. Instead, a more complicated regulatory network senses oxygen, nitric oxide, nitrite and even Cu to ensure these genes are expressed under denitrifying conditions in the cell.

NNR regulates the *nir* and *nor* genes in *P. denitrificans*, a transcription factor which is sensitive to NO [23] and O_2 [24]. NNR activity is heme dependent [25] and in the presence of NO, NNR activates both *nir* and *nor* expression. NO can be a toxic gas to the cell and so sensing and switching on systems to remove NO is an important task for *P. denitrificans* in making sure the substrate is dealt with while at the same time ensuring that it can respire anoxically; therefore, this substrate is under tight regulation.

How N_2OR expression is controlled, is less clear. Early studies on mutants deficient in either *fnrP*, *nnr,* or both genes have shown the activity of N_2OR remains the same

within the cell regardless of the mutant [24]. Later studies showed *fnrP* mutants could reduce N_2OR, only if presented with nitrate; if nitrate was removed, nitrite could restore the expression of *nosZ* and whole cell N_2OR turnover[26]. Therefore, *nosZ* transcription is affected by low O_2 levels and NO. Functional N_2OR was also found to precede any measurable NIR or NOR activity [27] which revealed N_2O is not an inducer of *nos*. The two genes upstream to *nosZ, nosCR*, have been linked directly to lowering *nosZ* expression in the absence of Cu, as shown recently by Sullivan et al [28]. The organisation of *nosCR* alongside *nosZ* and further accessory genes to *nosZ* in *Paracoccus denitrificans* are described in Figure 1.10.

1.2.1 Biochemistry of Denitrification

The four chemical reductions that make up denitrification are carried out by distinct metallo-proteins that are associated with the inner membrane and periplasm of *P. denitrificans*. Each enzyme carries out a single reaction step in the denitrification pathway, and no two proteins contain the same set of metal cofactors, as illustrated in Figure 1.3. The catalytic enzymes responsible are: Nar/ Nap *(*nitrate reductase), Nir (nitrite reductase), Nor (nitric oxide reductase) and Nos (nitrous oxide reductase).

Transition metals found at the catalytic centres of these enzymes include molybdenum, Cu and iron. As transition metals, they have partially filled d orbitals which can polarise the otherwise inert nitrogen bonds to an activated state and allows the reduction reaction to take place. Interestingly, the nitrite reductase and nitrous oxide reductase are unique in that they contain cofactors which have not been identified in any other biological system, so far. This exclusivity suggests a specific evolution of these metal centres for nitrogen oxide reduction in denitrifying bacteria. Figure 1.3 describes the metalloenzyme topology among the periplasm. This figure includes the cytochrome bc_1 complex, from which electrons are donated to the electron carriers, cytochrome *c*550 and pseudoazurin.

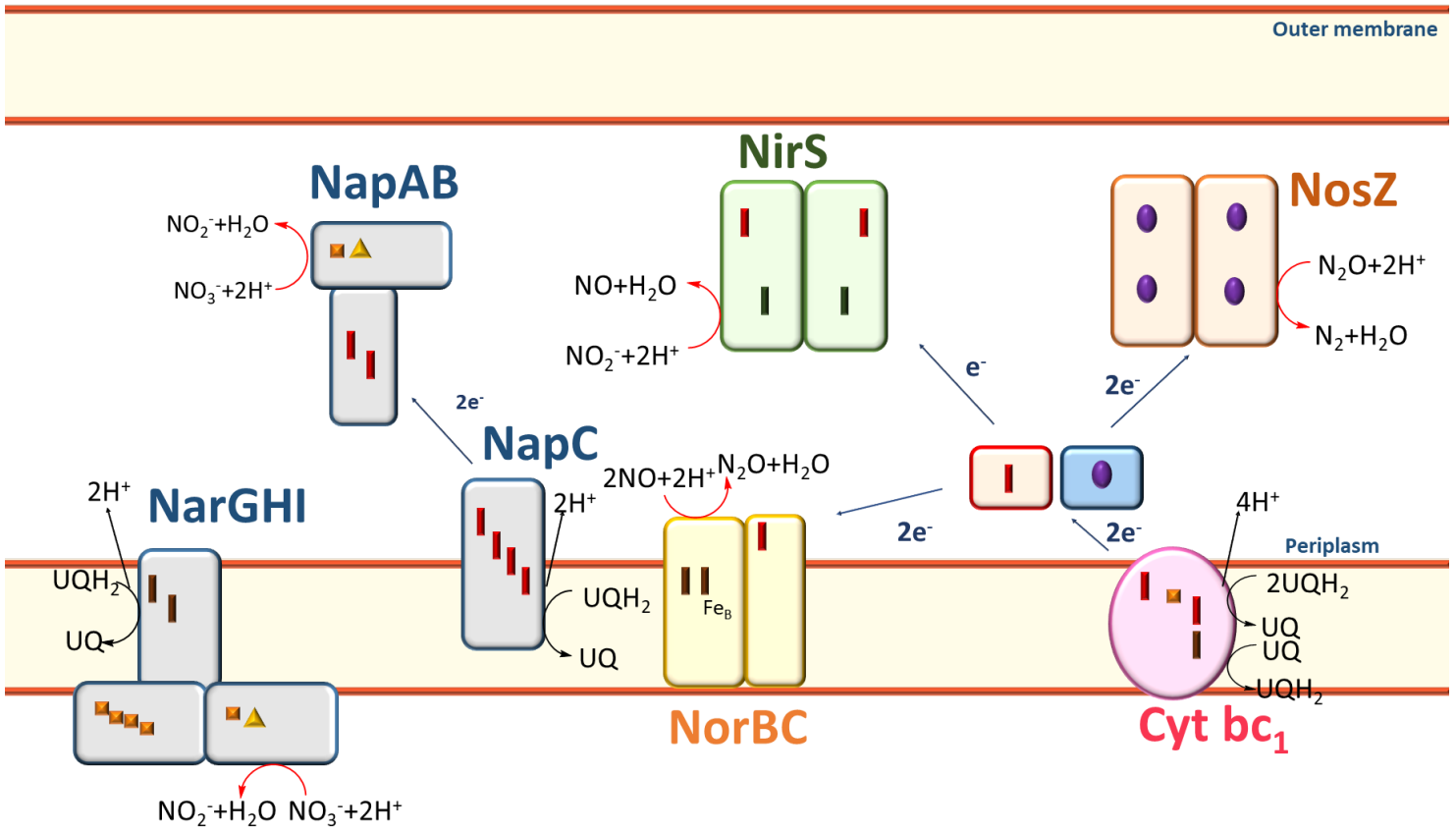

Figure 1.3: Organisation of the metallo-enzymes involved in denitrification within the periplasm and inner membrane of *P. denitrificans*. Within each protein, the metal cofactor is depicted. These cofactors range from hemes such as *c*, *b* and the unique d_1 (■, ■ , ■, respectively), iron sulfur cluster (■), molybdenum complexes (▲) and Cu (●). The electrons used to reduce substrates originate from cytochrome bc_1 Q-cycle and the oxidation of ubiquinol to ubiquinone which also releases 4 protons across the membrane, contributing to the net electrochemical gradient, driving the synthesis of ATP

Nitrate reductases

Denitrification begins with most oxidised form of nitrogen in the N-cycle, nitrate, which is reduced by two possible enzymes under denitrifying conditions: Nap and Nar, which contain molybdenum, heme and iron-sulfur cofactors. Nar (respiratory nitrate reductase) is associated with the inner membrane and consists of 3 protein subunits. An intrinsic membrane subunit (NarI, 25 kDa), an iron sulfur redox centre subunit (NarH, 60 kDa) and a catalytic subunit (NarG, 140 kDa) containing a molybdenum cofactor where nitrate is reduced at the face of the cytoplasm [29, 30]. Nap, the soluble periplasmic nitrate reductase is present as a heterodimer comprising a NapA subunit (90 kDa) with a molybdopterin guanine dinucleotide (MGD) cofactor, while NapB (16 kDa) contains two hemes [31]. A variety of molybdoenzymes are present in nature, such as formate dehydrogenase and polysulfide reductase [29], which present a MGD cofactor that cycles between the Mo^{IV} and Mo^{V} oxidation states [30]. In total 2 electrons are donated from the oxidation of a quinol for nitrate reduction and 2 protons are also released to the periplasm, which contribute to a proton electrochemical gradient used to synthesise ATP.

Nitrite reductases

Nitrite is reduced by a single periplasmic enzyme in *P. denitrificans*, cytochrome cd_1, which is a 120 kDa homodimer. Each monomer consists of 2 domains, each with a distinct heme moiety, a *c* and d_1 type heme. The *c*-type heme accepts electrons from small donors such as cytochrome c_{550} or pseudoazurin present in the periplasm, passing electrons to the unique d_1 heme, which is the site of nitrite reduction. The d_1 heme is a non-covalently bound, partially reduced porphyrin ring, which is unique to nitrite reductase and is thought to have evolved for specialised nitrite reduction. An alternative metal centre catalysing the same reaction can be found in *Achromobacter cyclolastes,* where a di-Cu centre reduces nitrite.

Nitric oxide reductase

Nitric oxide is a powerful cellular inhibitor when it reacts with iron and Cu centres. As an intermediate in the denitrification pathway it is important that it is dealt with and removed quickly. NOR is expressed strictly under anaerobic conditions directly in response to NO. The mature protein consists of 2 subunits, NorB (56 kDa), an intrinsic membrane protein made up of 12 helices, and NorC (17 kDa), a periplasmic soluble catalytic subunit [32]. The integral NorB shares sequence similarity with the cytochrome oxidases, but it contains non heme Fe instead of a Cu centre (discussed

later). The NorB subunit of *P. denitrificans* contains a low spin *b* type heme that is magnetically coupled to a non-heme Fe [32]. The subunit NorC contains a covalently bound *c*-type heme that accepts electrons from small electrons donors in the periplasm to pass to the NorB cofactor where the catalytic binuclear centre is located close to the periplasmic face of the membrane [29].

There are overlapping subnetworks in the inner membrane which use the same protein and quinol pool. The Q/QH_2 pool is used to distribute electrons either directly to the nitrate reductases, or via oxidation of quinol to quinone by the cytochrome bc_1 complex, as shown in Figure 1.3, which then passes electrons to small periplasmic electron donors such as cytochrome c_{550} and azurin. Finally, these, in turn pass electrons to Nir, Nor and Nos for the reduction of their respective substrates.

The final reaction in denitrification is carried out by nitrous oxide reductase (NosZ, from herein N_2OR), the only protein in this pathway in *P. denitrificans* to contain Cu as the cofactor. Both Clade I and Clade II members of N_2O reducing bacteria contain a Cu bound N_2OR, to be discussed in section 1.4.

1.3 The Chemistry and Biological Chemistry of Copper

1.3.1 Chemistry of Cu

A few fundamental chemical principles must first be covered to understand how Cu interacts with biological macromolecules/proteins. First, the d orbital electron configuration and how this relates to the Hard Soft Acid Base theory (HSAB). Cu(I) is a diamagnetic d^{10} species where all d orbitals are full. This means that Cu(I) is a soft acid based on the HSAB principles and will only react with soft bases - those with empty orbitals and are highly polarizable. Amino acid residues which represent these preferential soft ligands are sulfur based such as cysteine and methionine. Cu(II), with one electron less than Cu(I) has a partially filled d orbital and is paramagnetic, therefore detectable by EPR. It is also a borderline/hard acid and will interact with nitrogen and oxygen-based residues such as histidine and glutamate.

Metals have a preferred binding geometry based on the number of valence d electrons and the number and type of coordinating ligand, as explained through ligand field theory (LFT). Cu(I) is d^{10} and does not have geometric preferences based on the ligand field stabilisation energy, as all d orbitals are full. It is found coordinated by 2,3,4 ligands in linear, trigonal planar and tetrahedral geometries [33]. Cu(II) is a d^9 system and exhibits geometric preferences for 4, 5 or 6 ligands in square pyrimidal,

square planar or axially distorted octahedral [33]. Cu(I) is often found in tetrahedral geometry, though geometry imposed on Cu(II) forms an entactic state which increases the reduction potential of the centres and thus electron affinity and activity [34].

The Irving-Williams series orders the ability of transitions metals to form stable complexes and sits Cu at the most stable end, making it highly competitive with other metals. An example is the displacement of the Zn(II) ion in the zinc finger DNA binding domain of human oestrogen receptor by Cu(II), which renders it no longer active for its role in hormone-dependant signal transduction [35].

1.3.2. The Biology of Cu

Copper is located on the earths surface where it is mined and commonly used as wiring as it is an electrical conductor, but also used to prepare alloys with other metals, such as zinc to make brass, or with tin and zinc to make bronze. Cu is a vital element for life on earth and is the second most prevalent biological transition metal behind iron. It was made biologically available due to the oxygenation of the earth's atmosphere some 2.5 billion years ago. This event solubilised the metal via oxidation of Cu(I) to Cu(II) and enabled its incorporation into the biosphere. With two stable oxidation states, Cu is an ideal candidate as a protein cofactor involved in redox chemistry. Though Cu will redox cycle both as a protein cofactor and when it is freely available, this activity poses a significant problem within the cellular environment. Free Cu(I) species react with superoxide and hydrogen peroxide to produce harmful radical species, carrying out similar reactions to that of Fenton chemistry. Radical species produced are the prime cause of oxidative damage to nucleic acids and proteins [36] where the damage often goes on to cause cancer, disease of the nervous system and ageing in mammals [35]. Equations 1.4-1.6 demonstrate the redox cycling and Fenton like chemistry carried out by Cu species in the cell. These produce reactive oxygen species (ROS) including $OH^{\cdot}$, the hydroxyl radical, Equation 1.6.

$$Cu^{2+} + O_2^{-} \longrightarrow Cu^{1+} + O_2 \qquad \text{(Eq. 1.4)}$$

$$Cu^{1+} + H_2O_2 \longrightarrow Cu^{2+} + OH^{-} + OH^{\cdot} \qquad \text{(Eq. 1.5)}$$

$$\text{Net: } O_2^{-} + H_2O_2 \longrightarrow O_2 + OH^{-} + OH^{\cdot} \qquad \text{(Eq. 1.6)}$$

Harmful radical species are not the only threat Cu poses to the cell. While free Cu can result in these harmful species, it is still a highly important metal in the active sites of proteins. Such systems where Cu plays a vital role include respiration, photosynthesis, detoxification and neurological function [36], specifically in enzymes such as cytochrome *c* oxidase (COX), superoxide dismutase (SOD) and the iron uptake protein FetB.

There are 3 common classes of Cu centres in biology which are distinguished based on nuclearity, electronic structure and geometries which are shown in Table 1.1.

Table 1.1 The 3 types of Cu centres found in biology, based on [33].

Type	
I	• "Blue" Cu proteins, including electron transfer proteins such as azurin and plastocyanin. • Mononuclear centres are arranged in a trigonal or distorted tetrahedral geometry • Typical ligands are a cysteine, 2 histidine residues and a further axial ligand. • Positive reduction potential >0.25 V versus Standard Hydrogen Electrode (SHE) • Intense blue comes from S(Cys)-Cu(II) Ligand to Metal Charge Transfer (LMCT) bands with an absorbance ~600 nm.
II	• The "non-blue" Cu proteins such as superoxide dismutase. • Mononuclear centres are often trigonal bipyrimidal or distorted square planar geometry. • Typically, liganded by histidines and oxygen-based residues.
III	• Binuclear centres, such as hemocyanin involved in O_2 transport in invertebrates and the Cu_A site of cytochrome c oxidase. • Vary in geometry from tetrahedral to trigonal bipyramidal, and bind cysteine, histidine and oxygen based amino acids. • Each Cu is bound to 4/5 ligands depending on the oxidation state.

As Cu is a metal which can interfere with cellular homeostasis, not only redox cycling ROS but also displacing other metals, there is a clear requirement within the cell for

a mechanism to regulate, chelate and compartmentalise Cu. Cells must sustain a sufficient supply of Cu to incorporate the metal into the active sites of cupro-proteins but also must restrict access and thus reactivity of Cu within the cell by using protein chelators that minimise the toxic effects of this metal.

1.3.3 Cu trafficking systems

Strategies used by the cell to control and maintain Cu levels in both eukaryote and prokaryote systems have been well sudied over the past 20 years. Importantly, studies have revealed a structural and functional conservation of Cu metabolism throughout life [35]. The most common system involves the use of metal ion chaperones which bind and transport Cu(I) ions (ATX1 in Figure 1.10) to a specific partner/transporting (a P_{IB}-type ATPase in Figure 1.10) which deliver the Cu to a protein, compartment of the cell or organelle in the case of eukaryotes. The two main objectives of this delivery are, to either incorporate the metal in a protein, or to deliver it to a Cu ion exporter to relieve the cell of toxic Cu(I).

In bacterial cells, the primary role for such systems is to alleviate the toxicity of Cu(I) by coordinating it in the cytoplasm and exporting it out of the cell. These systems are important in eukaryotes, not only for the aforementioned, but also for maturation of cupro-proteins and if not controlled, serious health problem can result from Cu. Mutations in the human Cu transporters result in Cu metabolism disorders such as Menkes syndrome and Wilson's disease, which arise due to an accumulation (Wilson's) or acute deficiency (Menkes) of Cu within the cell. ATP7A and ATP7B known as Menkes and Wilson's proteins, respectively, are the membrane associated P-type ATPase transporters responsible for copper trafficking in human cells. Menkes disease presents symptoms such as neurological impairment, delayed development, connective tissue abnormalities and is fatal, often resulting in death within the first few years of life [17]. Wilson's disease is an autosomal recessive disorder, which results in a toxic accumulation of copper in the liver and is fatal if not treated by chelation. A patient suffering from this disease will experience depression and psychiatric abnormalities [17]. While the fatal phenotype of these mutations is a clear indication of how necessary it is to transport Cu correctly, this metal is essential for a number of proteins and cellular processes such as respiration.

Our understanding of Cu homeostasis in prokaryotes is now well established and an overview of systems used by bacteria to alleviate Cu is presented in Figure 1.4.

Homologues of the chaperone (ATX1) and transporter (P_{1B}-typ ATPase) discussed are found in prokaryotes. Once Cu is transported from the cytoplasm to the periplasm of a Gram-negative bacterium, 3 further systems are known to deal with it. During aerobic growth, CueO, an oxidase, oxidises Cu^{1+} to the less harmful Cu^{2+}. During anaerobic growth this system is redundant, and some Gram-negative bacteria have the Cus system, such as *E. coli*, that transports Cu^{1+} completely out of the cell. Other bacteria such as *Salmonella* have CueP, which functionally substitutes the Cus system and has been linked not only to Cu storage in the periplasm, but also to maturation of superoxide dismutase II to supress oxidative stress arising from free Cu in the cell [37]. These systems, including their biochemistry, will be explored further in Chapter 6.

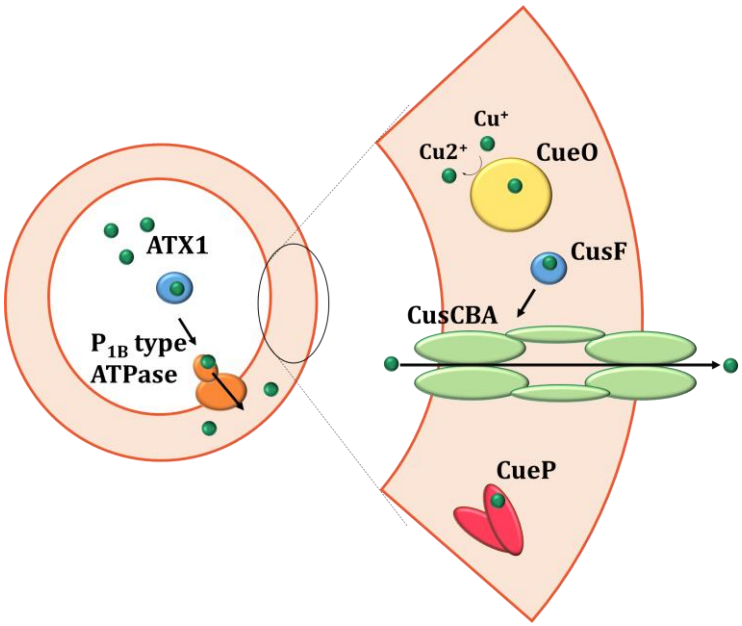

Figure 1.4: Various Cu detoxification systems used by Gram-negative bacteria to relieve the cell of cytotoxic free Cu. These include the ATX1 chaperone and P-type ATPase which relieves the cytosol of cytotoxic Cu, transporting it to the periplasm; the Cus system which ensures export of Cu to the out of the bacterium and into the extracellular environment; CueO is a Cu oxidase which oxidised Cu^{1+} to Cu^{2+} and CueP which has been linked to Cu detoxification, particularly in enteric *Salmonella* species.

1.4 Nitrous oxide reductase

Nitrous Oxide Reductase (N_2OR) has been purified and studied in various proteobacteria including *Pseudomonas stutzeri* (previously *perfectomarina*) [38], *Paracoccus denitrificans* [39] (Figure 1.5), *Pseudomonas aeruginosa* [40], *Thiosphaera pantotropha* [30] and *Achromobacter cycloclastes* [41], *Marinobacter hydrocarbonoclasticus* [42]. These studies confirm that N_2OR is a multi-Cu homodimeric protein with a mass ~ 130kDa.

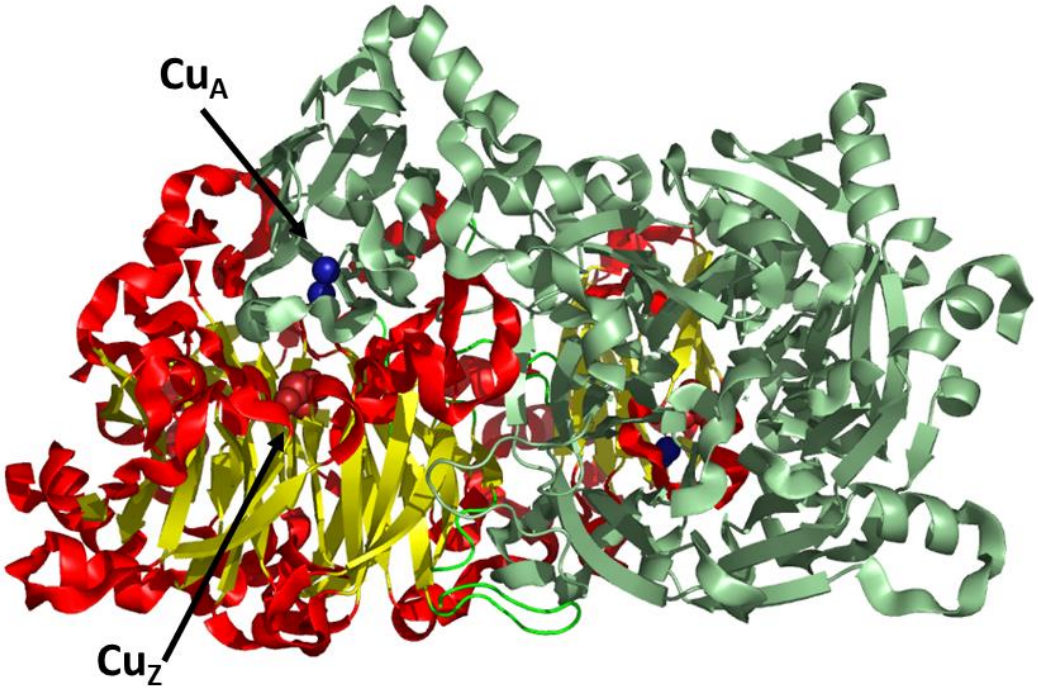

Figure 1.5: Nitrous Oxide Reductase dimer from *P. denitificans*, PDB file: IFWX [43]. A single monomer is coloured according to the secondary structure, α-helices (red) and β-sheet (yellow), the other monomer is in green. Blue spheres represent Cu atoms at the Cu_A centre and red spheres, the Cu_Z centre. The reaction catalysed by the dimer is described in Equation 1.7.

$$N_2O + 2H^+ + 2e^- \longrightarrow N_2 + H_2O \quad E_0'(N_2O/N_2) = +1.35\ V\ vs\ SHE \qquad \textbf{(Equation 1.7)}$$

Two distinct clades of N_2O reducing bacteria have been identified. Each clade uses a separate method to export N_2OR to the periplasm for maturation. As *P. denitrificans* is a clade I member, N_2OR (*Pd*N_2OR) is transcribed and translated from the gene *nosZ*

with a matured mass of 66.2 kDa per monomer (this work, Chapter 4). The signal sequence of N_2OR carries a twin-arginine motif, which is a Tat leader sequence that directs the apoprotein in the folded homo-dimeric state to the periplasm where the N-terminal signal sequence is cleaved. Evidence for the insertion of Cu only once the protein is in the periplasm comes from mutational analysis of the *tatC* gene in *P. stuzeri,* the membrane bound translocator of the folded protein. In this mutant, *Ps*N_2OR accumulated as an unprocessed, dimeric, apoprotein in the cytoplasm of the cell [44]. Similarly, the mutation of an arginine in the tat leader sequence of *Ps*NosZ gave the same result [45]. Once the protein enters the periplasm, N_2OR is matured to the holoprotein with 12 copper atoms and 2/4 sulfide atoms, per dimer. The variation in the sulfide total depends on the presence or absence of oxygen during purification. 4 sulfur atoms per dimer have been identified in the crystal structure obtained from an anaerobic preparation of N_2OR and has since been proposed as the biologically relevant form of the protein [46].

The tertiary structure of a single N_2OR monomer reveals 2 distinct domains with an N-terminal seven-bladed β-propeller domain and a C-terminal cupredoxin like domain as described in Fig. 1. 6. The tetranuclear Cu_Z site and the binuclear Cu_A site reside in the N- and C- termini respectively.

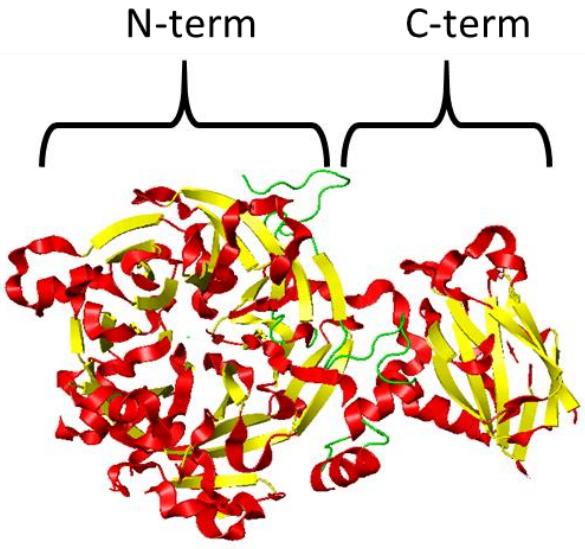

Figure 1.6: Structural representation of the two domains in a monomer of N_2OR. The 7-bladed β-propeller N-terminus and a cupredoxin-like fold at the C-terminus.

Each centre plays an important role in the reaction described in Equation 1.7. The Cu_A site is involved in electron transfer and receives electrons from an external donor then passes them to the catalytic Cu_Z site where 2 electrons are used to reduce one

N_2O substrate. Figure 1.7 demonstrates the distance between the two sites in the monomer and the dimer. The total distance between the 2 centres in a monomer is ~39.5 Å, which is too far for electrons to pass directly. The protein dimer is orientated in a 'head to tail' position, placing the Cu_A site of one monomer in close proximity to the Cu_Z of the other. The distance between the two centres of different monomers is 10 Å, well within the accepted distance for electrons to be transferred.

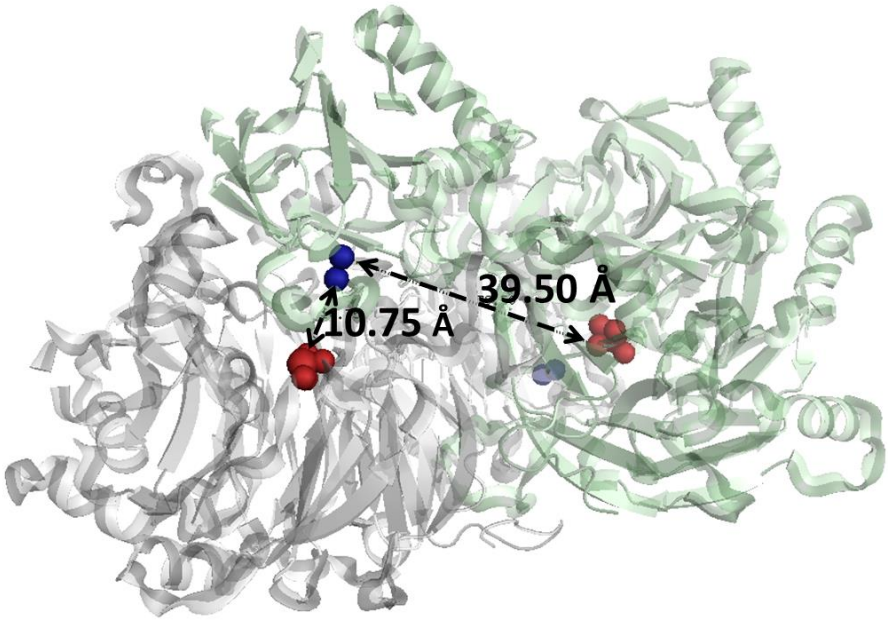

Figure 1.7: The distance between the Cu_A site (blue spheres) and the Cu_Z site (red spheres) within the monomeric protein and the dimer. Each N_2OR monomer is coloured grey and light blue. Electron transfer between the 2 centres is not possible in the monomer, but a more reasonable distance of ~10 Å means it is possible between the dimer.

Electrons used to reduce N_2O are donated from small periplasmic electron donor proteins that contain either a heme or Cu centre. Studies in *Rhodobacter capsulatus* first identified cytochrome c_2 as being crucial as the electron donor for N_2OR reduction [47]. In *Paracoccus*, a knock-out mutant of the cytochrome c_{550} did not result in an accumulation of N_2O [48]. In the absence of this cytochrome it was concluded through further work that a Cu containing protein must be responsible for the electron transfer, likely pseudoazurin [49]. The interaction between electron donors and the Cu_A site of N_2OR is electrostatic in nature [50]. Well conserved residues on the surface of this domain are involved in the electron transfer pathway including aspartate, asparagine, histidine, valine and leucine [50]. The electrostatic

surface of the region around the Cu_A centre, and proposed electron entry site, is overall negative while the donors are predominantly positive in charge allowing for a transient complex to form and transfer of an electron [50] . Once at the Cu_A site, electrons are passed across the dimer interface to the N-terminal domain containing the Cu_z site housed in a seven-bladed β-propeller, where N_2O reduction takes place to produce N_2 and water.

1.4.1 The Cu_A centre

The Cu_A site resides in the C-terminal domain of N_2OR which is configured in a cupredoxin fold similar to that of subunit II cytochrome *c* oxidase and type II Cu centres with a tetrahedral geometry [51]. The centre itself is a *bis*-thiolate-bridged dinuclear Cu center where the two Cu atoms are held, each with a histidine and another, either methionine or tryptophan ligand along with 2 cysteine residues (Figure 1.8). These cysteines bridge the two Cu atoms resulting in a binuclear mixed valent [$Cu_A^{+1.5}$:$Cu_A^{+1.5}$], S=1/2 [52] centre with an unpaired electron that is detected by EPR in the oxidised resting state which resolves into a distinct 7 hyperfine splitting pattern [53].

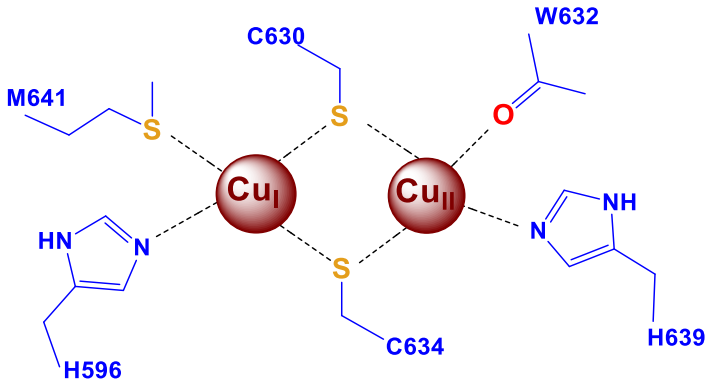

Figure 1.8: The Cu_A site of N_2OR. Two Cu atoms are bridge by sulfur donating cysteine residues. Other ligands to the Cu include histidines, a methionine and a tryptophan.

The Cu_A site appears to be di-nuclear in order to permit fast electron transfer, as it has low reorganisation energy between the two oxidation states [54]. This centre is not unique to N_2OR; homology with the Cu_A located in subunit 2 of cytochrome *c* oxidases (COX) in both eukaryotes and prokaryotes is apparent where its role is to

transfer electrons for the reduction of O_2 to water in the final step of respiration. The spectroscopic properties of the Cu_A site, as observed in mitochondrial COX, are similar to those of N_2OR, consistent with the close similarities of the site. The 2 Cu atoms identified in a Cu_A site did not account however for the total 4 Cu atoms which were first detected per N_2OR monomer [55], so another Cu cofactor site was predicted to be present. The then described Cu_Z site was believed to be a variant of the Cu_A site and early magnetic circular dichroism data showed sulfur ligation was also present at the site.

1.4.2 The Cu_Z centre

Located in a seven-bladed β-barrel motif lies the Cu_Z centre of N_2OR. The first crystal structures of *Ps*N_2OR and *Pd*N_2OR showed 4 Cu atom at the centre, bridged by what was thought to be an O_2 atom [56]. However, further analysis of an improved resolution structure showed it was in fact a bridging sulfur [57]. A version of N_2OR with no Cu_A site was used to characterise the Cu_Z centre by removing any overlapping spectral signal from both centres. Substantial metal-ligand covalency indicative of sulfur ligation was observed in the magnetic circular dichroism [58] and electron paramagnetic resonance (EPR) spectra of this reduced N_2OR variant [59]. This bridging sulfur species was predicted to be an inorganic, acid labile sulfide, not resulting from a sulfur based amino acid; this was further confirmed by metal analysis and the observation of shifts in the resonance raman spectrum of isotopically labelled sulfur and Cu species [59] along with the crystal structure. The Cu population of the Cu_Z site remains the same in every structure solved, but the total number of sulfur atoms vary depending on whether O_2 is present resulting in either a [4Cu-S] or [4Cu-2S] cluster. All the crystal structures agree there is a bridging sulfur species, but the ligand coordinating the Cu_I and Cu_{IV} atoms, varies (described in Figure 1.9). In the presence of O_2 this was found to be a water or hydroxide, while in the presence of the inhibitor iodide, this atom also bound at the same bridging position [46]. From this it was speculated that this is the substrate binding site. Since the first aerobic crystal structures were solved for *Ps*N_2OR, *Pd*N_2OR [51] and *Ac*N_2OR, a structure of the anaerobically purified *Ps*N_2OR has been solved which shows a second sulfur atom at this 1-4 bridging positions [46]. The nature of the Cu_Z centre with regard to sulfur content and oxidation states will be described in more detail in the introduction to Chapter 4. The remaining ligands to the Cu_Z centre are all histidine residues (Figure 1.9) that are well conserved across all N_2OR's, in a histidine rich motif.

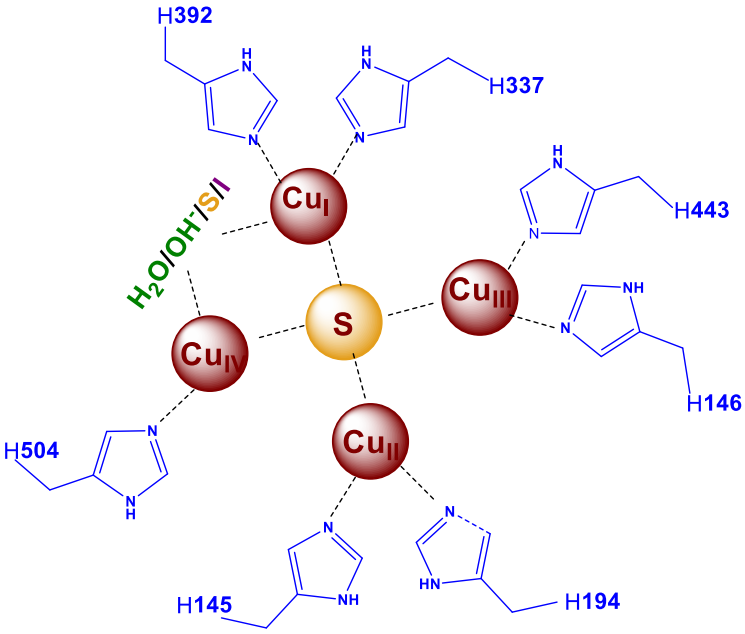

Figure 1.9: The Cu_Z site ligands are 7 histidine residues and one bridging sulfide. In total, each dimer requires 12 Cu atoms to produce a functional N_2OR. [60].

The unique CuS cluster, once fully reduced and at its most active, has a strong electronegative electron withdrawing ability that is ideal for polarising the N-O bond for electrophilic attack on the oxygen atom from a proton, for the reduction of N_2O to N_2. This analogue of the common redox active FeS cluster is unique and its evolution must be specialised for N_2O reduction, possibly through binding of the oxygen of N_2O to the bridging sulfur [59]. The activity itself is slowly becoming better understood as further crystal structures of the protein are published along with complementary spectroscopic studies, revealing further insight into the catalytic mechanism and which form of the Cu_Z centre is the active form [61, 62].

1.4.3 Mechanism of nitrous oxide reduction

There are currently two views on the mechanism used by N_2OR for overcoming the reaction barrier of N_2O reduction; each with a separate position where the substrate can bind.

The first is at the disputed Cu_1-Cu_4 bridging ligand edge, where the ligands vary depending on O_2 availability or the presence of the inhibitor, sodium iodide. In this mechanism N_2O binds at this position when all 4 Cu atoms in the cluster are reduced ($4Cu^I$) and is bound in a bent mode, with back-bonding from the Cu d orbitals to the pi-antibonding orbitals of N_2O allowing for N_2O activation [63]. The N-N and N-O bonds are also elongated during this state and leave the oxygen atom activated towards electrophilic attack from a proton [63]. A conserved second sphere lysine residue close to the N_2O binding site provides hydrogen bond stabilisation to one nitrogen atom and then the electron is transferred from the Cu_{IV} atom to N_2O [64]. The role of the acid labile sulfur in this mechanism is to stabilise the semi oxidised form of the cluster after the first electron has passed. This is through charge delocalisation and σ super exchange pathways, the electronic reorganisation energy between the fully reduced and oxidised states is minimised promoting activity [63]. The cluster then returns to its resting state as N_2 and water are released.

In light of a recently solved structure of the physiologically active *Ps*N_2OR with a [4Cu:2S] Cu_Z centre and also N_2O bound, an alternative N_2O binding position and mechanism has been proposed. The first mechanism assumed electrons were passed from the Cu_A site to the Cu_Z as the Cu_Z centre has a less positive reduction potential than the Cu_A [65]. This alternative mechanism, however, takes into account a ligand gate which is observed at the Cu_A site. The His583 ligand to Cu_I of the Cu_A site (H596 of *Pd*N_2OR) binds the Cu atom, as shown in the crystal structure of N_2OR exposed to O_2 or bound to N_2O, but, anaerobic, oxidised *Ps*N_2OR Cu_A centre lacked this ligand and the H583 was rotated 130˚ away from the Cu_A site [66]. Interestingly, this residue, even when rotated, remains hydrogen bonded to a conserved aspartate residue (D576). This aspartate residue reaches the protein surface and has been implicated in the electron entry toure to the Cu_A centre [50]. This change in His583 ligation at the Cu_A site is initiated at the Cu_Z centre based on the state of the cluster, as mentioned above, suggesting a functional coupling of the two metal centres [66]. H583 is believed to act as a molecular gate for electron transfer to the substrate by N_2O binding to the Cu_Z centre, the rotation of the histidine back to the Cu_A site allows for the gate to open, and electrons to pass from the surface to the substrate. The crystal

structure of N_2O infused crystals of *Ps*N_2OR revealed a substrate binding site between the two Cu centres, though at a distance too far for direct binding of substrate at the metal cluster [66]. The Cu_Z site in this mechanism provides a flat metal-sulfide surface composed of 3 Cu and 2 sulfide ions which lie below the N_2O which sits in a pocket above the cluster. Above N_2O in this conformation is the histidine ligand to the Cu_A site which would allow for the donation of electrons directly to N_2O [66] unlike the first mechanism which uses the electrons to reduce the cluster to activate the substrate and then passes the electrons to reduce N_2O.

Previous work on the mutation of this H583 residue has shown it produces a catalytically inactive Cu_Z site, with the loss of 2 spectroscopic features associated with the purified anaerobic protein [67], and so the mutant has the spectral features of N_2OR exposed to O_2. Additional information based on the activated and transient forms of the center in the second mechanism is needed to distinguish how plausible the method is. Inorganic small molecule mimics may be useful in trying to decipher the true role of the Cu_Z centre in this reaction, such as a Cu_4S model supported by nitrogen donating ligands [68].

1.4.4 The nos gene cluster

The DNA in *P. denitrificans* is organised into three elements: chromosomes I and II (2.9 Mb, 1.7 Mb, respectively) and a single plasmid (653 Kb). Together the genome encodes the sequence of 5077 proteins. The genes encoding a *cbb*$_3$-type oxidase, *caa*$_3$-type oxidase and the nitric oxide reductases lie on chromosome I, while genes encoding the nitrate, nitrite and nitrous oxide reductase enzymes are located on chromosome II. The plasmid does not provide the genetic information of any key respiratory enzyme.

In *P. denitrificans*, the *nosZ* gene encoding N_2OR is located on chromosome II and lies within the *nos* gene cluster (NGC). The role of the genes located in the NGC is to assist with expression and maturation of N_2OR in the cell. The cluster and the protein products are described in Figure 1.10A and 1.10B, respectively.

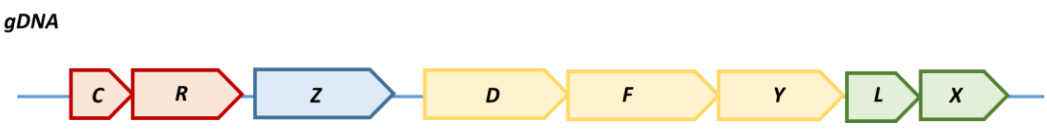

Figure 1.10A

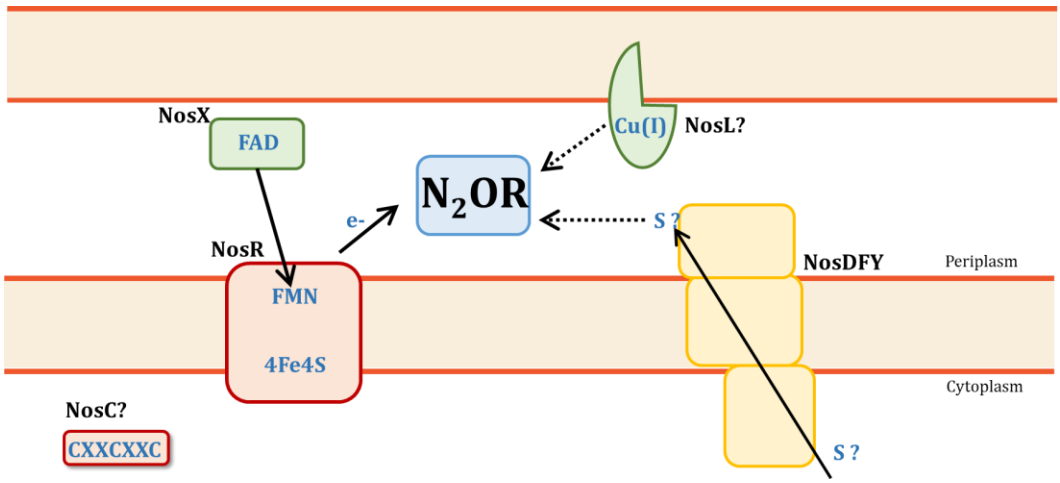

Figure 1.10B: The *nos* gene cluster in *Paracoccus denitrificans* (Fig. 1.10A) and organisation of the protein products of the NGC (Fig. 1.10B). NosCR (red) are regulatory genes which supress transcription of *nosZ* under Cu limitation. In the case of nosR, it is expected to bind Fe-S clusters and flavin mononucleotide. NosZ (blue) is the polypeptide chain of N_2OR which is folded and transported to the periplasm via the tat pathway. NosDFY (yellow) are proposed to form a trimeric complex with the potential to transport a sulfur species which provides the sulfide species, populating the Cu_Z centre. NosLX (green), further accessory proteins with putative roles in Cu delivery (NosL) and enzyme turnover (NosX).

As mentioned, there are 2 clades of N_2O reducing bacteria, each with a separate mechanism of translocation across the cell membrane [16]. An atypical *nosZ* from clade II features a SEC leader sequence while members of clade I, which are predominantly proteobacteria, have a Tat leader sequence. The *nos* gene cluster from clade II members, shares similarity to the NGC of the clade I members. Both clade I and II feature a N_2OR with a Cu_Z centre and therefore, retention of accessory genes needed to mature such a cofactor between the clades, shows they must be important for complete maturation of N_2OR. The organisation of the following accessory genes among the two clade's is discussed further in Chapter 3, in particular Figure 3.1.

NosCR

The *nosC* gene is translated into a small hypothetical protein, typically 8 kDa in size, and has a CXXCXXC motif which could bind a redox active centre. Mutation analysis in *P. denitrificans* has shown the removal of the *nosC* generates a partial Nos$^-$ phenotype [28]. Transcriptome analysis has shown that *nosC* regulates and reduces the level of *nosZ* transcription in the cell under Cu limited conditions. The *nosZ* gene becomes de-regulated in the absence of *nosC*, and therefore *nosZ* is switched on

permanently, even in the absence of Cu. Transcription of the *nosC* gene is up-regulated in the presence of low Cu [28] and low zinc [69]. NosR has been overexpressed, purified and characterised from *P. stutzeri* as an integral inner membrane, FeS flavoprotein [70]. Similar studies to those for *nosC* describe a Nos$^-$ phenotype in a Δ*nosR* strain under both Cu-low and Cu-high growth conditions. Like *nosC*, inactivation of the *nosR* gene removes regulation of *nosZ* and levels of transcription of *nosZ* become independent of Cu concentration [28]. Analysis of the protein has shown it spans the inner membrane using 5 core helices, with two flanking hydrophilic domains: the periplasmic N-terminus contains a FMN cofactor and the cytoplasmic cysteine rich C-terminus houses a [4Fe-4S] cluster [70]. The protein is processed through the SEC pathway and loses its SEC leader sequence as it is imbedded within the membrane. Two conserved CXXXCP motifs are found at the C-terminus of NosR are also observed in other redox proteins such as the thioredoxin like Sco proteins that may be a property of Cu binding or the protein acting as a disulfide switch during the maturation of C*c*O. The exact role for NosR within the cell is unclear. Based on the redox centres present, NosR could have not only a regulatory function but it could also pass electrons directly to N_2OR, as protein purified from the *nosR*$^-$ background has the spectral features of Cu_A and Cu_Z sites indicating a lack of activation [71]. Deletion of the C-terminal soluble domain of the protein produced a redox-inert Cu_Z species, while deletion of the N-terminal flavin binding domain resulted in a similar phenotype to one which lacks an electron donor to N_2OR.

NosDFY

The accessory genes *nosDFY* encode proteins that form a large heterotrimeric ABC-type transporter located in the inner membrane. NosD belongs to a family of proteins with carbohydrate binding domains and faces the periplasm, NosF is a cytoplasmic facing protein with ABC (ATP binding cassette) binding motifs, and NosY is a hydrophobic putative membrane protein based on the prediction of 6 transmembrane helices which joins the two [72]. Three of these genes have been implicated in the production of the Cu_Z site in *P. stutzeri*: a transposon Tn5-induced mutant in *nosD* produced a catalytically inactive form of the enzyme with only the Cu_A site [73] implying the importance of these genes in the maturation of the Cu_z site. The presence of ABC binding motifs would suggest that assembly of the cofactor sites require energy and could be supported by the hydrolysis of ATP/GTP to generate energy for the translocation of an unknown species. Sequence similarity between the NosDFY complex and the ATM1 transporter involved in yeast FeS cluster biogenesis

suggests it may function similarly to transport a sulfur species required for assembly of the Cu_Z site [74]. The importance of *nosRZDFY* in producing enzymatically active N_2OR was shown by cloning the cluster from *P. aeroginosa* into the non-denitrifying bacterium *Pseudomonas putida,* to generate an active N_2OR holoenzyme [75]. This experiment suggested only *nosRZDFY* genes are necessary for the production of active holo-N_2OR in *Pseudomonas* genus.

NosLX

These final genes in the cluster are the focus of this thesis. NosL is a small lipoprotein and, based on sequence analysis, is believed to be anchored to the outer membrane once matured through the localisation of lipoproteins (LOL) system [76]. Work on the protein from *Achromobacter cycloclastes* has shown it binds one Cu(I) atom and therefore could function as a Cu chaperone to N_2OR [77]. NosX is a soluble periplasmic protein, matured through the Tat pathway and is a putative maturation factor of NosR, flavinylating the periplasmic face of NosR with a single flavin mononucleotide [78]. Further information about the importance of these genes for N_2O reduction is now needed.

1.4.5 Strategies to mitigate N_2O

It is clear that the rising global population and the introduction of artificial fertiliser have undoubtedly resulted in the global rise in N_2O by 20% in the past century [10]. Two key approaches on how to reduce N_2O emissions have been described: to manage soil chemistry and microbiology, ensuring denitrification goes to completion, and to engineer crop plants to fix nitrogen with more efficiency so that they are not reliant on anthropogenic nitrogen sources [10]. The first approach is dependent on developing a greater understanding of the enzymology of N_2OR. The environmental factors that may be limiting the synthesis of N_2OR need to be assessed, and a greater understanding of the assembly of the active site of the enzyme is also required. If the environmental factors affecting the loss of activity in this enzyme could be determined, then a strategy can be put in place to tune or alter soil microbes and their environment, to increase the efficiency of this enzyme. This is where this work may help: understanding the impact a changing Cu environment has on the bacterium and pinpointing specific proteins that are necessary for whole cell N_2O reduction will

assist with developing strategies to help mitigate rising global N_2O emissions from our soils.

1.5 Aims of the project

Great knowledge on the enzymology of N_2OR, especially the activity and structure, is already available but much remains to be discovered about the biosynthesis of the metal cofactors. This project aims to identify genes and subsequent protein products that traffic Cu to N_2OR or indirectly mature the protein. This will develop the understanding of Cu cofactor biogenesis within N_2OR.

The accessory genes *nosLX* have not yet been fully studied in *P. denitrificans.* Mutational analysis of these genes will be conducted, and the impact of these deletions on the N_2OR Cu centres will be evaluated using spectroscopic methods. Further biochemical studies will be employed to determine the nature of either protein, if a phenotype is found.

A bioinformatic analysis of the *Paracoccus denitrificans* genome will be used to identify recognisable Cu trafficking/detoxification or handling proteins. RNA-Sequencing will be used to evaluate the *P. denitrificans* transcriptome under Cu excess, leading to the identification of the systems encoded within the genome that deal with Cu.

Together this work will begin to draw together new insights into the potential involvement of NosL and NosX in the maturation and activation of the metal centres in N_2OR and to develop the understanding of optimum N_2O reduction and Cu homeostasis in *P. denitrificans.*

CHAPTER 2

Materials and Methods

2.1 Strains, growth media and genetic methods

2.1.1 Bacterial growth

2.1.1.1 Escherichia coli

Escherichia coli strains JM109 and JM101 were used as plasmid storage strains. *E. coli* BL21(DE3) was used as an expression host. All strains of *E. coli* were grown at 37 ˚C in Luria-Bertani (LB) medium or on agar plates consisting of LB with 1.5% (w/v) agar (LB agar). Antibiotics used where appropriate, at the given concentration, as shown in Table 2.1.

Table 2.1: Antibiotics used in this study. A 1000x stock was made and diluted into media where necessary.

Antibiotic	**Concentration (µg/ml)**
Ampicillin (*amp*)	100
Kanamycin (*kan*)	50
Gentamycin (*gen*)	20
Spectinomycin (*spec*)	25

2.1.1.2 Paracoccus denitrificans – aerobic and anaerobic growth

Paracoccus denitrificans (PD1222) and mutant strains were always cultured at 30 ˚C. As a basic rule, starter cultures were prepared in 10 ml LB (10 ml in a 25 ml glass vial) with the appropriate spectinomycin and agitated at 180 rpm. After 24 hours of growth, this culture was used as a 1% inoculum to 10 ml minimal media (Table 2.2) supplemented with Vischniacs trace elements (Table 2.3). Antibiotic was not used in the minimal medium.

A typical aerobic growth experiment used a 1% inoculum from the 10 ml minimal media culture into the larger volume (50 ml media in a 250 ml concical flask). A typical anaerobic growth experiment again used a 1% inoculum into a final volume of 400 ml minimal medium in a 500 ml sealed Duran bottle.

Table 2.2: Components of 1 L minimal media, pH 7.5.

Component of media	Concentration
Succinate	30 mM
Nitrate	20 mM
Dihydrogen potassium phosphate	11 mM
Disodium hydrogen phosphate	30 mM
Magnesium sulfate	0.4 mM
Ammonium chloride	1 mM

The minimal medium was supplemented with Vischniacs trace elements to give the final concentration in Table 3.3. Prior to use, the solution was filter sterilised using a 0.2 μm sterile filter. Prior to bacterial culture inoculation, 2 ml/l of the stock trace elements was added to the minimal media. Table 3 describes 'Cu High' supplementation of the media which is typically a final concentration of 13 μM. Cultures grown under 'Cu low' conditions simply omitted the Cu salt from the Vischniacs trace element stock below.

Table 3.3: Vischniacs trace elements [79] used to supplement minimal media. The EDTA and metal salts were dissolved in 1 l water in the order shown below

Component	Stock concentration (mM)	Final concentration (μM)
EDTA	130	260
$ZnSO_4.7H_2O$	7.64	15.28
$MnCl_2.4H_2O$	25	50
$FeSO_4.7H_2O$	18.5	37
$NH_4\ Mo_7O_{24}.4H_2O$	0.89	178
$CuSO_4.5H_2O$	6.4	12.8
$CoCl_2.6H_2O$	6.72	13.4
$CaCl_2.2H_2O$	37.4	74.8

2.1.2 DNA isolation, restriction digests and ligations

Plasmid DNA was isolated from 5 ml cultures of *E. coli* using plasmid mini-prep kit (Qiagen). Genomic DNA was isolated from *P. denitrificans* using a Wizard ® Genomic DNA Purification Kit (Promega).

Restriction digests

To isolate a fragment of DNA from plasmid DNA, the following digest mixture was prepared (Table 2.4), using FastDigest enzymes from Thermo Scientific.

Table 2.4

Component	**Volume**	
Restriction enzyme buffer (10x conc)	2 µl	1x
Restriction enzyme	1 µl	1 unit
Plasmid DNA	x µl	1 µg
Water	17 µl - x µl	
Total Volume	**20 µl**	

The mixture was incubated at 37 ˚C for 30 minutes. The DNA fragment was separated using agarose gel electrophoresis (see section 2.2) and extracted using a DNA gel extraction kit (Qiagen).

Ligation of DNA fragment with plasmid DNA

Plasmid DNA and DNA fragments were digested using restriction enzymes which cut the DNA to produce 'sticky ends'. Ligations were prepared as shown in Table 2.5 using T4 DNA ligase from New England Biosciences. A total of 50 ng vector was used in each ligation and a mass ratio of 1:3 or 1:7, plasmid:insert, was used.

Table 2.5

Component	**Volume**	
Ligation buffer	2 µl	
Vector DNA	V µl	50 ng
Insert	I µl	-
T4 DNA ligase	1 µl	1unit
Nuclease free water	Up to 20 µl	
Total Volume	**20 µl**	

Reactions were left at 16 ˚C overnight and used to transform fresh competent *E. coli* JM101 cells.

2.1.3 Transformations

E. coli cells were made competent by the calcium chloride method [80] and stored at –80 ˚C. For a single transformation, 100 ng of plasmid DNA was added to a 0.2 ml aliquot of competent cells and incubated on ice for 40 min (unless the plasmid is the result from a ligation, in which case 50 ng of plasmid is avaiable for the transformation). The cells were heat shocked for 2 min at 42 ˚C and returned to ice for 5 min. Pre-warmed LB (0.7 ml at 37 ˚C) was added to the cells and incubated at 37˚C for 60 min. The cells were pelleted by centrifugation at 11337 x g for 2 min and 0.7 ml of the supernatant was removed. The pellet was resuspended in the remaining ~0.2 ml then plated onto LB plates with the given antibiotic (Table 2.1) and left overnight at 37 ˚C.

2.1.4 Conjugating plasmid DNA into PD1222 for - complement experiments, expressing nosZ and gene knock outs

Plasmids in *E. coli* host strains were conjugated into wild-type *Paracoccus denitrificans*, here on referred to as PD1222, and mutant strains using the *E. coli* helper plasmid pRK2013. A 50 ml PD1222 culture in LB medium was cultured at 30˚C for 36 hours with no antibiotic. The 10 ml cultures of *E. coli* (the plasmid to be transferred and of *E. coli* containing pRK2013) were cultured at 37 ˚C overnight with

antibiotic. A 50 µl aliquot from each of the 3 cultures was pipetted onto a LB agar plate with no antibiotic, mixed and left at 30 ˚C for 2 days. A sterile loop was used to collect cells from the plate and transfer them to a new plate with *spec* and *gen* antibiotics, screening for successful uptake of the *gen* resistant plasmid by *P. denitrificans.*

Note the conjugation method to produce genetic knock outs was different. The full strategy and method used to knock-out genes in *P. denitrificans* is described in section 3.4.

2.1.5 PCR

Colony PCR was used to amplify fragments from *P. denitrificans* genomic DNA to confirm whether a mutant had been made successfully. A single colony from plated culture of *P. denitrificans* was picked into 20 µl water, heated to 100 ˚C for 10 min and cooled on ice for 5 min. Cell debris was removed by centrifugation at 11337 x g for 2 min and the supernatant containing genomic DNA (gDNA), i.e. the template, was used in the reaction mixture described in Table 2.6. MyTaq™ Mix from Bioline was used as a premix of dNTP's and DNA polymerase.

Table 2.6: Components of a PCR reaction using MyTaq

Component	**Stock concentration**	**Volume**
MyTaq	2 x	10 µl
Template DNA		2 µl
Forward Primer	20 µM	4 µl
Reverse Primer	20 µM	4 µl
Total Volume		**20 µl**

The thermal cycler programme was set as shown in Table 2.7 and each cycle was repeated 35 times. The annealing temperature was optimised for each pair of primers.

Table 2.7: A single cycle of the MyTaq PCR

Process	Temperature	Time	
Initial denaturation	95˚C	90 s	
Denaturation	95˚C	15 s	1 cycle
Annealing	58˚C	15 s	
Extension	72˚C	30 s	
Final extension	72˚C	5 min	

2.2 DNA analysis: Agarose gel electrophoresis

A 1% (w/v) agarose gel was prepared using agarose dissolved in TAE buffer (Tris-acetate-EDTA, pH 8.0, 50x concentrate, from Fischer) and heated in a microwave for 3 min for a typical 120 ml solution, to dissolve the agarose. The solution was cooled to 60˚C and ethidium bromide was added to a final concentration of 1 μg ml^{-1}. The gel was poured into a casting unit and left to set. Agarose loading dye was added to the DNA sample (typically a 10x dilution) and loaded into the gel. Gels were run at 130 V for 1 hr and DNA bands were visualised under a UV light source.

2.3 Protein Overexpression and Purification

2.3.1 Overexpression and purification of N_2OR-Strep-tag II from P. denitrificans strains

The expression plasmid was produced by Manuel Soriano-Laguna and is described in section 2.12. The *pden_4219* gene was synthesised and sub-cloned into pLMB511, a derivative of pLMB509, to produce pLMB511-*pNosZ*-Strep-tag II and stored in *E. coli* JM101 with gentamycin (25 mg L^{-1}). The pLMB511-*pNosZ*-Strep-tag II plasmid was conjugated into WT (PD1222) and mutant strains produced during this work, Δ*nosL* (PD2501) and Δ*nosX* (PD2502), using the *E. coli* pRK2013 helper strain, as described in section 2.1.4. Successful conjugants were screened for both gen^R/$spec^R$ and first cultured in 10 ml LB overnight at 30 ˚C, then in 50 ml minimal media supplemented with the necessary VS and finally used to inoculate 5 L minimal media, again supplemented with VS trace elements and left at 30 ˚C, as explained in section 2.1.1.

Expression of N_2OR-Strep-tag II from the plasmid was induced at an $OD_{600\ nm}$ 0.6 with 10 mM taurine and the culture left to stand for 24 hours at 30 ˚C. Cells were harvested by centrifugation at 5000 x g, 4˚C (Beckman JLA 8.100) and resuspended in binding buffer (20 mM HEPES, 150 mM NaCl, pH 7.2) with protease inhibitors (cOmplete™ ultra tablet, Roche) and lysed by passing through a French press pressure cell at 1000 psi, twice. The cell lysate was centrifuged at 205 000 x *g* for 1 hour at 4 ˚C and the supernatant applied to a Hi-Trap HP Strep II affinity column (5 ml, GE Healthcare). The N_2OR Strep-tag II was eluted using elution buffer (20 mM HEPES, 150 mM NaCl and 2.5 mM desthiobiotin, pH 7.2). The eluted protein was concentrated, and buffer exchanged back into binding buffer using a 30 kDa MWCO centricon.

2.3.2 Overexpression and purification of recombinant NosL in E. coli BL21(DE3)

A truncated sequence of *nosL* was synthesised, codon optimised for *E. coli* and sub-cloned into pET-21a(+) using 5'*Nde*I and 3' *Eco*RI restriction sites (the exact protein sequence shown in Figure 5.1). The pET-21a(+)*trnosL* plasmid was used to transform *E. coli* BL21(DE3) competent cells, to confer ampicillin resistance, and plated on LB agar plates containing 100 µl/ml ampicillin and incubated overnight at 37 °C. Colonies were picked and used to inoculate 0.5 l LB with 100 µl/ml ampicillin and grown for 2 hrs at 180 rpm, 37 °C, until an OD_{600nm} of 0.6 was reached. Expression was induced using 500 µM IPTG and cells continued to be incubated at 37 °C, 180 rev/min for 5 hr. Cells were harvested by centrifugation at 4000 x g for 15 mins at 4˚C and resuspended with buffer A (50 mM MES, pH 6.5). Cells were lysed by sonicating 3 x 8 min 20 s (0.2 sec intervals, 50% power) in a microbiological cabinet. The cell lysate was centrifuged at 40000 x g for 45 mins at 4 ˚C to remove cell debris. The supernatant was applied to a DEAE column (HiPrep DEAE FF 16/10; GE Healthcare) equilibrated in buffer A. NosL eluted using a 0-50% gradient of buffer B (50 mM MES, 1 M NaCl, pH 6.5). Fractions containing NosL were buffer exchanged using a 10 000 Da MWCO centrifugal filter membrane (Centricon) into buffer A and applied to a Q sepharose column (HiPrep Q FF 16/10; GE Healthcare) and eluted using a 20%-50% gradient of buffer B. NosL fractions (as determined by SDS-PAGE) were pooled and, as a final step, applied to an S-100 gel filtration column (120 ml prepacked) equilibrated in buffer A and eluted in the same buffer. Fractions containing the pure protein were combined and dialysed against buffer A with 1 mM EDTA overnight at

4 ˚C and buffer exchanged into 100 mM MOPS, 100 mM NaCl, pH 7.5, fo storage at –80 ˚C.

2.4 Protein analysis: SDS PAGE and Western Blot

2.4.1 Sodium dodecyl sulfate polyacrylamide gel electrophoresis (SDS PAGE)

Both 12% (v/v) and 15% (v/v) gels were prepared depending on the size of the protein being analysed (often 12% for N_2OR and 15% for NosL). A discontinuous gel was prepared constituting stacking and resolving layers with the components shown in Table 2.8

Table 2.8: SDS PAGE gel components

Component	**12% Resolving**	**15% Resolving**	**Stacking**
1 M Tris buffer	(pH 8.8) 1.4 ml	(pH 8.8) 1.4 ml	(pH 6.8) 625 µl
Water	160 µl	500 µl	3.5 ml
30% Acrylamide	1.25 ml	1.61 ml	850 µl
10% (w/v) SDS	37.5 µl	37.5 µl	50 µl
10% (w/v) Ammonium persulfate	25 µl	25 µl	37.5 µl
TEMED	12.5 µl	12.5 µl	12.5 µl
Total	**3.225 ml**	**3.225 ml**	**5.075 ml**

For a typical protein sample, 15 µl of loading dye (Table 2.9) was added to a 15 µl protein sample, heated to 100 ˚C for 5 min. The protein concentration of a sample was determined using a Bradford assay and bradford reagent supplied by BioRad. Typically, 10 µg protein was loaded into each lane of the gel. The SDS PAGE gel was run at 180 mA, 200 V for 50 min in running buffer (25 mM Tris, 0.2M glycine and 3.5 mM SDS). Bands were stained using either Instant Blue from Expedeon or a mix of 50% (v/v) methanol, 10% (v/v) acetic acid, 0.1% (v/v) Coomassie, 39.9% (v/v) H_2O and then de-stained with water or 10% (v/v) methanol, 20% (v/v) acetic acid, 70% (v/v) H_2O, for each respective staining method.

Table 2.9: SDS Loading dye

Component	
1M Tris, pH 6.8	1 ml
DTT	0.31 g
20% SDS	2 ml
Bromophenol Blue	1 mg
Glycerol	2 ml
Total volume	**5 ml**

2.4.2 Western blot

A 12% SDS PAGE (Table 2.8) and the separated protein transferred to a polyvinyldienefluoride (PVDF) membrane using the arrangement shown in Figure 2.1.

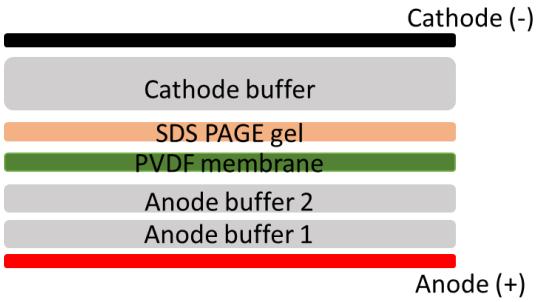

Figure 2.1: Arrangement of the western blotting apparatus; 3 filter papers soaked in anode buffer 1 (Tris HCl 0.3M, pH 10.4, in 20% v/v methanol), 3 filter papers soaked in anode buffer 2 (Tris HCl 25 mM, pH 10.4, 20% v/v methanol), PVDF membrane soaked in 100% methanol for 1 min, SDS PAGE gel soaked in anode buffer 1 for 1 min and 6 filter papers were soaked in cathode buffer (Tris HCl 25 mM, pH 9.4, 40 mM aminocaproic acid, 0.1% SDS, 20% v/v methanol). Once layered, the cathode was attached, and the trans-blot SD cell was run for 1 hr at 85 mA.

Once finished the PVDF membrane was removed and blocked for 20 mins at 4 °C in blocking solution (Phosphate Buffered Saline with Tween 20 (PBST) - 8% (w/v) NaCl, 1.44% (w/v) Na_2HPO_4, 0.2% (w/v) KCl, 0.24% (w/v) KH_2PO_4, 0.1% (w/v) Tween 20) and 5% (w/v) milk powder.

The primary antibody for NosZ, raised from sheep, was added in a ratio of 1:10 000, in PBST buffer and incubated at 4°C for 16 hrs. The membrane was washed with 3x

PBST buffer and 3x PBS (PBST without tween 20) and blocked with 5% milk in PBST at 4°C for 15 min. Anti-sheep horse radish peroxidase (HRP) conjugate (Thermo Fischer Scientific) was added in a ratio of 1:1000 in PBST buffer and incubated at 4°C for 1 hr. The 6 rinsing steps were repeated. The presence of antibody was confirmed using chemiluminescence western blot detection kit from Thermo Fischer. The luminescence was detected using a FujiFilm LAS-3000 imager.

2.5 Column chromatography: Anion exchange, gel filtration and affinity protein purification

Anion exchange chromatography separates molecules based on their charge. Pre-packed columns filled with resin were purchased from GE Healthcare. The stationary phase is made of beads of sepharose, a polysaccharide polymer, which is covalently attached to charged groups via stable ether linkages. The charged groups are dependent on the type of chromatography and the strength of charge necessary for the chromatographic step. Both weak and strong anion exchange resins were used in this work, a diethylaminoethanol (DEAE) sepharose and Quaternary ammonium (Q) sepharose columns are shown in Figure 2.2.

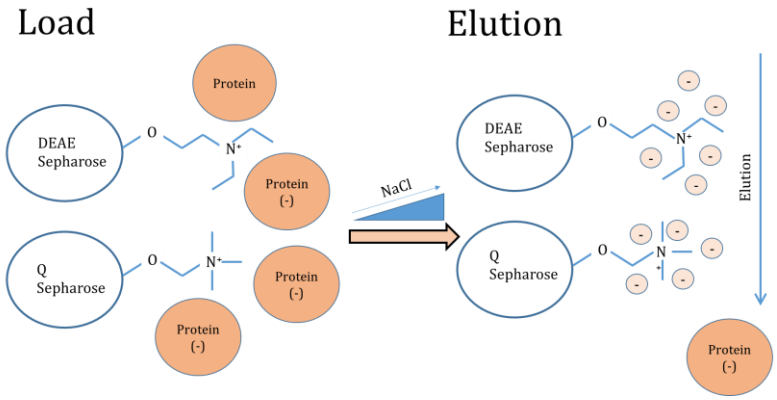

Figure 2.2: DEAE and Q sepharose column operations.

The positively charged resin (negatively charged in the case of cation exchange) is accompanied by negatively charged counter ions in solution. Proteins with a net negative charge will bind to the column through electrostatic interactions. Bound protein can then be eluted by increasing the concentration of counter ions in solution, i.e. increasing the salt concentration in the sample, which in turn weakens the electrostatic interaction between the protein and the resin, displacing the protein.

Like ion exchange chromatography, gel filtration size exclusion chromatography columns contain a polysaccharide-based resin, but in this case Sephacryl is used. These fine beads are not charged but have a specific pore size. In this work, a Sephacryl S-100 column was used which contains a resin with pore size designed to separate proteins between 1-100 kDa in mass.

Sample is loaded onto a column already equilibrated in the same buffer as the sample and then passed through the column at a suitable flow rate. The main principle is that smaller molecules will take a longer route to the end of the column than larger molecules which are less able to fit in the small pores of the resin, passing through the column faster, therefore eluting first, see Figure 2.3.

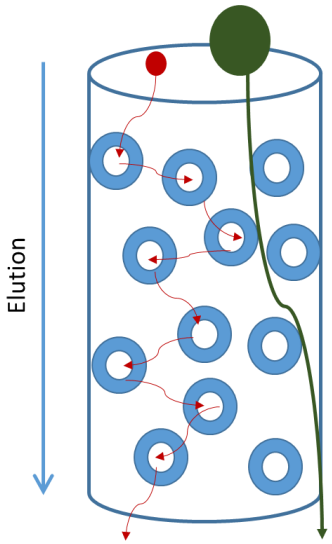

Figure 2.3: Diagram of larger v smaller proteins passing through a column

This method is typically used as a final clean up step, removing any remaining impurities with ease if the molecular mass of impurities is sufficiently different to the protein of interest.

Affinity chromatography exploits the affinity of a ligand for a protein, much like ion exchange chromatography but the interaction is more specific. In this work we exploited the high affinity interaction between streptavidin, protein purified from *Streptomyces avidinii* and h-biotin. The next generation Strep-tag II has a high affinity for Strep-Tactin, an engineered form of streptavidin which is attached to the Sepharose based column resin. The column used was a 5 ml HP StrepTrap column (GE Healthcare).

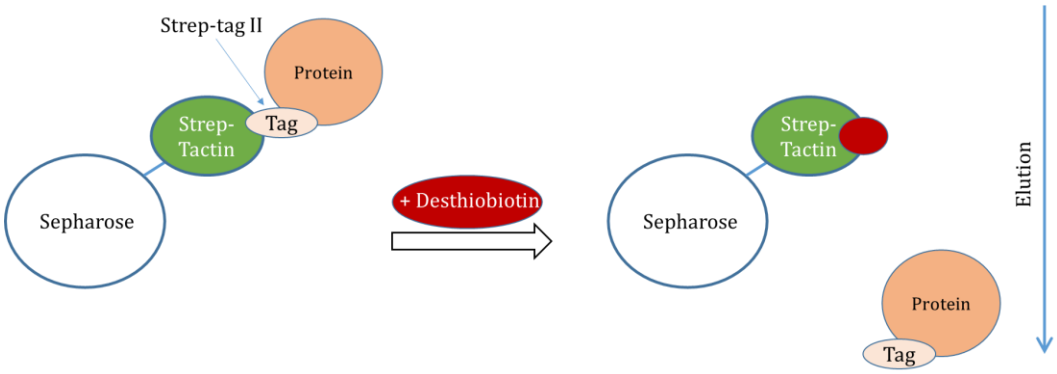

Figure 2.4: Operation of a StrepTrap affinity column.

The strep-tag II is a synthetic peptide made up of 8 amino acids residues (TSHPQFEL), which can be attached to the N- or C- terminus of a protein by introducing the coding sequence for these amino acids into the gene on a plasmid to be used during recombinant expression. Once translated, the protein then has a Strep-tag II attached. As the tagged protein meets the column it will bind while other, non-tagged proteins pass through. During the elution step, the tagged protein is outcompeted by desthiobiotin which binds tightly to the biotin binding pocket of Strep-Tactin, and thus removed from the column. This method allows for a rapid one step isolation of the protein from the cell lysate.

2.6 Determining an extinction coefficient using guanidine hydrochloride assay

The extinction coefficient of a purified protein was determined using the method of Pace et al [81], in which guanidine hydrochloride is used to denature the protein, exposing aromatic residues and cysteines which absorb with highly characteristic extinction coefficients, allowing the total $\varepsilon_{280\,nm}$ for the protein to be calculated. From this an estimated concentration of the protein was calculated using the Beer-Lambert law.

2.7 Copper assay

The concentration of Cu in a protein sample was determined using a Bathocuprionedisulfonic acid (BCS) colorimetric based assay. 100 µl of sample was heated with 100 µl 21% (v/v) HNO_3 and heated to 95˚C for 30 min. The solution was left to cool and then neutralised with 0.6 ml saturated sodium acetate. 100 µl of 100

mM hydroxylamine was added to reduce the Cu to Cu(I) and then 100 µl of 10 mM bathocuproinesulfonic acid (BCS) was added. The complex of BCS_2-Cu(I) absorbs at 483 nm and was used to determine the concentration of copper. A calibration curve was generated using standard copper sulfate solution (1 mg/ml) from Sigma Aldrich.

2.8 Metal ion additions

Copper solutions were prepared anaerobically in either 1 mM of 5 mM stocks. CuCl was dissolved in 1 M NaCl, 100 mM HCl while $CuCl_2$ was dissolved in water. Additions to protein solutions were made anaerobically for Cu(I) or aerobically for Cu(II) using a Hamilton syringe.

2.9 Methyl viologen activity assays

The first assay to detect nitrous oxide reduction was established in 1980 by J.K. Kristjansson and T.C. Hollocher [82]. Methyl viologen is a dye which can be redox cycled. The two forms, which form the basis of the assay, are the oxidised MV^{2+} which is colourless, and MV^{+} which is blue. The aim of the assay is shown in Figure 2.5. The reduced MV^{+} species acts as the electron donor to N_2OR, nitrous oxide is then added and the acceptance of electrons from MV to N_2OR to reduce the substrate results in the oxidation of MV^{1+} to MV^{2+}, resulting in a colour change from blue to colourless. The change in absorbance at 600 nm is monitored. An extinction coefficient, $\varepsilon_{600\ nm}$ = 13 600 M^{-1} cm^{-1} is then used to determine the concentration of MV^{+} oxidised and thus the concentration of N_2O reduced (given that the latter requires two electrons).

For each assay, N_2OR was pre-incubated in a 500-fold excess of reduced methyl viologen to protein. Aliquots of this stock were then taken at 15 mins time increments and used in the final assay as described in Table 2.10. 20 µl of a 10 mM N_2O solution, produced by passing N_2O through 5 ml HEPES/NaCl buffer in a sealed vial, for 2 mins, was added to initiate the reaction.

Table 2.10

Component	Volume	Initial concentration
Protein stock	5 µl	40 µM
Methyl viologen	25 µl	20 mM
Dithionite	25 µl	10 mM
Buffer	1925 µl	
N_2O buffer	20 µl	
Total volume	2 ml	

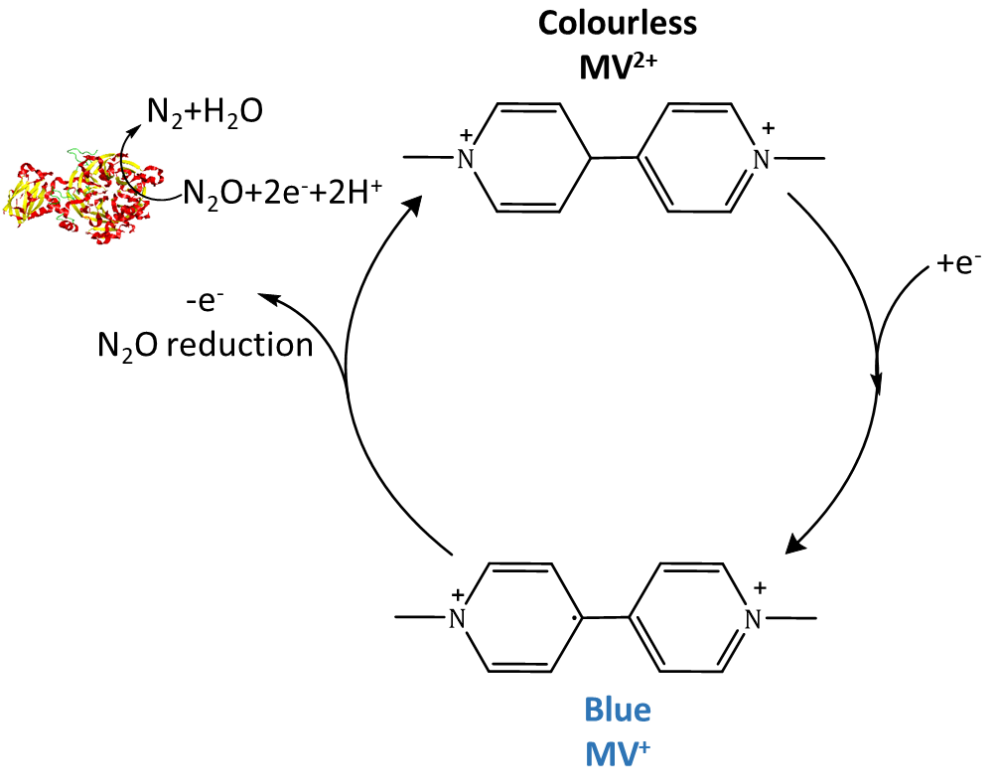

Figure 2.5: A schematic overview of the methyl viologen activity assay. Oxidised MV is reduced using sodium dithionite to produce the reduced blue form of MV which absorbs at 600 nm. The rate of absorbance decrease 600 nm as reduced MV is oxidised by the turnover of N_2OR in the presence of substrate (N_2O), is recorded and converted to a specific activity (µM N_2O min^{-1} mg^{-1}).

2.10 Spectroscopic techniques

2.10.1 UV-visible absorption spectroscopy

Electromagnetic radiation interacts and is absorbed by matter through the process of resonance. This electromagnetic radiation at a given frequency can induce electric dipoles and as a result, molecules gain energy and are excited to a higher energy level. This is the process of absorption. The intensity of these absorptions of a given wavelength of radiation can be obtained using absorption spectroscopy in which excited states correspond to a change in electronic configuration. Characteristic absorptions of certain molecules such as chromophores or aromatic amino acids are useful to protein biochemists wishing to identify a cofactor, metal oxidation state or to quantify a protein sample.

The instrument used to measure the amount of radiation in the UV and visible range of the electromagnetic spectrum absorbed by a sample is a spectrophotometer. Electronic transitions between valence electron orbitals are induced using light sources in the UV and visible region. A common set up for these instruments consists of 4 components: a light source, monochromator, sample compartment and detector/data processor.

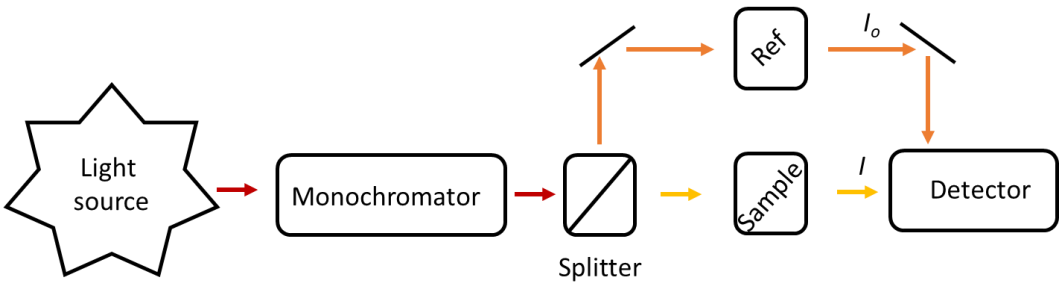

Figure 2.6: Components of a double beam spectrophotometer

The light source has 2 lamps, one a tungsten lamp covering the visible region of the spectrum, typically 340-800nm, and the other a deuterium lamp for the UV region covering 200-350 nm. The light emitted from the source is focused through a monochromator, where a prism or grating separates the radiation into its component wavelengths, to be passed through the reference and sample in turn. Any radiation passing through both cells is then detected. As a result, a spectrum of absorbance (A) as a function of wavelength (λ/nm) is produced.

The absorbance at a specific wavelength can be used to quantify the sample using the Beer-Lambert law, as shown in Equation 2.1, which states that absorbance is equal to the product of concentration of sample (c/M), extinction coefficient ($\varepsilon/M^{-1}cm^{-1}$), which is a number characteristic of the absorbing molecule, and the pathlength of the of the sample (l/cm). This can be rearranged to calculate the concentration of a sample.

$A = \varepsilon.c.l$ **Equation 2.1**

Absorbance spectroscopy is useful for determining an accurate concentration of a protein sample or for identifying cofactors bound within a protein and for observing changes in the oxidation state of metals and other cofactors within a protein.

Some examples of assigned absorptions include hemoproteins, in which the delocalised porphyrin ring of a *b* heme absorb in the 400-550 nm region. The characteristic Soret and α/β bands are due to $\pi \longrightarrow \pi^*$ transitions. Ligand to metal charge transitions arise in iron-sulfur clusters, from the S⟶Fe in the region of 350-600 nm. In this work, the Cu_A and Cu_Z centres of N_2OR are studied and they absorb in the region of 450-800nm. Absorbance in the 500-580 nm region is the result of the Cu_A centre where transitions in this energy range fit a typical $S \longrightarrow Cu^{2+}$ LMCT band from the bridging cysteine residue to the Cu.

UV-visible absorbance spectra were recorded on a Jasco V550 spectrophotometer and recorded between 900 and 250 nm in a reduced volume 1 cm pathway length quartz cuvette.

2.10.2 CD Spectroscopy

Circular Dichroism (CD) spectroscopy is useful for studies of any sample which has chirality. This technique compares the absorbance of left- and right-circularly polarised light by a sample in the UV and visible range of radiation. CD is defined as the normalised difference in molar extinction coefficient, shown in Equation 2.2

$\Delta\varepsilon = \varepsilon_R - \varepsilon_L$ **Equation 2.2**

The instrument operates similarly to an absorbance spectrometer, only that after the monochromator there is a photo-elastic modulator which generates left- and right-circularly polarised light at the given wavelengths.

The raw data is observed as an angle of ellipticity, theta, in millidegrees. This can be converted to the more recognisable Δε via Equation 2.3, using the known concentration of the sample (c) and pathlength of the cuvette (l).

$$\Delta\varepsilon = \Theta / 3298.c.l \qquad \textbf{Equation 2.3}$$

This technique is useful for examining secondary structures of polypeptides, with alpa helices and beta sheets giving rise to distinct CD spectra and thus for examining folding-unfolding transitions. Other uses include changes in the oxidation states or ligand environment of metal cofactors and changes in the potentials of certain chiral cofactors within a protein. Not all cofactors are chiral, but the pocket within the protein in which they sit can induce chirality. CD spectra were recorded on a Jasco J-810 spectropolarimeter using a 1 cm pathlength quartz cuvette.

2.11 ESI Mass Spectrometry

Mass spectrometry (MS) analyses ions based on their mass and charge. The two methods described below were carried out using a Bruker micrOTOF-QIII electrospray ionisation (ESI) time-of-flight (TOF) mass spectrometer (Bruker Daltonics).

2.11.1 Non-denaturing protein mass spectrometry

As opposed to traditional harsher methods of ionisation, supramolecules remain intact as a gas phase ion during the process of soft electrospray ionisation [83], allowing studies of, in this case, proteins under non-denaturing conditions.

The aim of the instrument is to impart a charge by the addition (in this case in positive ion mode) of H^+ ions to generate ions. The sample is loaded and passed through a fine needle like tip and heated capillary which has a certain high voltage applied, generating charged droplets that are subsequently dried to remove solvent leaving protonated forms of the protein. These ions pass through a quadrapole which stabilises and directs them through to the mass analyser. The m/z of an ion is determined by accelerating the ions using the same voltage for all, then measuring the time it takes for the ions to reach the detector. Such soft methods, if used correctly, will not result in fragmentation of a protein and therefore it is possible to observe native oligomer formations by maintaining the quaternary nature of the protein. This technique is also useful to those studying non covalently attached cofactors, or the formation and break down of prosthetic groups as a chemical reactions takes place,

such as the FeS cluster conversion in FNR, in response to O_2, identifying key intermediates in the process [84].

In order to perform non-denaturing MS, the protein was first exchanged into a volatile buffer such as ammonium acetate. The concentration and pH of the buffer was determined through trial and error, to observe the best ionisation by the given protein. Concentrations commonly used were in the range of 20-200 mM and pH 6-9.

The instrument was calibrated in the m/z range 300-2000 using ESI-L Low Concentration Tuning Mix (Agilent Technologies). Protein samples were loaded into a Hamilton syringe and then directly infused into the ESI source at a rate of 300 µl per hour. Data was aquired in 5 min increments with ion scans between 500-3000 m/z, or up to 4000 in some cases. MS acquisition was controlled using Bruker oTOF Control software. The data were collected as raw mass-to-charge ratio (m/z). The gas phase ions measured normally acquire multiple charge states due to the nature of the proteins with surface exposed residues that can protonate. This raw m/z spectrum can reveal whether the protein has undergone unfolding. For example, a protein with a small m/z and therefore many charges, is likely to be unfolded as many surface-exposed residues will be able to protonate. A larger m/z is indicative of fewer charges and the protein is likely to be more folded with fewer residues able to protonate.

NosL mass spectra (*m/z* 1000-3000) were recorded with acquisition controlled by Bruker qTOF Control software, with parameters as follows: dry gas flow 4 L/min, nebuliser gas pressure 0.8 Bar, dry gas 180 ˚C, capillary voltage 4000 V, offset 500 V, ion energy 5 eV, collision RF 1000 Vpp, collision cell energy 20 eV.

An automated, maximum entropy deconvolution algorithm was used to deconvolute the m/z spectra recorded to generate a neutral mass based on the packets of charged species identified in the m/z spectrum. The software responsible for this is was Compass DataAnalysis version 4.1 (Bruker Daltonik). The mass ranges used in the algorithm were varied depending of the size of the protein being explored, for monomeric NosL, the range was 18 kDa to 20 kDa.

2.11.2 Liquid chromatography mass spectrometry (LC-MS)

A traditional liquid chromatography method was used to determine exact masses of protein samples. 50 µl of a 50 µM protein sample was diluted 10 times using 2% (v/v) acetonitrile and 0.1% (v/v) formic acid. Samples were loaded into the LC-MS via an autosampler using an UltiMate 3000 HPLC system (Dionex). A 20 µl injection volume of the protein was applied to a ProSwift reversed phase RP-1S column (4.6 50 mm;

Dionex) at 25 ˚C. A Gradient elution was performed at a flow rate of 200 mL min^{-1} using solvents A (0.1% formic acid) and B (acetonitrile, 0.1% formic acid). Once loaded the following chromatographic method was used: isocratic wash (2% B, 0–2 min), linear gradient from 2–100% B (2–12 min), followed by an isocratic wash (100% B, 12–14 min) and column re-equilibration (2% B, 14–15 min). Mass spectra were acquired throughout using the following parameters: dry gas flow 8 L min^{-1}, nebuliser gas pressure 0.8 bar, dry gas 240 ˚C, capillary voltage 4500 V, offset 500 V, collision RF 650 Vpp. Mass spectra from manually chosen elution volumes were averaged and deconvoluted using the Compass DataAnalysis software. This experiment allowed the protein mass and any covalently attached molecules to the protein to be determined.

2.11 Gas chromatographic determination of N_2O produced by cultures

N_2O emissions from cultures of *P. denitrificans* were monitored by collecting 3 ml samples from the headspace of 400 ml cultures. These samples were stored in a 3 ml Exetainer evacuated vial (828W). The gas samples were analysed using a Perkin Elmer Clarus 500 gas chromatographer with an electron capture detector and Elite-PLOT Q (a DVB Plot) column, 30 m, 0.53 mm lD. Carrier gas was N_2, make-up gas was 95% (v/v) argon/5% (v/v) methane. The column temperature was at 90 ˚C and the injector at 115 ˚C. 50 µl of sample was injected each time.

The instrument output is an area that can be used to generate a standard curve of known N_2O concentrations in N_2 (5, 100, 1000, 5000, 1000 ppm, Scientific and Technical Gases). The gradient of the line was used to convert the GC output into ppm N_2O. This was then converted from ppm to mM N_2O using the relationship:

$$1 \text{ ppm} = 1/1000000 \text{ g/g}$$

$$= 2.272 \times 10^{-8} \text{ moles } N_2O \text{ in 1 ppm } N_2O.$$

The number of moles of N_2O in 1 ppm is equal to 1 $x10^{-6}$ g divided by the mass of nitrous oxide, 44.013 g/mol. The number of moles can then be multiplied by the ppm of N_2O calculated from the GC to give the number of moles of N_2O in the headspace of the culture.

N_2O is soluble in aqueous solutions and so the concentration of N_2O in the headspace is multiplied according to Henry's law for N_2O at 30 ˚C, K_H^{cc} of 0.5392, to determine the amount in solution.

Calculating the concentration of N_2O in total

Both headspace and solution N_2O are added together and then multiplied by 2. As there is one nitrogen atom in nitrate and 2 in N_2O, this correction gives the amount of nitrate which is converted into N_2O. With 20 mM nitrate reacted, you would expect 10mM in the form of N_2O product

2.12 Strains, plasmids and DNA sequences used to prepare mutants in *P. denitrificans* PD1222

Table 2.11

Strains	
P. denitrificans PD1222	Wild-type, $spec^R$
P. denitrificans PD2501	Unmarked Δ*nosL* (*pden_4215*) deletion, $spec^R$
P. denitrificans PD2502	Unmarked Δ*nosX* (*pden_4214*) deletion, $spec^R$
P. denitrificans PD2503	Unmarked, Δ*nosL* and 5 amino acid deletion from the *nosX* N terminus., $spec^R$
P. denitrificans PD2504	Unmarked *Δpden_0521* deletion, $spec^R$
P. denitrificans PD2505	Unmarked Δ*nosZL* double deletion, $spec^R$
P. denitrificans PD2506	Unmarked *Δpden_0926* deletion, $spec^R$
E. coli BL21 (DE3)	Host for recombinant overexpression from pET construct
E. coli JM109	Host for pK18*mobsacB*-based and pLMB511-based plasmids
E. coli JM101	Host strain for pET21a(+) overexpression vector
Plasmids	
pRK2013	Mobilizing plasmid in triparental crosses, kan^R

pK18*mobsacB*	Allelic exchange suicide plasmid, sucrose - sensitive, *mob*$^{+}$, *kan*^{R}
pK18*mobsacBΔnosL* [a]	Construct for *nosL* deletion, *kan*^{R}
pK18*mobsacBΔnosX* [a]	Construct for *nosX* deletion, *kan*^{R}
pK18*mobsacBΔnosLX* [a]	Construct for *nosLX* deletion, *kan*^{R}
pK18*mobsacBΔPden_0521* [a]	Construct for *pden_0521* deletion, *kan*^{R}
pK18*mobsacBΔPden_0926* [a]	Construct for *pden_0926* deletion, *kan*^{R}
pLMB511NosZ [b]	Overexpression construct for NosZ (*pden_4219*) with C-terminal enterokinase cut site and Strep-II tag, *gen*^{R}
pLMB511NosL [b]	Complementation plasmid for PD2501 (*pden_4215* sequence cloned into pLMB511 as a *Nde*I-*Eco*R1 fragment), *gen*^{R}
pLMB511NosX[b]	Complementation plasmid for PD2502 (*pden_4214* sequence cloned into pLMB511 as a *Nde*I-*Eco*R1 fragment), *gen*^{R}
pET-21a(+)*trnosL*	Overexpression plasmid for *nosL* in *E. coli*, *amp*^{R}
Primers	
PD2501 F' Check	cccctgcttctgacctatcc
PD2501 R' Check	gaggctgaggatgttttcca
PD2502 F' Check	cctgttcttcagccaggttc
PD2502 R' Check	gaatcggatgtttcccagaa
PD2503 F' Check	ctggtggtgctttacgacct
PD2503 R' Check	gccggtatcgatcagaatgt
PD2504 F' Check	aagtccttcgagaccacgac
PD2504 R' Check	ggacaagggttctcagcatc
PD2506 F' Check	ctgcctgatcctgctgatg
PD2506 R' Check	ccgctctaccagaacctcaa

[a] These plasmids include regions upstream and downstream of the specified gene to be removed, ligated into the cut pK18*mobsacB* plasmid using *Eco*RI and *Pst*I.

[b] The pLMB511 plasmid is a derivative of the pLMB509 plasmid, produced by Dr M. Soriano Languna.

Table 2.12. DNA Sequences used to produce pK18*mobsacB* suicide vectors.

The full gene knock out strategy and the process of producing knock outs is described in 3.2.

Sequence Information	**DNA Sequence**
nosL flanking regions[a] cloned into pK18*mobsacB* to produce pK18*mobsacBΔnosL*	GAGAATTCacctcgctggccgtctatctggtgccgctgctggcgctg ctgatgagcttcgacgccgtcgccggcgaggtcgagcgcggcacgct gcccctgcttctgacctatccgtcgcacgggccgaagttctggcgg gcaagctggtcgcgcatatggcgatcctggcgctggcggtcggcgcg ggctacggcgccgccgcgctggcggcggtctggaccgatccggcctc gacggccgggctgccggcgctgtggcggctgatgtggagctccaccc tgctgggcgcgaccttcctgggcgcgggctacgcgctttccagcatc gcgcggcggccctcgggcgcggcgggactggcggtcgggctgtggct ggggctggtggtgctttacgacctgggcctgctggcgctgatcgtcg ccgatggcggcggcggcttcaccaccgaggtgctgccggtcgcgctg cttgcgaaccctgccgacgccttccgcctgttcaacctctcggccgc ccaggccaccgctgccgctgccggcgtgggcggggccgccgcgacca tcccgctttggcaatcggctctgtcggtcctggtctggccgctggcc gcgcttggccttgccatcgccgcattccgaaaggtcacgccatgaga catTCTAGAtgactgactgaccgatttcctgaaccgcctgcgcgcgc tgagccaacccaaggagcccgcgacatgagcctgtcccgccgtcgct ttctgaccatcaccgccgccgtcgcgctgctgcccgcggggctgcgc gcccagcccggcaggcattgggtcgggcaggcgcttggcgcccgcgc ctcgatccgcatcgaccaccccgaggccggggcgatcaccgcccgct gcctggccgagatcgaccggctggaaaacatcctcagcctctatcgc cccggcagcgcgcttgcgcgcctgaaccgcgacggcgtgctggatgc gccgccctttgaattgctcgactgcctgtcgctggccggcgccgtgc atcgcgccagcggtgggctgttcgacccgaccgtgcagccgctctgg tcgctctgggccgaggccgccgtgaatggccgccgtcccacgcccga ggagcggcgcgatgcgctggcacggacgggctgggatcgggtgcggc tggacgcggcgcgcatcacgctggagccggggatggccctgacgctg aacggcatcgggcagggctatgtcgccgaccgtgtcgccgcgctgct tgaggccgaggggctgggcgacattctgatcgataccggcgaattgc gggccctgggcggccggcccgatgggcgcgactggccggtccggctg gccgagggcggcgcggCTGCAGTC
nosX flanking regions[a] cloned to produce pK18*mobsacBΔnosX*	GAGAATTCccgccgcgaccatcccgctttggcaatcggctctgtcgg tcctggtctggccgctggccgcgcttggccttgccatcgccgcattc cgaaaggtcacgccatgagacatgcgttgctgctggtgctgctgctg ggccttgtcgcctgccgcgaggaggtggcgcaggatacggcgccggt cgagatgaacgcccagacactcggccatttctgccagatgaacctgc tggagcatcccggccccaaggcccaggtgcatctggaggggatgccc ggcacgccccctgttcttcagccaggttcgcgacgccatcgcctatgc ccggatgccggagcaaagccatccgatcctggcgatccaggtcaacg acatgggcaagccgggcgccacctgggacgatcccgggcagggcaac tggatcgacgccgcggacgccttttttcgtcatgggctcggcccaggc cgggggcatgggggcgcccgaggcggtgccctttttccagccgcgagg ccgccgaaacctttgtcgccgcgcagggcgggcaggtgatgcggctg gacgcgatccccgacgaaatggtgctcgcgcccgaggaaaccgtgcc cgacagcagcaccgaggccgatttcctgaaccgcctgcgcgcgctga gccaacccaaggagcccgcgacatgagcctgtcccgccgtcgctttc tgacTCTAGAtgactgactgaggagatccgtgcgctgctggacaggt tcgacggcacccggctggaagccgcgcagcgccaggcatagccacag gcccgccgggccttgatgccgccgcgcatggctgcgtggcggctttc gcatgtcccgtacccgcctggggccggatatctgacggggttgtgaa tattttacaaaaacagcgatcttatcgtcaatttatttacaaaaaaa

	tctttgaaaaaaaatgatttactggaaatgaaaagtttgattaacat tcgtcgcaatcggttttccgatgtccgttgcggcaccttgaggaggg tgtgggcgtcccgaaccgacccctgtcgcgagtagaggaggcgcgca tgaccattgaaacttctgggaaacatccgattccgccgggttttggg gatgccctggtccagcctggcgattacgcccgcatgtatgccgaatc gatctcggaccctgacgggttctggggccgcgagggcaggcggctgg actggatccacccctattccagggtgaagaacaccgatttcgccatg ggccaggtctcggtgaagtggttcgaggacggcatcctgaacgcctc ggtcaactgcatcgaccgccacctgcccgggcgcgcgaaccaggccg cgatcatcttcgagccggacgacccggaccagccggcgcgccacatc acctatgcggaactgtcCTGCAGTC
nosL flanking regions[a] including the first 15 bp of *nosX,* cloned to produce pK18*mobsacB ΔnosLX*	GAGAATTCacctcgctggccgtctatctggtgccgctgctggcgctg ctgatgagcttcgacgccgtcgccggcgaggtcgagcgcggcacgct gcccctgcttctgacctatcccgtcgcacgggccgaagttctggcgg gcaagctggtcgcgcatatggcgatcctggcgctggcggtcggcgcg ggctacggcgccgccgcgctggcggcggtctggaccgatccggcctc gacggccgggctgccggcgctgtggcggctgatgtggagctccaccc tgctgggcgcgaccttcctgggcgcgggctacgcgctttccagcatc gcgcggcggccctcgggcgcggcgggactggcggtcgggctgtggct ggggctggtggtgctttacgacctgggcctgctggcgctgatcgtcg ccgatggcggcggcggcttcaccaccgaggtgctgccggtcgcgctg cttgcgaaccctgccgacgccttccgcctgttcaacctctcggccgc ccaggccaccgctgccgctgccggcgtgggcggggccgccgcgacca tcccgctttggcaatcggctctgtcggtcctggtctggccgctggcc gcgcttggccttgccatcgccgcattccgaaaggtcacgccatgaga catTCTAGAgtcgctttctgaccatcaccgccgccgtcgcgctgctg cccgcggggctgcgcgcccagcccggcaggcattgggtcgggcaggc gcttggcgcccgcgcctcgatccgcatcgaccaccccgaggccgggg cgatcaccgcccgctgcctggccgagatcgaccggctggaaaacatc ctcagcctctatcgccccggcagcgcgcttgcgcgcctgaaccgcga cggcgtgctggatgcgccgccctttgaattgctcgactgcctgtcgc tggccggcgccgtgcatcgcgccagcggtgggctgttcgacccgacc gtgcagccgctctggtcgctctgggccgaggccgccgtgaatggccg ccgtcccacgcccgaggagcggcgcgatgcgctggcacggacgggct gggatcgggtgcggctggacgcggcgcgcatcacgctggagccgggg atggccctgacgctgaacggcatcgggcagggctatgtcgccgaccg tgtcgccgcgctgcttgaggccgaggggctgggcgacattctgatcg ataccggcgaattgcgggccctgggcggccggcccgatgggcgcgac tggccggtccggctggccgagggcggcgcggtgggcctgcgcgcccg ggcgctggcgacgtccgcgccgctgggcaccagcttcgacgaggcgg gccgcgacggccatatcctcgacccgctgagCTGCAGTC
Pden_0521 flanking regions[a] cloned to produce pK18*mobsacB Δpden_0521*	GAGAATTCtagcggaccgcccggcccggtgcgacgacgtggtaaagg aagaagtccttcgagaccacgacgatgctgccgacctcgaaatcgtt gcggatcgagacttcggtcggggcataggggtcgcgcttgggctcgg cctgcgtggtcagcgccgcgggctgcgcctgtgccagggccagcgag ggcacggccaccagcggcaaggcggccatcagcatctgtctgcggtt catctgtccgtcctgaatccttgcgtttcttgatcatgcgcctaacc gcttgggcgcccgggatcaactcaaagcgccgtgacgcggttgaaac gcgcggcaagcgtgcctagcttgcatcgggaaaggaccgcccgccat gacttgtgcgacctgtgccgccattccccgcccgccgcgccggcccg ccacgcgtgccccgcatctgtgccggggccggggcgggcgcggttgc cgctgccatgtcgcggcccgcccgcatctggcccgccccgtgctggc cggcgacggccatccgctgcgctggcgccgggaaccaggcgacgggc cgcagcccgggcagatcctgcaccatccgccgcaatatccgcaggct ccgccgatccctgtctgaatcgcgtctttttcgccattctgacagga caatccgatgaaacatcTCTAGAtgactgactgaggggccggggcga tggcgctttcctcggtcttcgtggtcagtaacgcgttgcgattgagg cgtgccgcatgatgctgagaacccttgtcctgatcctggcccttgcg gccgtgccggcggcagcgacgccgctgcgcatcttggccttcggcga cagcctgaccgaaggctacggcctgccccgcaaggacgggctggtgc

	cgcaattgcaggactggctgagggcacgcggccatgacgtgctggtg ctgaacggcgggctctcgggcgacaccacagcgggcgggcgggtgcg gatcggctattcgctggcccgccacaagcccgatgcggtgatcgtcg agctaggcggcaacgacctgctgatgggctttgccccgcagatggtc gagggcaacctggattcgatcctgggccaggccggcaggggcggccg gccgctgctgctggtcggcatcgcctcgcccgaccacgacgaccccc tgcgccgcgactgggccgggatctggccgcgcatggccacgcagcac gatgccctgctgatggagaacctgtaccagccgcttttcgacctgcc gggcgacggctacaaggccatgctgcaacccgacgggctgcatgcct cggccaagggcgtcggcctgatcgtgcaatcgctgggccccaaggCT GCAGTC
pden_0926 flanking regions[a] cloned to produce pK18*mobsacB Δpden_0926*	GAATTCgctgggcgaagagctttcgctgccggccgtgctgggcgtcg cgctttcgacggcgggcgtcgccatggcggtgctgggccgggccggg cgctcgggcgggcatcgtttcgaggcggtgcagggctcggtctggat cgcctcgggcttcgggctgatggcggcggcggggcaggcgctggggt cgctgatcgcgcggccggtgatggctgcgggcttcgacccctatgtc gcctcgctggtgcgggtgggcgtggcggtggcctgcctgatcctgct gatggcgctgccgctccgcgcggtccagccactgggccggcccacgc cgcgcgtgatggtgctgacggcgctttccggcctgatcgccatggtc accggcatgacgctgctgatgttcgcgctgcaaggcggcaaggtcgg tatcgtctcgacgctttcggcgctgtcgccggtgctgatcctgccgg tgctctgggcgatgaccggggcgcggccctcggcgacctcatgggcg ggggcgctgatcgcggtggcgggcatggcgctgctcttcttgcgctg acgggtttgtcatttgccgccggtgccttgccgcgcttctctctgcg catcgtcacgacaggagaaTCTAGAtgactgactgaccgtccttcct gctcaagatggccggtccggccctgaggggtgggaccggccgggcta aggcccttgccctcagcccagcaggcgctgcgcttcctggatggcaa agcggtcggtcatgccggcgacgtaatccagcaccacccgggcgcgc ccggtctcgtcccccgcggcctcggcggcctggaaccaggtccgcgg catcttcgaggggtcgtccaggaacagcgggaacagcccgttcagca tctcggtcacccgccgccgctcgaccaccaccgagggcgcgcgatac atgcgctggaacaggaacagcttgatcgccttgaggttctggtagag cggcttggaaaagcggatgatcggcccttccatgtcgcgaatctcct gcacgttttgcggTtgcaggctggccagccggttctgcgccactgcg atcacatcctcgaccatgacgccaaagacccggcgcagcgcctcgtg ccggcgtcgcatcggctccagccccgggtgcagcgcatcgacgcggg caagagcctcgccgacgacgggcagttccgccaggtccgcctcggtg aacagccccgcgcgcagcccgtcatgcaggtcgtgatggttataggc cacgtcgtcggccacggcCTGCAG

[a] The sequence highlighted in yellow (a marker *Xba*I site) separates the *nosL* 5'- and 3'-flanking regions. *Eco*RI and *Pst*I sites used for cloning are in capitals and underlined. Sequences in red indicate the primers used to confirm the deletions in *P. denitrificans* PD1222.

2.13 Plasmid maps

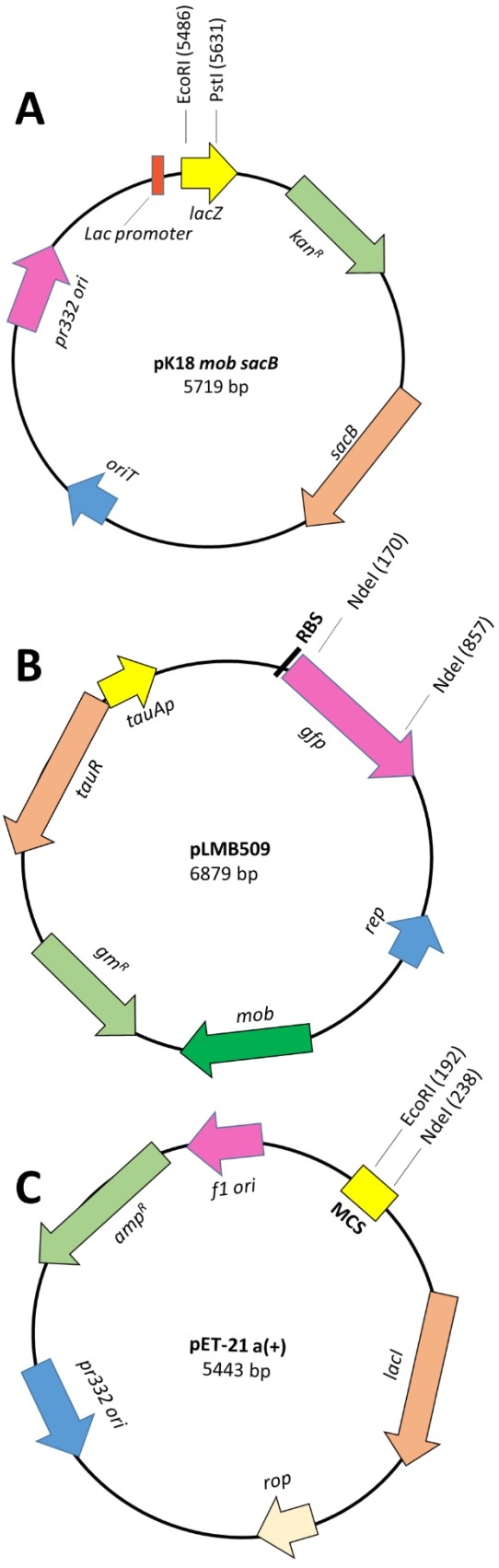

CHAPTER 3

Investigation of the phenotypes of three mutant strains of *Paracoccus denitrificans*: Δ*nosL,* Δ*nosX* and Δ*nosLX*

3.1 Introduction

The *nos* gene cluster (NGC) in *P. denitrificans* is comprised of 8 genes that are transcribed from 3 transcription initiation sites (Figure 3.1).

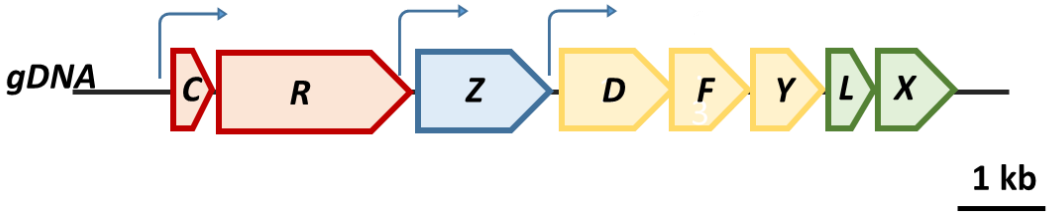

Figure 3.1: The *nos* gene cluster. Arrows indicate the start sites for transcription of *nosCR* (red), *nosZ* (blue) and *nosDFYLX* (yellow and green) from 3 start sites.

The conservation of these NGC elements across the 2 clades of N_2O reducing bacteria, is described in Figure 3.2. The *nosC* and *nosR* genes in *P. denitrificans* have been identified as Cu responsive units which encode proteins that regulate the transcription of *nosZ* [28] as mentioned in Chapter 1. Under Cu limited conditions, they reduce the transcription frequency of *nosZ*. The *nosC* gene itself is highly conserved across α-proteobacteria, in particular, it shares >50% sequence identity within *Paracoccus* species, so this gene will likely have a specific role for this class of bacteria. The mechanism by which *nosR* regulates the transcription of the *nosZ* gene is still unknown, though it is important for whole cell N_2O reduction and is well conserved across clade I members, see Figure 3.2.

Five accessory genes downstream of *nosZ*, *nosDFYLX*, are transcribed in a single transcriptional unit. Only 4 elements are common across the NGC's of other denitrifying bacteria from clade I, these are *nosDFYL* (Figure 3.2). The *nosL* gene was identified in all but one gene cluster. *Opitutus terrae*, a clade II member, lacked *nosL* but it does, however, feature a type I Cu binding protein upstream of *nosZ*, which may functionally replace NosL, which, is a putative Cu chaperone. The final gene in the cluster, *nosX*, is predominantly found in α- and β- proteobacteria NGC's but not γ-proteobacteria among clade I and does not feature in clade II clusters.

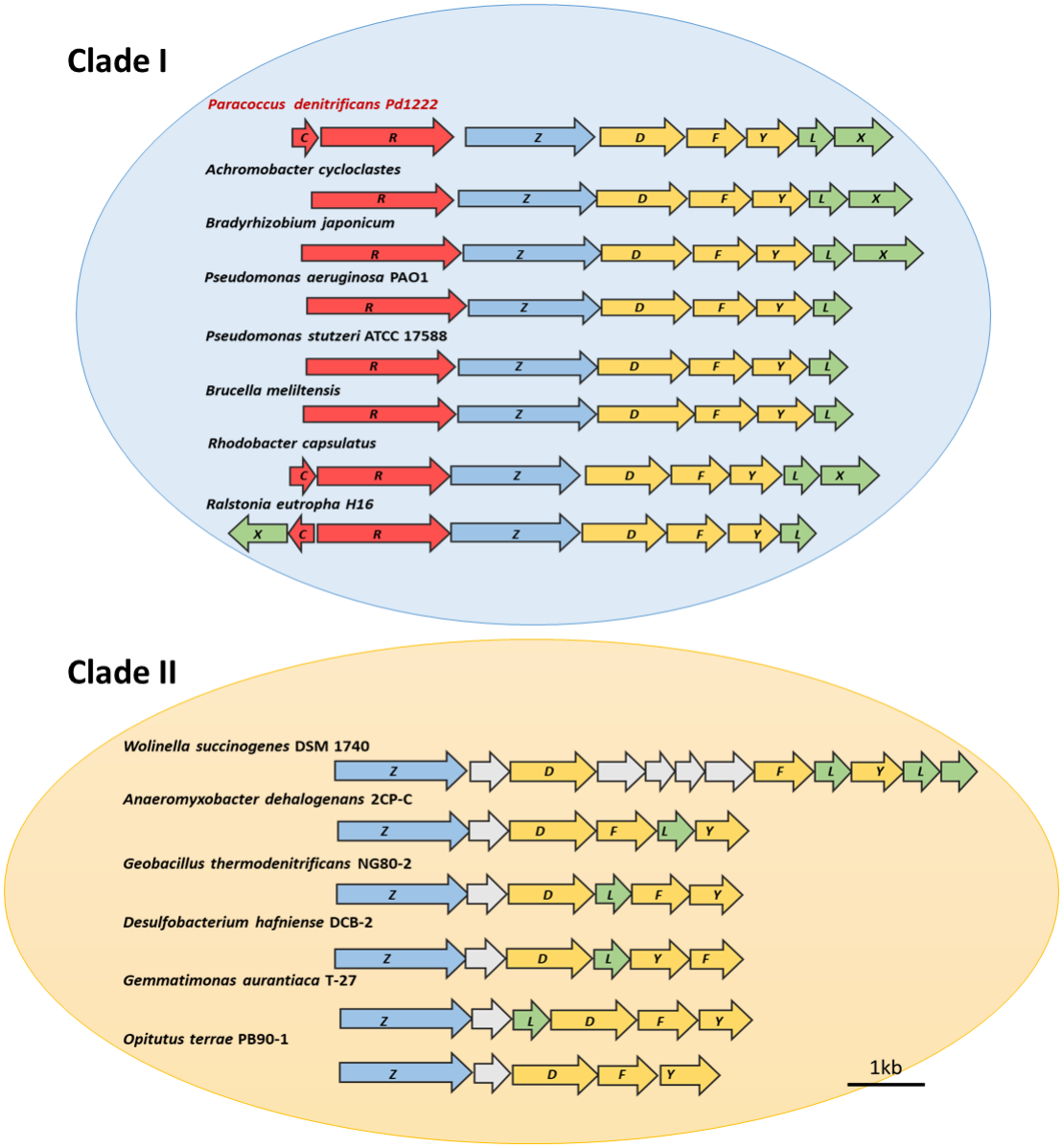

Figure 3.2: A comparison of the NGC from clade I (blue) and clade II (yellow) members of N_2O reducing bacteria.

The consequence of a *P. denitrificans* strain lacking a *nosL* gene has yet to be evaluated. A mutation study of nos*X* in *P. denitrificans* did not reveal a clear Nos$^-$ phenotype. Only the disruption of both *nosX* and its homologue *nirX* resulted in a Nos$^-$ phenotype [85].

An early insertional mutant disrupting the *nosDFY* genes of *P. stutzeri* illustrated their role in the maturation of the Cu_Z centre when N_2OR purified from this background was missing the key spectroscopic signals of this centre [73].

Figure 3.2 describes the N_2OR phylogeny which has two groups, clade I (blue) and clade II (yellow). As discussed in section 1.4 , one of the main differences between the clades is the method used to translocate N_2OR to the periplasm. Clade I members are also most likely to be full denitrifiers as explained by the presence of a nitrite reductase, *nirS* or *nirK,* in their genome. In contrast, 51 % of clade II members are non-denitrifying N_2O reducers [86] and therefore act as N_2O sinks. Clade I, denitrifying proteobacteria, have *nosR,* a well-conserved regulatory gene which has not been annotated across clade II members. Interestingly, some members of clade II have Fe-S and flavin protein encoding genes in close proximity to the *nosZ* gene which could functionally replace the role of *nosR* [86]. The other gene not found in clade II NGC's is *nosX,* a putative partner to *nosR.* 51% of this clade does not have *nirS* or *nirK,* a gene cluster in which a *nosX* homologue is found. Therefore, it is likely they have another functional homologue.

The key similarity between the two clades is the *nosDFYL* operon. The genes are not necessarily in the same order as those in clade I but present nonetheless. The strict conservation of these genes within the NGC implies an essential role in the maturation of N_2OR. *nosDFY* have already been implicated in the maturation of the Cu_Z centre in *P. stutzeri* and studies of NosL from *Achromobacter cycloclastes* [77] have shown it can bind copper and is, therefore, a potential copper chaperone to N_2OR.

An analysis is presented in this chapter, of 3 mutant backgrounds: Δ*nosL,* Δ*nosX* and Δ*nosLX*. Double recombinant allelic exchange methodology was employed using the suicide plasmid pK18*mobsacB* to generate the new mutant strains of *P. denitrificans.*

3.2 Gene knock out strategy

3.2.1 Preparation of suicide plasmid pK18mobsacB, with gene inserts for the knock out process

DNA sequences relating to the fragments illustrated in Figure 3.3, were synthesised by Genscript. *Eco*RI and *Pst*I restriction sites flanked 2 sections of DNA corresponding to the ~750 bp sequences upstream and downstream of the gene to be removed (see 2.12 for exact DNA sequences). The 5' upstream region of DNA chosen was synthesised and 2 further elements were incorporated: 3 stop codons and an *Xba*I restriction site, at the 3' end. Stop codons in all 3 frames were essential to ensure

translation of the gene upstream finished and that translation did not carry through, translating downstream. An *Xba*I restriction site was incorporated following on from the 3 stop codons; this restriction site acted as a marker to confirm the gene knock-out. The synthesised DNA was cloned into pUC57 using *Eco*RI and *Pst*I restriction sites and further sub cloned into pK18*mobsacB* using the same sites. The pK18*mobsacB* vector [87] exhibits *kan*^{R}, mobility genes and sacB sucrose sensitivity which are used as markers during the knock-out strategy. The resulting pk18*mobsacB* plasmid was used to transform competent *E. coli* JM101 cells, which were plated onto *kan* LB agar. Transformations were subsequently used as sources of the suicide vectors: pK18*mobsacB*Δ*nosL,* pK18*mobsacB*Δ*nosX* and pK18*mobsacB*Δ*nosLX*.

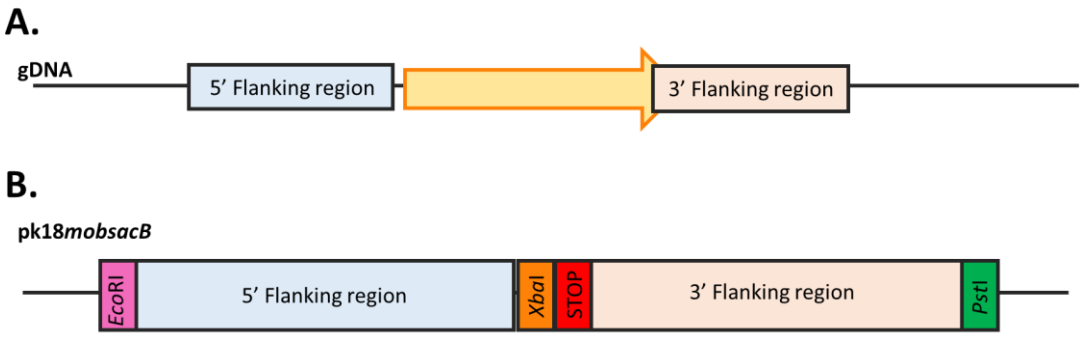

Figure 3.3: The strategy used to remove genes in PD1222. 5' and 3' regions flanking the yellow gene to be deleted (A) were synthesised by Genscript along with additional restriction sites: a 5' *Eco*RI, 3' *Pst*I and, a *Xba*I site along with 3 stop codons, which were sandwiched between flanking regions. This was cloned into pUC57 and subsequently sub-cloned into the suicide vector, pK18*mobsacB* (B).

3.2.2 Conjugation of suicide plasmid and double recombination

By means of a triparental mating strategy the pK18*mobsacB* plasmid derivations were conjugated into *P. denitrificans* with the assistance of the *E. coli* pRK2013 helper strain. The following cultures were prepared using a 1% inoculum from a 10 mL LB pre-culture of the relevant strain, grown for 24 hours, shaking at 180 rpm at 30 ˚C for PD1222 and 37 ˚C for *E. coli* strains.

- 50 ml of WT PD1222 with no antibiotic was grown for 36 hrs in LB at 30 ˚C to stationary phase (approx. ~1.8 OD at 600 nm)
- 50 ml of the *E. coli* pK18*mobsacB* JM101 containing the appropriate suicide vector was cultured in the absence of antibiotic for 4 hours at 37 ˚C to mid-exponential phase (~0.7 OD at 600 nm).

- 50 ml of the *E. coli* helper strain pRK2013 was cultured without antibiotic both was cultured for 4 hours at 37 ˚C to mid-exponential phase (~0.7 OD at 600 nm).

The 3 cultures were harvested in one tube, resuspended using 1 ml of the remaining LB and pipetted onto a sterile 0.22 µm filter paper on a plain LB agar plate. The conjugation mix was left for 3 days at 30 ˚C to allow for the first recombination event to occur.

First recombination event

Once the helper strain (pRK2013) has assisted with the transfer of the pK18*mobsacB* KO plasmid into PD1222, homologous regions of the PD1222 genome on the pK18*mobsacB* plasmid can be incorporated into the genome of PD1222 in two stages. The first single recombination event results in the complete incorporation of the plasmid DNA into the chromosomal DNA (Figure 3.4). Once in the genome, the resulting strain from the single recombination event is now kan^R from the plasmid and $spec^R$ from the PD1222 genome. The conjugation mixture was plated onto a mixed *spec*/*kan* plate, and colonies were chosen from this plate and cultured for 1 day at 30˚C for the second recombination event to occur.

Second recombination event

During the second round of DNA recombination, the other flanking region is recognised and forms a loop as it is incorporated into the genome. During this step, the gene to be deleted incorporates into the plasmid and the plasmid is removed from the genome. The pK18*mobsacB* plasmid with the deleted gene cannot replicate in PD1222 and is lost thus removing its kan^R and other genetic components such as *sacB* from the cell. After the second recombination event, the cells were screened on 6% sucrose LB agar plates. Those with the suicide plasmid including the *sacB* gene still incorporated into the genome cannot survive as the *sacB* gene in the presence of sucrose is lethal. Cultures insensitive to sucrose were either a wild type revertant that had removed the plasmid from the genome and degraded it or was a successful conjugant that had undergone a double recombination event. To further confirm this, sucrose resistant colonies were screened on *spec* and *spec*/*kan* plates. Those that grew on *spec* but not *spec*/*kan* were wild type revertant or double recombinants and were taken forward for colony PCR to amplify the region deleted.

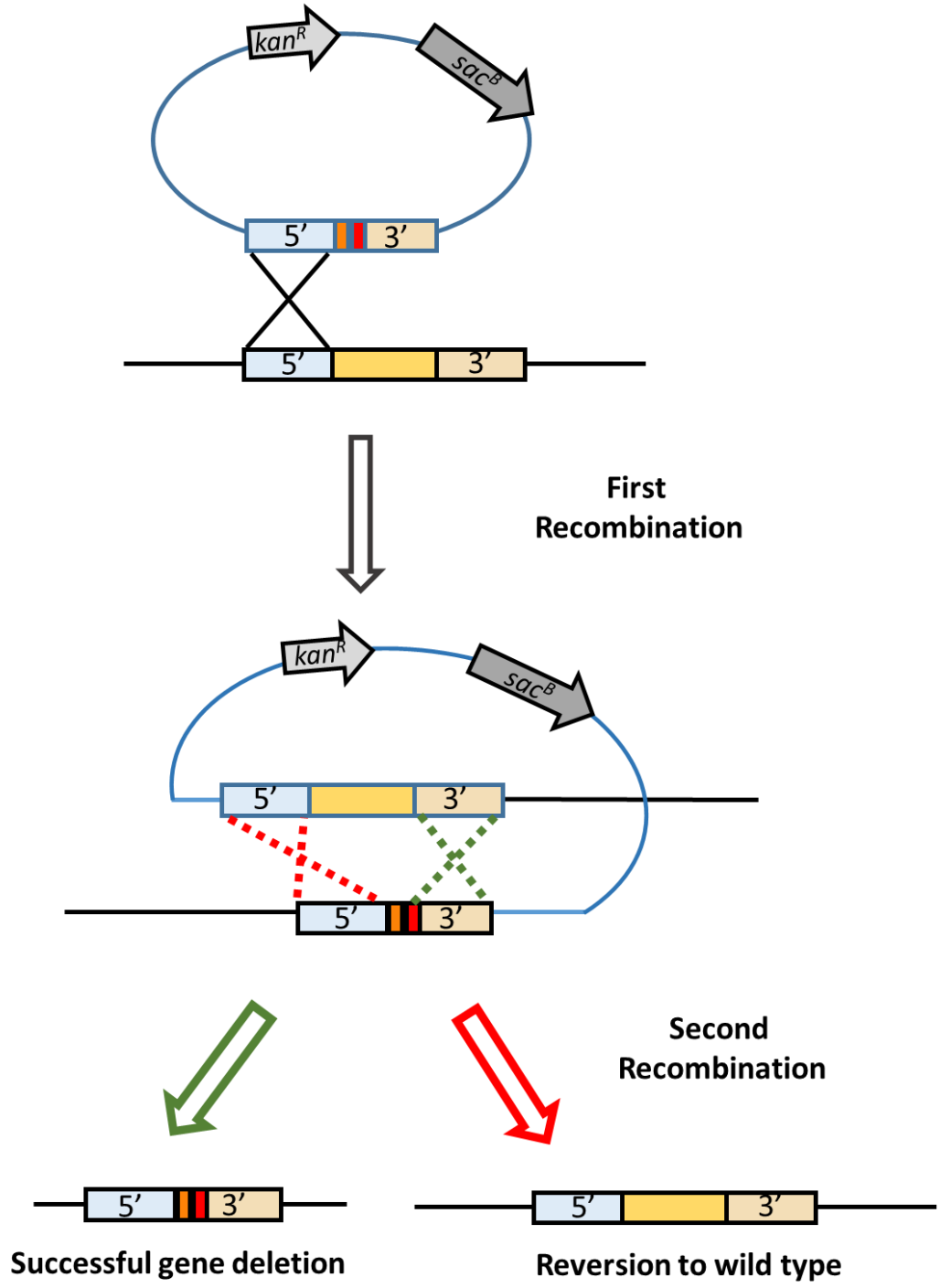

Figure 3.4: Schematic of recombination events used to generate gene knock out in *P. denitrificans.* The 2 events include initial homologous integration of the pK18*mobsacB* mutant plasmid into the genome, and the second recombination event, generating the knock out as shown or alternatively the reversion back to parental strain genotype.

3.2.3 Confirmation of a successful gene knock out

To establish where the gene knock-out was successful, colony PCR was used to analyse colonies growing on the *spec* plate and not on the *spec*/*kan* (Setion 2.1.5). To further confirm this, the PCR was also performed on extracted gDNA. Primers used in the PCR were designed to start on the flanking 5' and 3' fragments and extend across the *Xba*I site in the middle, which was used as a marker to even further confirm the loss of the gene.

In a typical PCR, if the gene was not lost the fragment of DNA amplified would be longer, as it still contained the gene (Figure 3.5). Positive knock-outs were therefore shorter, and the amplified fragment was extracted from the agarose gel using a gel extraction kit (Qiagen), and sequenced (Eurofins). The presence of an *Xba*I site in the amplified fragment was taken as confirmation that the knock out had been successfully produced.

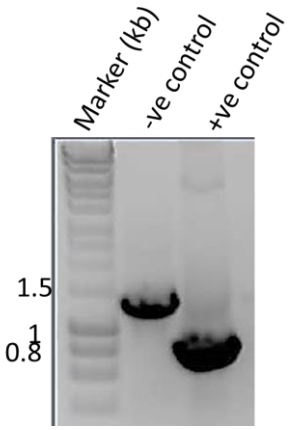

Figure 3.5: Agarose gel electrophoresis of PCR fragments from *spec*^{R} colonies after the second recombination event. Those with the gene removed are shorter and based on primer sequence, should result in a fragment ~750 bp like the starting pK18*mobsacB* plasmid which offers a positive control. The negative control is genomic DNA with the gene still intact and therefore the DNA product of the PCR is longer. For this example, the Δ*nosL* strain, the wild-type length was 750 bp along with the length of *nosL*, 573 bp, to give a total length of 1.3 kb.

3.3 Growth characteristics of mutant strains of *P. denitrificans*

Three mutant strains of *P. denitrificans* were produced: a *ΔnosL*, *ΔnosX*, *ΔnosLX*. All 3 mutant strains, wild-type and a *nosZ* null mutant, were grown anaerobically in batch culture in minimal media, under copper sufficient (13 μM) or limited (<0.5 μM) conditions as described in section 2.1.1. 400 ml cultures were inoculated with 1% of pre-conditioned cells (10 ml minimal media, Cu-high and Cu-low cultured for 24 hrs at 30˚C). Samples of the culture (1 ml) and of the headspace (3 ml) were collected at regular time intervals. Samples were analysed using GC and method in 2.11. Figures 3.6A and 3.6B illustrate the positive and negative controls, wild type and Δ*nosZ* respectively, which are easy to compare with the mutant strains.

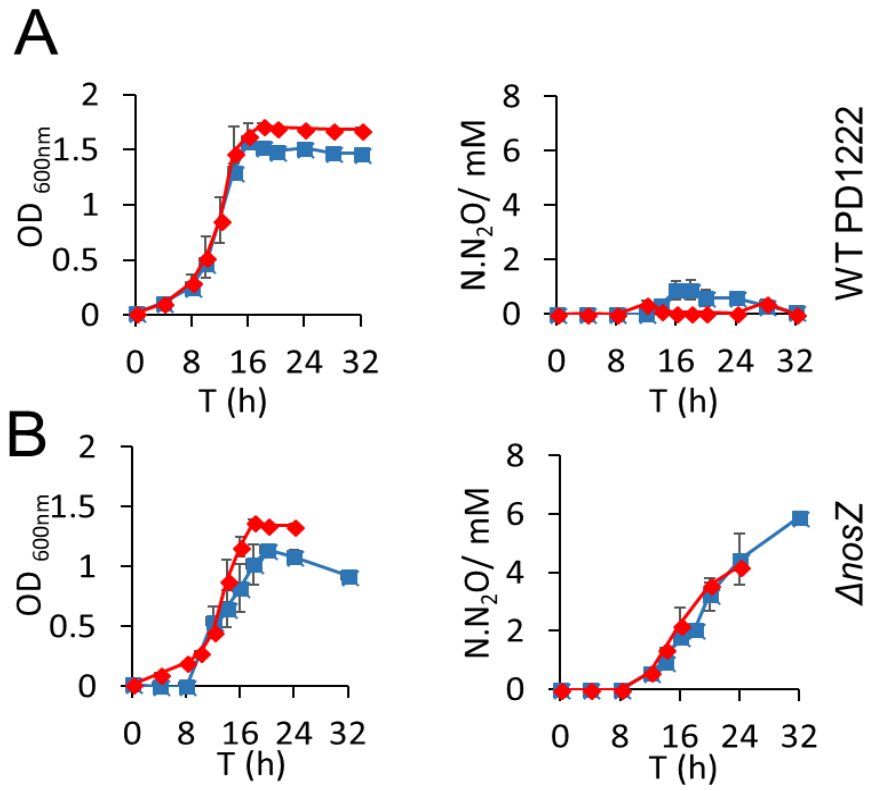

Figure 3.6: Growth and N_2O production characteristics of *P. denitrificans* strains wild type PD1222 (A) *ΔnosZ* PD2303 (B) in anaerobic batch culture in Cu-High media (♦) and Cu-Low media (■). Left, Optical density (OD 600 nm) and right, $N.N_2O$ (millimolar N in the form of N_2O) for each strain. Cultures were grown in triplicate and bars represent SE.

The wild type cultures did not accumulate a significant concentration of N_2O under Cu-limited conditions. The ~ 1 mM N_2O which was produced during the exponential phase of growth was reduced and N_2O was not detected after 28 hours of growth. In

the Δ*nosZ* strain, after 32 hours of growth, 6 mM N_2O was produced by the culture. The minimal media contains 20 mM nitrate and we expect 10 mM N_2O to be produced from a *nosZ* deficient mutant. The increase in N_2O emissions was reaching a linear phase and so it would be expected that after another 12 hours of growth, the 10 mM N_2O in the headspace would have been reached, consistent with the starting nitrate being converted to N_2O. The maximum growth reached by the 2 strains during stationary phase varies slightly depending on the amount of Cu in the cell and whether the *nosZ* gene is present. The point of reducing nitrogen oxide species under anaerobic conditions is to generate a proton motive force which will, in turn, generate enough ATP for the bacterium to survive. Electrons also play a role in this and N_2OR acts as an electron sink in the periplasm under such conditions. If these electrons are not being used to reduce nitrous oxide, then only 5 of the possible 7 electrons needed to reduce nitrate to nitrogen gas are being used. Under these circumstances, the electrochemical gradient is effected and the periplasm has an excess of electrons and therefore the cell has to wait for the electrons to be used up before it can pass more through from the ubiquinol pool and cytochrome bc_1. For this reason, fewer ATP molecules are synthesised and therefore the culture grows to a lesser density and we see a fall in approximately 20% of the growth maximum (OD_{600nm} ~1.7 for WT and ~ 1.4 for the Δ*nosZ* mutant, Figure 3.6). A less obvious growth reduction is observed in the WT background, in response to Cu limitation. This is due to the fact that under Cu-limited conditions, *nosZ* transcription is reduced due to regulatory effects from *nosCR,* and therefore less N_2OR is present compared to optimum conditions. The WT strain responded to Cu limitation by producing up to 1 mM N_2O during its exponential phase of growth, Figure 3.6A. This accumulation of N_2O is the cell responding to less N_2OR, and if N_2O can not be reduced, then fewer ATP molecules are synthesised, and the OD is down compared to when the full fleet of denitrification enzymes are in place.

Once clear growth and N_2O characteristics for the two control strains were documented, the same methodology was applied to culture and analyse the 3 mutants (Figure 3.7).

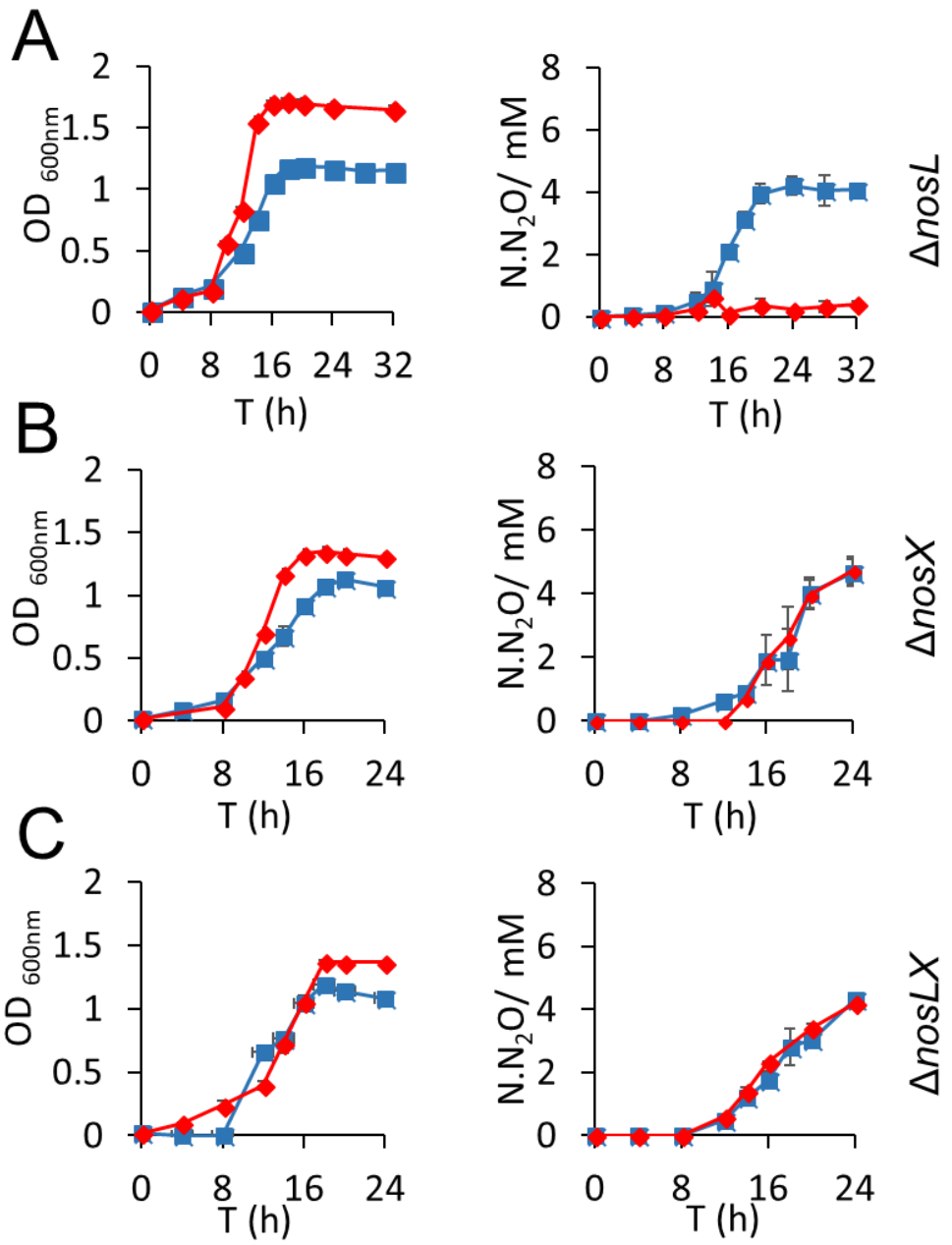

Figure 3.7: Growth and N_2O production characteristics of *P. denitrificans* strains Δ*nosL* PD2501 (A), Δ*nosX* PD2505 (B) and Δ*nosLX* PD2503 (C) in anaerobic batch culture conditions in Cu-High media (♦) and Cu-Low media (■). Left, Optical density (OD 600 nm) and right, N.N_2O (millimolar N in the form of N_2O) for each strain. Cultures were grown in triplicate and bars represent SE.

Five clear phenotypes were observed having analysed the three mutant strains under Cu-sufficient and Cu-limited conditions. The only strain and one condition presented a phenotype: the Δ*nosL* (PD2501) strain under Cu-high growth conditions. A Nos$^-$ phenotype was only observed in this strain when Cu was limited, Figure 3.7A. After

24 hours of growth, and once the cells had reached stationary phase, up to 4 mM N_2O was detected in the headspace of the cultures, which is comparable to the Δ*nosZ* strain.

The *nosLX* strain (PD2503) is composed of a *nosL* deletion with the additional loss of the first 15 base pairs of the *nosX* gene, which resulted in a *nosL* deletion and assumed to be non-functional *nosX*. Analysis of this strain, under both copper regimes, showed a clear Nos^- phenotype, like that of the Δ*nosZ* strain. Once again, the growth maximum was below an $OD_{600\ nm}$ of 1.5 (characteristic of maximum growth in wild type copper sufficient conditions) and N_2O levels in the culture headspace was above 4 mM after 24 hours of growth.

Examination of the Δ*nosX* strain PD2502 (Figure 3.7B) presented the same clear growth and N_2O emissions characteristics as the Δ*nosLX* (PD2503) strain. Therefore, it appears that the double mutant strain is dominated by the loss of *nosX* transcription, which resulted in one of the following: the catalytic inactivation of N_2OR, incomplete maturation of N_2OR or loss of *nosZ* transcription.

The growth maximum for all strains presenting a phenotype, was below 1.5 OD_{600nm}, as expected when N_2O, one of the 4 substrates in the denitrification pathway, is not reduced.

3.4 Complement experiments

Each, single knock out strain, was complemented with a plasmid *in trans*. The genes corresponding to *nosL* and *nosX, pden_4215* and *pden_4214* respectively, were synthesised by Genscript with flanking 5' *Nde*I and 3' *Eco*RI restriction sites and cloned into pUC57. The gene was subcloned into a derivative of pLMB509 called pLMB511 (produced and supplied by Dr M. Soriano-Laguna). pLMB509 is a high copy number plasmid developed for expression and purification of polyhistidine-tagged proteins in alpha-proteobacteria [88]. The genes to be complemented were then sub-cloned into pLMB511 using *Nde*I and *Eco*RI, and competent *E. coli* JM101 cells were transformed with the plasmids. The pLMB plasmid series confers gentamycin resistance, which when conjugated into the knock out strains using method 2.1.4, results in a $spec^R/gen^R$ strain.

Batch cultures were prepared and grown anaerobically, as described in section 2.1.1. Expression of the gene from the pLMB511 plasmid was induced with 1 mM taurine at the start of growth or taurine was omitted from the cultures as a control. Cultures

were incubated, without shaking, at 30 ˚C. Samples of the culture density and the headspace were collected at regular intervals for analysis.

3.4.1 ΔnosL (PD2501) complement

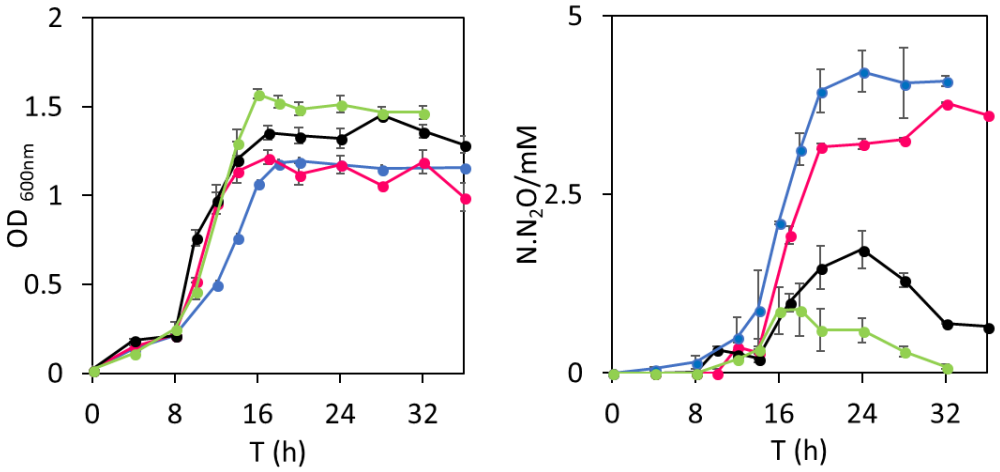

Figure 3.8: Growth and N_2O production characteristics of the mutant Δ*nosL* complementation under Cu-low conditions in batch culture. The anaerobic growth optical density (OD 600nm), left, and N.N_2O (mM N in the form of N_2O), right. The pLMB511*nosL* plasmid was conjugated into the *ΔnosL* PD2501 strain and cultured in the absence of taurine (●) and presence of 1 mM taurine (●). For reference, data for the *ΔnosZ* PD2303 strain (●) and wild type PD1222 (●) are shown. Experiments were repeated in triplicate and bars represent SE.

The phenotype of the Δ*nosL* strain was rescued by complementation with *nosL* encoding, taurine inducible plasmid. Under Cu-limited conditions in wild type PD1222, there was up to 2 mM N_2O released from the culture and some N_2O accumulation is also observed in the complementation. After the cells were into late exponential/stationary phase at ~18 hours, the level of N_2O fell in the *nosL* complemented strain, which is consistent with the wild type data.

3.4.2 ΔnosX (PD2502) complement

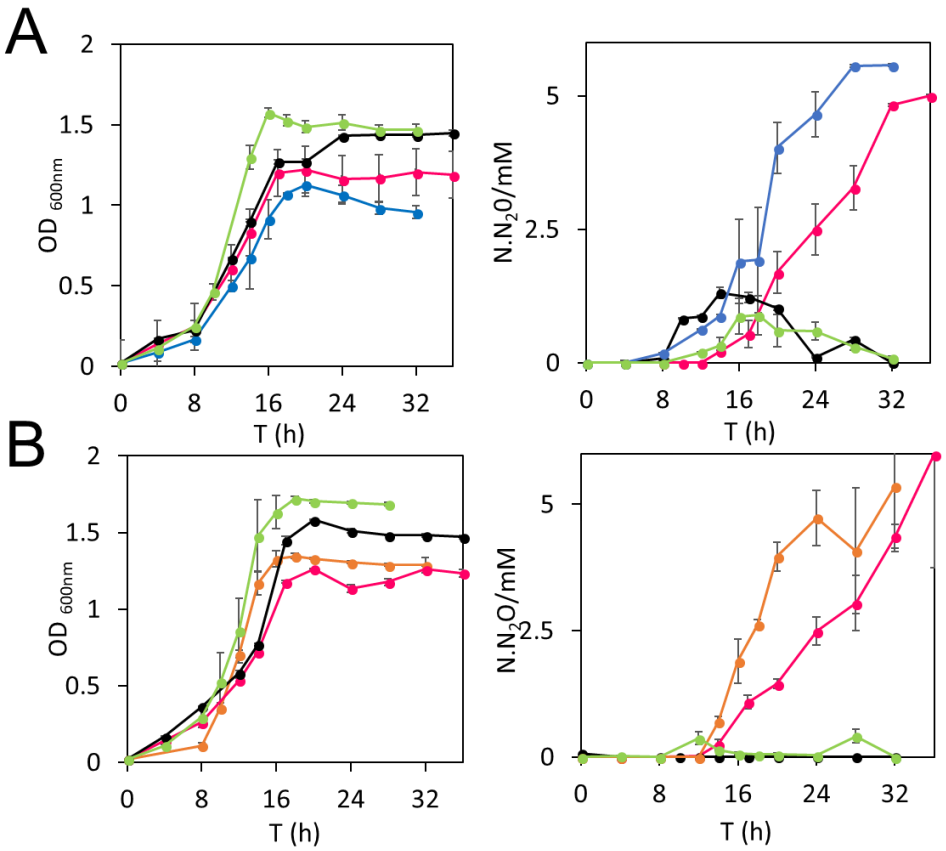

Figure 3.9: Growth characteristics and N_2O production of the mutant Δ*nosX* PD2502 complementation under Cu-low (A), and Cu-High (B) conditions in batch culture. The anaerobic growth optical density (OD 600nm), left, and N.N_2O (mM N in the form of N_2O), right. The pLMB511*nosX* plasmid was conjugated into the Δ*nosX* PD2502 strain and cultured in the absence of taurine (●) and in the presence of 1 mM taurine (●). For reference the Δ*nosZ* PD2303 strain (●/●) and wild type PD1222 (●) are shown. Experiments were repeated in triplicate and bars represent SE.

The phenotype of the *nosX* mutant was rescued under both Cu conditions. Under Cu-limitation, N_2O accumulated and subsequently decreased over time, as observed in the *nosL* complementation. In the presence of Cu, very little N_2O accumulated in the headspace during the complementation, typically <1 mM.

3.5 Discussion

Functional N_2OR requires 12 Cu atoms to produce a catalytically active dimeric holo-enzyme. As the genes deleted in this experiment encode factors that potentially mature the Cu centres of N_2OR, the effect of Cu being present and absent was likely to play an important role in observing a phenotype. Minimal media used in the experiments was advantageous as the Cu content of each experiment could be manipulated. This was an important advantage that allowed us to distinguish whether a strain was Cu dependent or not.

The turbidity of a culture correlates with the number of bacterial cells and in turn, feeds back as to how well the bacteria are coping under the condition. A growth difference between the positive (WT PD1222) and negative (Δ*nosZ*) control strains was apparent and the final OD_{600nm} was ~1.7 and ~1.4, respectively, under Cu replete conditions. The lower maximum turbidity in the Δ*nosZ* strain is presumably due to 3 of the 4 substrates in the denitrification pathway being metabolised, as discussed in section 3.3. Comparing the growth of a culture is a subtle method of finding a phenotype, but the more decisive method employed here was the analysis of the headspace for N_2O.

Growth and N_2O analysis of the Δ*nosL* strain under Cu-high conditions showed no phenotype, as it was similar in growth and N_2O emissions to the wild type strain. Under Cu limited conditions, however, a clear Nos^- phenotype was observed. Both the maximum growth and N_2O emissions from the culture were similar to those found in the Δ*nosZ* mutant, see Figure 3.6B and 3.7A for Δ*nosZ* and Δ*nosL,* respectively. Chemical complementation was clearly possible in the Δ*nosL* strain by adding Cu. Biological complementation with an *in trans* version of the *nosL* gene was necessary under Cu limited conditions and this was demonstrated using the taurine inducible system as shown in Figure 3.8. The only previous mutational study carried out on *nosL* was in *P. stutzeri* which demonstrated a gentamycin cassette inserted towards the C-terminus of *nosL*, 399 base pairs in, produced an active holo-N_2OR and no phenotype, other than slightly lower growth rate than the wild-type [89].

By using the 2 Cu regimes, a sensitivity to Cu was identified in the *nosL* mutant. This sensitivity leads to the conclusion that the gene is likely to affect the ability of the Cu centres to assemble under Cu limited conditions. The concentration of Cu under Cu limitation is predicted to be <0.5 μM based on ICP analysis of the media using the exact methods carried out by Sullivan et al [28]. In this environment, the wild type background can still scavenge enough copper to produce sufficient amounts of

functional N_2OR, while a strain that is without *nosL* cannot. Under Cu-limited conditions, it is known that transcription of *nosZ* is reduced, so there are fewer N_2OR proteins to populate. Therefore, if there was 0.5 μM Cu, it could be used to populate 420 nm N_2OR (assuming 12 Cu atoms per dimer 0.5 μM divided by 12). What remains is enough active N_2OR to turn over N_2O in exchange for little accumulation of N_2O in the headspace of the culture. This is plausible as we know *nosZ* transcription is down under Cu limited conditions. There are therefore fewer N_2OR proteins to populate when Cu is limited within the cell and in turn, the chance of obtaining holo-protein, is higher. The Δ*nosL* strain did not produce as much N_2O as the Δ*nosZ*, under Cu-limitation. It could be that the residual Cu in the media (<0.5 μM) produces enough active N_2OR that we do not see all the N_2O expected in a Nos^- strain. This sensitivity and the impact on N_2OR Cu centre maturation within each mutant condition will be explored in the next chapter.

The Δ*nosLX* mutant is comprised of a complete *nosL* gene deletion along with the first 5 amino acids of the downstream *nosX* gene, effectively removes the starting methionine residue of NosX. The knock-on effect of this could either be halting the transcription of *nosX*, or, as *nosL* and *nosX* are in the same frame, the lack of the first 5 residues destabilises NosX and it degrades, therefore rendering NosX as non-functional. Phenotype analysis of this mutant (labelled Δ*nosLX* PD2503) generated a replicate of the Δ*nosZ* phenotype, regardless of the total Cu in the media. This result contradicts a previous report of a *nosX* gene mutation in *P. denitrificans*. An antibiotic cassette inserted 469 bp into the *nosX* gene was reported not to affect the ability of the cell to reduce N_2O [85]. A homologue *nirX* was identified in the genome and only when this gene was also interrupted was N_2O emitted from the culture and N_2OR activity diminished, as recorded by methyl viologen assay.

Based on this unexpected finding, a single *nosX* complete deletion strain was generated to understand whether the *nosLX* phenotype was dominated by *nosX.* The growth and N_2O analysis of this strain was an exact replica of the Δ*nosLX* mutant, where ~6 mM N_2O was emitted, and the growth maximum was reduced under both Cu sufficient and limited conditions, like the Δ*nosZ* strain. The common Cu independent phenotype found in both the *nosLX* and *nosX* strains means the loss of *nosX* dominates the former strain. Biological complementation of the single *nosX* mutant was successful under both copper regimes, and both growth and N_2O analysis represented the WT background once restored (Figure 3.9).

N_2OR activity is lost when *nosX* is removed. As the phenotype is independent of Cu, it is likley that NosX carries out one of 3 possible roles: it is crucial for inserting Cu and maturing the Cu centres of N_2OR, or it is involved in N_2OR activity, or it is important for *nosZ* transcription. It was previously shown that *nirX* exists as a functional homologue to *nosX* in *P. denitrificans*, in its absence. Further mutant studies using a Tn5 insertion 31 nucleotides into the total 966 nucleotide sequence downstream of *nosDFY* in *Sinorhizobium meliloti*, what is now recognised as *nosX,* abolished N_2OR activity [90]. This bacterium does not have a *nosX* homologue. Therefore, examples are available where *nosX* is functionally redundant in one denitrifier, and important to the overall N_2OR activity, in another. No attempt was made to look at Cu sensitivity in either experiment though the Nos^- phenotype was observed in *Sinorhizobium meliloti* in the presence of Cu, in keeping with our findings.

NosX is a member of the AbpE protein family which was recently shown to bind flavin adenine dinucleotide, as illustrated by a crystal structure of *Salmonella enterica* ApbE [91]. Their function was later described as a flavinyl transfer-ase. The AbpE from *Vibrio cholera* was shown to mature NqrC post-translationally by covalently attaching a flavin mononucleotide (FMN) to a threonine residue in NqrC [92]. NosX is not commonly conserved across the clades; it is primarily only located within α-proteobacteria NGC's and those of some β-proteobacteria. Work on one of these homologues from the γ-proteobacterium *Pseudomonas stutzeri* (which does not have a *nosX* gene in the NGC) identified the AbpE family member as a flavin protein which can mature the regulatory protein NosR by attaching a FMN to the periplasmic facing side of NosR, which contains the conserved threonine/FMN binding motif found in NqrC [78]. A potential role for NosX in the indirect activation, and not the maturation, of N_2OR, via NosR is therefore likely.

If NosX is involved in the maturation of NosR then a Nos^- phenotype would be expected from a Δ*nosR* strain. Based on the finding of Sullivan et al., this is the case; a PDΔ*nosR* strain presents a phenotype independent of the Cu in the cell [28]. The properties of purified N_2OR from these mutants will be explored in the next chapter.

CHAPTER 4

Studies of the copper centres in N_2OR purified from Δ*nosL* and Δ*nosX* mutants of *P. denitrificans*

4.1 Introduction

In this chapter, N_2OR purified from two mutant strains of *P. denitrificans* (Δ*nosL* and Δ*nosX*) is examined following on from the previous work described in chapter 3 which showed that both genes are important for whole-cell N_2O reduction.

P. denitrificans N_2OR (*Pd*N_2OR) is a homo-dimeric protein, with a monomeric mature mass of 66251.59 Da (as described by LC-MS analysis in Figure 4.3). There are three different types of inorganic ions associated with the protein which were revealed by structural studies. Six Cu atoms and one or two acid-labile sulfur atoms are present per monomer, as well as calcium. Copper and sulfur are required for catalytic function while the role of calcium, located at the inter-subunit sites, is to ensure stable dimer formation[43, 51, 93, 94].

The spectroscopic signature of N_2OR has been well covered in the literature [42, 65] using protein purified in the presence and absence of oxygen, each possessing a discrete difference in one of the Cu centres. In total there are three forms of N_2OR and they are summarised in Figure 4.1.

The behaviour of the Cu_A site, as a bi-nuclear Cu centre, has been characterised in its oxidised and reduced state. Discrepancies in the absorption spectra of N_2OR are most likely to arise due to variations in the Cu_Z centre. The oxidised Cu_A centre is easily detectable by EPR due to its distinctive 7-line hyperfine pattern arising from the mixed valent [$Cu^{1.5+}$:$Cu^{1.5+}$] species of spin S=1/2 [52] due to an unpaired electron being delocalised across the 2 nuclei. This site becomes EPR silent once reduced as both Cu atoms are reduced to the [Cu^{1}:Cu^{1}] state, with the $3_d{}^{10}$ shells filled, such that the centre becomes diamagnetic.

While the Cu_A site remains the same independently of the exposure of the enzyme to oxygen [55, 95], the Cu_Z is purified either as a [4Cu-S] cluster or a [4Cu-2S] cluster in the presence and absence of O_2, respectively. There are five possible oxidation states that the Cu_Z centre can exist in, and these depend on the sulfur content of the cluster (Figure 4.1).

Three forms of the protein have been isolated to date. Purple N_2OR (form I) is purified under anaerobic conditions and has the Cu_Z centre in a resting mixed valent $[2Cu^{II}:2Cu^{I}:2S]^{2+}$ state [60] which is believed to be the physiologically relevant and readily active form of N_2OR. Pink (form II) N_2OR is purified under aerobic conditions and is only active once it has been reduced with methyl viologen for an extended period of time [51, 63]. When the pink form is purified, the majority of the CuZ centre

is found as the $[1Cu^{II}:3Cu^{I}:S]^{3+}$, Cu_Z* species, which is EPR active (S=1/2). Studies tracking the loss of this EPR active Cu_Z centre once it is reduced by methyl viologen, showed as the EPR signal was lost, the $[4CuI:S]^{2+}$ is generated, known as the blue (form III) N2OR, which is active [63]. In fact, reduction of both pink and purple forms to the fully reduced state, produces blue N_2OR[66]. Importantly, the main difference between the purple and pink form of N_2OR is that they contain 2 and 1 sulfur atoms in the Cu_Z centre, respectively.

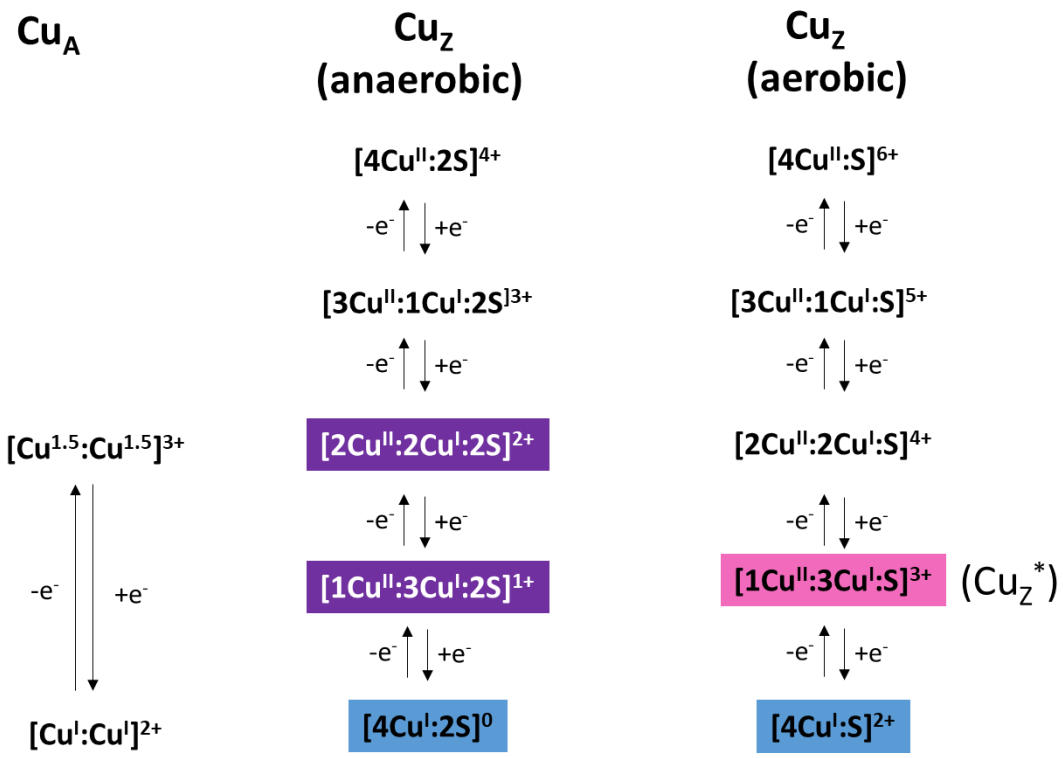

Figure 4.1: Overview of the possible redox-states of the Cu_A centre (left)n and Cu_Z centre, with and without oxygen (right). Colours depict the purple form I of the Cu_Z centre, purified from an anaerobic preparation which, when reduced forms the fully active blue Cu_Z centre. The pink form II is purified from aerobic preparations, this centre is also known as the Cu_Z^*, which once reduced with a strong reductant such as reduced MV, will form the fully reduced, blue, active form III.

The spectroscopic signature of pink form II N_2OR was used to determine whether the Nos^- phenotypes detected in the Δ*nosL* and Δ*nosX* strains are associated with inadequate N_2OR Cu centre maturation, by comparison with pink N_2OR purified from a WT background. The total Cu in each monomer as well as the specific activity of

purified N_2OR, were also determined to highlight any further differences between the samples.

There are two plausible reasons for observing the N_2O-genic phenotypes in Chapter 3. Either the method of activating N_2OR by supplying the electrons for the reduction was lost and therefore it was unable to reduce the substrate, or, the maturation of the Cu centres in N_2OR was affected, rendering them unable carry out the reduction. The aim of this work was to understand if, and how, the Cu centres of N_2OR were affected when the *nosL* or *nosX* gene was removed from the genome.

4.2 Characterisation of N_2OR-Strep-tag II

4.2.1 SDS PAGE analysis of N_2OR-Strep-tag II

pLMB511NosZ was conjugated in to WT PD1222, Δ*nosZ (*PD2303) Δ*nosL (*PD2501) and Δ*nosX (*PD2502) using the method described in 2.1.4 and subsequently overexpressed and purified using the method in 2.3.1 to produce N_2OR-Strep-tag II. The presence of this protein in the eluted fractions was confirmed using a western blot and the sample purity was determined using SDS/PAGE analysis, Figure 4.2. Protein concentration was determined using a Bradford Assay with Bradford reagent from *BioRad* and bovine serum albumin to generate a standard curve.

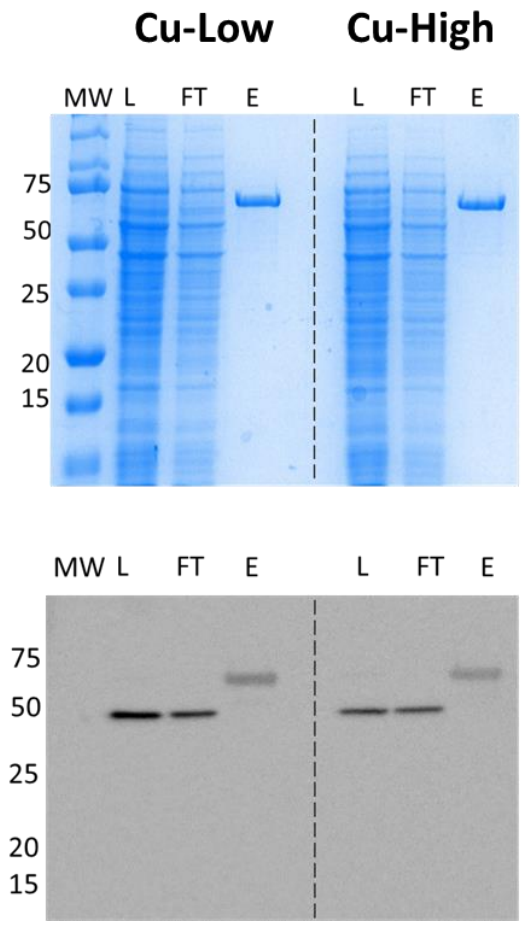

Figure 4.2: SDS-Page analysis (upper panel) and Western blot analysis (lower panel) of the purification of N_2OR-Strep-tag II from a wild type *P. denitrificans* background. The SDS-PAGE gel that was used in the transfer for the western blot was run exactly as the SDS-PAGE above. The load on to the column (L), flow through (FT) and eluent (E) are shown for a purification from Cu-Low (left) and Cu-High (right) cultures. Non-specific binding of the antibody to a beta propeller like domain in the L and FT have been recognised previously, though this could also be the Cu_Z domain which has an estimated mass of ~ 50 kDa [96]. The Strep-tagged N_2OR, with an expected mass ~70 kDa, was pure in the eluted fraction.

4.2.2 LC-MS analysis

To ensure the protein eluting from the affinity column had the correct sequence, the eluted fraction was analysed by LC-MS. The most intense masses were associated with the processed form of N_2OR that is found in the periplasm. Some unprocessed, full length N_2OR was also observed, see Figure 4.3.

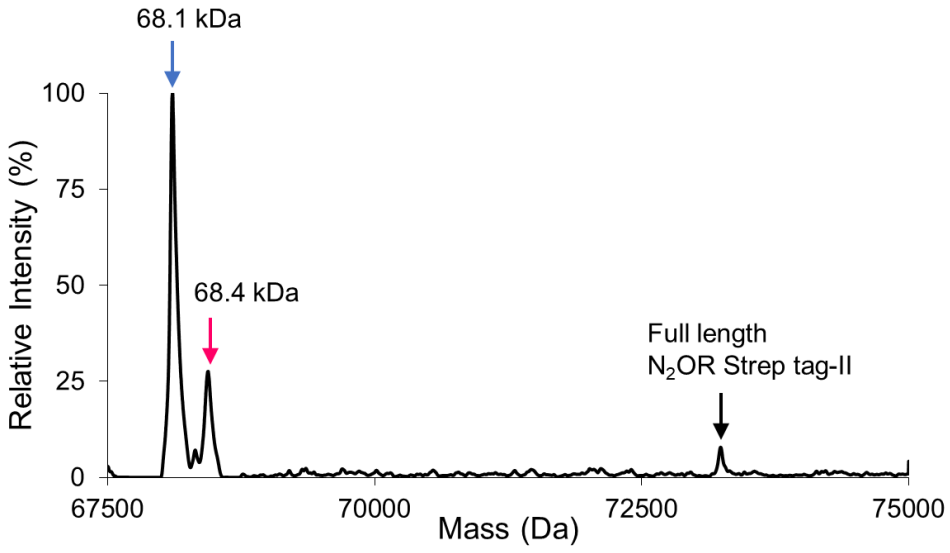

Figure 4.3: LC-MS of 20 µM N_2OR purified from a wild type Cu-high background. Sample was in 2 % (v/v) acetonitrile, 0.1 % (v/v) formic acid.

The amino acid sequence relating to the masses observed in the LC-MS (Figure 4.3) are described in Table 4.1 and the first amino acids in the sequence for each mass, is demonstrated in Figure 4.4.

Table 4.1: Expected and observed masses for N_2OR from LC-MS mass spectroscopy.

Observed Mass (Da)	Expected Mass (Da)	Amino acid cleavage site/ Start site
73239.43	73240.1	Full length protein
68440.8	68435.91	SG/AALAA
68106.71	68105.51	A/ASGDGSV
Not observed	66251.59	Mature *Pd*N_2OR - A/ASGDGSV, minus the EK cut site and Strep-tag II

MESKQEKGLSRRALLGATAGGAAVAGAFGGRLALGPAALGLGTAGVATVAGSG/AALA/ASGDGSVAPGQLDDYYGFWS
SGQSGEMRILGIPSMRELMRVPVFNRCSATGWGQTNESLRIHERTMSERTKKFLAANGKRIHDNGDLHHVHMSFTEGKYD
GRFLFMNDKANTRVARVRCDVMKCDAILEIPNAKGIHGLRPQKWPRSNYVFCNGEDETPLVNDGTNMEDVANYVNVFTA
VDADKWEVAWQVLVSGNLDNCDADYEGKWAFSTSYNSEKGMTLPEMTAAEMDHIVVFNIAEIEKAIAAGDYQELNGVKV
VDGRKEASSLFTRYIPIANNPHGCNMAPDKKHLCVAGKLSPTVTVLDVTRFDAVFYENADPRSAVVAEPELGLGPLHTAFDG
RGNAYTSLFLDSQVVKWNIEDAIRAYAGEKVDPIKDKLDVHYQPGHLKTVMGETLDATNDWLVCLSKFSKDRFLNVGPLKP
ENDQLIDISGDKMVLVHDGPTFAEPHDAIAVHPSILSDIKSVWDRNDPMWAETRAQAEADGVDIDNWTEEVIRDGNKVRV
YMSSVAPSFSIESFTVKEGDEVTVIVTNLDEIDDLTHGFTMGNYGVAMEIGPQMTSSVTFVAANPGVYWYYCQWFCHALH
MEMRGRMLVEPKEA**PG**DDDDK**WSHPQEFK**

Figure 4.4: The amino acid sequence generated from the pLMB511-*pNosZ*-Strep-tag II plasmid. The sequence shown includes the C-terminal enterokinase (EK) cut site (green) and Strep-tag II (red), along with the 2 cleavage sites that result in the dominant masses observed in the mass spectrum.

The observed mass for full length, unprocessed, Strep-tagged N_2OR was 73239.43 Da. It was expected that full-length protein would be present as the purification was carried out on whole cells and therefore unprocessed cytoplasmic N_2OR, not yet exported to the periplasm, was likely to be present. The masses that remain on the LC-MS spectrum are the mature protein that has been processed through the TAT pathway and cleaved at the N-terminus in the periplasm, as shown in the Table 4.1. Thus, the LC-MS data confirm that the purified protein is mostly processed, periplasmically located N_2OR. The final theoretical mature mass of the monomer, without the C-terminal enterokinase cut site and Strep-tag II was 66251.59 Da.

4.3 Spectroscopic characterisation of N_2OR Strep-tag II purified from wild type and mutant backgrounds

N_2OR was purified and examined from four backgrounds, these were: the wild type strain, a Δ*nosZ* null mutant and the two Δ*nosL* and Δ*nosX* strains produced. Once purified, N_2OR was buffer exchanged back into 50 mM HEPES, 100 mM NaCl, pH 7.2 and subsequently oxidised with potassium ferricyanide and reduced with sodium dithionite under anaerobic conditions (5 mg/ml stocks of each were prepared and 1 µl was titrated into 1 ml protein in a 1 cm pathlength, reduced volume, quartz cuvette, until the spectrum no longer changed). From here on Strep-tagged N_2OR purified from each background is referred to according to the background from which it was isolated, for example, N_2OR from the Δ*nosZ* strain is referred to as Δ*nosZ*N_2OR.

4.3.1 UV-visible absorbance spectroscopy

The oxidised spectrum of N_2OR delivers information on the two Cu centres, together. In reducing the sample, the Cu_Z spectrum can be observed, alone, while a difference spectrum obtained by subtracting the reduced spectrum from the oxidised, provides detail on the Cu_A site.

Oxidised spectra were normalised to $\varepsilon_{580\ nm}$ 5000 M^{-1} cm^{-1} per monomer as described by Rasmussen et al [65]. Pink, oxidised N_2OR had features at 480, 540 and 640 nm in agreement with the previous literature on N_2OR from *P. pantotrophus* (*Pp*N_2OR) [65], *Pseudomonas stutzeri* (*Ps*N_2OR) [38], *Pseudomonas natuica* (*Pn*N_2OR) [97], *Achromobacter cycloclastes* (*Ac*N_2OR) [98] and *Marinobacter hydrocarbonoclasticus* (*Mh*N_2OR) [42]. Features in the absorption spectrum at these wavelengths arise from S^{2-} to Cu(II) charge transfer bands and additional optical bands due to interactions between the Cu(I) and Cu(II) ions of the centres [65]. The values plotted on the absorbance spectra indicate the extent to which the Cu centre are populated in the sample. It is clear to see in Fig. 4.5A that the extinction coefficients of bands in the region of 450-550 nm, which correspond to the Cu_A centre, are equal in intensity, in all samples. The 640 nm Cu_Z centre band in the pink form of N_2OR is dominated by what we assume is the Cu_Z^*, the pink form II, purified with only a single acid-labile sulfur atom. Changes in the intensity of this 640 nm peak depend on which recombinant N_2OR is being analysed. The lower absorption coefficient for the WTN_2OR and Δ*nosL*N_2OR, indicate a deficiency of Cu_Z cluster and therefore a lower occupation of this centre [65].

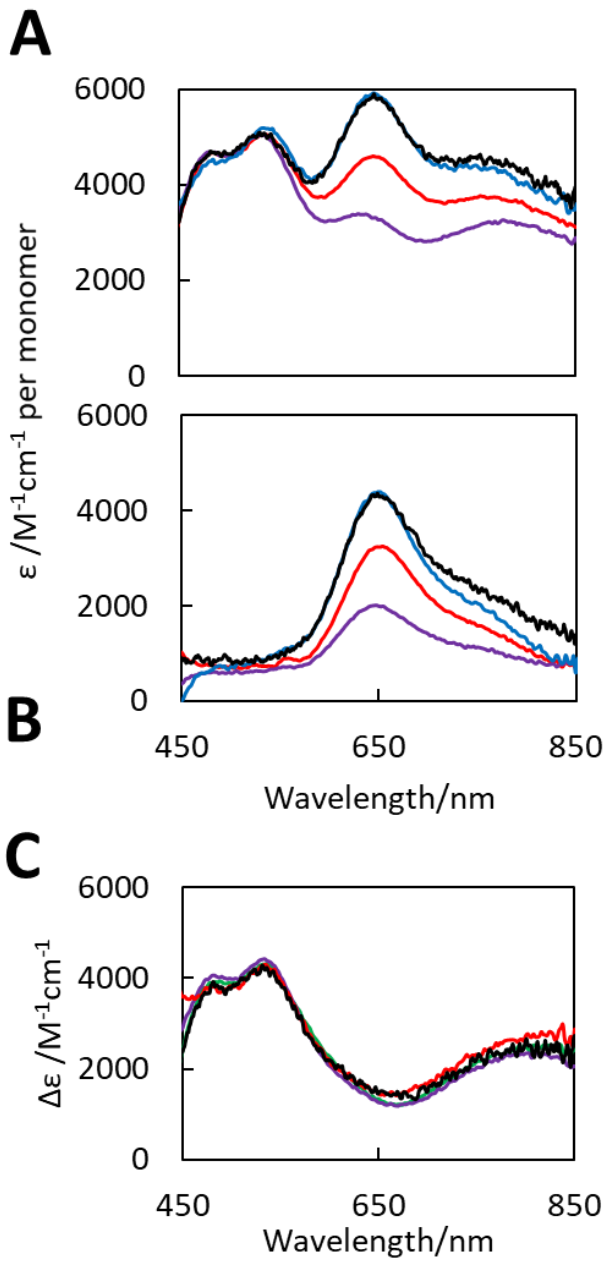

Figure 4.5: UV-Visible absorbance characterisation of N_2OR-Strep-tag II purified from Cu-High media from the mutant backgrounds. WT (●), Δ*nosL* PD2501 (●), Δ*nosX* PD2502 (●) and Δ*nosZ* PD2303 (●) were in 20 mM HEPES, 150 mM NaCl, pH 7.2. Spectra of ferricyanide-oxidised **(A)**, sodium dithionite-reduced **(B)**. The ferricyanide-oxidised minus dithionite-reduced difference spectrum is also shown **(C)**.

Reduction of the N_2OR samples in Figure 4.5A with dithionite, reduces the Cu_A centre to a [Cu^1:Cu^1] diamagnetic species which is colourless and thus does not contribute in the visible region. Thus in Figure 4.5B, bands at 480, 540 and 900 nm are removed

to leave a Cu_Z^* signature with a peak at 640 nm in agreement with the literature for pink N_2OR [65].

The apparent variability amongst the Cu_Z centres in the samples, looking at the oxidised spectra, was confirmed in the reduced spectra, Figure 4.5B. This is further demonstrated in Figure 4.5C where an overlay of the difference spectra, representing the Cu_A site, shows identical spectra for all four samples.

4.3.2 Circular dichroism spectroscopy

CD spectra were also recorded for each N_2OR sample, see Figure 4.6. The CD spectrum demonstrates there are asymmetric cupric centres at both sites [40].

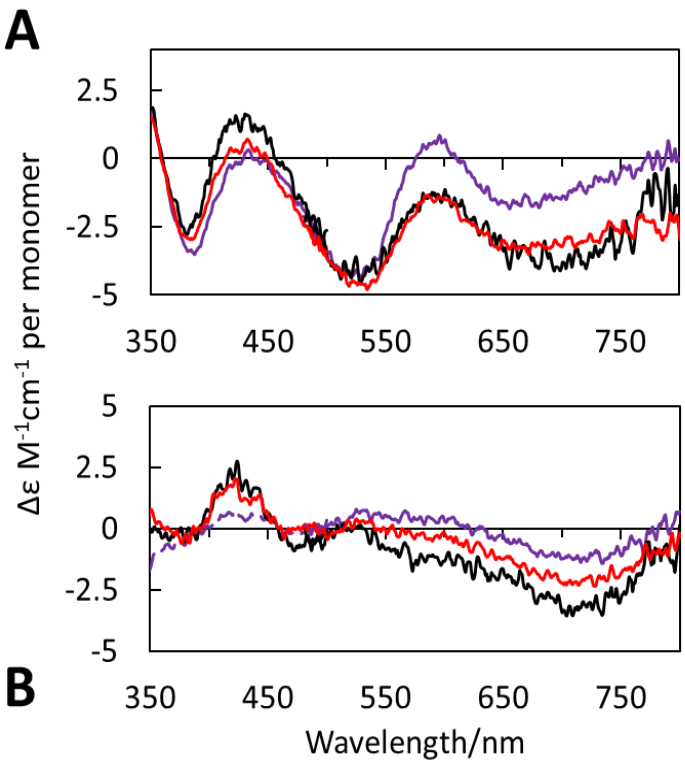

Figure 4.6: CD spectra of ferricyanide-oxidised N_2OR-Strep-tag II (A), dithionite-reduced (B). Samples purified from copper high media from a WT PD1222 background (●), Δ*nosL* PD2501 (●) and Δ*nosX* PD2502 (●), recorded in 20 mM HEPES, 150 mM NaCl, pH 7.2.

Positive features were identified in the oxidised spectrum at 430 and 590 nm and negative features at 380, 475 and more broadly at 650 nm. Some absorbance bands partially overlay with the bands observed in the CD spectra.

Less intense bands in the Δ*nosL*N_2OR spectrum compared to those of WTN_2OR were observed. CD spectra of the oxidised WTN_2OR and Δ*nosX*N_2OR were of similar intensity. After the samples were reduced by dithionite the remaining features were at 440 and 720 nm, which match those of PpN_2OR from Rasmussen et al [65] and, again, weaker features were observed for the Δ*nosL*N_2OR protein, indicating a lower population of Cu_Z centres.

4.3.3 Determining the specific activity of N_2OR-Strep-tag II

The activity of pink N_2OR was determined by following the oxidation of methyl viologen (MV) in an assay as described in section 2.9. Reduced MV is blue and absorbs at 600 nm. As electrons are donated to N_2OR to reduce N_2O, the resulting oxidised MV is colourless and so the absorbance decrease at 600 nm over time is monitored. The decrease in absorbance can be used to calculate the specific activity of the N_2OR enzyme, via the MV extinction coefficient, $\varepsilon_{600\,nm}$ = 13600 $M^{-1}cm^{-1}$ [82].

As the N_2OR purifications were carried out aerobically, the enzyme contained a Cu_Z* centre. This pink form of N_2OR is only active once it is incubated in an excess of dithionite-reduced methyl viologen to generate the blue form III, [$4Cu^1$] site [63, 97]. At specific time points, a sample of the protein was taken and used in the final activity assay. Over time the activity increased nearly 6-fold, from 29.65μmol $N_2O{\cdot}min^{-1}{\cdot}mg^{-1}$ after 5 minutes of incubation, to 171.13 μmol $N_2O{\cdot}\ min^{-1}{\cdot}\ mg^{-1}$ after 150 mins for the protein purified from a WT background, see Figure 4.7 and Table 4.2. There are only limited data for the activity of N_2OR using this activation method in the literature. Preincubated *Ps. Nautica* 617 N_2OR had a turnover of 23 ± 14 μmol $N_2O{\cdot}\ min^{-1}{\cdot}\ mg^{-1}$ of $enzyme^{-1}$ after 5 minutes of incubation and in a different study the same protein had an activity of ~20 ± 8 μM $N_2O\ min^{-1}mg^{-1}$ after 5 minutes incubation and 275 μM $N_2O\ min^{-1}mg^{-1}$ after 120 minutes [63]. The protein concentration used in the assay affects the specific activity of the protein as explained by Prudencio et al [97] where an exponential decrease was observed as the stock concentration was diluted from 10 to 1 mg/mL and left for 3 hours to yield approximately 1 μmol $N_2O{\cdot}\ min^{-1}{\cdot}\ mg^{-1}$ [97]. The activity for WTN_2OR and Δ*nosX*N_2OR were almost identical after a 120 min incubation with the reduced methyl viologen. The initial activity of both proteins after 5 minutes of incubation was comparable to the literature with ~ 30 μM $N_2O\ min^{-1}mg^{-1}$ activity, see Figure 4.7 and Table 4.2 The lower maximum activity in the WTN_2OR and Δ*nosX*N_2OR, of ~170 μM $N_2O\ min^{-1}mg^{-1}$ after a 150 min pre-incubation, could be

due to the protein dilution effects mentioned. In comparison, the Δ*nosL*N_2OR had a much lower maximum activity with 95.7 μM N_2O $min^{-1}mg^{-1}$ detected after a 150 min incubation.

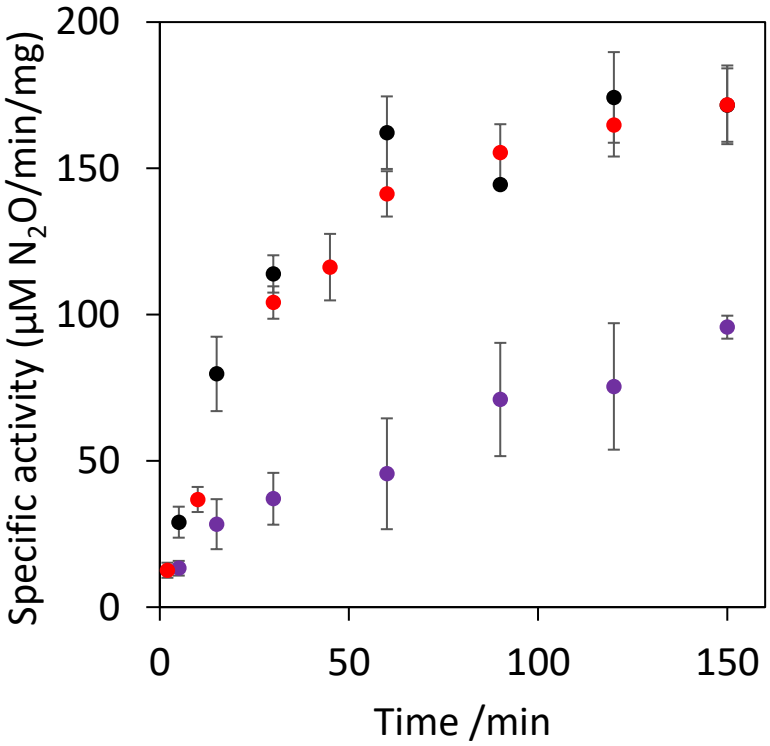

Figure 4.7: **Specific activity of Strep-tag II N_2OR purified from WT PD1222 (●), Δ*nosL* PD2501 (●), and Δ*nosX* PD2502 (●).** Protein was pre-incubated in 500- fold excess of reduced methyl viologen for the time shown before aliquots were used in the final assay to determine the rates of specific N_2O reducing activity by N_2OR-Strep-tag II. Reactions were carried out in triplicate and the SE is plotted.

Copper analysis using the colorimetric assay based on the Cu chelator BCS, revealed that WTN_2OR and Δ*nosX*N_2OR were fully occupied with Cu as expected from the spectroscopic data. The slightly lower level of Cu in the WTN_2OR is likely to be due to a deficiency at the Cu_Z site (see Figure 4.5.). Nevertheless, the N_2O reducing activity of the protein was as high as that of the Δ*nosX*N_2OR. Two controls were included in this experiment. One was N_2OR purified from a *nosZ*⁻ background, such that the strain contained only plasmid encoded N_2OR (*p*N_2OR) and no chromosomal encoded N_2OR (*g*N_2OR). The other was the WT background which provides information for a strain that contains both chromosomal encoded untagged N_2OR, and plasmid encoded tagged N_2OR. The total Cu content per monomer of each N_2OR is shown in Table 4.2.

Table 4.2: Summary of some characteristics of Strep-tagged N_2OR from *P. denitrificans* strains PD1222, PD2501 and PD2502. Total copper per monomer was determined using a BCS Cu assay. N_2O reducing activity was determined using a reduced methyl viologen assay. Protein was pre-incubated with a 500-fold excess of reduced methyl viologen and used in the final assay after 5 min and 150 min incubation. All reactions were carried out in triplicate and StDev is shown.

Strain	Cu ions / monomer	Specific activity after 5 mins (μmol $N_2O \cdot min^{-1} \cdot mg^{-1}$)	Specific activity after 150 mins (μmol $N_2O \cdot min^{-1} \cdot mg^{-1}$)
WTPD1222::pLMB511-*nosZ*Strep-tag II	**5.6 ± 0.11**	**29.24 ± 0.74**	**171.13 ± 13**
Δ*nosL*PD2501::pLMB511-*nosZ*Strep-tag II	**4.1 ± 0.43**	**11.31± 0.85**	**95.7 ± 3.9**
Δ*nosX*PD2502::pLMB511-*nosZ*Strep-tag II	**6.38 ± 0.19**	**30.07 ± 0.53**	**171.63 ± 12**
Δ*nosZ*PD2303::pLMB511-*nosZ*Strep-tag II	**5.92 ± 0.56**	**-**	**196.2 ± 9**

In the WT background, both pN_2OR and gN_2OR forms of N_2OR compete for Cu. The cell is limited to 13 μM Cu in the medium so it is reasonable to expect that sharing this Cu between at least double the number of N_2OR proteins compared to the *nosZ*- mutant, would result in fewer occupied Strep-tagged N_2OR proteins overall. This was the case when Strep-tagged N_2OR was purified from a WT background: its Cu_A site was fully assembled, but its Cu_Z site was not. For the activity assay, however, this did not impact on the activity after incubation with reducing MV.

The competition for Cu is still relevant in the *nosL*- background and the sample can be compared to the WTN_2OR. Four Cu atoms per monomer of Δ*nosL*N_2OR were detected, on average. The Cu_A site was clearly fully occupied based on spectroscopic data in 4.6C, which leaves 2 Cu atoms per monomer remaining, on average, for the Cu_Z site. If these 2 remaining Cu atoms per monomer were to be used to form a complete 4Cu

core of the Cu_Z cluster, then half the total protein would be holoprotein and half would have no Cu_Z centre. If the holoprotein is fully active in the Δ*nosL*N_2OR then half the maximum activity of the WTN_2OR would be expected. The overall maximum activity of Δ*nosL*N_2OR is ~55% of the WTN_2OR.

4.4 Spectroscopic characterisation of N_2OR-Strep-tag II purified from a Cu-Low background

Copper limited conditions were difficult to replicate during experiments as *P. denitrificans* appeared to be able to scavenge Cu from the surface of the bottles in which the cultures are grown, suggesting that it has a high affinity for copper. There was variability in the results obtained under Cu low conditions depending on the history of the bottles used for growth and particularly the number of Cu- low experiments that had been carried out on the bottles beforehand. For the purposes of achieving a satisfactory level of consistency, all the following experiments employed bottles which had previously been used for growth under Cu-high conditions. Any Cu found by *P. denitrificans* was not presented in the trace elements added to the minimal media, but from the bottles themselves.

As mentioned before there were two controls in this experiment, the WTN_2OR which represents the *p*N_2OR and *g*N_2OR and the Δ*nosZ*N_2OR presenting the *p*N_2OR only. All spectra in Figure 4.8 are normalised to the concentration of the protein determined by a Bradford assay. The oxidised, reduced and difference spectra are shown in Figure 4.8.

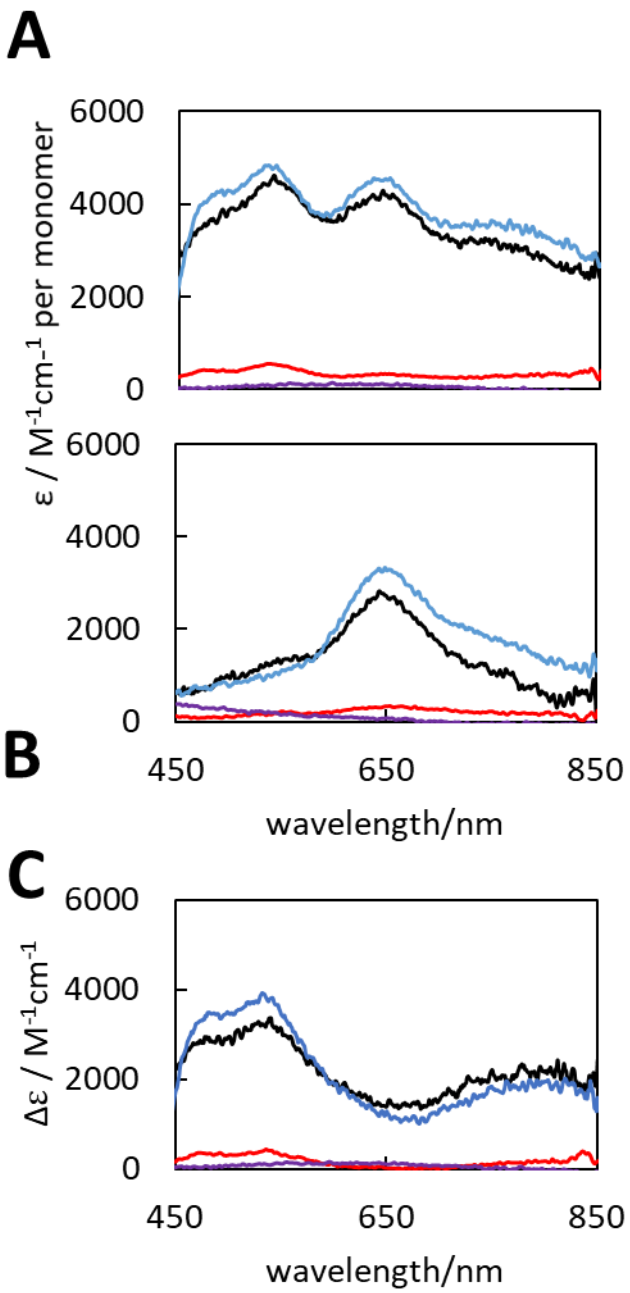

Figure 4.8: UV-Visible absorbance characterisation of N_2OR-Strep-tag II purified from Cu-low media from the specific backgrounds. WT (●), Δ*nosL* PD2501 (●), Δ*nosX* PD2502 (●) and Δ*nosZ* PD2303 (●) in 20 mM HEPES, 150 mM NaCl, pH 7.2. Spectra of ferricyanide-oxidised **(A)**, sodium dithionite reduced **(B)**. The ferricyanide-oxidised minus dithionite-reduced difference spectrum is also shown **(C)**.

Both the WTN_2OR and Δ*nosL*N_2OR had a very little absorbance in the visible region in Figure 4.8. The Δ*nosL*N_2OR absorbance spectrum does not display Cu_Z or Cu_A bands and the BCS assay yielded no detectable Cu. In the WTN_2OR there are weak signs of both centres and once reduced, a 640 nm peak indicative of the Cu_z centre appears though it is 6 times less intense than the signal from the sample in Figure 4.8B and only 0.3 Cu ions/monomer were detected in the sample. If the 0.3 Cu atoms on average were added up to generate a fraction of holoprotein then only 5% of the total protein would be fully occupied and 95 % apo. No N_2O reducing activity was detected in the MV assay.

In contrast, Δ*nosZ*N_2OR and Δ*nosX*N_2OR were almost identical by spectroscopic analysis and both proteins were purified with partially occupied Cu sites. Under Cu-limited conditions the majority of trace Cu obtained by *P. denitrificans* appears to have been utilised to populate the *p*N_2OR in the Δ*nosX*N_2OR, whereas in the WT background very little Cu was directed to *p*N_2OR. Absorption spectral forms observed for the pink Δ*nosZ*N_2OR and Δ*nosX*N_2OR were similar to those under Cu-high, though the intensity was reduced. Evidence for the reduced occupancy of the Cu centres in the absorbance spectra was supported by the Cu detection assay. The Δ*nosX*N_2OR sample contained 4 Cu atoms per monomer, and the Δ*nosZ*N_2OR contained slightly more with 4.8 Cu atoms per monomer. This result unambiguously demonstrates that the function of *nosX* is not associated with Cu centre biogenesis of N_2OR.

Table 4.3: Summary of some characteristics of N_2OR-Strep-II tag from *P. denitrificans* strains PD1222, PD2501 and PD2502 and PD2303. Total copper per monomer was determined using a BCS Cu assay.

Strain	Cu ions/monomer
WTPD1222::pLMB511-*nosZ*Strep-tag II	**0.3 ± 0.57**
Δ*nosL*PD2501::pLMB511- *nosZ*Strep-tag II	**0**
Δ*nosX*PD2502::pLMB511- *nosZ*Strep-tag II	**4.18 ± 0.17**
Δ*nosZ*PD2303::pLMB511- *nosZ*Strep-tag II	**4.8± 0.42**

4.5 Exploration of a Δ*nosZL* mutant background

In section 4.3, a competition between *g*N_2OR and *p*N_2OR for Cu in the cell was observed in the WTN_2OR sample. Holo-N_2OR contains 6 Cu ions per monomer; however, WTN_2OR contained on average 5.6 Cu/monomer compared to Δ*nosZ*N_2OR with 5.92 Cu/monomer. Where WTN_2OR was previously deficient in Cu, it was reflected in the reduced absorbance spectrum 640 nm band, which was less intense and was therefore associated with fewer Cu_Z centres. The same was observed in *ΔnosL*N_2OR where around only a half of the total protein sample was occupied with a Cu_Z centre. We ask whether the Δ*nosL* strain was also subject to this competition between the plasmid and chromosomal version of N_2OR. To remove this uncertainty a double Δ*nosZL* mutant was produced and N_2OR-Strep-tag II was purified from this background and analysed (Δ*nosZL*N_2OR). This will demonstrate the true nature of Δ*nosL*N_2OR in section 4.3 and determine whether it was due to the loss of *nosL*, or simply an artefact of the competition mentioned.

A Δ*nosL* knock out mutant was produced in a Δ*nosZ* background using the same method described in section 3.2. Essentially, the PD2303 (Δ*nosZ*) strain was used during the initial conjugation along with the Δ*nosL*pK18*mobsacB* suicide vector. From there the method remained the same, the mutant was confirmed using PCR to amplify the *nosL* region, and N_2O sampling of the culture headspace confirmed N_2O was being produced even under Cu-sufficient conditions (data not shown).

The Strep-tagged N_2OR was first purified from a Cu-sufficient Δ*nosZL* background and compared to the Δ*nosZ*N_2OR protein, Figure 4.9. Our previous data showed the Δ*nosL*N_2OR contained on average, ~4 Cu/monomer, and had the spectroscopic feature of fewer Cu_Z centres.

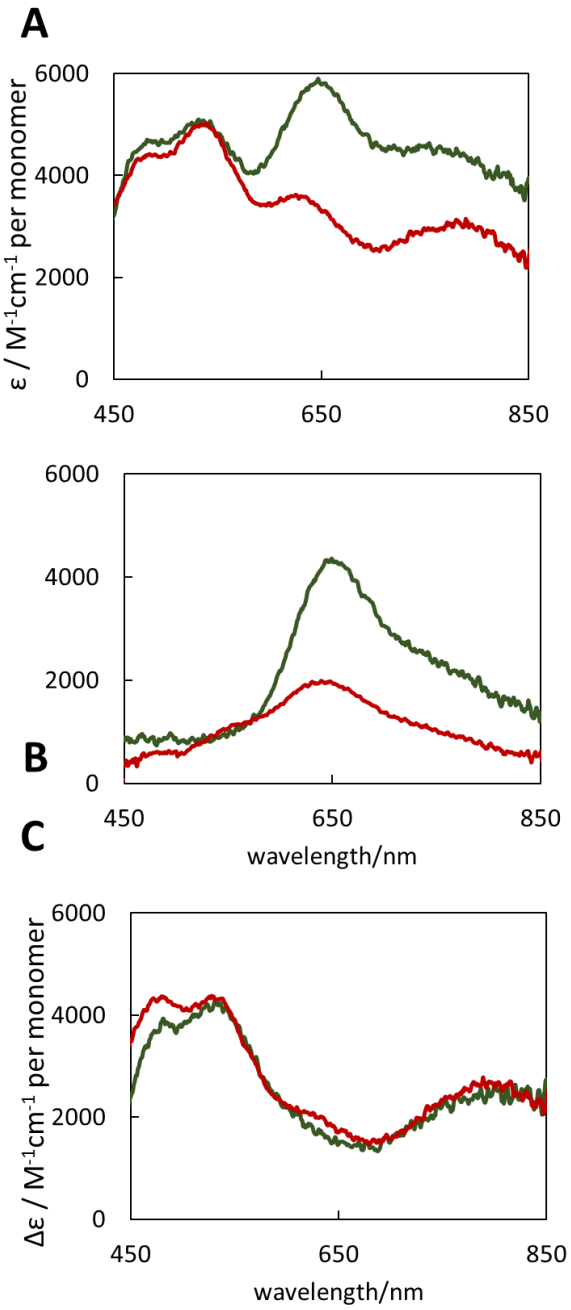

Figure 4.9: UV-Visible absorbance characterisation of Strep-tag II N_2OR purified from Cu-high media from Δ*nosZ* PD2303 (◆) and Δ*nosZL* PD2505 (◆) in 20 mM HEPES, 150 mM NaCl, pH 7.2. Spectra of ferricyanide-oxidised **(A)**, sodium dithionite reduced **(B)**. The ferricyanide-oxidised minus dithionite-reduced difference spectrum is also shown **(C)**.

The oxidised UV-visible absorption spectrum of pink Δ*nosZL*N_2OR was similar to that of Δ*nosL*N_2OR in that the Cu_A bands indicate full occupancy while the Cu_Z bands indicate a significant population deficiency (Figure 4.9A). The reduced spectrum of Δ*nosZL*N_2OR (Figure 4.9B, burgundy) displayed a lower absorption coefficient at 640

nm which once again demonstrates fewer Cu_Z centres among the total protein while the difference spectrum demonstrates the Cu_A site was fully occupied (Figure 4.9C), in agreement with the results in section 4.3. A BCS assay also confirmed ~3.4 Cu ions/monomer and the MV assay revealed a lower activity than for the Δ*nosZ*N_2OR, both results are in agreement with fewer occupied Cu_Z sites. By ensuring that *p*N_2OR was the only N_2OR present, we could corroborate that the nature of the Cu loading in Δ*nosL*N_2OR, in particular the Cu_Z centre, under Cu sufficient conditions, was due to the loss of the *nosL* gene and not related to competition between *g*N_2OR and *p*N_2OR for Cu.

Δ*nosZL*N_2OR was also purified from a Cu limited background and the results were once again in keeping with the data for Δ*nosL*N_2OR under Cu-limitation: Δ*nosL*N_2OR was found in an apo form, while Δ*nosZ*N_2OR contained 4.8 Cu ions per monomer, as described in Table 4.4.

Table 4.4: Overview of Strep-tagged N_2OR purified from the Δ*nosZ* (PD2303) and Δ*nosZL* (PD2505) strain under Cu sufficient and limited conditions.

Strain	Cu condition	Cu atoms/monomer	Specific activity – 5 min (μmol $N_2O \cdot min^{-1} \cdot mg^{-1}$)	Specific activity – 150 min (μmol $N_2O \cdot min^{-1} \cdot mg^{-1}$)
Δ*nosZ*PD2303::pLMB511-*nosZ*Strep-tag II	**+**	5.92 ± 0.56	-	196.2 ± 9
Δ*nosZL*PD2505:pLMB511 - *nosZ*Strep-tag II	**+**	3.43 ± 0.26	6.23 ± 2.61	93.6 ± 0.8
Δ*nosZ*PD2303::pLMB511-*nosZ*Strep-tag II	**-**	4.8 ± 0.42	**-**	**-**
Δ*nosZL*PD2505::pLMB511- *nosZ*Strep-tag II	**-**	0 ± 0	**-**	**-**

P. denitrificans are able to scavenge Cu from the Duran bottle and the water used to make the media in order to populate N_2OR under Cu-limitation. Interestingly however, Δ*nosL*N_2OR is entirely apo once again and deficient in a Cu_A and Cu_Z site. This was unexpected because it is known that the simple addition of Cu can reconstitute the Cu_A site *in vitro*, and we know from the Δ*nosZ*N_2OR that some Cu remains even when we attempt to remove it all and is directed to N_2OR [99]. This result is interesting because it suggests NosL is needed to mature the Cu_Z site when Cu is present, but more importantly, when Cu is limited, NosL plays a vital role in providing Cu to either Cu centre in N_2OR.

The activity of Δ*nosZ*N_2OR was high, as expected for a fully occupied N_2OR, with a rate of 196 μmol $N_2O \cdot min^{-1} \cdot mg^{-1}$. The activity of Δ*nosZL*N_2OR was lower at 93.6 μmol $N_2O \cdot min^{-1} \cdot mg^{-1}$ which is representative of fewer sites for substrate turnover (Cu_Z centres). The figure for Δ*nosZL*N_2OR activity was as high as that of Δ*nosL*N_2OR in section 4.3, even though the latter contained on average 1 more Cu per monomer. A change in temperature between experiments is likely to be the reason for the higher activity. The set of methyl viologen assays recorded for Δ*nosZL*N_2OR was in excess of ~28 ˚C, closer to the temperature at which *P. denitrificans* are cultured and therefore potentially optimum for N_2OR activity, instead of the 22 ˚C which was used in 4.3.

4.6 Discussion

Analysis of Strep-tag II-N_2OR purified from the Δ*nosL* and Δ*nosX* mutants, and wild type and Δ*nosZ* control strains, revealed the *nosL* gene encodes a protein that has a function in the maturation of N_2OR and that *nosX* does not.

Data reported in Chapter 3 showed that the Nos^- phenotype was only recognised in the Δ*nosL* strain during Cu limitation. Unexpectedly, then, there was a difference between purified Δ*nosL*N_2OR under Cu-high conditions compared to WTN_2OR. Characterisation of the oxidised and reduced Δ*nosL*N_2OR protein by UV-visible absorbance spectroscopy revealed the Cu_A site was fully occupied, but only a partial number of the Cu_Z sites were populated, leaving a proportion of the total Δ*nosL*N_2OR with no Cu_Z site. A comparison between Δ*nosL*N_2OR and all other strains analysed revealed they all had an identical oxidised-reduced difference spectrum and therefore all contained fully occupied Cu_A centres (Figure 4.5). The reduced spectra were evaluated in Fig. 4.5B and revealed a striking difference in the intensity of the Cu_z band. The lower absorption coefficient at 640 nm in the Δ*nosL*N_2OR reduced

spectrum was an indication that there were fewer occupied Cu_Z sites. Both absorbance and CD spectroscopy indicated fewer fully occupied Δ*nosL*N_2OR proteins with a Cu_Z centre, and this was further supported using a BCS assay to determine total Cu in the protein and a catalytic activity assay. This result was a surprise as it was assumed the protein was fully assembled based on the knowledge that no phenotype was found under Cu-sufficient condition. However, the fewer Cu_Z centres present among the total N_2OR was apparently enough for the cells to turn over N_2O without observing an accumulation of the gas.

The loss of the *nosL* gene under Cu limitation was clear cut in terms of why a phenotype was observed under such conditions: Δ*nosL*N_2OR from this background was purified as an apo protein and therefore no active site was present to carry out the reduction of N_2OR. While the Δ*nosZ*N_2OR was partially populated with both centres and the WTN_2OR also, though to a lesser extent, the remaining Cu among the media and bottles was unable to be incorporated into Δ*nosL*N_2OR. The Cu_A centre can be reconstituted using Cu alone [99] and consequently it was expected that some assembled CuA centre would be observed if indeed the function of *nosL* is to directly and specifically mature the Cu_Z centre. However, under Cu limitation, Δ*nosL*N_2OR showed no sign of either Cu centre. It is important to note that under Cu limited conditions the level of *nosZ* transcription is down in comparison to Cu sufficient and this is due to transcriptional regulation by the *nosCR* genes [28]. For that reason, the majority of the N_2OR in the cell would have been *p*N_2OR and therefore the *p*N_2OR would have competed with a small amount of *g*N_2OR for the residual Cu. In the Δ*nosZ* strain, the complete absence of *g*N_2OR would have resulted in more Cu being directed to the Δ*nosZ*N_2OR (plasmid only), and for this reason, we see the discrepancy in the Cu centre occupations. The fact Δ*nosL*N_2OR was entirely apo means that, especially under Cu limitation, *nosL* is involved in directing Cu in general to N_2OR for the population of both centres.

The partial occupancy of Δ*nosL*N_2OR under Cu-high and complete lack of Cu under Cu-low conditions in Δ*nosL*N_2OR were further verified using a Δ*nosZL* strain, where the only source of N_2OR in the Δ*nosL* background was the plasmid version, thus removing any potential for competition for Cu between N_2OR proteins in the cell. The Δ*nosZL*N_2OR purified under Cu-high conditions showed once again the number of Cu_Z centres matured when the *nosL* gene has been removed, is lower, and therefore activity and Cu ions detected was lower in Δ*nosZL*N_2OR. The same apo state of Δ*nosZL*N_2OR from Cu limited growth conditions was once again observed. This work

demonstrates a role for *nosL* directly in the maturation and incorporation of Cu into the unique Cu_Z cluster of N_2OR under Cu sufficient conditions. The sensitivity of the Δ*nosL* strain during Cu limitation, resulted in the complete failure to incorporate Cu into N_2OR, suggesting NosL plays a broader role in sensing and directing Cu in the periplasm. The fact the Δ*nosZ*N_2OR was purified with Cu incorporated into its Cu centres, when all assembly factors are present in the cell is consistent with this. The observation of an apo form of the protein under Cu limitation supports the phenotype analysis in chapter 3, where the Nos^- phenotype was only observed under the same condition in the Δ*nosL* strain. This work has also provided an explanation for why we do not see a phenotype under Cu sufficient conditions in the Δ*nosL* strain, as N_2OR, allbeit with only a fraction of Cu_z centres occupied, is catalytically active and can turn over N_2O at a rate which does not see N_2O accumulate in the headspace of the culture. The response to Cu in the *nosL* mutant is clear, and the function of the *nosL* encoded chaperone is investigated further in Chapter 5.

The Δ*nosX* strain in Chapter 3, produced a phenotype under both high and low Cu conditions. The Δ*nosX*N_2OR was fully occupied with Cu when it was purified from a Cu sufficient background, with all 6 Cu ions per monomer present and as active as the WTN_2OR (Figure 4.5). While a comparison to WTN_2OR can be made, the N_2OR that Δ*nosX*N_2OR resembled the most, spectroscopically, was the Δ*nosZ*N_2OR in which there is the only *p*N_2OR. It is puzzling that the *nosX*$^-$ mutant strain produced *p*N_2OR almost identical to that isolated from the *nosZ*$^-$ mutant. There are a few possibilities for why this might be; *p*N_2OR could out-compete the *g*N_2OR for Cu in the *nosX*$^-$ mutant or, these data raise the possibility that *nosZ* transcription is lost in the *nosX*$^-$ mutant. In either case, this experiment has shown that *nosX* is not involved in the maturation of the Cu centers and therefore, likely involved in the *in vivo* catalytic activity of N_2OR, so without *nosX*, N_2O reduction cannot be achieved in the cell.

Δ*nosX*N_2OR did not resemble the WTN_2OR protein in the Cu limited experiment, instead, it was most similar to the Δ*nosZ*N_2OR protein, in that it contained significant amounts of Cu. We have seen competition for Cu in the WT background, and this result perhaps indicates that, in the Δ*nosX* background the Strep-tagged N_2OR is the only N_2OR present in the cell.

There is literature on the properties of N_2OR purified from a double *nosX* and *nirX,* kanamycin insert mutant which exhibited a Nos^- phenotype [85]. N_2OR purified from this double mutant revealed spectroscopic characteristics not of the purple form I N_2OR, but instead, a pink Cu_Z* centre with an absorbance at 634 nm in the oxidised

spectrum [71]. The Cu_Z* centre in the *nosX/nirX* mutant is the same as the centre purified in this work, from the single Δ*nirX*. However, the pink form reported in this work was generated by aerobic purification of Δ*nosX*N_2OR, with *nirX* remaining in the genome. Our result is in agreement with the previous mutant work: N_2OR was matured with Cu_A and Cu_Z centres and was catalytically active once treated with reduced MV. The main difference is that this work describes this finding as a result of a single *nosX* deletion. This work confirms *nosX* is a gene that is highly likely to be involved in sustaining catalytic activation and reduction of specifically, N_2OR, and that *nirX* cannot substitute for *nosX*. The mechanism of activation is most likely indirect, through the maturation of NosR [78]. *Pd*NosX is a putative FAD binding protein and member of the AbpE family of proteins which can flavinylate a target, in this case, the periplasmic domain of NosR [78].

A recent study has been carried out to characterise an AbpE protein from *P. stutzeri* (PsAbpE), a denitrifying bacterium which is missing a *nosX* gene in the *nos* gene cluster. ApbE is a homologue of *nosX* and recombinant expression of the protein in *E. coli* established that it is a monomeric FAD-binding protein [78]. Further to this, studies showed PsAbpE could serve as a flavin donor for NosR maturation *via* covalent flavinylation of a threonine residue [78] .The post-translationally modified, FMN bound NosR is then a putative electron donor to N_2OR. Thus, a NosX-like protein functions indirectly in maintaining the reaction cycle of N_2OR by flavinylating another accessory protein, NosR. There are 3 AbpE type proteins in *P. denitrificans*: NosX, encoded by *pden_4214*, NirX (*pden*_2485) and *pden_3291*, the first two of which are are exported to the periplasm via the Tat pathway, the remaining one is cytoplasmic. An FAD binding ApbE protein has been characterised from *Salmonella enterica* [91]. The residues involved in FAD binding in NosX (Pden_4214) are predicted to be Serine 68, Tyrosine 70, Threonine 174 and Glycine 256, based on sequence similarities with the SeApbE. If these are important for NosX function, then the mutation generated in *Pd*NosX previously, which was an insert 366 bp into the gene, would have missed the conserved serine 68 and tyrosine 70 and NosX may have been able to function, which would account for why a phenotype was not observed in the single mutant.

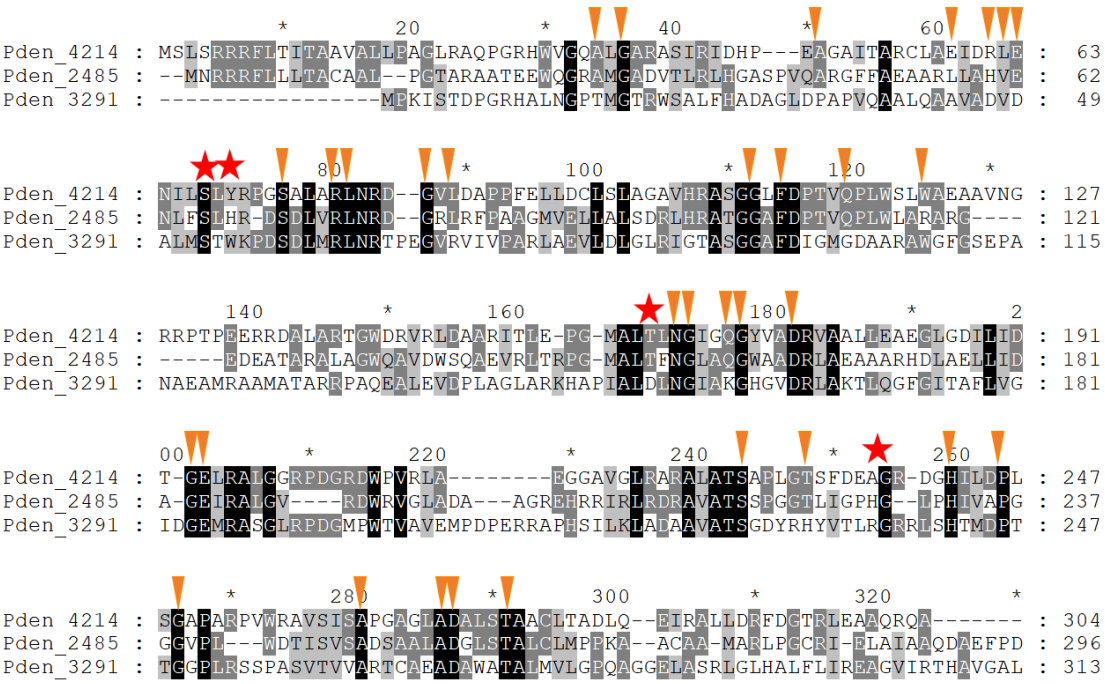

Figure 4.10: Analysis of residues conserved across 3 AbpE protein in *P. denitrificans* (Pden_4214, 2485 and 3291). 100 % conservation (black), 80 % conservation. 100% conservation with other proteobacteria AbpE proteins determined by a Blast search are revealed by orange triangles. Serine 68, Tyrosine 70, Threonine 174 and Glycine 256 are also conserved in *Salmonella enterica* AbpE which binds FAD using these residues (red stars).

The findings in this chapter explain why we observed the phenotypes in Chapter 3. *nosL* is a crucial gene for N_2O reduction under Cu limitation as, without it, both N_2OR Cu centres are unpopulated. Under Cu sufficient conditions the loss of *nosL* results in fewer Cu_Z centres, though enough are assembled for N_2O to be turned over at a rate sufficiently high that it does not accumulate.

Conversely, the loss of *nosX* did not affect the Cu population of N_2OR and, therefore, it is likely, based on sequence homology, that *nosX* functions in the same way as *Ps*AbpE, maturing NosR, so in turn, it can donate electrons to N_2OR and maintain the catalytic reaction cycle.

CHAPTER 5

Copper binding studies of NosL

5.1 Introduction

In Chapter 4, N_2OR was purified from a Δ*nosL* strain of *Paracoccus denitrificans* with fewer assembled Cu_Z centres than N_2OR from a wild type background, even when the strain was grown under Cu replete conditions. Under Cu limited conditions the *nosL* gene was found to be even more crucial for populating the two Cu centres of N_2OR. These findings were verified by comparing Strep-tag II N_2OR purified from a Δ*nosZ* and Δ*nosZL* strain which allowed for a direct comparison of N_2OR from each background without the genomic version of N2OR interfering and competing for Cu. Thus, Chapter 4 gave a clear indication that NosL responds and has a function related to Cu which, in turn, impacted on the Cu centre maturation of N2OR in the periplasm.

The *Paracoccus denitrificans nosL* gene (*pden_4215*) encodes a 20 kDa lipoprotein with the amino acid sequence shown in Figure 5.1, with a mature mass of 18 862 Da. The N-terminal of the protein peptide constitutes the Sec export signal necessary to export NosL in an unfolded state to the periplasm, where further processing of the lipoprotein precursor relocates NosL to the outer membrane using the localisation of lipoproteins (LOL) pathway. Once in the periplasm, the N-terminal cysteine forms a thioether link with the diacylglycerol of the polar head on the lipid bilayer [100]. The signal peptide upstream of the cysteine is cleaved by a lipoprotein signal peptidase and the N-terminal cysteine is further acylated ready for recognition of LolA, a chaperone that transports the lipoprotein to its final destination in the outer membrane and facing in towards the periplasm [100].

The sequence of *P. deniritrificans* NosL along an alignment with other NosL proteins from proteobacteria is shown in Figure 5.22. Early studies in *P. stutzeri* identified the product of an open reading frame downstream of *nosDFY* as a protein with a disulfide isomerase signature and named it NosL (*Ps*NosL) [89]. *Ps*NosL was assigned this role based on a histidine and methionine rich C-terminus and an N-terminal CXXC motif which could potentially reduce disulfide bridges in N_2OR [89]. Contradicting this assessment was the *Sinorhizobium meliloti* (SmNosL) protein in the nitrogen fixing bacterium *Rhizobium meliloti* (now *Sinorhizobium meliloti*), which does not contain the complete CXXC motif, but one single conserved cysteine and the same conserved N-terminal maturation sequence indicative of a lipoprotein [90].

An *in vitro* study using recombinantly expressed NosL from the β-proteobacterium *Achromobacter cycloclastes* identified *Ac*NosL as a Cu binding protein, specifically binding Cu(I) [77]. Based on sequence similarities and EXAFS data, the putative ligands to the Cu atoms are thought to be a mix of both sulfur and N/O based [77].

Further insight into the structure of apo-NosL was obtained using solution NMR, revealing two independent homologous domains with an unusual ββαβ topology [101].

This chapter describes an investigation into the function and role of *P. denitrificans* NosL (*Pd*NosL) using a recombinantly expressed truncated version of the protein. The first 16 amino acids of *Pd*NosL encoding the export signal was removed and replaced with a single methionine residue to yield the final sequence (Figure 5.1). The new sequence ensured a soluble protein was produced and avoided difficulties with export and maturation of the protein in *E. coli.* Copper binding studies were then performed with the purified NosL protein.

5.2 Purification and characterisation of recombinant NosL from *E. coli*

A truncated sequence of NosL (Pden_4215) was expressed in and purified from *E. coli* BL21(DE3). The sequence is shown in Figure 5.1.

MREEVAQDTAPVEMNAQTLGHFCQMNLLEHPGPKAQVHLEGMPGTPLFFSQVRDAIAY
ARMPEQSHPILAIQVNDMGKPGATWDDPGQGNWIDAADAFFVMGSAQAGGMGAPEAV
PFSSREAAETFVAAQGGQVMRLDAIPDEMVLAPEETVPDSSTEADFLNRLRALSQPKEPA
T

Figure 5.1: Primary sequence of truncated NosL produced from the overexpression of the pET-21a*trnosL* plasmid. Expected mass of the protein is 18890.21 Da.

5.2.1 SDS-PAGE Analysis of NosL

After each chromatographic step in the purification of NosL, protein samples were collected and run on a 15% SDS-PAGE to determine the purity of the eluted sample, as shown in Figure 5.2, until the final gel filtration step which yielded pure NosL protein.

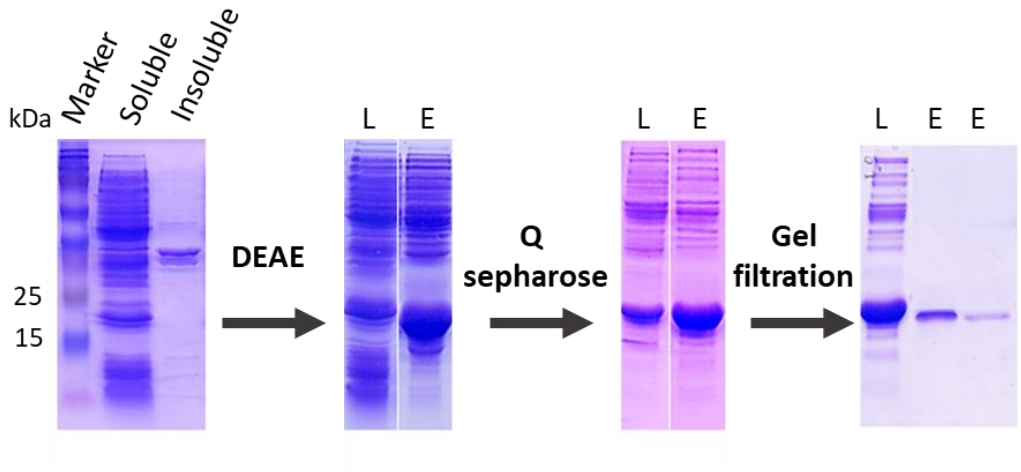

Figure 5.2: SDS-PAGE analysis of each step in the purification of NosL. The soluble and insoluble fractions of the cell lysate were separated and NosL was purified from the soluble fraction until pure NosL remained (18890 kDa). The load (L) and elution (E) from each column is demonstrated above.

5.2.2 LC-MS analysis of NosL

Liquid chromatography mass spectrometry (LC-MS) was carried out using a MicrOTOF- Q III instrument with a Dionex Ultimate 3000 HPLC system. Protein was diluted 10-fold in 2% (v/v) acetonitrile, 0.1% (v/v) formic acid to a final protein concentration of 5 µM and applied to a ProSwift reverse phase RP-1S column (4.6 x 50 mm; Dionex) in 20 µL aliquots. NosL was eluted with an increasing acetonitrile concentration with the column temperature at 25 °C (further details on the LC-MS analysis are included in section 2.11.2). The MS identified a mass of 18889.1 kDa which is in good agreement with the expected mass of 18890 kDa (Figure 5.3). Under the conditions of LC-MS the protein was in the apo state with no covalently attached adducts.

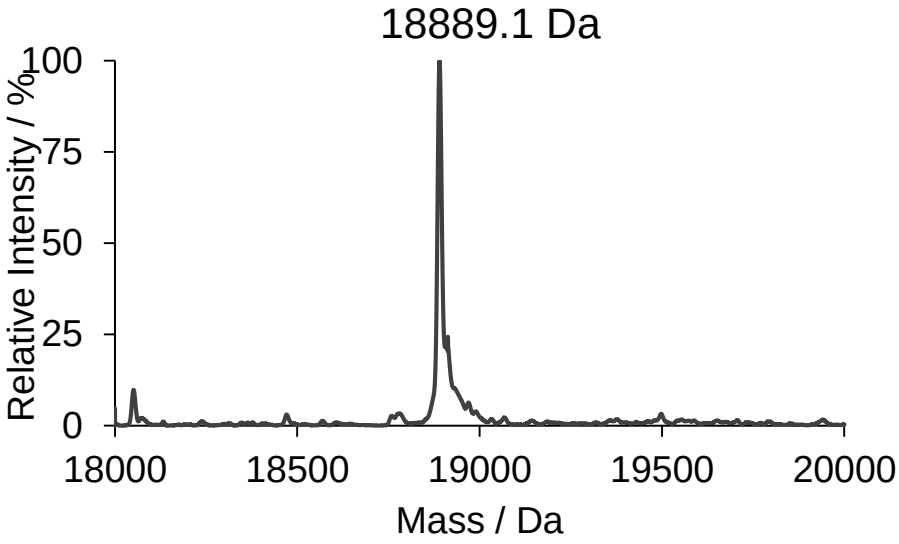

Figure 5.3: Deconvoluted LC-MS spectrum of purified NosL. 5 μM NosL in 2% (v/v) acetonitrile, 0.1% (v/v) formic acid was loaded onto a reverse phase column at 25 ˚C and eluted by increasing acetonitrile concentration.

5.3 Spectroscopic studies of copper(I) binding to NosL

Absorbance spectra were recorded on a Jasco V550 Spectrometer. All titrations unless stated were carried out under anaerobic conditions in a glove box where the total oxygen was kept below 2 ppm. The extinction coefficient of apo-NosL was determined as 11 923 $M^{-1}cm^{-1}$ ± 5.2 using a guanidine hydrochloride assay [81].

Prior to starting the Cu titrations, it was necessary to establish whether the single cysteine remaining in NosL was forming a disulfide bond and therefore a dimer with another NosL protein, or whether it was available to bind Cu. A 5,5'-dithiobis-(2-nitrobenzoic) acid (DTNB, Ellmans reagent) assay was used to determine the free cysteine content of the protein [102]. Stock solutions of DTNB (2 mM, 1 mM, and 250 μM) in 100 mM Tris, pH 8.0 were prepared. To this, a total of 15 μM NosL was added. DTNB contains a highly oxidising disulfide bond which is reduced by free thiols to release a yellow 5'-thio-nitrobenzoic acid (TNB^{2-}) product. The free cysteines reduce DTNB to produce stoichiometric amounts of TNB to free cysteine thiol. The absorbance was monitored at 412 nm and converted to a concentration using the extinction coefficient 13 600 $M^{-1}cm^{-1}$ [102]. The results, shown in Table 5.1, demonstrate that the average number of free cysteines in NosL was 1.03, indicating

no disulfide dimer formation in NosL and that the cysteine was available for reaction. It was, therefore, unnecessary to treat the protein with a reductant to reduce disulfide bonds when preparing for the titration. The protein was used from the freezer and left to equilibrate in a glove box overnight to remove all oxygen from the sample.

Table 5.1: Ellmans reagent (DTNB) assay to determine oxidised, free cysteines. Absorbance at 412 nm was monitored after 10 minutes and the concentration of TNB^{2-} was determine using $\varepsilon_{412\ nm}$ = 13 600 $M^{-1}cm^{-1}$.

[DTNB], mM	$[NosL]_{TOTAL}$, µM	$[TNB^{2-}]$, µM	Free cysteines/NosL
2	15	15.3	1.02
1	15	15.8	1.05
0.25	6	6.18	1.03

5.3.1 UV-visible absorbance spectroscopy

Cu(I)Cl was prepared as described in section 2.8 and titrated into the protein at 0.1 Cu atoms per monomer (Figure 5.4). Cu(I)Cl was also titrated into the same MOPS buffer the protein was in, as a control, and subtracted from the protein-Cu spectrum. At higher Cu concentrations during the titration (typically >1 Cu/protein) there was noticeable precipitation of free Cu as Cu went from high salt (1M in the Cu stock) to low salt in the MOPS/NaCl buffer mix and this absorbed in the region of 240 – 250 nm. Therefore, subtraction of free Cu, in the MOPS/NaCl buffer was necessary to observe the true interaction between the protein and Cu.

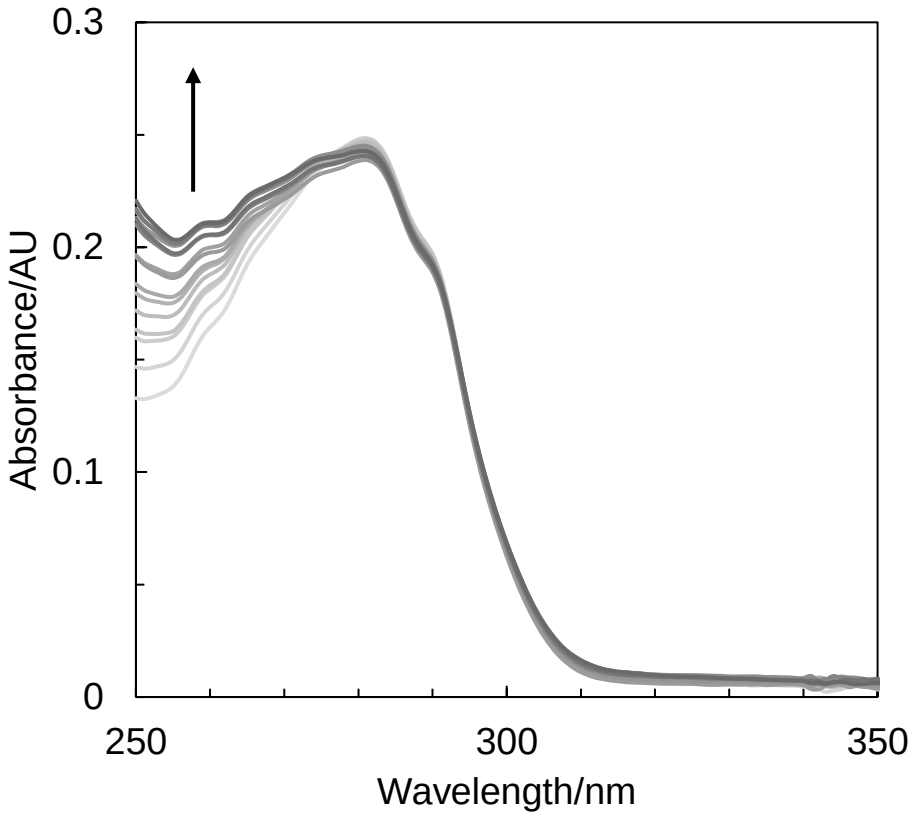

Figure 5.4: Overlaid UV-vis absorbance spectra of NosL following the addition of 0.1 to 2 Cu atoms per protein molecule. 21 μM NosL was in 100 mM MOPS, 100 mM NaCl, pH 7.5 with 2 μl additions of 1 mM Cu(I)Cl from 0.1 to 1 Cu/protein, then 4 μl additions of Cu(I)Cl up to 2 Cu/protein. The starting volume of the titration was 1 ml in a reduced volume, 1 cm pathlength, quartz cuvette.

Absorbance values were corrected using the final concentration of NosL after each addition, giving a plot of change in extinction coefficient as a function of wavelength (Figure 5.5).

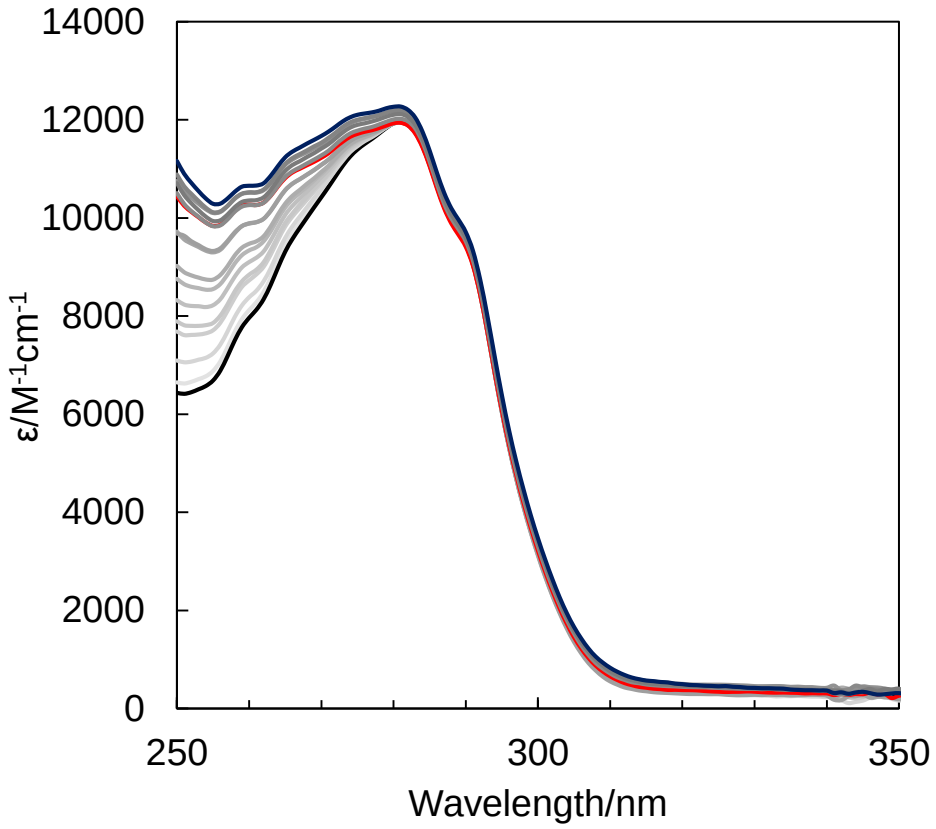

Figure 5.5: Overlaid spectra of apo NosL (black) following the addition of 0.1 to 1 Cu atom equivalent (red) to 2 Cu atoms (blue) per protein molecule. Grey scale indicates the additions in between the set equivalents. UV-vis titration of 21 μM NosL in 100 mM MOPS, 100 mM NaCl, pH 7.5 with 2 μl additions of 1 mM Cu(I)Cl.

An increase in intensity in the UV region of the spectrum is apparent as Cu is titrated into the apoprotein. Plots of the change in extinction coefficient at 266 nm and 260 nm, as a function of the total Cu atoms per monomer of NosL, are shown in Figure 5.6.

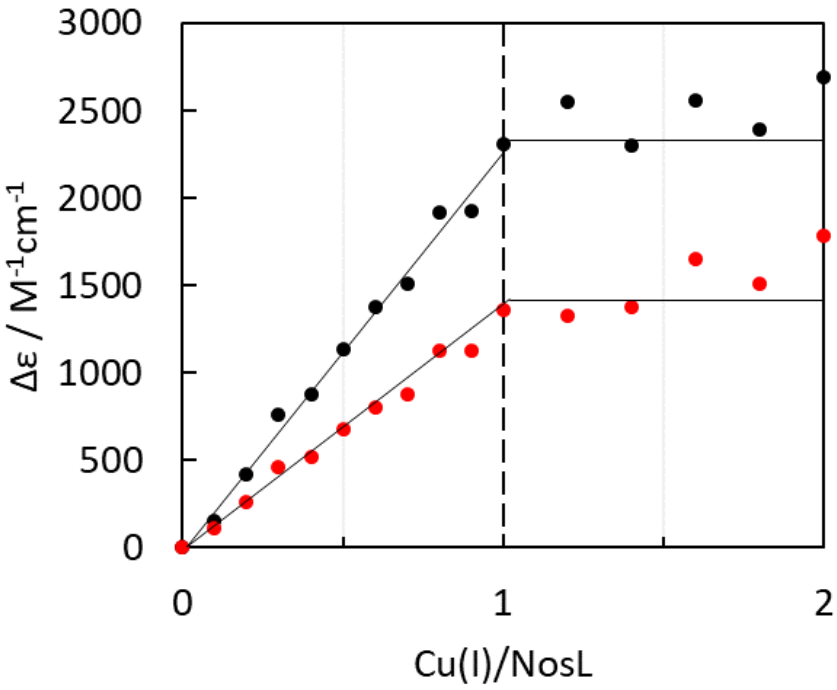

Figure 5.6: Plots of extinction coefficient at 260 nm (black) and 266 nm (red) as a function of Cu(I) ions per NosL protein.

As 0-1 Cu atoms per NosL are titrated in, there is a linear increase for both wavelengths. The change in absorbance plateaus from 1 to 2 Cu atoms, though the 266 nm band continued to rise slightly. The absorbance in this region is indicative of sulfur to Cu, ligand-metal charge transfer transition arising from a cysteine to Cu(I) interaction [103]. As the *d*-orbital shell is full in Cu(I) it behaves as a soft Lewis acid interacting with the *p* orbitals of the sulfur in cysteine, which is a polarizable soft Lewis base.

Figure 5.6 demonstrated that only one Cu(I) atom is bound to NosL. The addition of greater than 1 Cu(I) atom gives rise to somewhat noisy data but with no significant change in intensity. The noisy data are a result of Cu(I) precipitation as the Cu goes from a high salt concentration in the stock, where it is soluble, to be free in the buffer which has a lower concentration of salt. To confirm that NosL binds a single Cu atom, a NosL sample containing 2 Cu atoms per protein was loaded onto a PD10 (GE Healthcare) de-salting column and eluted using the MOPS buffer described. Figure 5.7

clearly shows that passing the 2 Cu loaded protein down a PD10 de-salting column removes the excess Cu and the spectrum of a single Cu(I) bound NosL is retrieved.

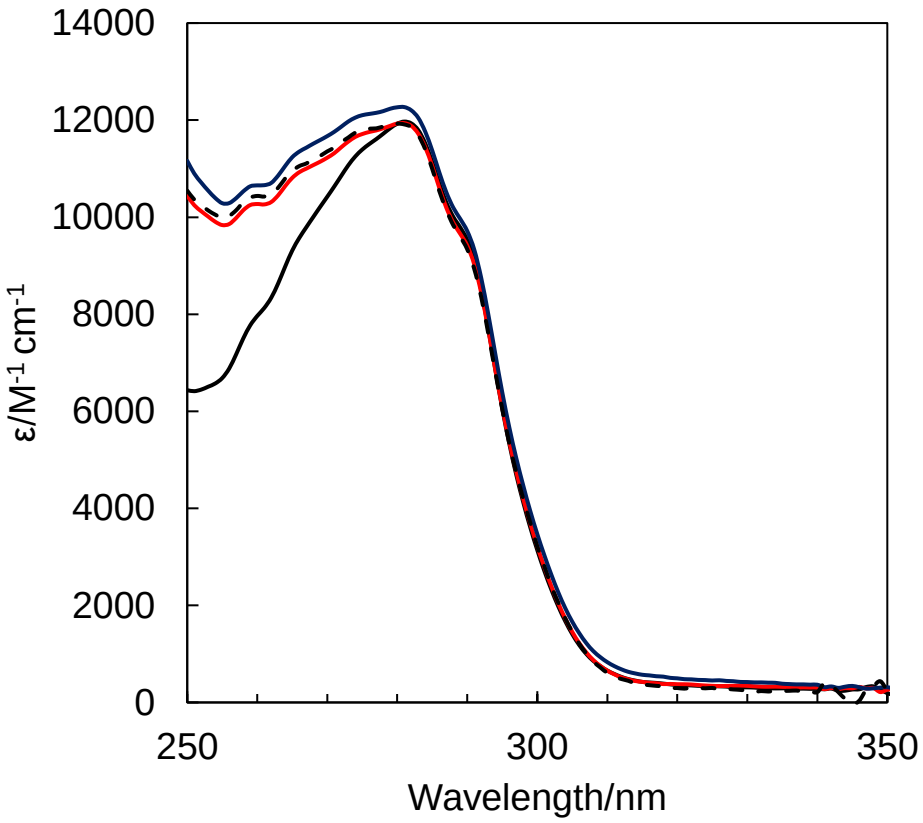

Figure 5.7: Overlaid spectra of 0 (black), 1.0 (red) and 2.0 (blue) Cu(I) ions per protein. The 2 Cu ions per NosL samples was passed down a PD10 column (dashed black) equilibrated with 100 mM MOPS, 100 mM NaCl, pH 7.5.

5.3.2 Circular dichroism spectroscopy

Cu(I) binding to NosL was monitored using circular dichroism spectroscopy, Figure 5.8.

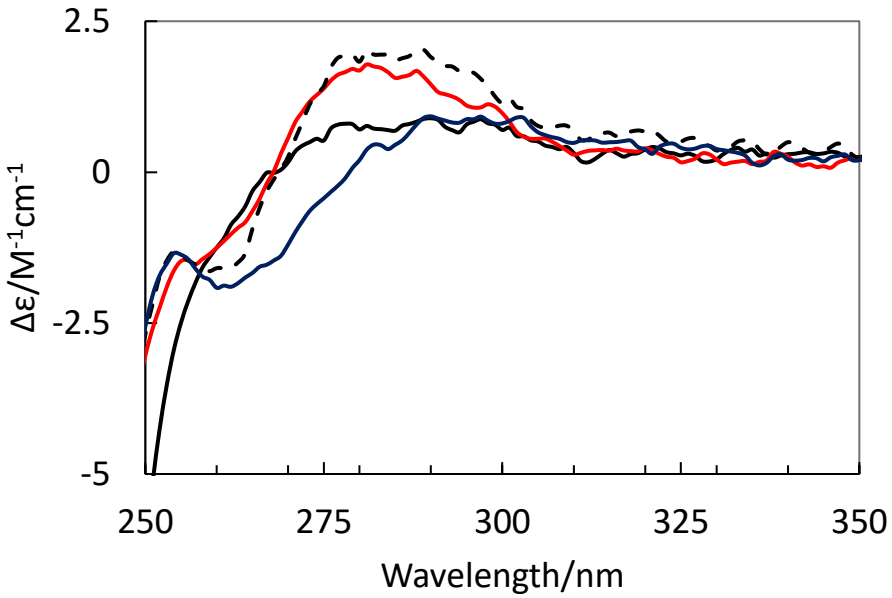

Figure 5.8: Overlaid circular dichroism spectra of apo-NosL (black) and with 1 or 2 (blue) Cu(I) ions per NosL. 14.5 μM NosL in 100 mM MOPS, 100 mM NaCl, pH 7.5 with the addition of 1 and 2 Cu(I) ions per protein. The 2 Cu(I)/protein sample was passed down a PD10 column equilibrated in 100 mM MOPS, 100 mM NaCl, pH 7.5 and the spectrum re-measured (dashed black).

The CD spectrum of apo NosL contained no significant features above 260 nm though there is a negative band below this wavelength. Negative regions in the far UV are indicative of the secondary structure of the protein but is not a focus of this work. As Cu was titrated into the protein, changes to the CD signal arise from Cu binding to a chiral centre, which can absorbance circularly polarized light. As the Cu is titrated, the intensity of the 270 – 300 nm band increases and a local maximum feature at 255 nm appears in the single Cu ion bound form of the protein (Figure 5.8, red). Addition of further Cu ions shifted the 270-300 nm band and the intensity dropped back to that of the apo-protein, yet the feature at 255 nm remained. The spectrum of 1 Cu loaded NosL was obtained once after the 2 Cu loaded NosL was passed down the PD10 column. The data suggest that the additions of >1 Cu per protein lead to an interaction that affects the CD spectrum. However, whatever the nature of this interaction, it is

weak and was readily removed by passage down the PD10 column. Thus, the CD data confirm that a single Cu(I) ion binds tightly to NosL.

5.3.3 Electrospray Ionisation Native Mass Spectrometry

To investigate Cu(I) binding to NosL further, mass spectrometry under non-denaturing conditions was employed. Apo and Cu bound forms of NosL were ionized in an aqueous volatile buffered solution, enabling the protein to remain folded with the cofactor bound. All samples were measured in ammonium acetate, 50 mM pH 7.8 and under anaerobic conditions unless otherwise stated. In the apo-protein sample, the same mass (18890.1 Da) as in the LC-MS, was observed (Figure 5.9). In addition to the main peak at 18890 Da, a number of peaks to higher mass were also observed, ranging from 17 to 22 Da, arising from non-covalent adducts.

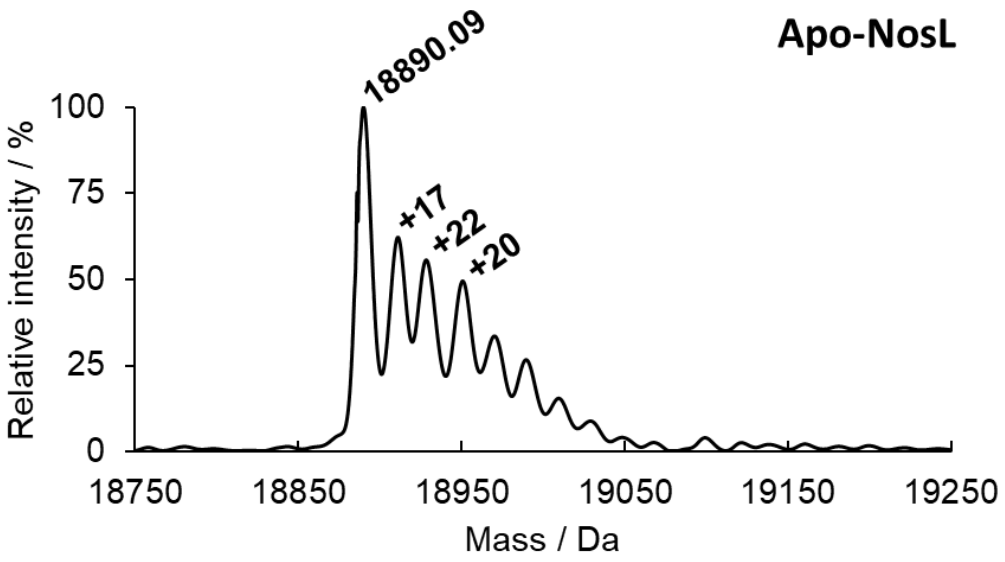

Figure 5.9: Deconvoluted ESI-MS of 20 µM apo-NosL in ammonium acetate, 50 mM, pH 7.8.

These adducts observed are most likely a product of the buffer used and therefore are very likely to be ammonium ions (NH_4^+, +17 Da) or sodium ions (Na^+, observed around +22 Da) which are a component of the NaOH used to generate the correct pH of the buffer. Further attempts were made to remove the adducts observed by altering the buffer concentration and pH (Figures 5.10 and 5.11).

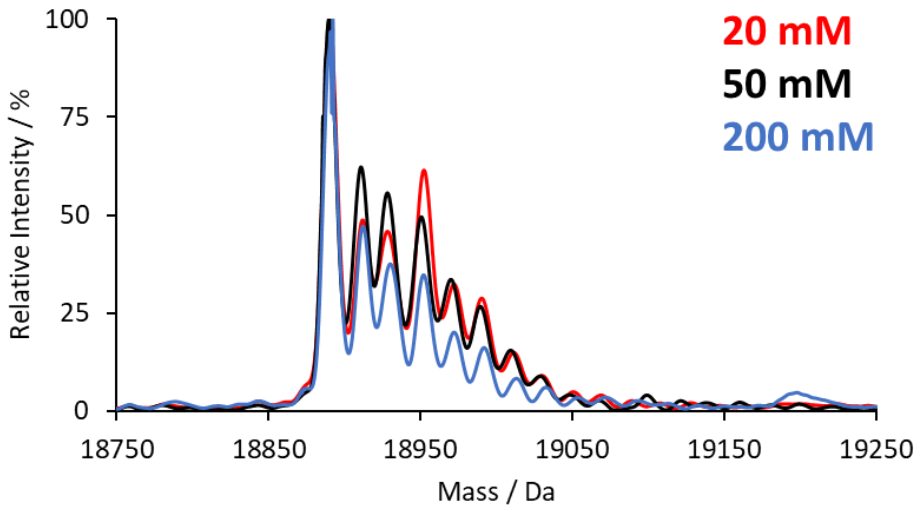

Figure 5.10: Deconvoluted ESI-MS of 20 µM apo-NosL in ammonium acetate, 20 mM pH 7.8, 50 mM, pH 7.8 and 200 mM pH 7.8.

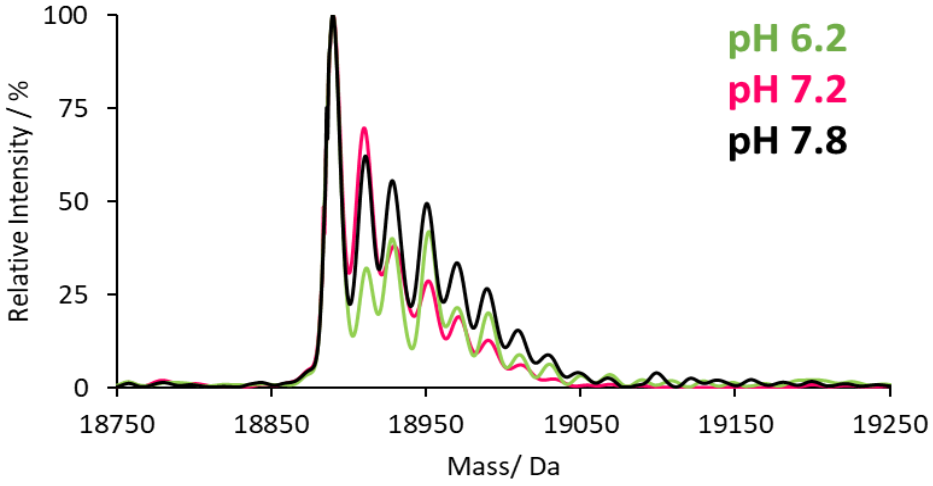

Figure 5.11: Deconvoluted ESI-MS of 20 µM apo-NosL in 50 mM ammonium acetate pH 6.2, pH 7.2 and pH 7.8.

It is imaginable that these small molecules are buried or have a strong attraction to the surface of the protein and therefore remain bound during the measurement. If the protein was not properly buffer exchanged and some MOPS buffer, which the protein was stored in, remained, then MOPS was observed in the native mass spectrum and could only be removed by in source collision induced dissociation (CID); a method used which imparts more energy to the molecule which then collides with neutral molecules, resulting in non-covalent bond breakage. By increasing the in-source CID

gently, the 'sticky' MOPS was removed (results not shown). In source CID was attempted with the NosL sample in Figure 5.9 but was not successful in removing the adducts.

Although altering the buffer concentration resulted in changes in adduct peak intensities, with increased concentration and lower pH giving the most significant reduction in intensity, unfortunately, the adduct peaks could not be removed entirely. Despite the presence of adduct species, the ESI-MS spectrum of Cu-NosL was measured under non-denaturing conditions, see Figure 5.12. Importantly, a shift of the peak envelope to +63 Da was observed, consistent with the binding of one Cu(I) per NosL.

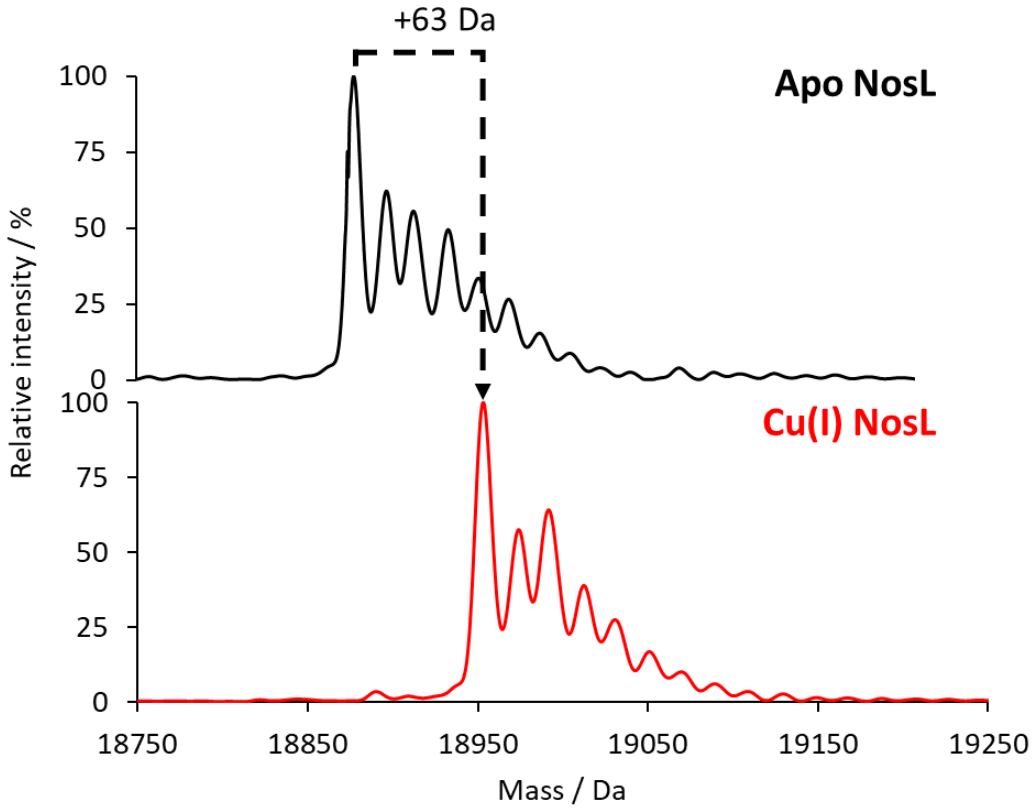

Figure 5.12: Deconvoluted ESI-MS native mass spectrum of 20 µM apo and Cu(I) bound NosL in ammonium acetate, 50 mM, pH 7.8.

5.3.4 Competition assays with BCS

BCS is a nitrogenous bidentate ligand which binds Cu(I) with an extremely high affinity [104] to form a $[CuBCS_2]^{3-}$ complex, which exhibits an absorbance at 483 nm which can be used to quantitate the concentration of copper in a sample. BCS was titrated into Cu(I)-NosL and the absorbance spectrum recorded (Figure 5.13).

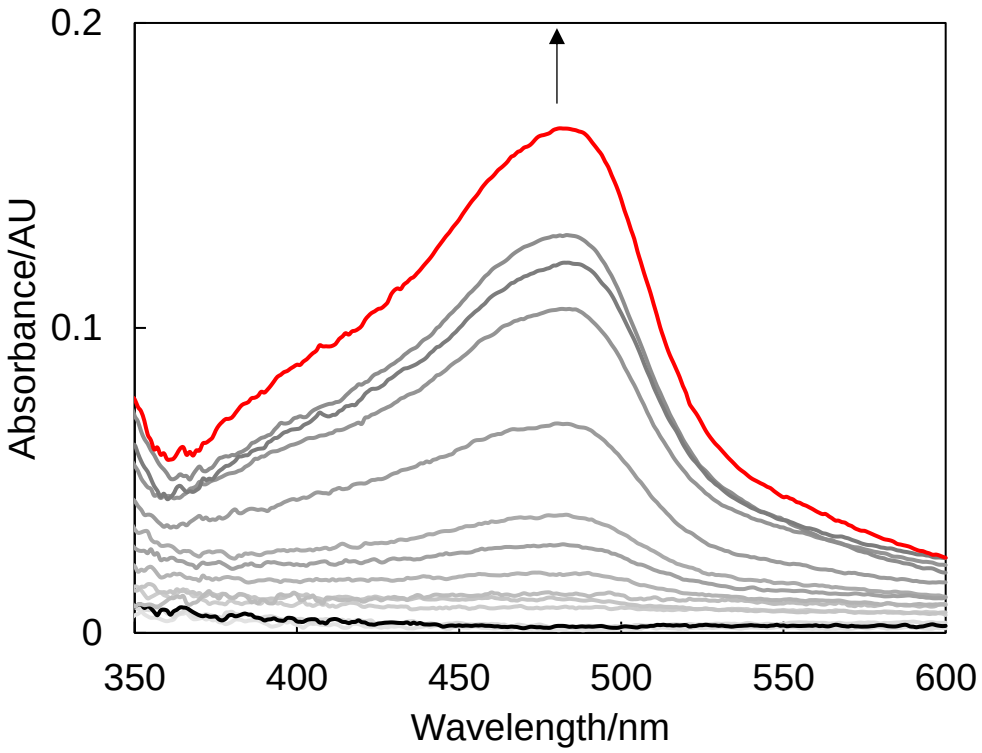

Figure 5.13: Overlaid UV-visible absorbance spectra of Cu(I)NosL with increasing amounts of BCS. Spectra correspond to Cu(I)-NosL with 0 BCS (black) to 50 equivalents of BCS/NosL (red). An extinction coefficient value of ε_{483nm}=13 300 $M^{-1}cm^{-1}$ was used to calculate $[CuBCS_2]^{3-}$ concentration [105]. 16 µM Cu(I)-NosL was in 100 mM MOPS, 100 mM NaCl, pH 7.5 with additions of 1 mM BCS in water.

As BCS is titrated into Cu-NosL the intensity of the band at 484 nm corresponding to $[CuBCS_2]^{3-}$ increases. Figure 5.14 describes the formation of $Cu(BCS)_2$ throughout this titration and the significance of a 50 fold excess of BCS:NosL which is necessary for the complete transfer of Cu to BCS.

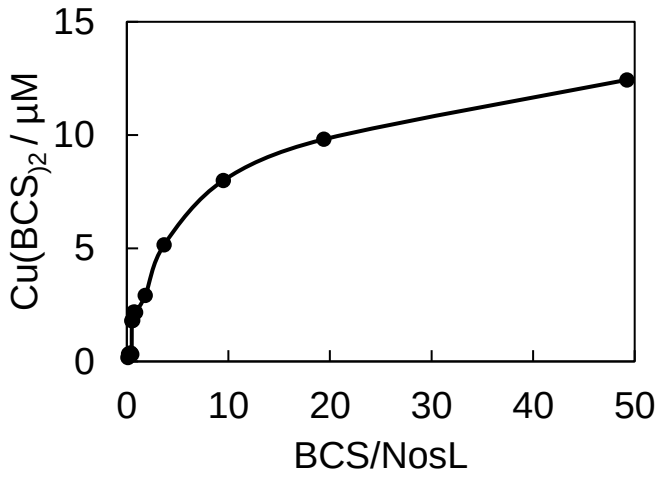

Figure 5.14: Plot of change in $[CuBCS_2]^{3-}$ against the ratio of BCS/NosL. At the start of the titration NosL was at 16 µM and was corrected for dilution effects. After 50 equivalents of BCS to NosL had been added, all Cu had transferred to BCS to form the $[CuBCS_2]^{3-}$ complex.

Initial experiments showed Cu transfer was possible from Cu(I)-NosL to BCS^{2-} but that the reverse was not apparent at the limited range of NosL excess concentrations tested, see Figure 5.15. The data indicate that the affinity of NosL for Cu was less than that of BCS for Cu.

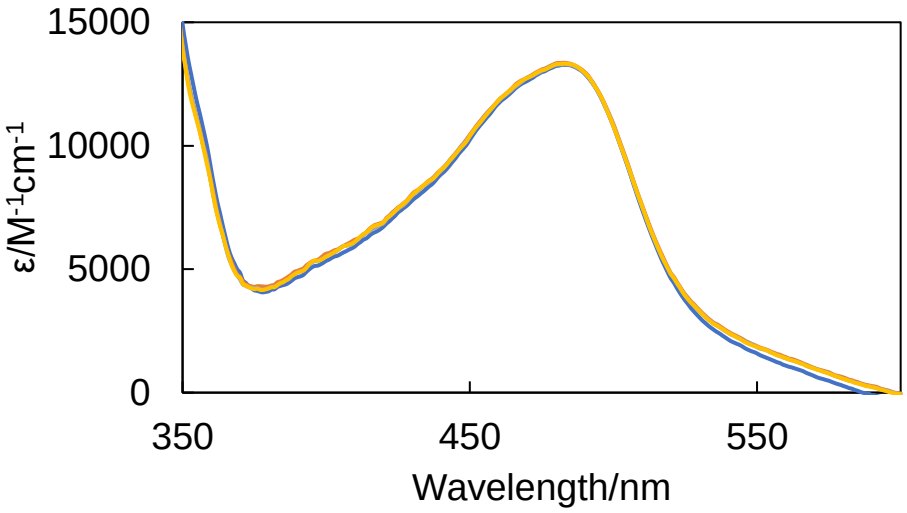

Figure 5.15: Overlaid UV-visible absorbance spectra of $[CuBCS_2]^{3-}$ with increasing amounts of apo-NosL. 7 µM $[CuBCS_2]^{3-}$ (blue), with 7.6 µM apo-NosL (red) 10.8 µM apo-NosL (grey) and 14 µM apo-NosL (yellow). These values are equivalent to 1, 1.5 and 2 NosL: $[CuBCS_2]^{3-}$.

The titration of BCS into Cu-NosL was used to determine a dissociation constant for Cu binding.

Determination of the dissociation constant for copper binding to NosL

The binding of Cu to BCS can be described as follows:

$BCS^{2-} + Cu(I) \rightleftharpoons (BCS)Cu(I)^{-}$ **Equation 5.1**

$(BCS)Cu(I)^{1-} + BCS^{2-} \rightleftharpoons (BCS)_2Cu(I)^{3-}$ **Equation 5.2**

Where the association constants K_1 and K_2 can be described as:

$$K_1 = \frac{[BCSCu(I)^{1-}]}{[BCS^{2-}][Cu(I)]}$$ **Equation 5.3**

$$K_2 = \frac{[BCS_2Cu(I)^{3-}]}{[BCS^{2-}][BCSCu(I)]}$$ **Equation 5.4**

The formation constant (β_2) for this complex is described as:

$$\beta_{2(BCS)} = K_1K_2$$ **Equation 5.5**

This can also be written as:

$$\beta_{2(BCS)} = \frac{[BCSCu(I)][BCS_2Cu(I)^{3-}]}{[BCS^{2-}][Cu(I)][BCSCu(I)][BCS^{2-}]}$$ **Equation 5.6**

This can be simplified to:

$$\beta_{2(BCS)} = \frac{[(BCS)_2Cu(I)^{3-}]}{[BCS^{2-}]^2[Cu(I)]}$$ **Equation 5.7**

It has been demonstrated above that NosL binds one single Cu ion. Therefore, the association for Cu binding to NosL can be written as:

$NosL + Cu(I) \rightleftharpoons Cu(I)\text{-}NosL$ **Equation 5.8**

The association constant for this reaction can then be described as:

$$K = \frac{[NosLCu(I)]}{[NosL][Cu(I)]}$$ **Equation 5.9**

Through the addition of BCS to Cu(I)-NosL, the concentration of free Cu(I) in solution is limited by BCS and the value of K can be determined. The free Cu(I) concentration, $[\mathrm{Cu(I)}]_f$, during this experiment is given by:

$$[Cu(I)]_f = \frac{[(BCS)_2Cu(I)^{3-}]}{\beta_2[BCS^{2-}]^2} \qquad \textbf{Equation 5.10}$$

The concentration of free BCS can be found by subtracting the concentration of Cu bound BCS from the total BCS $[\mathrm{BCS}]_T$:

$$[BCS^{2-}] = [BCS]_T - 2[(BCS)_2Cu(I)^{3-}] \qquad \textbf{Equation 5.11}$$

Substituting the above equation into Equation 5.10 gives:

$$[Cu(I)]_f = \frac{[(BCS)_2Cu(I)^{3-}]}{\beta_2([BCS^{2-}]_T - 2[(BCS)_2Cu(I)^{3-}])^2} \qquad \textbf{Equation 5.12}$$

By substituting the above into the expression for NosL (Equation 5.9). The association constant for NosL can be determined using:

$$K = \frac{[TrNosLCu(I)]}{[TrNosL]} \times \frac{\beta_2([BCS^{2-}]_T - 2[(BCS)_2Cu(I)^{3-}])^2}{[(BCS)_2Cu(I)^{3-}]} \qquad \textbf{Equation 5.13}$$

The ratio of Cu bound NosL to free NosL can be expressed as θ/1- θ, where θ is the fraction of NosL present as the Cu bound form of the protein.

$$\theta = \frac{([\mathrm{Cu}]_T - [Cu(BCS)_2{}^{3-}])}{[P]_T} \qquad \textbf{Equation 5.14}$$

Therefore:

$$K = \frac{\theta}{1-\theta} \times [Cu]_f \qquad \textbf{Equation 5.15}$$

By measuring the formation of $[\mathrm{BCS_2Cu(I)}]^{3-}$ as BCS is titrated in to the reaction mix, a value of K can be determined and from this value the dissociation constant for Cu binding to NosL is obtained ($K_d = 1/K$).

A set of experiments were set up, titrating BCS^{2-} into NosL loaded with a single Cu(I) ion. After each addition the solution was left for 10 minutes to equilibrate and the

concentration of $[CuBCS_2]^{3-}$ was calculated using the extinction coefficient $\varepsilon_{483\ nm}$ = 13 300 $M^{-1}\ cm^{-1}$ [105] and a value for the formation constant of $Cu(BCS_2)^{3-}$, $\beta_{2=}\ 10^{19.8}$ [105].

$[P]_t$ (µM)	15.3	14.8	13.6
$[BSC]_t$ (µM)	160	320	800
$[Cu]_t$ (µM)	15.3	14.8	13.6
$[Cu(BCS)_2{}^{3-}]$ (µM)	7.9	9.8	12.4
Θ, Cu occupancy	0.483	0.33	0.088
Cu_f (10^{-18} M)	6.02	1.72	0.32
K_d (10^{-18} M)	6.44	3.49	3.38
Average K_d (10^{-18}M)	**4.44 ± (1.73)**		

Table 5.2: *K* was calculated using Equation 5.15 and 1/*K* was used to determine the K_d.

The determined K_d value is 4.44 x 10^{-18} M, i.e in the atto molar range.

5.4 Spectroscopic studies of copper(II) binding to NosL

5.4.1 UV-Visible absorbance spectroscopy

The specificity of NosL for Cu(I) was explored through studies of Cu(II) binding. In initial experiments in an anaerobic glove box, the result from Cu(II)Cl_2 dissolved in water when titrated into NosL was unexpected. The resulting UV-visible absorbance closely resembled that obtained in the Cu(I) titrations and no bands in the visible region of the spectrum were observed, which are common for proteins containing Cu(II).

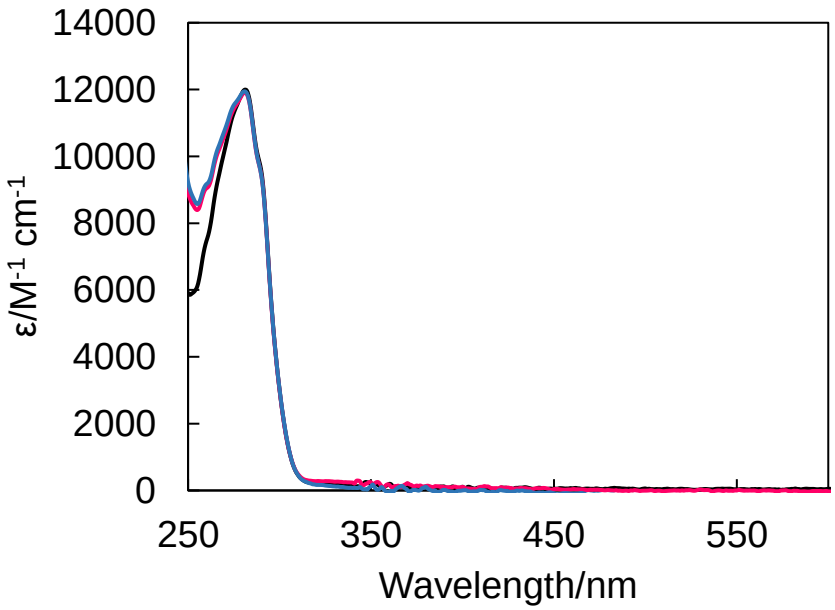

Figure 5.16: Overlaid UV-visible absorbance spectra of NosL following additions of 0 (black), 1 (pink) and 2 (blue) Cu(II) ions per NosL. 16 μM NosL was in 100 mM MOPS, 100 mM NaCl, pH 7.5 with 1.6 μM additions of 1 mM Cu(II)Cl_2. Starting volume was 1 ml, spectra were recorded in a reduced volume, 1 cm pathlength cuvette.

Spectral changes in the UV region were apparent. A closer look at this region and a comparison with the Cu(I)-NosL spectrum is shown in Figure 5.17.

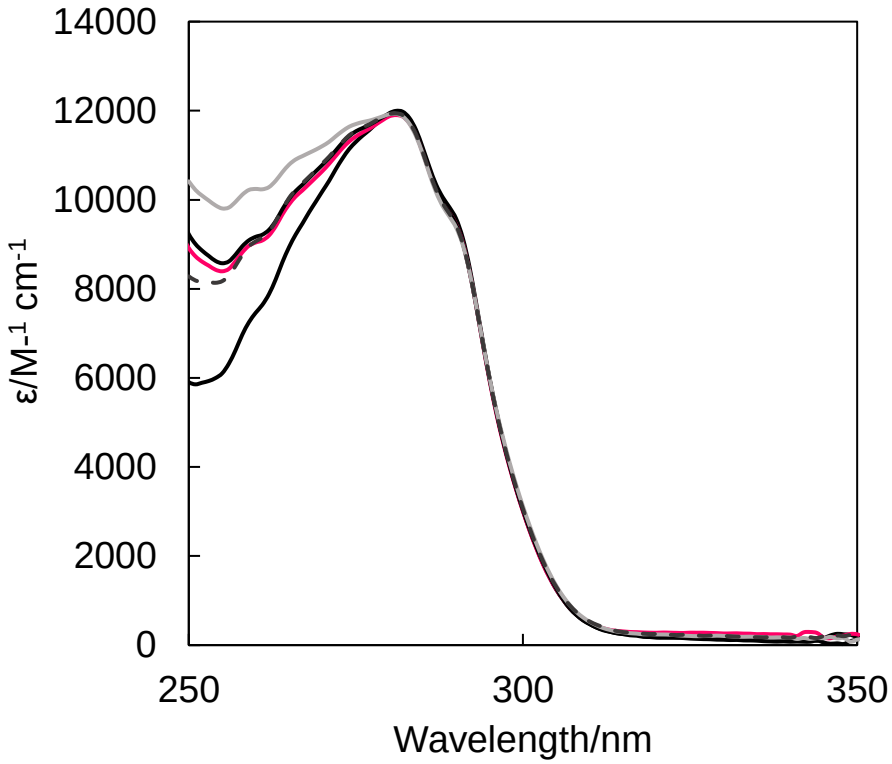

Figure 5.17: Overlaid UV-visible absorbance spectra of NosL following additions of Cu(II)Cl_2 or Cu(I)Cl. Apo-NosL (black), 1 Cu(II) equiv. (pink), 2 Cu(II) equiv. (blue), 0.5 Cu(I) equiv. (black dash) and 1 Cu(I) equiv. (light grey).

Samples were incubated with Cu(II) for 5 mins before recording spectra. After two equivalents of Cu(II) had been added to NosL, the sample had been left for 10 mins. In comparison to the Cu(I)-NosL absorbance spectrum, the spectrum of the Cu(II) loaded sample resembled that of 0.5 Cu(I) ions per NosL, including the peak at 260 nm and the shoulder at 266 nm. This preliminary result suggests that half of the Cu(II) added was reduced to Cu(I) and bound to NosL. EPR was used to investigate whether auto-reduction of Cu(II) to Cu(I) was taking place.

5.4.2 EPR studies on Cu(I) and Cu(II) loaded NosL

NosL loaded with either Cu(I) or Cu(II) was subjected to EPR measurements to identify the nature of the copper bound to NosL. As Cu(I) has a d_{10} electron configuration with filled orbitals, it is therefore diamagnetic, and no signal is detected by EPR. Cu(II), however, has a partially filled *d* orbital and an unpaired electron which is detectable.

The failure to observe the characteristic signal for S=1/2 Cu(II) could result from auto-reduction of Cu(II) to Cu(I), however, it is also possible that Cu(II) in solution could form a dimer that is EPR silent due to magnetic coupling of the two Cu(II) ions. To investigate this possibility a further set of experiments were performed which involved the same Cu loaded samples but also included an equivalent of EDTA. If any Cu (II) was free in solution it would be chelated by the EDTA rather than forming dimers and should result in an EPR signal.

EPR measurements were made using an X-band bruker EMX EPR Spectrometer with an ESR-900 helium flow cryostat. A 98 μM Cu(II) with EDTA standard was used to estimate Cu(II) concentrations by comparing the signal intensity of the protein sample with the standard. These experiments and calculations were carried out by Dr Dimitri Svistunenko, School of Biological Sciences, University of Essex.

Absorbance spectra of the Cu loaded NosL samples sent for EPR analysis are shown in Figure 5.18. Based on the knowledge that the Cu(I) loaded NosL is fully loaded, the loading of the Cu(II)-NosL sample can be calculated using the intensity of the 260 nm LMCT band. It was therefore estimated that 75% of the Cu(II) had been auto-reduced to Cu(I) and bound by NosL after a 20 min incubation.

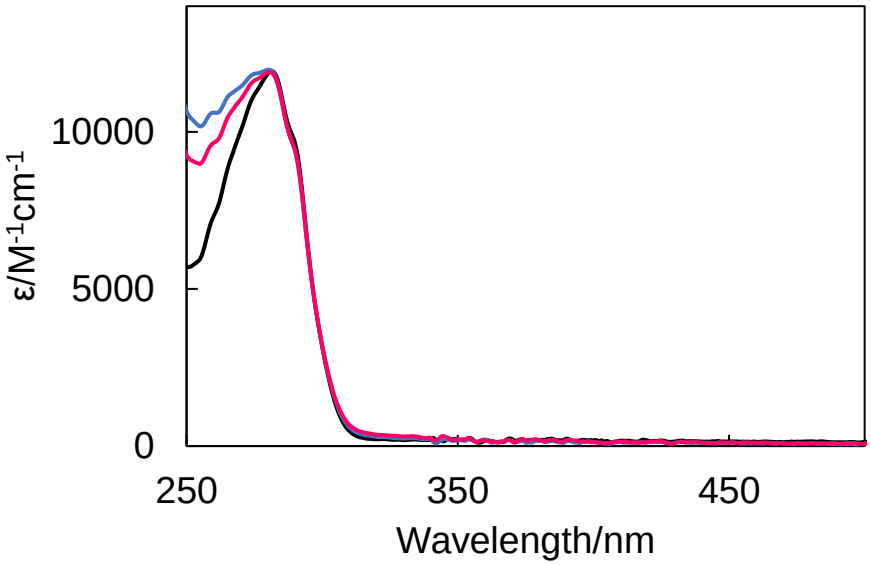

Figure 5.18: UV-visible absorbance spectra of samples of NosL sent for EPR analysis. Apo-NosL (black), Cu(II) loaded NosL (pink) and Cu(I) loaded NosL (blue).

EPR spectra recorded for the same samples are shown in Figure 5.19. Double integration of the EPR signals due to Cu(II) for all samples recorded are given in Table 5.3.

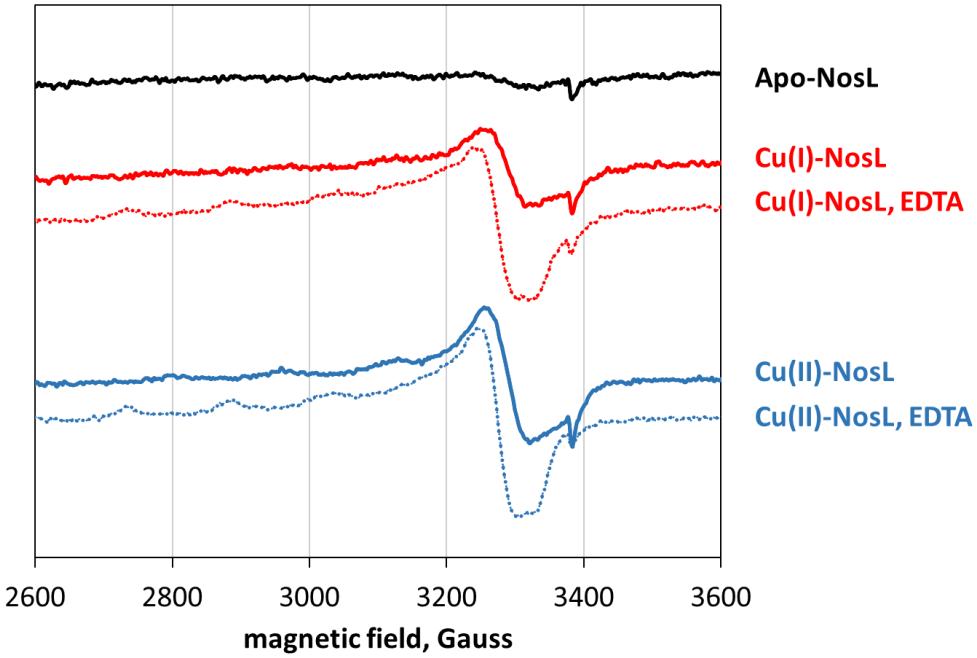

Figure 5.19: EPR spectra of Cu loaded samples of NosL.

Using the Cu(II) standards discussed, signal intensities were then compared and the concentration of Cu(II) in each sample was recorded (Table 5. 3).

Table 5.3: Concentration of Cu(II) detected in each NosL spectrum shown in Figure 5.19.

Sample ID	$[Protein]_T$ (μM)	$[Cu]_T$ (μM)	$[EDTA]_T$ (μM)	[Cu(II)] detected by EPR (μM)	Cu(II) atoms/NosL, (%)
Apo-NosL	195			1.2	0.62
Cu(I)-NosL	185	186		7.7	4.2
Cu(I)-NosL, EDTA	186	186	200	14.9	8.1
Cu(II)-NosL	186	187		14.7	7.9
Cu(II)-NosL, EDTA	186	187	201	20.6	11.1

As expected, in the Cu(II)-NosL samples, Cu(II) was largely reduced to Cu(I). Therefore, it is concluded that NosL significantly favours Cu(I) over Cu(II) and, if necessary, will find an electron to reduce and bind Cu at its centre even in the absence of an exogenous reductant. These data are consistent with the high affinity of Cu(I) binding to NosL reported above.

5.5 Solution studies of excess Cu binding to NosL

Attempts were made to crystallise Cu(I)-NosL for X-ray crystallography. As yet, diffraction quality crystals have not been generated. The Cu-NosL was detected by mass spectrometry as a monomer, but during the final step of purification on a gel filtration column, the protein eluted as a broad band indicating a possible monomer dimer mixture. To test this, a native PAGE was run using NosL samples loaded with varying amounts of Cu(I) and transferred into a HEPES/salt buffer to be run under native conditions (Figure 5.20).

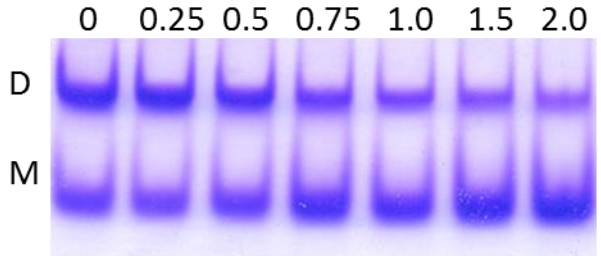

Figure 5.20: Native-PAGE analysis of NosL loaded with varying ratios of Cu(I). 20 μL of NosL in 100 mM MOPS, 100 mM NaCl pH 7.5 was loaded with varying Cu ratios to protein and buffer exchanged into 60 mM HEPES, 40 mM NaCl, pH 7.2, to be run on a 12% Native PAGE gel.

Apo-NosL gave rise to two bands on the gel that are interpreted as the monomer and dimer forms. Increasing the Cu(I) loading in the protein up to 1 Cu(I) per protein, increased the intensity of the monomer band at the expense of the dimer band. These data indicate NosL is not entirely a monomer in solution.

To explore the monomer/dimer species in more depth, samples of apo and Cu(I)-NosL were passed down a size exclusion column containing SeptFast gel filtration media (Generon) which was able to separate proteins between a mass range of 3 and 70 kDa. The column was calibrated with protein standards (Figure 5.21B) so the protein mass corresponding to the elution peak of NosL could be determined.

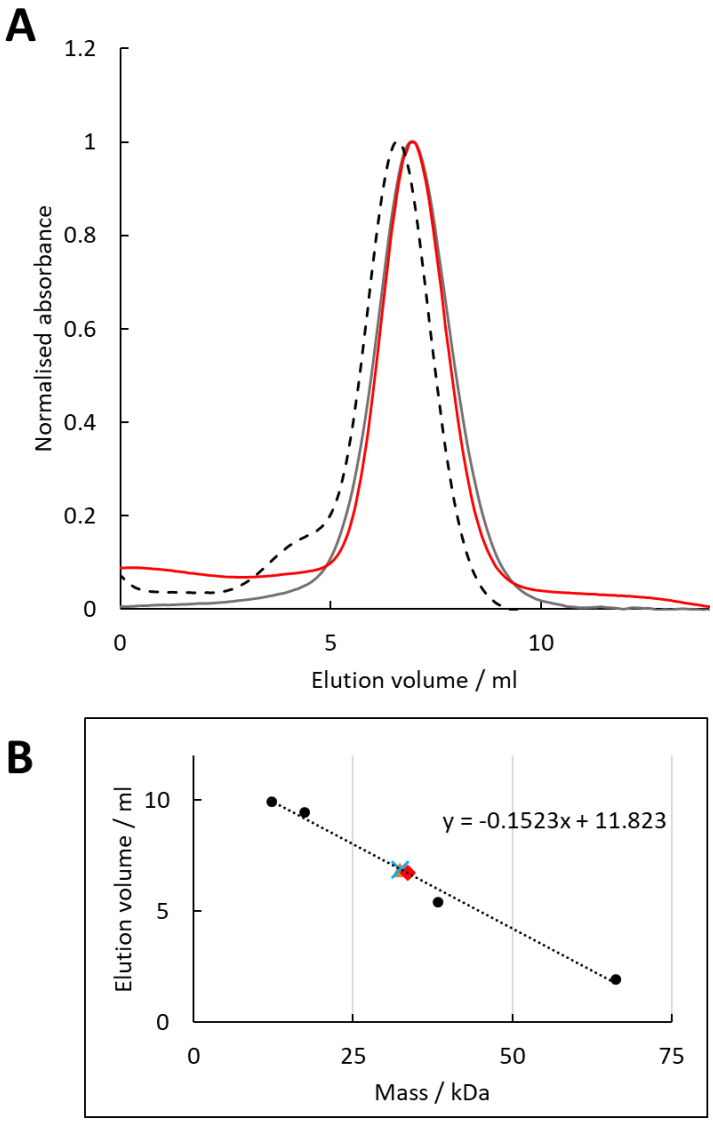

Figure 5.21: (A) Elution of apo-NosL (grey), 1 Cu/NosL (red) and 2 Cu/NosL (dashed black) from the Generon gel filtration column. (B) A calibration curve was produced using Cytochrome *c* (12.4 Da), Myoglobin (17.6 Da), RsrR (35 Da) and Bovine serum albumin (66.5 kDa), black dots. Each volume corresponding to the elution with maximum absorbance at 280 nm in 5.21.A, was plotted on 5.21.B. Apo-NosL (orange triangle), 1 Cu/NosL (blue cross) and 12 Cu/NosL (red) . The column was run using 100mM MOPS, 100mM NaCl, pH 7.5.

NosL eluted from the gel filtration column as a mixed monomer-dimer. Table 5.4 shows the mass of the protein eluting from the column, determined using the calibration curve. Neither the monomeric mass of NosL (18 890 Da) or dimeric mass (37 780 Da) was observed. Therefore, these data together with the native-page

suggest the protein is in a mixed monomer/dimer equilibrium. According to the gel filtration data, Cu(I) binding has little effect on association state.

Table 5.4

Protein sample	Eluted volume / ml	Estimates mass / Da
Apo-NosL	6.94	32.06
1 Cu/NosL	6.94	32.06
12 Cu/NosL	6.7	33.63

The protein sample which eluted after 1 Cu/NosL was passed down the gel filtration column, was collected and analysed using native-PAGE and denaturing SDS-PAGE. As Figure 5.22 shows, the protein remains in a mixed monomer/dimer species.

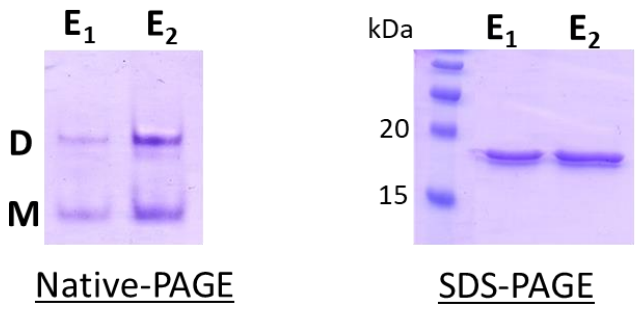

Figure 5.22: Analysis of the Cu(I)-NosL elution maximum in Figure 5.21A, by native-PAGE (left) and SDS-PAGE (right). The native-PAGE demonstrates the mixed monomer/dimer species whereas the denaturing SDS-PAGE reveals a single band corresponding to the monomeric NosL.

5.6 Discussion

A recombinantly expressed, truncated and soluble form of NosL was characterised by Cu binding. Apo-NosL was titrated with Cu(I) and revealed specific binding of a single Cu(I) atom. Additional Cu(I) that bound to the protein could be readily removed by passing the sample down a de-salting column. The affinity of NosL for Cu(I) was determined using a BCS competition assay, resulting in a K_d of 4.44×10^{-18} M.

Cu(II) binding studies revealed an absorbance spectrum like the Cu(I) bound form of NosL, implying the Cu(II) had been reduced to Cu(I), which was binding to NosL. This hypothesis was confirmed using EPR, where only ~8% of the total Cu(II) added to a sample of NosL was detected as Cu(II). The remaining ~92% of the Cu(II) had been reduced to Cu(I) and was bound to the protein. The EPR result identified a greater percentage of the Cu(II) had been auto-reduced than the crude calculation from the absorbance spectrum (Figure 5.18). This discrepancy is most likely due to the extra time taken between recording the absorbance spectrum and then transferring the sample to the EPR tube before flash freezing, which would allow more time for auto-reduction and binding of Cu(I) to NosL after the spectrum was recorded.

Together, these data are consistent with a Cu site in NosL that has a strong preference for Cu(I) over Cu(II). Thus Cu(II) added to NosL is highly oxidising, undergoing reduction even in the absence of an exogenous reductant. In this case, the source of the electron is most likely the protein itself through a reaction similar to that carried out in the Lowry protein assay [107]. This colorimetric assay used to determine protein concentration starts with the chelation of Cu(II) by peptide bonds under an alkaline condition which in turn reduce the cupric ion to cuprous Cu(I) and then subsequent detection of Cu(I).

NosL, in both apo and Cu(I)-loaded forms, was analysed by ESI-MS under non-denaturing conditions. Both forms appeared as monomers, with a number of adducts which, despite significant effort, could not be removed. These adducts are likely to be ammonium and sodium ions and do not represent a covalent modification of the protein. This conclusion was confirmed by LC-MS which showed only one major peak that matched the expected mass of NosL (Figure 5.3). Solution studies on NosL by gel filtration and native-PAGE revealed the association state of the protein is in a dynamic monomer/dimer equilibrium. This work has shown that the protein ionizes and is observed as a monomer when flown under native conditions in the mass spectrometer however, it is not unusual for weak protein-protein interactions to be lost in the mass spectrum. Work by Mcguirl et al. showed that *Achromobacter*

cycloclastes NosL was isolated anaerobically as a Cu(I) loaded monomeric protein and that aerobic metal-depleted cultures resulted in a 50/50 mixture of monomeric and dimeric apo-NosL leading the authors to propose that disulfide bond formation between monomers might be the cause of dimerisation [77]. Our data are partially consistent with this finding, as native-PAGE data showed an increasing amount of monomeric NosL as the Cu(I) loading was increased, and that the apo form is a mixture of both monomer and dimer. However, in our study, no evidence of disulfide bond formation was found. Analysis of the protein by gel filtration showed the mass eluting from a calibrated gel filtration column was close to that lying between monomer and dimer (32 kDa, expected midway mass of 28 kDa) but that Cu binding did not cause a significant shift to favour monomer or dimer. Figure 5.22 shows the Cu(I)-NosL remained as a mixed species once passed down the column, as shown by analysing both the volume it eluted from the column and the protein samples itself by native-PAGE. The native-PAGE indicated Cu(I)-NosL favoured the monomeric species in contrast to the gel filtration studies which showed no significant preference for monomer or dimer.

While excess Cu effects NosL, it does not bind tightly, as shown spectroscopically in Figure 5.7, when excess Cu was removed by passage down a PD10 desalting column. The second Cu ion attaches to NosL but it binds weakly and although no significant change was observed in the absorbance spectrum, the CD spectrum of 2Cu(I)-NosL was unlike any other sample recorded (Figure 5.8). If 1 Cu atom binds tightly and the other weakly elsewhere, then this could lead to a change in the CD spectrum, as observed.

The data demonstrate that NosL remains in a dynamic equilibrium between a monomer and dimer. Whether this is physiologically relevant within the cell and if Cu(I) binding forces the dynamic equilibrium to distinctly favour the monomer, it remains to be shown. This could also be an artefact of removing the lipid anchor that tethers the protein to the membrane. The anchor could potentially stabilise one or the other association state.

The results from metal binding studies obtained in this work are, in principle, in agreement with those obtained by McGuirl et al using recombinantly expressed *Ac*NosL in *E. coli*: NosL binds a single Cu(I) atom [77]. Both studies used a recombinant expression system, replacing the N-terminal leader sequence with a methionine residue to allow for ease of purification. McGuirl et al showed that NosL could bind a single Cu(I) atom but oxidation of the Cu(I) to Cu(II) by ferricyanide

caused the Cu to dissociate. Our work, however, found that if presented with Cu(II), NosL could auto-reduce it to Cu(I) and bind Cu(I). The affinity of NosL for Cu(I) was high and close to the affinities exhibited by other periplasmic Cu chaperones (Table 5.5), such as SenC, which is involved in the maturation of the cytochrome *c* oxidase Cu_A centre.

Table 5.5: Dissociation constants for Cu(I) binding to periplasmic Cu binding proteins in prokaryotes. Amino acids residues involved in binding Cu are also described (C- cysteine, H-histidine and M- methionine).

Protein (species)-putative ligands	K_d	**Ref.**
Sco (*B. subtilisi*) – C/M/H binding	10^{-12} M	[108]
SenC (*R. capsulatus)* - C/H binding	3.25 x 10^{-15} M	[109]
Sco (*S. lividins*) – M/H	4.6 x10^{-17} M	[110]
PCCA (*R. capsulatus*) - M/H	8.25x10^{-16} M	[109]
CopC (*P. syringae)* - H/M_X	10^{-13} M	[111]
CopK (*C. metallidurans* CH34) – M	2 x 10^{-11} M – 2 x 10^{-13} M	[112]
NosL (*P. denitrificans)* (C/H/M)	4.44 x 10^{-18} M	This work

From spectroscopic studies, the increase in absorbance in the UV region, in particular with a band at 260 nm, indicates the involvement of a cysteine residue in binding Cu(I). Further information about how Cu(I) binds to NosL and the residues involved in this interaction can be deduced by comparing the peptide sequences of NosL from across a variety of N_2O reducing bacteria. Figure 5.22 describes a comparison of NosL sequences from the two clades of N_2O reducing bacteria. The first and most importantly conserved feature is a cysteine residue through which the protein is predicted to be anchored to the membrane (yellow). The only other cysteine is conserved and thus fits with our hypothesis that it binds Cu(I). The remaining conserved residues are; 2 methionines along with phenylalanine, alanine, valine and

glycine, all of which are hydrophobic. The other putative ligands mentioned by McGuirl et al to bind Cu were a methionine and histidine. These were predicted based on the energy of the Cu K X-ray absorption edge, the energy and shape of which was consistent with a three- or four-coordinate Cu(I) [77]. Fittings of the curve indicated the first-shell EXAFS for NosL is likely to assume a Cu-(O/N)S_2 coordination environment and that the light atom is likely histidine [77]. Only one histidine is semi-conserved across the prokaryotes as highlighted by a red box in Figure 5.22.

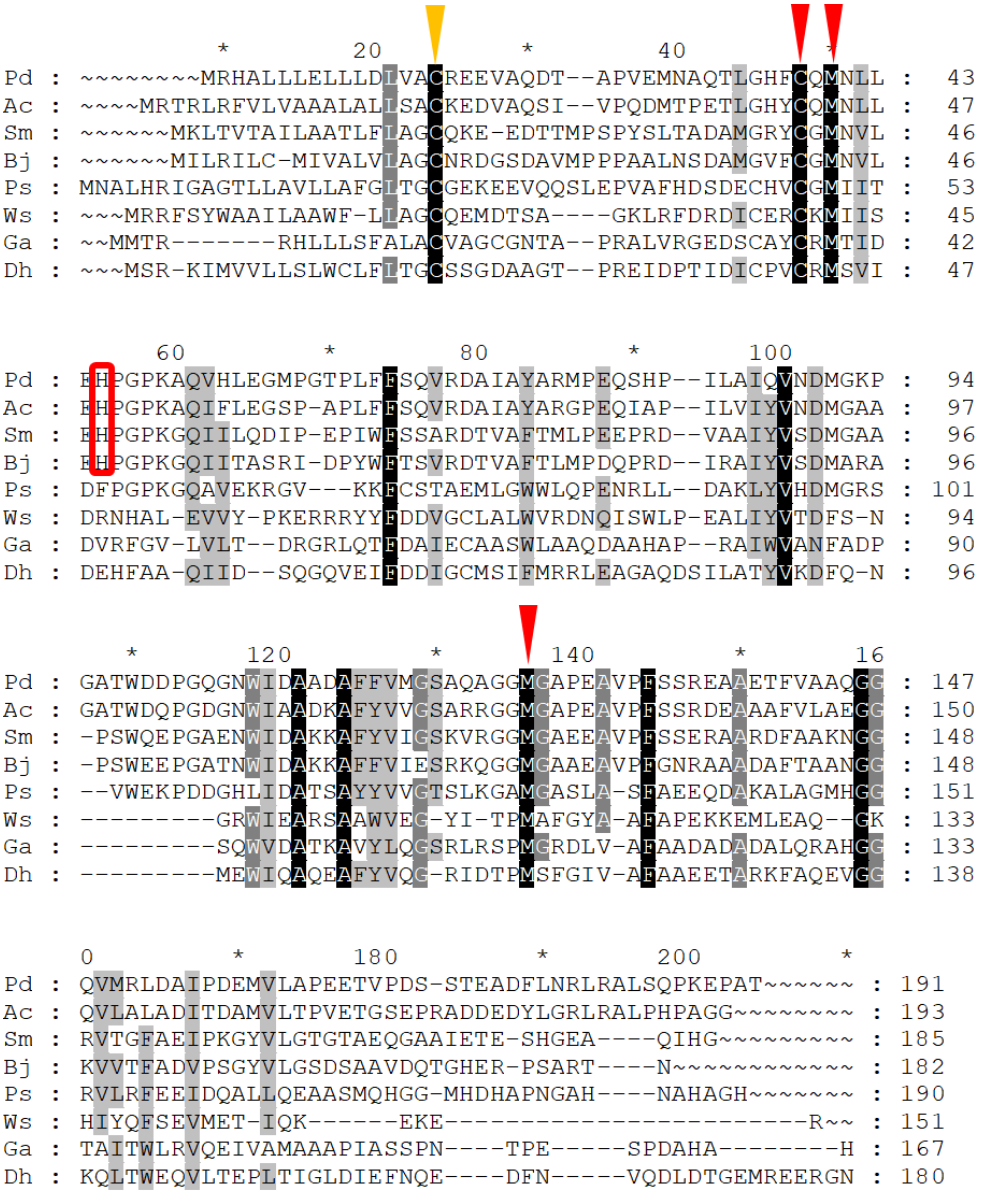

Figure 5.22: A comparison of the NosL sequence from N_2O reducing members of clade I (*Paracoccus denitrificans*-Pd, *Achromobacter cycloclastes*-Ac, *Sinorhizobium meliloti*-Sm, *Bradyrhizobium japonicum*-Bj, *Pseudomonas stutzeri*-Ps) and clade II members (*Wolinella succinogenes*-Ws, *Gemmatimonas aurantiaca T-27* -Ga *and Desulfobacterium hafniense DCB-2* -Dh). The conserved cysteine anchor (yellow

triangle) and CXM motif and further methionine are highlighted (red triangle) along with a conserved histidine in clade I (red box).

Figure 5.23 shows a part of the sequence alignment in Figure 5.22 with additional labels including histidine and a further cysteine residue close to the CXM motif identified in NosL. There are some interesting differences between the sequences close to the CXM motif between the two clades. Members of clade I have a well conserved histidine residue downstream of the conserved CXM motif, resulting in a possible $CXMX_4H$ copper binding motif. Members of clade II do not have such highly conserved histidine residues but do have an additional conserved cysteine resulting in a CXXCXM motif. This CXXC motif is also present in *P. stutzeri* and was the reason for the initial labelling of NosL as a disulfide isomerase. There is, however, some overlap between the two clades in the *Ps*NosL amino acid sequence. *P. stutzeri* is a clade I member, yet its sequence bears more similarity to the clade II NosL proteins. Studies in *Pseudomonas* have shown that only *nosRZDFY* are necessary to produce active N_2OR [73] in contrast to this work on a clade I member NosL, where we have shown, *nosL* was essential for N_2O reduction under Cu limitation. It may be possible that Cu binding site for clade I/II proteins might be different and this could reflect a functional difference between the clades.

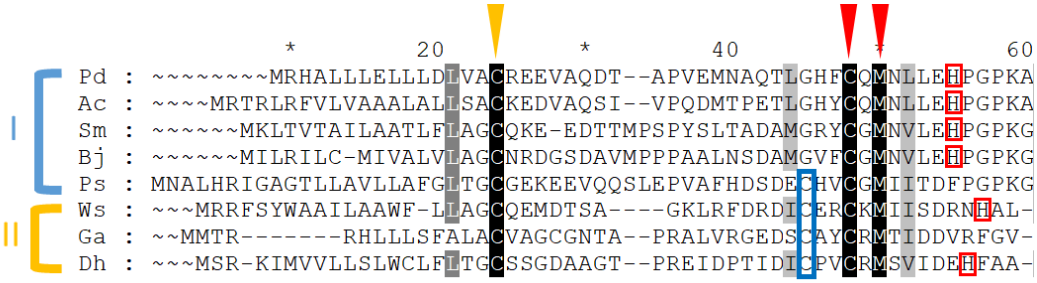

Figure 5.23: Further conserved residues in NosL across members of Clade I (blue) (*Paracoccus denitrificans*-Pd, *Achromobacter cycloclastes*-Ac, *Sinorhizobium meliloti*-Sm, *Bradyrhizobium japonicum*-Bj, *Pseudomonas stutzeri*-Ps) and Clade II (yellow) N_2O reducing bacteria (*Wolinella succinogenes*-Ws, *Gemmatimonas aurantiaca T-27* -Ga *and Desulfobacterium hafniense DCB-2* -Dh). Highlighted are a histidine residue close to the CXM motif (red square) and also a second cysteine (blue square) residue among Clade II members and *Ps*NosL. These amino acids could act as a third ligand to bind Cu.

This work has shown that NosL is involved in the maturation of the Cu_Z centre in *P. denitrificans* under Cu replete conditions and both Cu centres during Cu limitation, but how NosL obtains Cu is not known. One possibility is that NosL is part of a larger system in γ-proteobacteria in which it accepts Cu from an outer membrane importer, NosA [113], though this counterpart is not observed in *P. denitrificans.* In the periplasm of the cell where NosL is located, the environment is oxidising, and free Cu will likely be Cu(II). As shown in this work, Cu(II) can be auto-reduced to Cu(I) which binds tightly to NosL. Thus, NosL may not need a counterpart as it can simply make use of the Cu pool itself by auto-reducing and binding Cu(I). This could be a means of controlling Cu in the periplasm, while at the same time participating in the maturation of N_2OR under denitrifying conditions.

The work reported in this chapter has established that NosL binds Cu(I) tightly providing a clear indication of how it carries out its role in the maturation of the Cu centres in N_2OR.

CHAPTER 6

Investigating the *Paracoccus denitrificans* PD1222 transcriptome under Cu excess conditions to identify copper detoxification/trafficking systems

6.1 Introduction

The harmful and toxic effects of free Cu within the cell, as discussed in section 1.3.2 are limited in eukaryotes and prokaryotes by systems that bind and distribute Cu to specific compartments of the cell, either to secrete and alleviate cellular concentrations or to incorporate the metal into protein active sites.

P. denitrificans require Cu at the catalytic centres of key respiratory enzymes to metabolise and survive. Under anaerobic conditions, the penultimate substrate in the denitrification pathway is reduced by the multi-Cu N_2OR, which requires 12 Cu atoms to produce an active holoprotein. This is a much larger requirement than aerobic conditions which rely on 1 or 3 Cu atoms to produce a single active *Cc*O, to survive. *P. denitrificans* has a high demand for Cu not only for respiration purposes but also to produce other functional enzymes such as superoxide dismutase (SOD) and azurin, an electron transfer protein necessary for denitrification in *P. denitrificans*. We hypothesise that this bacterium contains at least one key Cu handling/trafficking systems to control Cu once inside the cell. An investigation was conducted on the *P. denitrificans* PD1222 genome, using the NCBI BLAST tool (Basic Local Alignment Sequence Tool) [114], to identify genes in the genome that encode homologues to well-known Cu handling systems. The primary amino acid sequence of well characterised members of Cu transport systems from separate kingdoms and phyla were used as query sequences to search against the PD1222 proteome. Primary amino acid sequence alignments were used to determine whether well-defined and conserved Cu binding motifs, which characterise these protein families, were present. A decision was then made as to whether hit sequences represented a true homologue.

Once candidate genes were identified, a transcriptome data set collected for PD1222 cultured under Cu deplete and replete conditions was scrutinised for each gene to determine whether their transcription was dependent on the presence of Cu in the cell.

6.2 Bioinformatic search of the *P. denitrificans* (PD1222) genome

6.2.1 Copper detoxification in the cell by copper chaperones and cognate P-type ATPases

ATX1-type copper chaperones

In the last 20 years, protein-based systems within the cytoplasm that bind and help to maintain low levels of free Cu(I) within the cell have come to light, in both eukaryota and prokaryota domains of life, which importantly reveals a functional conservation of Cu metabolism throughout life [2]. Even more interesting is the structural conservation of the residues which form the Cu binding motif. These small Cu metallo-chaperones primarily function to bind and transport Cu(I) ions to a specific partner/membrane transporter, the role of the partner will be discussed later.

The first Cu chaperone was discovered in *Saccharomyces cerevisiae* after studies of yeast mutants lacking the antioxidant enzyme, SOD, remained viable even in the absence of this gene. The newly discovered ATX1, a 8.2 kDa metallo-chaperone was responsible for shuttling Cu(I) from the cytosol to the Cu transporting ATPase Ccc2, located in the trans golgi networks, where the Cu is then inserted into processed proteins to produce active cupro-proteins [26]. ATX1 alleviated the cell of free cytotoxic Cu(I) in the cytoplasm and therefore limited the chemical cycling of ROS (section 1.3.2, Equation 1.4-1.7) and production of superoxide, which would under normal circumstances, be dealt with by SOD.

The first prokaryotic homologue to ATX1 was identified in the Gram-positive bacterium, *Enterococcus hirae*, where intracellular Cu is under the control of the *cop* operon consisting of 4 genes: *copA* and *copB* encoding P-type ATPases that transport Cu that is accepted from the chaperone encoded by *copZ* and finally *copY,* a transcriptional repressor [28]. EhCopZ, the bacterial equivalent of ATX1, traffics Cu(I) to the transporter and also play the role of sensing Cu and feeds back to the transcriptional repressor CopY, by metallating this protein, which in turn releases DNA and allows transcription of *copABZY* to commence [29], alleviating free Cu within the cell.

Another well-defined *cop* operon is in *Bacillus subtilis*, which comprises *copZ* and *copA*, both of which are under the control of a CsoR Cu-sensing repressor [30].

Inactivation of *copA* in *Bacillus* led to enhanced sensitivity to Cu in the cell, which indicated its involvement in the export of Cu(I) [31]. CopZ also makes a net contribution to Cu resistance even in the absence of CopA, implying a role in Cu sequestration when Cu levels exceed that which is safe in the cell [31].

Structure and physical properties of Cu chaperones

Comprised of 68 amino acid residues, ATX1 adopts a ferredoxin-like fold constituted by 2 alpha helices and a four stranded beta sheet (βαββαβ) [115] with the Cu binding site exposed on a loop to allow for the rapid transfer of Cu to the partnering P-type ATPase [116]. The copper binding motif (MXCXXC) is sulfur rich and optimised for stabilising the soft Lewis acid, Cu(I). The same tertiary structure and Cu binding motif is conserved in homologues from both kingdoms and is therefore a clear indicator of the metal which binds.

Copper transporting cognate P-type ATPases

A membrane bound P-type ATPase accepts Cu from their metallo-chaperone counterpart and transports Cu(I) safely across the lipid bilayer. The P-type ATPase superfamily is divided into 11 subfamilies with the P_{-1B}-type ATPase subgroup specifically transporting soft metals such as Cu [117]. As indicated by the name, the translocation of Cu across the membrane is coupled to the phosphorylation of an aspartate residue located on a single transmembrane helix using a phosphate derived from the hydrolysis of ATP. Further common structural features are recognised within this subgroup: 6 to 8 transmembrane (TM) spanning helices, imbedding the protein in the membrane and presenting DKTGT and CPX motifs. The first of these (DKTGT) is essential as the site of phosphorylation required for metal transfer across the membrane, while the second (CPX) is important for metal substrate specificity. Finally, the protein contains a number of (usually) N-terminal soluble metal binding domains (MBD) [117].

A strong resemblance between the tertiary structure of the N-terminal soluble domains of P_{1B}- ATPases and their chaperone counterparts, has been observed. Both structures have ferredoxin like folds and the specific metal binding motif (MXCXXC), which are optimised for Cu(I) binding and therefore allow for the efficient transfer of Cu between the two. This optimised conservation therefore reduces the risk of losing free Cu back to the cytoplasm. Interestingly, the number of MBD a P_{1B}-type ATPase

present varies among organisms, with higher eukaryotes possessing multiple domains, such as 6 in the human Menkes and Wilson proteins [118], whereas bacteria typically have 1 or 2 MBDs. Genes encoding the chaperone and cognate ATPase are commonly found alongside one another in the genome, providing another clear indication of function even in the absence of functional evidence.

Transcriptional regulators

Transcriptional repressors that sense Cu have been mentioned already, including CsoR and CopY. CopY binds Zn^{2+}, as a dimer, under Cu limited conditions. This allows CopY to bind DNA at the *cop* box and repress the expression of the cop operon. Only when Zn in displaced by Cu(I) is the DNA released and repression alleviated [119]. CsoR acts similarly by binding DNA in the apo-state as an oligomer (either a dimer or tetramer) and only once Cu(I) is bound, will it release the DNA [120]. An opposing function is carried out by CueR, a transcriptional activator and a member of the MerR family, associated with binding DNA through an N-terminal alpha helix-turn-helix motif. CueR has been identified in proteobacteria including the facultative photosynthetic bacterium *Rhodobacter sphaeroides*, which binds to the promoter region upstream of the ATPase and chaperone genes and allows for transcription of both under elevated Cu levels [121]. The Cu binding domain of CueR has a high affinity for Cu ($K_d \sim 10^{-21}$ M) using a cysteine coordinated site [122]. Unlike CopY, which is a repressor, CueR binds the DNA independent of Cu but once metallated, CueR distorts the DNA, remodelling the promoter region and enables transcriptional activation [123].

Copper detoxification in the periplasm of Gram negative bacteria – the Cue and Cus systems

E. coli has a P-type ATPase named CopA which is involved in the export of Cu out of the cytoplasm but also has periplasmic proteins which deal with the Cu(I) once it has been passed from the cytoplasm. CueO is a multi-copper oxidase that couples the oxidation of Cu(I) to Cu(II) to the reduction of dioxygen to water. CueO and CopA constitute the Cue system which is transcriptionally regulated a by CueR and, as expected, all 3 genes are transcribed during Cu stress when levels are elevated [124]. CueO can bind 4 Cu atoms at various sites, each with a function in either electron

transfer or dioxygen reduction [125] and methionine rich motifs provide these binding sites for exogenous Cu [126].

Under anaerobic conditions, the Cue system is, however, inactive, and the bacterium relies on an alternative, the Cus system, to deal with an elevated intracellular concentration of Cu. While, under aerobic conditions, the Cus system is functionally redundant for Cu homeostasis and the Cue system takes over. Each system is involved in Cu homeostasis but dependant on total oxygen concentration.

In *E.coli* the Cus system is composed of 4 proteins which respond by alleviating periplasmic Cu(I) levels: CusF, a periplasmic metallo-chaperone, binds and delivers Cu to the membrane spanning protein copper efflux pump CusCBA, which eliminate Cu entirely from the cell [127]. Homologues so far, have been identified across Gram-negative organisms and have 3 conserved methionines and an N/O donor, demonstrated in the sequence of CusA [128]. The periplasmic chaperone CusF presents a conserved histidine and 3 conserved methionines, identified from sequence alignments, which are favourable ligands for Cu binding in the periplasm [129].

Variations on the above systems have been discovered in *Salmonella* where the gene *cueP* encodes a protein that functionally replaces the Cus system, particularly during anaerobiosis [130]. CueP as a chaperone binds Cu and has also been linked to the maturation of Cu,Zn-SOD which is involved in virulence. Mutants missing the *cueP* gene were unable to mature SOD and presented a similar phenotype to the *cusCFBA* mutant when deleted under anaerobic conditions [130], therefore implying an increased occupation of the periplasm with free Cu. CueP has been identified in Gram-negative and positive bacteria, many of which are pathogens, thus, it may play an important role in Cu resistance against macrophage attack. The crystal structure of *Salmonella enterica sv typhimurium* apo-CueP has been solved to reveal a protein dimer with a C-terminal cysteine and histidine- rich region that is responsible for Cu binding [131].

Eukaryotes and bacteria have specialised yet widely distributed Cu trafficking and detoxification systems. These maintain Cu homeostasis within the cell so that Cu is supplied when necessary to apo cupro-proteins and when intracellular levels are too high, Cu can be exported out of the cell in a safe manner to alleviate cytotoxicity. Systems such as these are likely to be present in the PD1222 genome and should be easily identified by bioinformatic analysis.

6.2.1.1 Analysis of ATX1/P-type ATPase/MerR transcriptional regulatory systems in PD1222

A search of the PD1222 genome for an ATX1-like chaperone yielded a single hit on chromosome 2, identified as Pden_3894: a 71 amino acid residue protein annotated as a heavy metal binding detoxification protein. Directly downstream of *pden_3294* is a gene labelled as a heavy metal translocating P-type ATPase (encoding Pden_3295, 639 aa) which is encouraging when identifying these systems. However, neither protein product possesses the MXCXXC Cu binding signature, characteristic of these Cu transporting systems. The gene cluster is shown in Figure 6.1. The smaller chaperone-like protein displays 2 cysteine residues but no methionine; therefore, this may be a cation binding protein but not necessarily Cu specific.

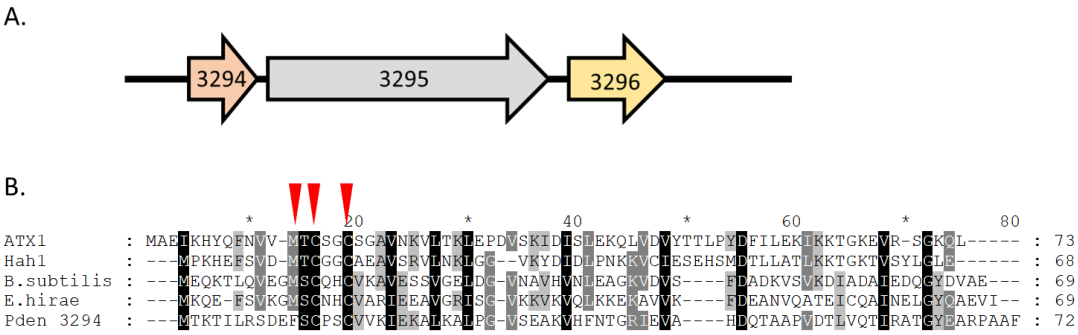

Figure 6.1: Gene cluster identified during search for an ATX1-like chaperone (A) and primary sequence alignment of the chaperone identified alongside well characterised ATX1 like proteins (B). Alignment of ATX1 from *S. cerevisiae,* Hah1 from *H. sapiens,* CopZ from *E. hirae* and *B. subtilis* and Pden_3294. Sequences were aligned using Clustal W2 (EMBL-EBI) [132] and Genedoc [133].

The partnering cation transporter to the chaperone above was aligned with known Cu export proteins. The transmembrane motifs which are key to ATP hydrolysis and metal transport specificity, are present, but no N-terminal soluble metal binding domain or Cu binding motif is present (Figure 6.2). Three further ATPases were identified on chromosome 1 and they all have N-terminal, soluble, heavy metal binding domains. Both Pden_0212 (758 aa) and Pden_0521 (807 aa) have all three signatures of the CopA like protein, including N-terminal MXCXXC motifs which together suggests they are Cu transporters. Pden_1842 (732 aa) is missing the full MXCXXC motif in its soluble N-terminal domain (red triangles, 6.2A) but does include the conserved DKTGT aspartate phosphorylation motif (blue triangles, 6.2C), along

with a CPX motif (yellow triangles, 6.2B) indicative of a Cu transporting ATPase and therefore could be a transporter of an alternative heavy metal such as cadmium. The alignment of all 4 transporter proteins discussed, with various known P_{1B}- type ATPases is shown in Figure 6.2. In each case, the gene is not co-located with a chaperone-like *copZ* gene. This is similar to that of the Gram-negative bacterium *E. coli*, which has the export apparatus but no *copZ* gene. In this case, it has been demonstrated that alternative translation of *copA* leads to the production of a truncated form that functions as a Cu chaperone [134]. The gene which based on this analsysis, looks like it could be part of Cu transporting system was the P-type ATPase, Pden_0212, which exhibited a transcriptional regulator of the MerR family upstream of the gene *pden_0211*.

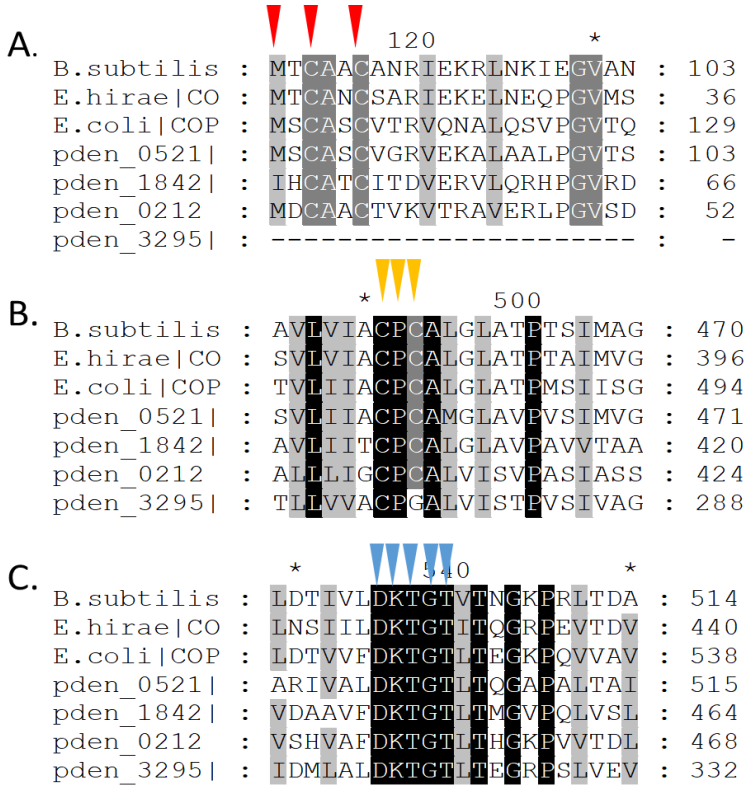

Figure 6.2: Alignment of the primary amino acid sequence of CopA from *B. subtilis*, *E. hirae* and *E. coli* with the 4 protein hits from the BLAST search, Pden_0212, Pden_0521 and Pden_1842 and Pden_3295. The N-terminal metal binding motif (A, red triangles), CPX Cu recognition sequence (B, yellow triangles), and phosphorylation site (C, blue triangles) are shown and specifically conserved amino acid residues highlighted.

It is important to note a further potential role for Cu transporting ATPases which includes the assembly of *cbb*$_3$ type, cytochrome *c* oxidase (C*c*O) in *Bradyrhizobium japonicum* [135]. The gene *fixI* encodes a homologue of the P-type ATPase and is located close to the *CcO* genes and if deleted, results in impaired oxidase activity that can be reversed by supplementing with Cu [135]. The same is true of CcoI, another highly homologous protein to CopA and whose removal from the gene leads to impairment of the *cbb*$_3$-type C*c*O in *Rhodobacter capsulatus* [136].

Interestingly, Pden_1842, which contains a single CXXC motif, is found amongst a set of genes that code structural gene and maturation factors to the *cbb*$_3$-type C*c*O, a protein which remove traces of oxygen during anaerobiosis [137], Figure 6.3.

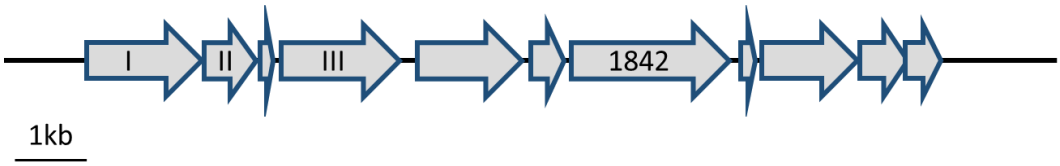

Figure 6.3: **Gene cluster for the cytochrome *c* oxidase, *cbb*$_3$-type (Pden_1848 and Pden_1847 and Pden_1845, subunits I, II and II).** Pden_1842 is the putative heavy metal translocating P-type ATPase and all other genes surrounding are linked to the maturation of the *cbb*$_3$ oxidase.

This observation alone indicates Pden_1842 would be a strong candidate as a Cu transporter involved in metal insertion at the active site of this particular C*c*O.

A search using transcriptional regulators associated with Cu regulation was undertaken. Regions up and downstream of the transporters mentioned previously, were also analysed. Transcriptional regulator hits only appeared from searches initiated using CueR sequences. Four proteins in total were highlighted, Pden_0211, 2343, 3477 and 4523. As mentioned above, only Pden_0211 is within proximity to any of the earlier genes highlighted, that is Pden_0212, a putative P-type ATPase with a single MXCXXC binding motif.

The proteins discussed above could play a role in Cu detoxification in *P. denitrificans*, but it is interesting to note the lack of a well-recognised *copZA* system in the PD1222 genome. Furthermore, there was also no sign of the Cue or Cus detoxification systems. It is strange that a bacterium with an appetite for Cu under anaerobic conditions does

not appear to have a system in place to minimise the effect of toxic free Cu(I) levels in the cell.

6.2.2 Proteins involved in the assembly of Cu_A sites in cytochrome c oxidase (CcO)

The investigation in 6.2.1 did not reveal a convincing Cu detoxification system in *P. denitrificans*. As a result, an investigation into possible periplasmic chaperones involved in maturation of cuproproteins was carried out to broaden the search into how *P. denitrificans* deal with Cu. Our interest lies particularly in the maturation of N_2OR in the periplasm and so a search of the systems known to mature Cu_A sites could provide answers as to how Cu is handled in this particular cellular compartment.

Cytochrome *c* oxidase (C*c*O) also known as complex IV, is the terminal electron accepting protein imbedded in the membrane of aerobic and facultative organisms which catalyses the reduction of O_2 to water. Eukaryotic C*c*Os typically have 11-13 subunits. Three are known as the catalytic domains and are conserved in prokaryotes and each domain plays a separate role in the reduction of oxygen to water; one is an electron transfer site while the other is the site of substrate reduction. As discussed previously, *cbb*$_3$-type oxidases have a single Cu atom located at a Cu_B site (single Cu and *a*-type heme). The more typical *caa*$_3$-type oxidases contain two Cu centres and 3 Cu ions in total across 2 subunits of the protein complex. Subunit II of this oxidase contains a binuclear Cu_A site whose role is to accept electrons and passes them to subunit I, where a Cu_B site is responsible for the reduction of oxygen to water [138]. There are 4 terminal oxidases in *P. denitrificans,* 3 of which need Cu to function. Therefore, Cu is a vital metal for respiration in this bacterium.

In the mitochondrion, three proteins have been linked to the maturation of Cu_A sites in these centres: soluble Cox17 and two membrane tethered proteins, Sco1 and Sco2. Human Cox17 is a cysteine rich protein which can form 3 pairs of disulfide bonds and has the ability to transfer Cu(I) and 2 electrons to oxidised Sco1, a thioredoxin-like protein. This Cu electron-coupled-transfer is ideal for the oxidising location of Sco1, where the cysteines are often oxidised and unable to bind Cu [26]. This reaction is not possible with Sco2, which can only receive Cu as a reduced protein. Once metallated, Sco2 interacts with subunit II of C*c*O and stabilises it prior to recruitment of metallated Sco1 which in turn metallates subunit II to produce the Cu_A site [139].

In prokaryotes, there is no *cox17* gene however a functional equivalent in Gram-negative bacteria has been identified as a *pCu$_A$C* (periplasmic Cu_A chaperone). Unlike

the cysteine rich Cu binding motif of Cox17, PCu_AC has histidine and methionine residues which make up the Cu binding motif, most likely in response to the oxidising nature of the periplasm. *Thermus thermophilus* PCu_AC has been shown to adopt a cupredoxin like fold with an extended, flexible, solvent-exposed β-hairpin and again contains a Cu binding motif composed of histidine and methionine residues and binds Cu in the sub-picomolar range [140]. This $TtPCu_AC$ metalates the Cu_A centre of cytochrome ba_3 oxidase directly as shown *in vitro* [141]. However, PCu_AC was also shown to first metallate the accessory protein to Cu_A assembly, Sco1, in *R. shpaeroides* which in turn matures Cu_A sites [142]. The latter system mentioned is more common, especially with eukaryote Cu_A system, with both chaperones working in unison and the two genes are normally within close proximity in the genome, implying a further dual action. Sco1 proteins have been shown to metallate Cu_A centres by binding Cu(I) but an alternative role has been offered, as a thiol-disulfide reductase involved in forming the reduced conformation of cysteine residues located at Cu_A sites, therefore facilitating Cu transfer and not directly involved [143]. Bacterial Sco proteins, such as that from *B. subtilis,* are homologues of the eukaryotic Sco protein mentioned above. Deleting the Sco gene reduces the expression of C*c*O and this can be recovered by supplementing the media with Cu, consistent with its importance in producing Cu bound C*c*O [144]. Cysteine and histidine residue conservation in this protein also suggests a functional role for these residues in Cu binding [144]. In other Gram-negative bacteria, such as *Rhodobacter sphaeroides*, the Sco homologue, SenC, has been implicated in the synthesis of biologically active cbb_3 type C*c*O, which only contains a Cu_B site [145]. Therefore, this protein may show some variability in the Cu site that it metalates.

6.2.2.1 Analysis of proteins associated with CcO metalation in PD1222

Two sets of homologues for PCu_AC and Sco were identified in the BLAST search. The two Sco homologues with gene IDs Pden_2780 (ScoA, 216 aa) and Pden_4443 (ScoB, 210 aa) are shown in Figure 6.4 alongside other Sco proteins. The *Pd*Sco proteins show a clear conservation of a CPXXCP motif [146].

Figure 6.4: Alignment of Pden_2780, Pden_4443, SenC from *P. stutzeri, R. capsulatus* and eukaryote Sco homologues from *H. sapiens* and *S. cerevisiae*.
The PCu_AC homologues are Pden_0519 (PCu2, 127 aa) and Pden_4444 (PCu1, 300 aa). Both proteins contain a C-terminal half with a conserved $H(M)X_{10}MX_{21}HXM$ motif in agreement with $TtPCu_AC$ and is known to bind Cu [146]. The genes Pden_4443 and Pden_4444 (ScoB and PCu1 respectively) are part of an up-regulated gene cluster, implicated in response to PD1222 Cu limitation under anaerobic denitrifying growth conditions [28].

All 4 genes mentioned here have also been studied in *P. denitrificans* with regard to C*c*O maturation, but only ScoB has, so far, been implicated in maturation of the Cu_A site, though the PCu proteins are thought to be direct interaction partners with the Sco proteins [146]. The machinery is therefore present in the periplasm of *Paracoccus denitrificans* for maturation of these dinuclear Cu centres.

6.2.3 Other copper resistance and regulatory proteins

The Cu resistance protein PcoC is plasmid encoded and allows strains of *E. coli* to survive in Cu rich environments (typically mM concentrations) [147]. Homologues of PcoC are found in *Pseudomonus* and are known as CopC proteins[111].

A high intraceullar Cu concentration induces the expression of *E. coli* PcoC in the periplasm along with other elements from this operon. PcoA, PcoE and PcoC are all soluble proteins that transport Cu to membrane proteins, PcoB and PcoD, located on the outer membrane and the inner membrane respectively [148]. PcoC has a soluble beta barrel structure and 2 separate metal binding sites; one that binds Cu(I) and one a Cu(II) ion, each liganded by His/Met and His/water, respectively, with affinities for Cu in the 10^{-13} M range and located 30 Å apart [148]. The conserved methionines and a single histidine (blue box in Figure 6.5) are possible ligands for Cu(II) while the Cu(I) ligands are histidines (red stars)[147].

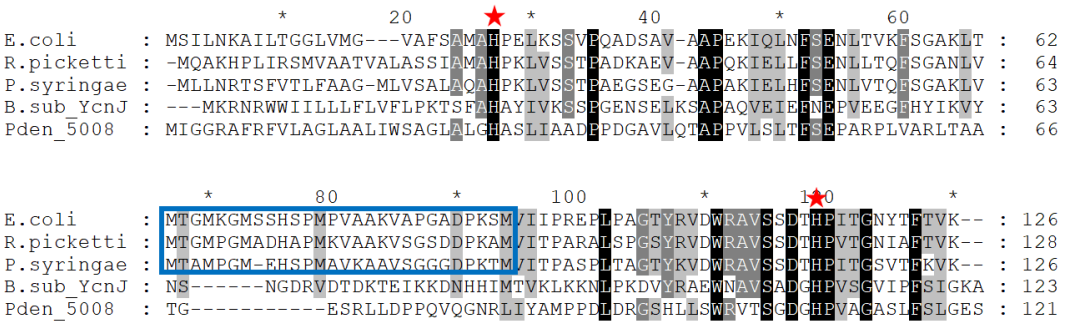

Figure 6.5: The alignment of Pden_5008 with CopC from *E. coli, P. syringae, R. picketti* and YcnJ from *B. subtilis*. Stars highlight the Cu(I) binding residues and the box contains conserved methionines and histidines linked to Cu(II) binding in *E. coli.*

Pden_5008 (513 aa) identified using BLAST only shares the Cu(I) binding ligands (starred histidines) and is similar in length to the *B. subtilis* YcnJ protein (541 aa). YcnJ is important for Cu metabolim in *B. subtilis* and when disrupted causes growth defects and a reduced intracellular level of Cu [149]. The N-terminal motif of YcnJ has been recognised as having strong homology with CopC and this domain has a high affinity for Cu(II) with a potential role in the uptake of oxidised Cu [149].

6.2.4 Parabactin and siderophores

Metals play key physiological roles as protein cofactors involved in metabolism, therefore, it is important to maintain a sufficient supply of these metals to the cell. Understanding the systems in place which allow a bacterium to obtain metals from extracellular sources and take up the metal is important for understanding the overall scheme of metal homeostasis within a bacterium.

Siderophores (Greek for iron carrier) are ferric binding compounds secreted by bacteria to chelate Fe(III) under Fe limitation. A compound containing catechol in *P. denitrificans* is released in response to Fe limitation and has been named parabactin. Once bound to Fe, the Fe(III)-parabactin complex is then imported back into the cell through an 80 kDa membrane bound TonB-dependent transporter protein which has a high affinity for Fe(III)- L-parabactin [150].

Anaerobically growing *P. denitrificans* has a high demand for Cu and it is possible that insufficient Cu would present a problem for the organism. The mechanism by which Cu may be acquired under Cu limitation by *P. denitrificans* has been proposed in the literature. Under Cu deprived conditions, coproporphyrin III is secreted from *P. denitrificans* into the medium [151]. It is possible that this could play a role as a

chalkophore. The coproporphyrin III is found in a Zn^{2+}-bound form, but this could be an artefact of the experiment where levels of Zn were high and the true chalkophore is without metal. The affinity of coproporphyrin III for Cu is high and the compound itself is a side product of the heme and chlorophyll biosynthesis pathway [151]. Once secreted the chalkophore needs to be imported back into the bacterium and there are putative systems which uptake metallated porphyrins including the gene Pden_4201 [151], a TonB dependent heme receptor/transporter.

Another known chalkophore is methanobactin, a small polypeptide featuring serine, tyrosine, glycine, cysteine and methionine residues with a mass of ~1200 Da. Methanobactin is found in high concentrations in the media from Cu depleted cultures of *Methylosinus trichosporium* OB3b and *Methylococcus capsulatus* [152]. It is then internalised into the cell to be associated principally with pMMO (particulate methane monooxygenase), a Cu protein central to the catabolism of methane [152].

These methods of scavenging metals from the environment can also be used as a defence mechanism for pathogenic bacteria [153]. For example, pathogenic strains of *E. coli* must deal with local high concentrations of Cu and therefore are able to fix and chelate metals they are subjected to. Therefore, the systems described may be useful in looking at a bacterium's response to a rise in metal concentrations outside the cell, and as a method to deal with toxic Cu levels.

The exact genes involved in the synthesis of coproporphyrin III are not fully known but any homologues to the traditional Hem-like proteins that respond to Cu may be highlighted in sections to come.

6.2.5 Discussion of the bioinformatic BLAST search

Analysis of the *P. denitrificans* genome using the Basic Local Alignment Search Tool (BLAST) did not identify a common Cu detoxification/trafficking system shared among prokaryotes and eukaryotes. The search did, however, identify single elements of some of these systems and the apparatus within the periplasm to assist with Cu_A assembly.

Microarray transcriptomics data from aerobic and anaerobic cultures of *P. denitrificans*, with (13 μM, Cu replete) and without (<0.1 μM, Cu deficient) Cu (Obtained by M. Sullivan, aerobic dataset unpublished) was used as a tool to assess whether any of the genes identified in the above search, respond and are up-regulated in the presence of Cu. Three of the genes identified from the BLAST search had significant expressional changes in response to Cu, as shown in Table 6.1. The

transcriptome data-set identified changes to the expression of other genes though these could not be obviously linked to Cu, and an overview of these can be found in Sullivan et al [28].

Table 6.1: Expression of gene selected by the BLAST search, taken from a PD1222 transcriptome data set collected under Cu depleted and replete growth conditions. The expression figure noted is an arbitrary absolute value based on the expression levels of RNA in the microarray experiment. Highlighted values are those that changed significantly in response to Cu. (The microarray data was collected by Dr M. Sullivan, aerobic dataset is unpublished)

		+O_2		**-O_2**	
Gene ID	**Function**	**+Cu**	**-Cu**	**+Cu**	**-Cu**
0211	Transcriptional regulator, MerR family	0.697	0.641	0.776	0.693
0212	P-type ATPase 1x MXCXXC motifs – now Zn related - *ZntA* [69]	0.697	0.641	0.776	0.693
0519	PCu2	2.39	2.33	2.00	2.05
0521	P-type ATPase 2x MXCXXC motifs	1.36	1.54	1.36	1.15
1842	Heavy metal translocating P-type ATPase 1x MXCXXC motif	3.07	1.49	5.75	5.39
2343	Putative Transcriptional regulator, MerR family	2.22	2.33	1.51	1.55
2780	SenC/ Sco2	2.14	1.95	2.36	2.35
3294	Heavy Metal Translocating / Detoxifying protein (no motif)	0.391	0.501	0.386	0.399
3295	Heavy metal binding ATPase (no motif)	0.24	0.290	0.307	0.29
3477	Putative Transcriptional regulator, MerR family	4.1	3.05	2.29	1.64
3629	Uroporphyrinogen decarboxylase	8.34	9.20	9.24	9.65
4523	Putative Transcriptional regulator, MerR family	0.878	0.80	0.729	0.572
5008	CopC/D	2.11	2.3	1.95	2.07

4443	SenC/ Sco	2.39	27.7	7.73	65.1
4444	PCu1	3.09	34.9	9.35	76.3

Transcription of the gene encoding the heavy metal P-type ATPase (Pden_1842), present upstream of genes encoding a *cbb*$_3$-type C*c*O, was greater in the presence of Cu under aerobic conditions. The *cbb*$_3$-type oxidases are commonly used in anaerobiosis, when oxygen levels are falling. The sensitivity of this gene's transcription was not observed under anaerobic conditions and levels remained the same irrespective of the Cu concentration. This aerobic response is likely to be of a transcriptional activator binding upstream of the gene, which is released once bound to Cu, allowing for greater transcription.

As mentioned above, two genes are linked to Cu_A site assembly, Pden_4444 and Pden_4443, encoding PCu1 and ScoB, respectively. The anaerobic data set from the microarray experiment showed ~10-fold increase in expression of both genes in the absence of Cu in both aerobic and anaerobic cultures. Cu limitation, therefore, imposes a need for a greater number of these Cu chaperones to be present in the periplasm of the cell to carry out their role in binding and trafficking Cu to Cu_A centres. Based on the homology with the Cu_A site found in N_2OR, these proteins are also putative chaperones to this centre and work is underway towards determining their role with regard to N_2OR maturation. The expression of all the other genes in Table 6.1 was not significantly higher or lower in the presence or absence of Cu. That is, the expression of no putative Cu transporter, Cu detoxification protein (CopC) or transcriptional regulator changed significantly in response to Cu.

Our interest also remains with the maturation of the multi-Cu N_2OR and the release of N_2O from the soil due to inefficient N_2OR activity. Therefore, a search of genomes among other proteobacteria that express N_2OR was carried out to try to understand whether there is a wide spread lack of Cu detoxification systems in N_2O reducing bacteria, or whether it is peculiar to *P. denitrificans*. The only α-proteobacteria with ATX1 like proteins with the MXCXXC motif are *Rhodobacter sphaeroides* and *Dinoroseobacter shibae.* It seems that while *P. denitrificans* lack an ATX1/P-type ATPase system specific to Cu trafficking, β- and γ-proteobacteria do have this system with the expected Cu binding motif (Figure 6.6).

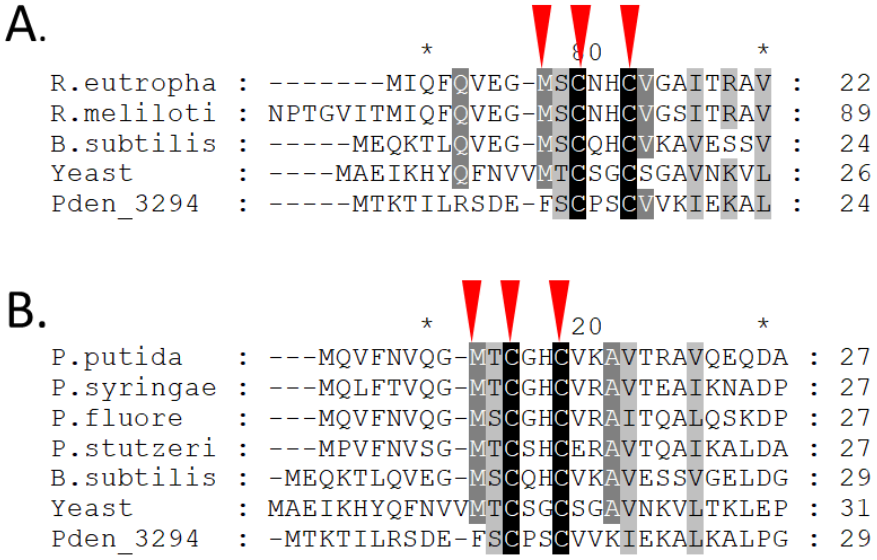

Figure 6.6: Alignment of the ATX1 like chaperones from β-proteobacteria (A)and γ-proteobacteria (B). ATX1-like proteins from *B. subtilis, S. cerevisiae*, *R. eutropha, R. meliloti* and Pden_3294 (A), alongside peptide sequences from *P. putida, P. synringae, P. flourescens* and *P. stutzeri* (B). All species share the common MXCXXC motif other than *Paracoccus* (highlighted by red triangles).

Denitrifying bacteria with ATX1-like proteins shown in Figure 6.6, are encoded in the genome alongside an ATPase and a putative MerR family regulatory protein. Conservation of this cluster of genes confirms ther role in Cu homeostasis. A transcriptome analysis under sub-toxic Cu conditions will be carried out to understand whether what the genes we have highlighted are the only method of regulating Cu in *P. denitrificans* or if there is a novel unidentifiable system.

6.3 Culturing PD1222 under sub-toxic copper conditions

Our aim in this experiment was to monitor Cu acclimation in *P. denitrificans* and not a cell death response to Cu.

We first established the appropriate sub-toxic concentration of Cu by identifying which concentration was toxic and then lowering this concentration until a comfortable growth rate was achieved, similar to that under Cu replete conditions. The minimal media in which *P. denitrificans* was cultured remained the same. The media was supplemented with 2 ml/l of the Cu deficient Vischniacs trace elements (section 2.1) and then further supplemented with the equivalent $CuSO_4$ to provide the

desired final concentration. All cultures started in a 10 ml LB grown overnight at 30˚C with spectinomycin, then pre-conditioned in 10 ml minimal media with a fixed Cu concentration for 24 hrs and finally into larger volumes, at high Cu concentrations, for the growth to be monitored. The volume of each aerobic culture was 50 ml in a 250 ml conical flask, and anaerobic cultures were 120 ml media in a 150 ml medicinal flask with a septum seal. Samples from the cultures were collected over a duration of 24 hours. Figure 6.7 shows growth curves for *P. denitrificans* grown under anaerobic conditions at increasing concentrations of Cu. Similar data under aerobic conditions is shown in Figure 6.8.

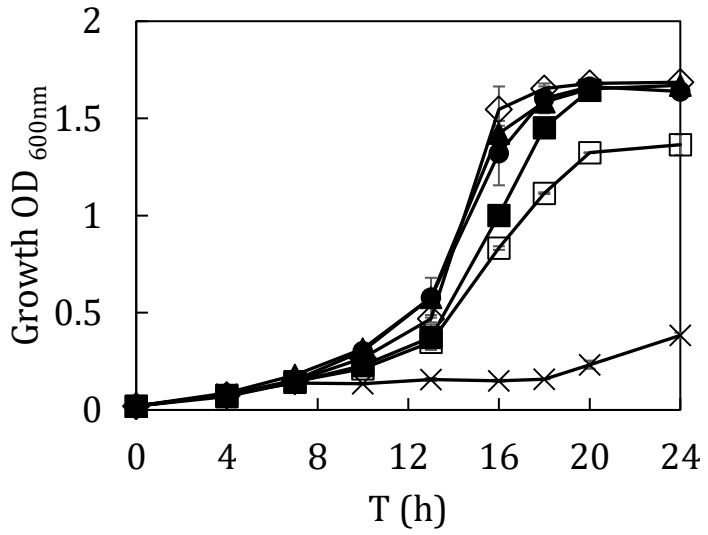

Figure 6.7: Growth of PD1222 anaerobically with increasing Cu in the media. Cells were cultured in minimal media supplemented with 0 V-S and varying concentrations of $CuSO_4$, 0 µM Cu (■), 13 µM Cu (◊), 25 µM Cu (●), 50 µM Cu (▲), 75 µM Cu (□) and 100 µM Cu (×), 30 ˚C, left static for 24 hours. Samples of the culture density (OD_{600nm}) were recorded at regular intervals.

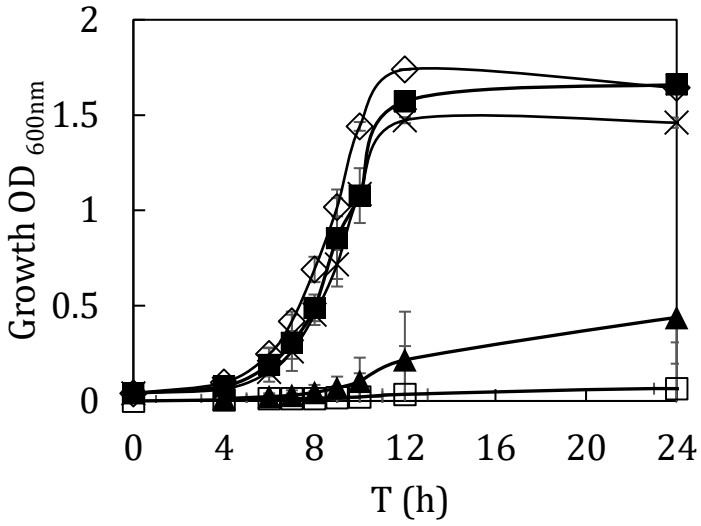

Figure 6.8: Growth of PD1222 aerobically with increasing Cu in the media. Cells were cultured in minimal media supplemented with 0 V-S and varying concentrations of $CuSO_4$, 0 μM Cu (■), 13 μM Cu (◊), 100 μM Cu (×), 125 μM Cu (▲) and 150 μM Cu (□), heated at 30 ˚C, 180 rpm for 24 hours. Samples of the OD_{600nm} were recorded at regular intervals.

The aerobic culture was able to tolerate a higher threshold of Cu than the anaerobic culture. In the absence of oxygen, Cu is likely to be found as the cuprous, Cu^{1+}, ion; the form which is involved in Fenton like chemistry and able to displace other metals and, therefore, more damaging to the cell. Based on this knowledge, it is reasonable to say *P. denitrificans* should be less able to handle excess Cu under anaerobic conditions. A severe reduction in growth was observed at Cu concentrations greater than 50 μM. The growth maximum fell to ~0.4 OD during stationary phase once the concentration of Cu reached 75 μM and *P. denitrificans* barely doubled in growth at 100 μM, see Figure 6.7. In the aerobic experiment however, a growth defect was apparent at concentrations above 100 μM Cu, see Figure 6.8. For these reasons the two Cu excess conditions selected for the RNA-Seq analysis were 50 μM for the anaerobic condition and 100 μM under the aerobic condition. The chosen concentrations generated a similar growth curve to PD1222 in the presence of our usual Cu replete, 13 μM Cu. This Cu replete condition was used as the baseline as a comparison in order to determine global changes to the *P. denitrificans* transcriptome during growth under Cu excess conditions.

6.4 RNA isolation and RNA-Sequencing methods

Cultures of *P. denitrificans* were grown under the conditions described in section 6.3 and supplemented with the given amount of Cu in the media; under aerobic conditions cultures with 13 μM and 100 μM Cu and under anaerobic conditions, 13 μM and 50 μM Cu. Biological triplicates were carried out for every condition. Cells were grown to early exponential phase (OD~0.4) and 30 ml of cells were transferred into 12 ml of ice-cold phenol-ethanol (95% v/v ethanol, 5% v/v phenol, stored at – 20 ˚C), then on ice. The mixture was left to incubate on ice for 30 mins and then centrifuged (4000 x g) for 10 mins at 4 ˚C. The supernatant was removed, and the cells were resuspended in any remaining supernatant, typically 0.5-1 ml. The resuspended pellet was transferred to a clean RNA free 1.5 ml tube and pelleted once more by centrifugation at 16 000 rpm for 2 mins. All supernatant was removed, and the pellets snap frozen in liquid nitrogen and stored at – 80 ˚C until RNA isolation was performed.

6.4.1 RNA Isolation

All equipment was treated with RNAse-ZAP (Ambion) to ensure the area remained as free of RNase as possible to limit RNA degradation. The cell pellets were thawed at room temperature for 5 mins. The basis of the following method uses components from the Promega SV total RNA kit. Lysosyme in RNase-free Tris-EDTA (100 mg/ml) was prepared and a total of 100 μl was used to resuspend the pellet. Cells were then incubated at 37 ˚C for 10 mins to begin cell lysis. 75 μl of lysis reagent was added to each tube, mixed by inversion, and to this another 350 μl of RNA dilution buffer was added, mixed and heated to 70 ˚C for 3 mins. The cell debris was pelleted by centrifugation at 11337 *x g*, 4 ˚C for 15 mins and the supernatant transferred to a clean RNase-free 1.5 ml tube supplied with the kit. To the supernatant, 200 μl of 100% ethanol (stored at – 20 ˚C) was added, mixed and transferred to a spin column supplied with the kit and centrifuged at 11337 x g for 30 s and the eluate discarded. The column was washed using 600 μl wash buffer and centrifuged as before for 30 s. A DNase stock mix was prepared; for each sample the following was added: 5 μl 90 mM $MgCl_2$, 40 μl DNase core buffer and 5 μl DNase. The DNase mix was added to the spin column matrix and incubated at 37 ˚C for 30 mins. 200 μl of a DNase stop solution was added to each column, which was then centrifuged at 11337 x g for 30 s. The column was washed using 600 μl wash buffer and centrifuged as before and washed once again with a further 250 μl wash buffer and centrifuged again. The column was

transferred to a clean RNase free 1.5 ml tube and to it 100 µl of RNase-free water was added and left to stand for 5 mins. The RNA was eluted by centrifugation of the unit at 4500 x g for 2 mins. A second DNase treatment step was performed using Turbo DNase kit (Ambion). To the 100 µl of RNA, 11 µl of buffer within the kit and 1 µl turbo DNase was added and incubated at 37 ˚C for 30 mins. 12 µl of the stop buffer was then added and agitated gently at room temperature for 5 mins. The mix was centrifuged at 11337 x g for 1 min to remove the DNase beads and the supernatant transferred to a clean RNase free tube for assessment of integrity by nanodrop and Experion Automated Electrophoresis platform (*BioRad*), using StdSens chips (*BioRad*) according to the manufacturer's manual, Figure 6.9. This analysis ensures the RNA is pure and of good enough quality for the sequencing and therefore not degraded. Defined bands in the region of 2600 and 1400 nucleotides relating to the 23S and 16S rRNA, respectively, were a clear visualisation that the RNA was ready for the RNA-Seq experiment.

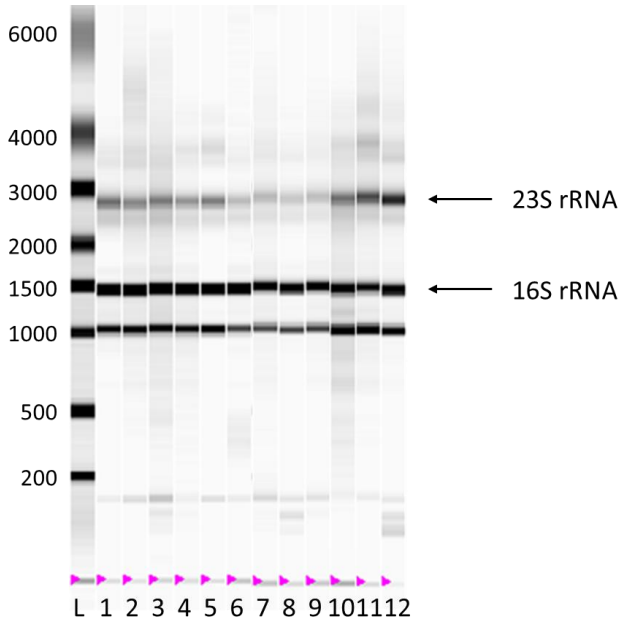

Figure 6.9: Experion RNA analysis to test the integrity of the RNA before RNA sequencing. All 12 samples were loaded, including a ladder (L). Triplicate repeats of the aerobic Cu replete (1-3), anaerobic Cu excess (4-6), aerobic Cu replete (7-9 and aerobic Cu excess (10-12). The abundant ribosomal RNAs are labelled.

6.4.2 RNA Sequencing

RNA was sent to Oxford Genomics for sequencing. The samples were treated with the Illumina ribozero rRNA treatment kit (bacteria) to remove ribosomal RNA and then libraries were prepared using the Illumina TruSeq stranded mRNA library prep kit to allow for 75 bp paired end reads. In total 12 libraries were prepared (4 growth conditions, 2 aerobic, 2 anaerobic and each in triplicate) and loaded onto a single lane on a Illumina HiSeq 4000 instrument which generated on average 25 million reads per sample.

6.4.3 Transcriptome analysis

All the work on the raw RNA-Seq data, including mapping the reads and the differential expression, was carried out by Dr Mark Alston at the Earlham Institute.
As this was a paired end experiment, the 2 fastq files obtained for each sample were interleaved and then the paired end read data was run in SortMeRNA to check the ribodepletion had worked efficiently, resulting in <2% rRNA, if done correctly. As the raw reads contain additional adapters used in the sequencing they must be removed. This was done using Trim_galore-0.4.2 paired end mode (phred-33, q20, length 30, stringency 5). This process typically removed ~0.2 % of the reads.
Reads were then mapped and quantified to the reference PD1222 transcriptome downloaded from the Ensembl Bacteria site as cDNA nucleotide sequences in FASTA format. The mapping was carried out using Kallisto v0.43.0, a newer alternative RNA-seq quantification program which aligns the reads and estimates transcript abundance ~two orders of magnitude faster than more traditional methods, including TopHat/Cufflinks approach [154]. The output was an abundance estimate for the transcripts as estimates counts and Transcripts Per Million (TPM).

The differential expression (DE) was carried out using the R (v3.4.0) statistical software Sleuth package. The first test for DE was a Wald-test and then the transcripts had to pass the more stringent, likelihood ratio test (LRT). A q-value of <=0.05 was accepted for a transcript being significantly differentially expressed under a given factor, in this case under Cu excess conditions. The 'b' value output is a measure of how the estimated counts are affected by the factor in question and can be used as an estimate of the fold change (values are in $\log_2$). Using these two values, q and b, a volcano plot was constructed for both aerobic and anaerobic growth datasets. A

positive 'b' value indicates genes have a higher expression under Cu excess and a negative value means the lower expression of the gene under Cu excess. Tables of the top DE genes are shown in the Appendix A, where *b* values are included along with transcripts per million (TPM) of the raw data counts before the DE was carried out. Often the *b* value is very similar to the fold change calculated by dividing the TPM in Cu excess by TPM in Cu replete. The expression of gene *pden_0970,* a housekeeping gene encoding the β subunit of DNA-polymerase III was analysed to ensure no significant up- or down-regulation was observed and that the data were good to use.

6.5 RNA Sequencing data

6.5.1 Anaerobic growth data

A volcano plot highlighting the 79 DE transcripts is represented in Figure 6.10. Those with positive log2 *b* values are 'UP' and are more highly expressed under Cu excess. Transcripts to the left with a negative *b* value are 'DOWN' under Cu excess conditions and therefore are transcribed more under Cu replete conditions.

Of the 5077 genes in *P. denitrificans*, 79 were differentially expressed in Cu excess conditions (1.56% of the total genome). Of these 79 genes, 70 were up-regulated (89%) and 9 were down-regulated (11%) under excess Cu. Over a fifth of the DE transcripts where either hypothetical proteins or those with domains of unknown function (22%) and therefore could not be assigned. Interestingly, 47% of the DE transcripts encoded proteins with an N-terminal signal sequence which demonstrates that nearly half of the encoded proteins were set up for export to the periplasm, membranes or for extracellular secretion.

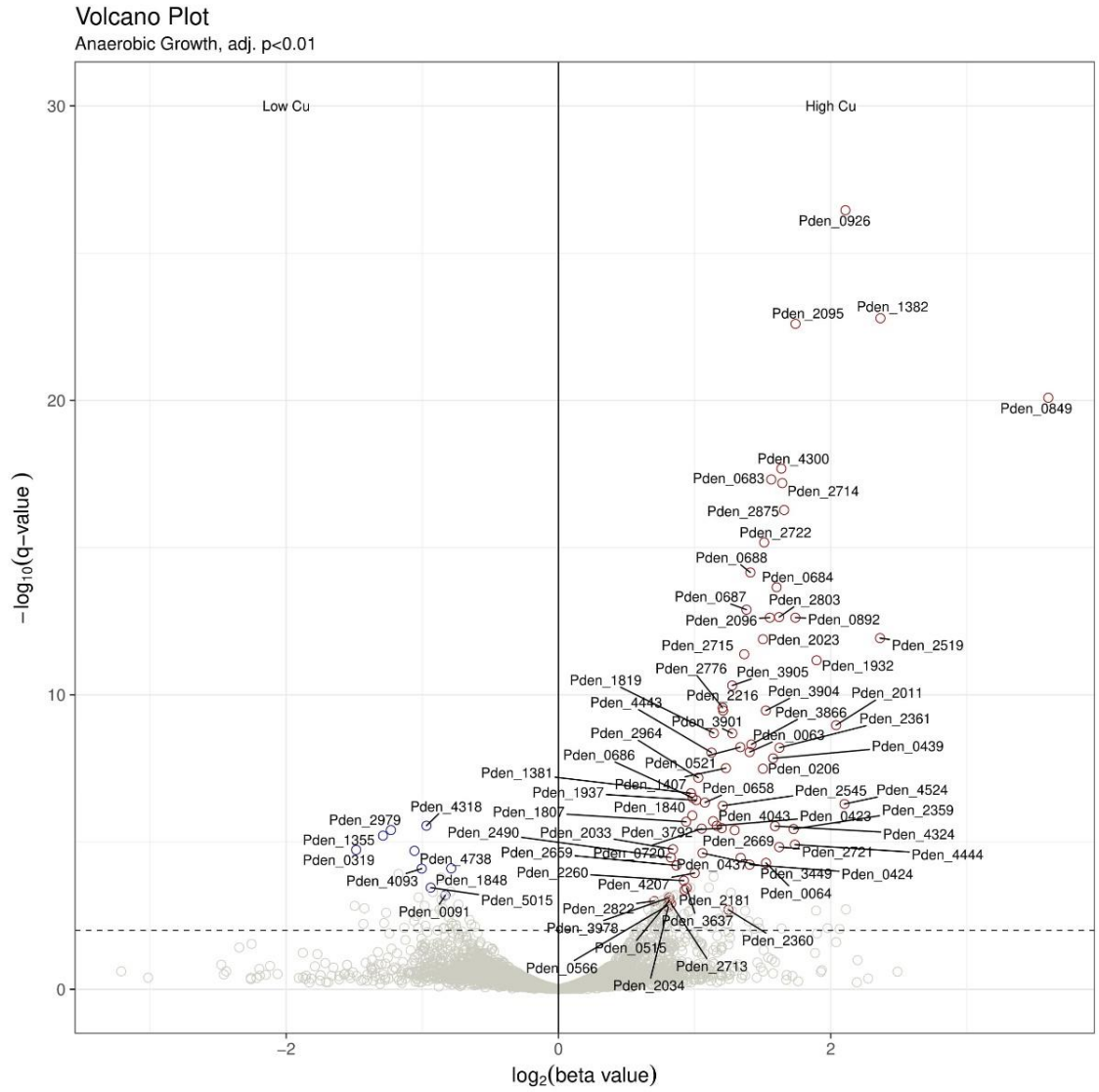

Figure 6.10: Volcano plot of the DE transcripts from the anaerobic data set, prepared by Dr M. Alston.

The 5 most up-regulated and 5 most down-regulared are described in Table 6.2, as red and blue, respectively.

Table 6.2

Gene ID	Role
Pden_0849	Putative outer-membrane protein
Pden_0926	Domain of unknown function
Pden_1382	Serine protease Do
Pden_2519	Hypothetical protein
Pden_4524	Hypothetical protein
Pden_1355	Mehtionine synthase (B12 independent)
Pden_2979	RNA polymerase, sigma 24 subunit, ECF subfamily
Pden_1848	Cytochrome *c* oxidase, *cbb*$_3$-type, subunit I
Pden_4318	Cytochrome c oxidase assembly protein CtaG/Cox11
Pden_4738	Periplasmic nitrate reductase

The transcripts annotated in the volcano plot in Figure 6.10 have been group into various categories including transporters, metabolism, oxidoreductases, biosynthesis, transcriptional/DNA related and miscellaneous and are included in Appendix A.

Analysis of the RNA-Seq data sets collected from Cu replete and Cu excess cultures of WT *P. denitrificans*, grown under anaerobic conditions, revealed 3 of the genes previously highlighted in section 6.2, are also up-regulated under Cu excess. Pden_0521, the P-type ATPase with 2 N-terminal Cu binding motifs indicative of a Cu transporter along with Pden_4443 and 4444, ScoB and PCu1, respectively, were all up-regulated in response to Cu excess. The latter genes have also been recognised previously during Cu and zinc limitation in *P. denitrificans* [28, 69] but not under Cu excess.

6.5.1.1 Up-regulated transcripts in Cu excess

Overall evaluation of the transcripts up-regulated shows there were no apparent signs of the Fenton like chemistry that could be expected to be induced by free Cu. SOD transcript up-regulation would have been expected if superoxide species were being produced. The two SOD genes, *pden_0518* and *pden_1634*, were more highly expressed in response to Cu excess, but only a fold change of 1.36 and 1.75 respectively, based on TPM reads. Importantly neither transcript made the list of 79 most DE and therefore was not among the most significant to change. Therefore, we maintain the response by PD1222 in the experiment was characteristic of the cell handling more Cu than is usually present and not the result of the negative impact from the redoc cycling of this metal which can catalyse superoxide formation.

From a general review of the 79 DE transcripts, 4 key groups of genes and one operon, were significantly up-regulated under Cu excess. Starting with genes encoding transporters, the most affected, with a *b* value of 2.49, was *pden_0849*, encoding a putative outer membrane protein, OmpA. Two further OmpA/MotB domain proteins, encoded by *pden_2875* and *pden_4324*, were also up-regulated under Cu excess, as was *pden_0687*, which sits among the operon to be discussed below. Based on the TPM value, a 12-fold increase was observed in *pden_0849*, while the remaining 3 transcripts were on average, up 3-fold.

OmpA in *E. coli* is an outer membrane protein which structurally has an N- terminal β barrel composed of 8 transmembrane helices as described by the crystal structure which also reveals the protein is an inverted micelle, with a hydrophobic surface and polar core [155, 156]. OmpA has been associated with the pathogenesis of *E. coli* K12 strains with a role in cell adhesion that allows the bacteria to invade cells and lead to sepsis [155]. OmpA is also a target for the innate immune system. After a cell is engulfed by neutrophils, it is subjected to oxidative and non-oxidative stress to cause cell death. These methods include releasing peptides from the neutrophil that permeabilise the membrane of the bacterium, through OmpA pores. OmpA is especially targeted by neutrophil elastase [155], a proteinase, though some septicaemic strains secrete OmpA in order to try and resist the neutraphil elastase by presumably saturating it before it reaches OmpA imbedded in the cell [155] . *P. denitrificans* is not an invasive bacterium but, perhaps the up-regulation of OmpA could be part of the stress response caused by Cu excess.

The expression of *pden_0687*, encoding another OmpA domain protein was up-regulated 3-fold in expression and sits among the up-regulated operon shown in Figure 6.11.

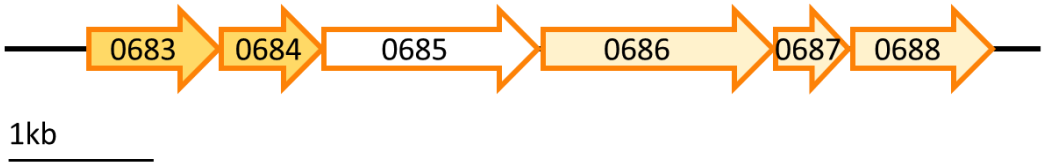

Figure 6.11: Operon identified in the anaerobic data set and upregulated under Cu excess. TolQ/ExbB protein (*pden_0683*), TolQ/ExbD protein (*pden_0684*), TolA (*pden_0685*), TolB (*pden_0686*), OmpA domain protein (*pden_0687*) and conserved hypothetical protein (*pden_0688*). The colour fill indicates the increasing fold change in expression, the greater the change, the more intense the colour.

The operon encodes elements of the Tol system: TolQ,R and TolB. The gene for the final element, TolA, was not highlighted in the DE but was up 3.6-fold based on TPM counts. The Tol proteins are necessary for outer membrane stability in Gram-negative bacteria. Studies in *E. coli* show mutants of the Tol system are hypersensitive to antibacterial agents and that they protect the membrane and periplasm. They have also been implemented in import of colicins, bacterial protein toxins [157], and some strains even export collicins to protect against invaders [158].

Interestingly as mentioned, just over half the DE transcripts have signal sequences which direct the protein for export to the periplasm. Maturation of some of these proteins, if bound to the membrane, will take place through the Lol system and consequently protein components of this system are highly expressed under Cu excess. LolC/E, the membrane component that releases lipoproteins from the inner membrane ready for export to the outer membrane via the lipoprotein carrier, LolA (*pden_1840* and *pden_2669*) were expressed more under Cu excess, 1.75 and 2.4-fold, respectively, based on TPM counts.

The second dominant group of up-regulated genes was the oxidoreductases. These included *pden_0063* and *0064*, encoding a molybdopterin protein and flavin oxidoreductase respectively, three DsbA oxidoreductases (*pden_1819*, *2095* and *3792*) and DsbD (*pden_0437*), which catalyses disulfide bond formation. All the above transcripts were up in the region of 2 to 3-fold in Cu excess. Disulfide bonds play an important role in folding and stability of proteins involved in transporting molecules in the cell, responding to environmental threats and assembly of the outer membrane [159]. DsbA is the thioredoxin like protein that functions as an oxidant to catalyse S-S bond formation. DsbB/D are redox transducers which sit within the innermembrane facing the periplasm and re-oxidise DsbA [159]. The role of DbsC is

as a disulfide isomerase, acting to correct any aberrant disulfide bond formation within the periplasm [159]. *pden_0437*, although a hypothetical protein, is annotated as DsbC in Pfam and was also up-regulated, appearing in the DE list and had a 2.5-fold increase in expression. The periplasm is an oxidising environment and the Dsb system is required to ensure the correct disulfide bonds are formed. Cu inside the cell is highly reactive with these available cysteines and can potentially bind to them or catalyse indiscriminate disulfide bond formation. Having observed an up-regulation of the Dsb system under Cu excess, this is consistent with the purpose of the system.

Two phage control/drug resistance proteins involved in response to a cellular attack were up-regulated; *pden_1381* and *1382*, encode an invasion associated protein and serine protease, respectively. One of the other most highly expressed genes in response to Cu was the serine protease (*pden_1382*) which was up-regulated 5-fold. Heat shock induced serine proteases have been implicated in protecting protein structures and even as far as enhancing bacterial survival under stress [160]. These proteases are important in the cell as they are involved in pathogenicity and cell viability and could be future antibiotic drug targets.

The transcript of peptidase M16 domain proteins encoded by *pden_2714* and *2715*, responded to Cu excess and have been annotated as proteins containing zinc. Whether these genes under optimum conditions are switched on by zinc and that mis-metalation by Cu has replaced zinc in transcriptional activation, could be a possible cause for the up-regulation of the genes. Alternatively, Cu stress could lead to dysfunctional proteins, and this promotes up-regulation of the peptidases in order to degrade such protein.

The biosynthesis of PQQ, a redox cofactor, mediated by *pden_2359-61* was also up-regulated [161]. PqqA is modified by PqqE (Pden_2359), a radical SAM protein, and PqqD (Pden_2360) serves as a chaperone to transport PqqA to PqqE, while PqqC (Pden_2361) acts as an oxidant to produce the final PQQ cofactor product [161]. Radical SAM enzymes contain at least one Fe-S cluster, which is generally sensitive to oxidative stress and perhaps directly to Cu toxicity. Indeed, it is known that a major route of Cu toxicity is to displace Fe from Fe-S clusters [162]. Up-regulation of PQQ biosynthesis may be a response to PQQ deficiency under Cu stress.

Genes involved in biosynthetic processes were also highly up-regulated. 3 heme containing proteins, the d_1 heme-binding protein, NirF (*pden_2490*), cytochrome b_{561} (*pden_2545*) and cytochrome *c* (*pden_1937*) were all up ~ 2-fold. NirF is an essential component of the d_1 heme biogenesis apparatus and *in vitro* studies have demonstrated its ability to bind the d_1 heme, in *P. pantotrophus* [73]. Once matured,

the unique d_1 heme is inserted into cytochrome cd_1 and is the site of nitrite reduction under anaerobic denitrifying conditions in *P. denitrificans*. The remaining *c*-type cytochrome up-regulated is involved in electron transport; one as a shuttle to, for e.g, the denitrification enzymes as a soluble periplasmic protein and the other, cytochrome b_{561}, is an integral membrane bound di-heme protein involved in regenerating ascorbate and reducing Ferric iron to be provided for transport across the membrane [163]. The fact that all these genes were up-regulated in response to excess Cu could be due to mis-metallation by Cu of the Fe sensing systems, or when the cell detemines that Cu is bound to a cofactor site it responds by producing more functional protein and cofactor, hense the transcription of the gene increases.

It is important to note that some of the most statistically relevant transcript changes were associated with hypothetical proteins. One transcript with the smallest q value and most significantly up-regulated was *pden_0926*. This protein is predicted to mature in the periplasm where it loses an N-terminal signal sequence to become a soluble protein with a mass of ~10 kDa. Of the putative 95 amino acids that remain, 10 are methionine residues; this could be consistent with a Cu binding function. A recent study in the cyanobacterium *Synechocytis* sp. PCC 6803, identified a Cu(I) binding protein called CopM, located in the periplasm and the extracellular space. With an affinity for Cu binding in the region of 10^{-16} M, CopM confers its Cu resistance mechanism by preventing the accumulation of Cu [164]. Interestingly this protein shares the same DUF 305 motif as Pden_0926 and is also a methionine rich protein, with methionine making up ~10% of the amino acid reidues. The DUF 305 motif is commonly found extracellularly according to Pfam [164], and therefore, the role of this motif could be to sequester Cu in the periplasm and the extracellular space to avoid accumulation. Nonetheless, up-regulation of this putative Cu binding protein is a sign of a Cu specific resistance mechanism in *P. denitrificans.*

6.5.1.2 Down-regulated transcripts under Cu excess

The remaining 11% of the DE transcripts were down-regulated under Cu excess and of these, some can be linked to Cu. Interestingly, two are related to C*c*O, specifically, *cbb*$_3$ oxidase subunit I (*pden_1848*) which is down and CtaG/Cox11 protein a maturation factor to C*c*O encoded by *pden_4138*. One possibility is that there could be less requirement for a Cu chaperone under Cu excess.

Other down-regulated transcripts included the B_{12} independant methionine synthase (*pden_1355*, *metE*) which possesses a catalytic Zn^{2+}. A study on *P. denitrificans* under Cu-limited conditions and therefore N_2O-genic, showed a higher level of expression

for this gene under such conditions; as a consequence it was found N_2O modulates vitamin B_{12} biosynthesis and B_{12} acts as a riboswitch, regulating *metE* [28]. The same riboswitch regulation of the B_{12}-independent methionine synthase of *Mycobacterium tuberculosis* has also been shown [165]. PD1222 cultured under Cu excess conditions, anaerobically, did not accumulate N_2O in the headspace (data not shown). Therefore, it is unlikely that N_2O was available to act as a riboswitch to this *metE* gene and therefore transcription is down. The alternative B_{12} dependant methionine synthase would have used all B_{12}, to maintain methionine synthesis. There are reports in *E. coli* that oxidative stress oxidises MetE and limits the amount of methionine in the cell [166]. In this experiment however, this is not the case as transcription of this methionine synthase was down under Cu excess and no other signs of oxidative stress or lack of methionine biosynthesis were observed in the up-regulated transcripts.

Finally, *napH* (*pden_4738*) is an integral membrane protein with 2, [4Fe-4S] motifs, each with 4 conserved cysteine residues and facing the cytoplasm as demonstrated in *E. coli* K-12 [31, 167]. The function of this protein is to transport electrons from ubiquinol to the periplasmic nitrate reductase. Cu interferring with the transctiption of this gene may be the reason for the lower expression.

All the genes discussed were down-regulated under Cu excess, but in most cases, by no more than 2-fold or more, based on TPM reads. The genes with the largest decrease in expression encoded hypothetical proteins such as *pden_0367*, *3352* and *4642*. *pden_3352* sits upstream of a cation diffuser facilitator family protein (Pden_3353), though the expression of the latter did not change.

The result from the anaerobic experiment was consistent with the initial BLAST finding: an absence of a conserved Cu trafficking system in *P. denitrificans* is still observed, with the exception of a potential Cu-transporting ATPase, with no chaperone counterpart and a putative periplasmic protein. Analysis of the genes identified in Table 6.1 with regard to the RNA-Seq data set showed only 3 genes responded to the rise in Cu: *pden_0521*, *4443* and *4444*. Two genes encoding MerR homologues and putative transcriptional regulators, *pden_3477* and *pden_4523*, were down, 0.57 and 0.7, based on TPM values, not quite a 2-fold reduction in expression. *scoA* and *pcu2* (*pden_2780* and *pden_0519*) were also unaffected whereas the homologues, *pden_4443*, and *pden_4444*, as mentioned were both up-regulated under Cu excess. The latter *scoB* and *pcuC* were up-regulated under Cu depleted conditions, so it is interesting that they also respond to Cu excess. Their secondary role could be to bind Cu when it is in excess and stop it from interacting in the periplasm as we know their homologues in other bacteria can bind Cu.

The bacterium responded to Cu excess by stabilising its periplasm and membranes, increasing the number of proteins which may combat Cu in the periplasm and switching on a Cu efflux ATPase. Periplasmic chaperones were also increased, which could bind Cu and mitigate the effects of free Cu within the cell. *P. denitrificans* also produced extra Dsb proteins to deal with aberrant disulfide bond formation in the periplasm, along with OmpA proteins which could be produced by *P. denitrificans* in response to an invasive attack. Finally, a methionine rich, periplasmic, Cu protein was identified as a hypothetical protein, encoded by *pden_0926* but could act as a part of a Cu resistance mechanism.

With this being an anaerobic experiment, at the point the cells were harvested, they would be moving into exponential phase and switching on the denitrification apparatus and particularly N_2OR, which would require Cu atoms from the two periplasmic chaperones mentioned. Therefore, this may limit the amount of Cu accessing the cytoplasm if Cu was being channeled to N_2OR. The expression of N_2OR and its gene cluster did not rise above 2-fold based on TPMs. The regulatory elements *nosCR* remained ~ 1-fold whereas *nosZDFYLX* all increased in expression, as shown in Figure 6.12.

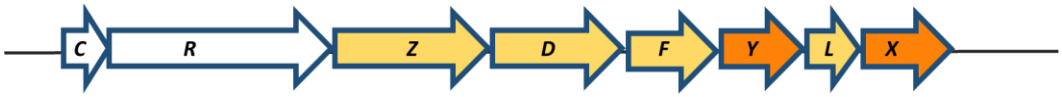

Figure 6.12: The *nos* gene cluster and the fold change increase in expression under Cu excess conditions. Genes with no change are white, between 1 and 1.5-fold increase yellow, and between 1.5 and 2.0-fold increase, orange.

6.5.2 Aerobic growth data

The same analyses were applied to the transcripts resulting from the aerobic data set, however, a more sensitive q-value <=0.001 was used to reveal 559 transcripts that were differentially expressed. The volcano plot in Figure 6.13 highlights the 75 most DE transcripts. In comparison to the anaerobic plot, many genes are down-regulated under Cu excess in the presence of oxygen within the media. Of these 75 genes, 16% were up-regulated under Cu excess and 84% were down-regulated. The percentage of proteins with an N-terminal signal sequence to direct the protein out to the periplasm was less than the previous experiment, at 15%. In the presence of oxygen, *P. denitrificans* could tolerate 100 µM Cu in the media, twice as much as the anaerobic

culture. Overall many more genes were differentially expressed than in the anaerobic experiment but, of the 75 most DE, the majority of DE transcripts were significantly less expressed under Cu excess. As before, to check for Fenton like chemistry, expression of the 2 SODs in PD1222 was analysed. Both *pden_0518* and *pden_1634* were up-regulated (2.1 and 1.91 -fold increase in Cu excess respectively), based on TPMs. This implies superoxide species were likely to have formed, consistent with an increasing concentration of free Cu and the presence of oxygen in these experiments, producing reactive species.

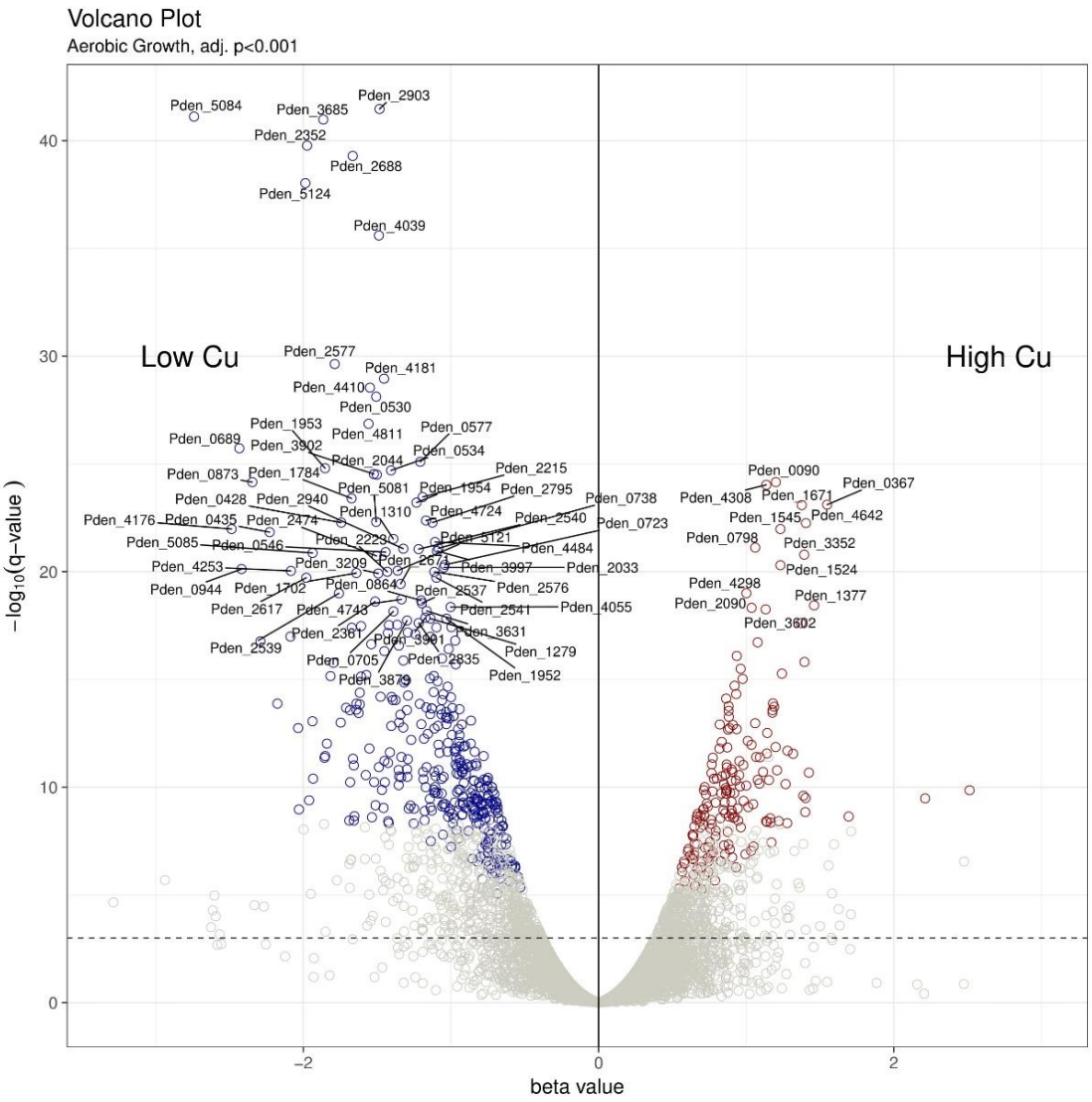

Figure 6.13: Volcano plot of the DE transcripts associated with the aerobic growth data set, prepared by Dr M. Alston.

When the conditions were chosen for this experiment, 100 μM Cu was deemed suitable, as the growth rate at the early exponential phase ($OD_{600\,nm}$, 0.4) was similar to that of Cu replete conditions (Figure 6.8). However, the stationary phase of growth and maximum OD was lower than for lower concentrations of Cu. This lower cell density means fewer cells reach the stationary phase of growth. Cu was the only varied factor and it is most likely the leading contributor to the lower growth, as neither carbon or nitrogen were limited. At 125 μM Cu, the cells struggled to grow, and in retrospect, a lower concentration of Cu may have been better. Having compared the logarithmic growth curves, 13 μM and 100 μM Cu media shared the same exponential phase indicating they were growing as expected but beyond this concentration, the exponential phase was affected, Figure 6.14.

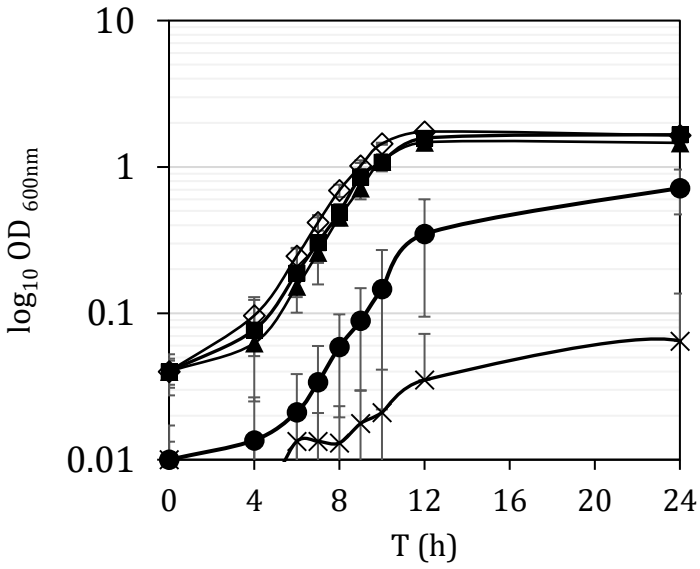

Figure 6.14: Log growth of PD1222 grown aerobically under increasing concentrations of Cu. Cells were cultured in minimal media supplemented with 0 Cu VS and varying concentrations of $CuSO_4$, 0 μM Cu (■), 13 μM Cu (▲), 100 μM Cu (◊), 125 μM Cu (●) and 150 μM Cu (x).

The 5 most up-regulated and 5 most down-regulared are described in Table 6.3, as red and blue, respectively.

Table 6.3

Gene ID	Role
Pden_0367	Hypothetical protein
Pden_1377	Redoxin domain protein
Pden_1671	Extracellular solute binding protein, family 5
Pden_3352	Domain of unknown function
Pden_4642	Hypothetical protein
Pden_0689	tRNA-lysidine synthetase
Pden_0873	Ribonuclease P protein component
Pden_0944	Transcriptional regulator, TetR
Pden_4176	HAD-superfamily hydrolase, superfamily IA, variant 3
Pden_5084	2-keto-3-deoxygluconate kinase

6.5.2.1 Down-regulated transcripts under Cu excess

A vast proportion of the down-regulated transcripts encoded proteins involved in transcriptional regulation and processing of DNA/RNA including the Rec proteins, RecF and RecN, Pden_2835 and Pden_4484 respectively. These proteins work to repair double stranded breaks in DNA. Studies in *E. coli* have shown RecN is necessary for DNA repair and suppressing DNA degradation, through an, as yet, unknown mechanism [168]. Down-regulation of these genes in Cu excess could mean they would not be able to fulfil their role in the cell in repairing DNA and thus damage was done to the DNA.

Other notable down-regulated transcripts include a number of one component transcriptional regulators (*pden_0723*, *0944*, *1784*, *2940*, *3991*), belonging to the TetR family (TRF) [169]. These regulators play an important role in many aspects of bacterial physiology from antibiotic resistance and toxins to metal homeostasis to catabolism of sugars and amino acid metabolism. They accordingly respond to a range of ligands to transduce signals, resulting in repression or activation [169]. The putative transcriptional regulators mentioned above including a catabolism/arabinose regulator, a regulator of virulence and antibiotic production (AraC), a regulator of quorum sensing (LuxR) and a LysR, a regulator of cellular

processes including cell division [170], methionine synthesis [171] and transporters involved in metal homeostasis [172], to name a few. Importantly all of these genes are suppressed by Cu excess, which results in them losing their activity, either activiating or repressing the transcription of their target genes.

A cluster of genes involved in porphyrin metabolism also presented a lowered expression under Cu excess, including *pden_2537*, *2539*, *2540* and *2541* (Figure 6.14). The protein products of these genes play a role alongside other proteins in transforming uroporphyrinogen I, a substrate in the heme biosynthesis pathway, into ultimately, vitamin B_{12} coenzyme. Down-regulation of these transcripts could be due to Cu inhibition of the pathway that regulates their expression.

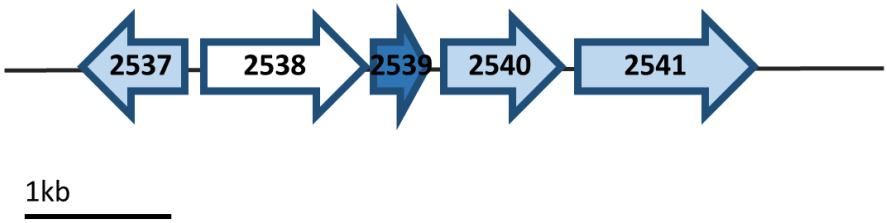

Figure 6.14: The gene cluster down-regulated and involved in porphyrin metabolism under Cu excess, aerobic growth conditions. The darker the blue, the lower the expression under Cu excess.

Of the genes in Table 6.1, the transcription of only one was affected by the increase in Cu. Pden _1842, a heavy metal translocating P-type ATPase with single N terminal MXCXXC motif, was expressed 3-fold less under Cu excess. Cu is a vital metal in aerobic respiration, at the active site of C*c*O. The ATPase described could be involved in suppling Cu to CcO. As the expression of this transporter is down, it would indicate that the target to which it could transport Cu, is not necessary under aerobic conditions.

The transcript with the lowest q value was associated with *pden_5084*, which was expressed 7-fold lower in presence of Cu excess. This gene encodes a 2-keto-3-deoxygluconate kinase involved in glucose metabolism [173].

6.5.2.2 Up-regulated transcripts under Cu excess

Although the two SOD genes were up-regulated, they did not reach the top 75 of most DE transcripts. Once again many of the DE transcripts were hypothetical proteins, in fact, over half of the up-regulated transcripts were hypothetical proteins with no clue as to their role. This includes *pden_0367* which produces a 98 aa long soluble cytoplasmic protein based on a lack of a signal sequence, and is up nearly 3-fold, yet, with no homology to any protein, it is hard to distinguish its role.

A variety of roles were represented by the few up-regulated transcripts remaining. The protein MetZ, encoded by *pden_4298*, is involved in cysteine and methionine metabolism, catalysing the formation of L-homocysteine from a serine derived molecule and hydrogen sulfide as the sulfur donor. Finally, a histone family protein involved in nucleoid restructuring was up-regulated, perhaps in response to DNA damage by oxidative species.

The aerobic data set failed to identify any transcripts which could be linked directly to Cu detoxification/trafficking.

6.6 Analysis of Δ*pden_0521*, Δ*pden_0926*, Δ*pden_4443* and Δ*pden_4444* strains under Cu excess conditions

We were particularly interested in four genes which were up-regulated in the anaerobic Cu excess data set in section 6.5, these were: *pden_0521*, the putative Cu transporter, *pden_4443* and *pden_4444*, ScoB and PCuC Cu chaperones, and finally *pden_0926*, the methionine rich putative periplasmic protein.

Δ*0521* (PD2504) and Δ*0926* (PD2506) complete gene deletion mutants were prepared, each using the same double recombination knock out strategy used in Chapter 3. Further details on the mutants is also found in 2.12. Two further mutants were supplied by Dr M. Sullivan and were deficient in *pden_4444* (PD2305) and *pden_4443* (PD2306). Each mutant was cultured in Cu replete and Cu excess media, under anaerobic and aerobic conditions as described in 2.1.1 and 6.3.

6.6.1 Aerobic growth

As a matter of completeness, aerobic studies were included in the analysis of the mutants, using 100 µM Cu as the Cu excess concentration in the media (Figure 6.15).

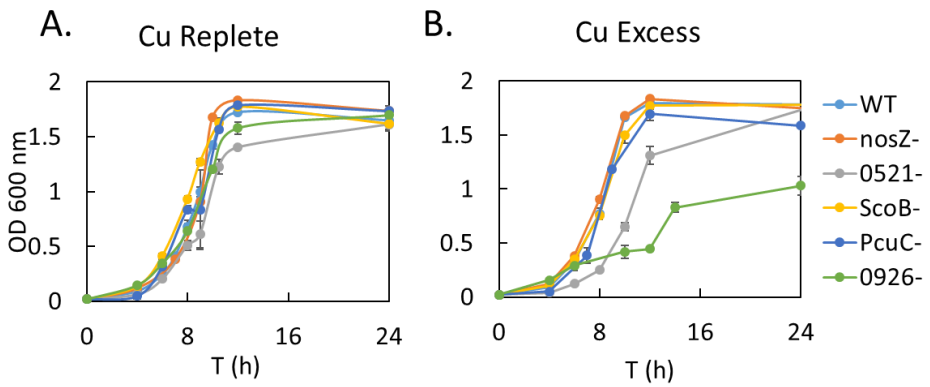

Figure 6.15: Aerobic growth of various *P. denitrificans* strains, wild type, Δ*nosZ* (PD2303), Δ*0521* (PD2504), Δ*ScoB* (PD2306), Δ*PCuC* (PD2305) and Δ*0926* (PD2506), in 50 ml minimal media under Cu replete (A, 13 µM Cu) and Cu excess (B, 100 µM Cu) conditions. Using the same approach as section 6.3, supplementing media with VS without Cu and then $CuSO_4$ to the desired concentration. 3 biological replicates were carried out and SE is plotted.

The four mutants in this analysis were not highlighted in the aerobic RNA-Seq dataset nevertheless, both Δ*0521* and Δ*0926* displayed a growth defect during aerobic growth under excess Cu. Previous analysis of *pCuC* and *scoB* mutants has shown their phenotype under Cu limitation is able to be chemically complemented with Cu [28], so it was unsurprising to not identify a phenotype under Cu excess. Δ*0521* gave a delayed lag phase under Cu excess and only reached the same maximum growth as the WT strain after 24 hours of growth. The Δ*0926* strain did not reach an OD higher than 1 after 24 hours of growth under Cu excess; therefore, the growth of this strain was sensitive to Cu.

6.6.2 Anaerobic growth

The same experiment was carried out under anaerobic conditions, using 50 µM Cu as the Cu excess concentration, Figure 6.16. In the RNA-Seq experiment, all 4 transcripts of the genes now mutated out of the genome were up-regulated in the RNA-Seq experiment.

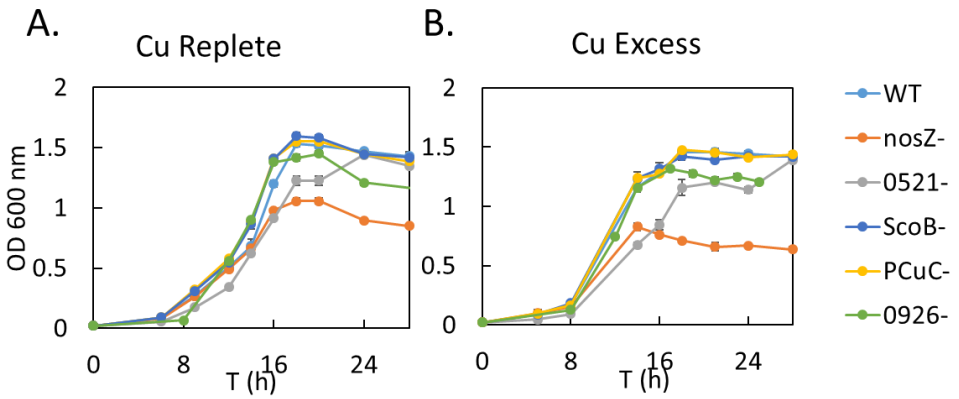

Figure 6.16: Anaerobic growth of various *P. denitrificans* strains, wild type, Δ*nosZ* (PD2303), Δ*0521* (PD2504), Δ*ScoB* (PD2306), Δ*PCuC* (PD2305) and Δ*0926* (PD2506) in 200 ml minimal media (in a 250 ml Duran bottle) under Cu replete (A, 13 µM Cu) and Cu excess (B, 50 µM Cu) conditions. Using the same approach as section 6.3, supplementing media with VS without Cu and then $CuSO_4$ to the desired concentration. 3 biological replicates were carried out and SE is plotted.

The Δ*pCuC* and Δ*scoB* strains were once again insensitive to Cu excess. The Δ*0521* strain displayed a similar growth pattern to the aerobic data, exhibiting an extended lag phase with slower exponential growth until it reached the stationary phase, approximately 8 hours after the WT strain. The same was true for both Cu replete and excess conditions and therefore is not strictly more sensitive under Cu excess. But this does mean this gene is likely to have a role in trafficking Cu. The Δ*0926* strain was able to grow identically to the WT strain regarding the initial lag and exponential phase, and it was only during stationary phase of growth that the variation occurred. The Δ*0926* mutant had a lower maximum OD than the WT strain consistently across both Cu regimes and it would seem the strain struggled to maintain cell density. N_2O analysis of the headspace was necessary as all the translated products of the genes studied were involved in potentially binding Cu, therefore it was interesting to

determine whether any of them could be potential chaperones to N_2OR during anaerobic respiration, by detecting an N_2O-genic phenotype, Figure 6.17. As expected the Δ*nosZ* strain produced N_2O. The WT PD1222, Δ*pcuC,* Δ*scoB,* and Δ*0926* did not produce any N_2O that was detectable by GC analysis. In the Δ*0521* strain, small amounts of N_2O were detected in the headspace, typically <0.1 mM under Cu replete and <0.15 mM under Cu excess. Even though this was a small fraction of what we expect from a Nos$^-$ phenotype, the fact that it was even detected is interesting as no N_2O was detected by the GC in all other mutants. Pden_0521 is a putative P-type ATPase, a protein which may have a role in translocating Cu, and maturation, of inner membrane enzymes such as C*c*O in *Rhodobacter* and *Bradyrhizobium*. This will be discussed further in the final discussion.

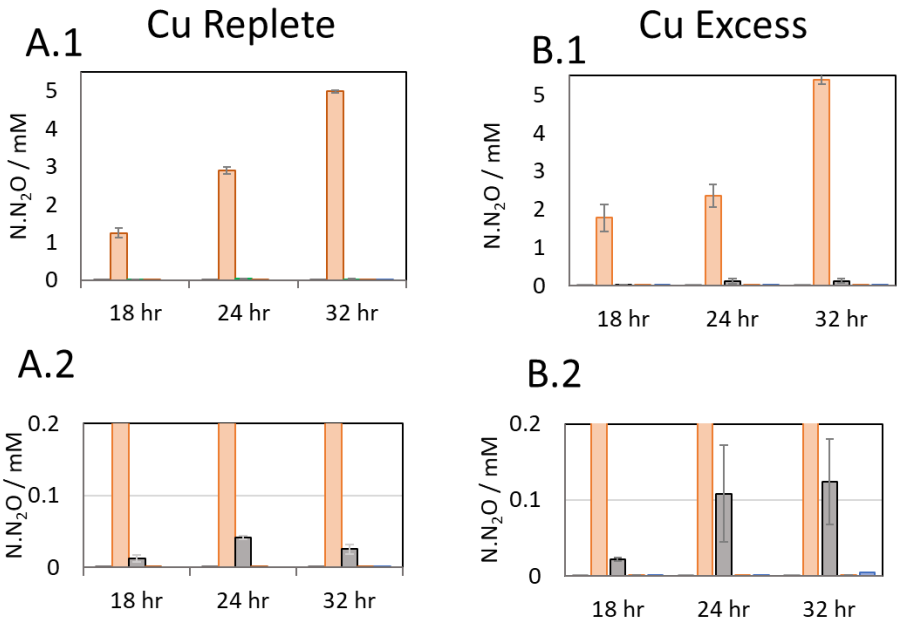

Figure 6.17: Headspace N_2O analysis of cultures shown in Figure 6.16, under Cu replete (A) and Cu excess (B). For lower concentrations of N_2O detected, i.e <0.1 mM, see A.2 and B.2. The Δ*nosZ* strain (orange) and Δ*0521* (grey) are clearly visible. The other samples strains did not produce N_2O at a concentration which could be clearly detected by the GC (Δ*pcuC*, Δ*scoB*, Wild-type, Δ*0926*).

6.7 Discussion

Our initial hypothesis was that by increasing the level of Cu within the cell significantly, we would elicit a transcriptional response from *P. denitrificans*, which would provide information on how this organism maintains Cu homeostasis.

This study in *P. denitrificans* has shown Cu excess has a greater impact on the transcriptome under aerobic conditions where 559 transcripts were DE, compared to the 79 DE transcripts under anaerobic conditions. The majority of DE transcripts in the anaerobic data set were up-regulated in response to Cu excess, whereas in an oxygenated environment the majority of transcripts were down-regulated.

Four genes that encode proteins predicted or known to bind Cu in bacterial cells, responded to Cu excess and were identified under anaerobic conditions: Pden_0521, a P-type ATPase Cu transporter and 3 periplasmic putative Cu chaperones, Pden_4443 and Pden_4444, ScoB and PCuC respectively, and the hypothetical protein, Pden_0926. A small proportion of the total DE was down-regulated and included a cbb_3 oxidase maturations factor, CtaG/Cox11, and the B_{12} independent methionine synthase, MetE. In contrast, the aerobic data did not reveal a Cu transporter or chaperone that could be associated with a Cu resistance mechanism.

The DE transcripts from each experiment were grouped into categories and the number of up- and down-regulated transcripts, under aerobic and anaerobic conditions, are presented in Figure 6.18. Across the 2 experiments, the number of hypothetical and biosynthesis based DE transcripts were similar yet, where the anaerobic experiment results show many within these categories were up-regulated, the anaerobic experiment was the opposite. For example; 10 biosynthetic transcripts were up-regulated in the anaerobic experiment whereas, 8 transcripts were down-regulated in the aerobic set. The same is true for many of the categories and can be visualised in Figure 6.18.

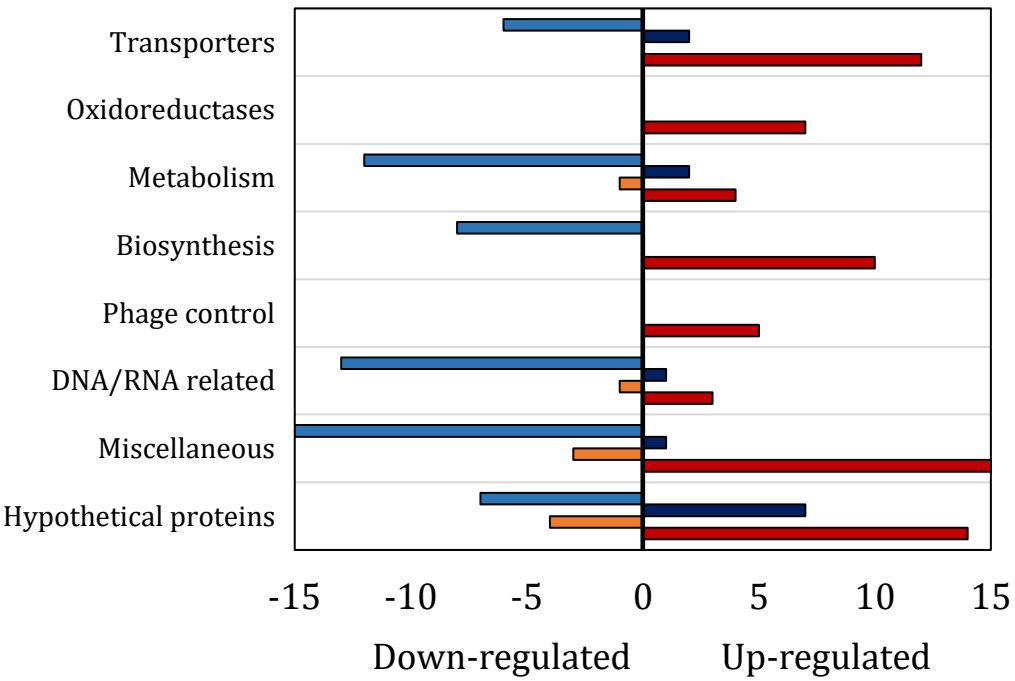

Figure 6.18: A representation of the number of DE transcripts in each category from either the anaerobic RNA-Seq dataset, up-regulated ( ), down-regulated ( ), or the aerobic dataset, up-regulated ( ), down-regulated ( ).

One unexpected result was the absence of a DE oxidoreductase transcript under aerobic conditions. Four oxidoreductases were up-regulated in the absence of oxygen, to deal with the activity of free Cu(I) within the periplasm. Perhaps the presence of Cu(II) and oxygen catalysing Fenton-like chemistry is more dominant than the power of Cu to interact and cause erroneous disulfide bond formation.

Very few transporters were identified in the aerobic dataset and none of which were related to metal transport. The transporters appeared to be involved in moving carbon/nitrogen substrates, e.g. Pden_4039, a nitrate/sulfonate transporter, and Pden_4181 a transporter of mannitol/sorbitol, and also the amino acid transporter, Pden_5081. Nonetheless, all of these were down-regulated and would, therefore, result in less transport of the substrate. In comparison, under anaerobic conditions, the up-regulated transporters were involved in stabilising the periplasm and outer membrane including the Tol system and 3 OmpA proteins along with the Cu transporter mentioned (Pden_0521). The anaerobic dataset also provided signs of a response within the cell to what it may think is an external attack and therefore stress upon the bacterium, in response to Cu.

Oxygen did, however, induce changes to 14 transcripts with links to DNA and RNA compared to only 4 DE transcripts in an anaerobic environment. This suggests perhaps oxidative stress may have damaged some of the DNA. However, instead of the machinery being up-regulated to repair the issues, all these genes were down-regulated. Metabolism was also largely affected in the presence of oxygen with many genes down-regulated, apart from MetZ, a protein involved in methionine and cysteine metabolism.

It is noteworthy that RNA-Seq analysis of the *Pseudomonas aeruginosa* transcriptome, employing the same method of inducing a response with sub-lethal amounts of Cu, was able to identify common Cu detoxification systems under aerobic conditions. These included the well-recognised CopZ/CopA, chaperone/transporter system along with CopR/S and CueR, as transcriptional regulators sensing Cu in the periplasm and cytoplasm respectively [174]. All these genes were highlighted using 0.5 mM Cu, fives time the concentration which *P. denitrificans* can tolerate.

Interestingly, another study in *Enterococcus faecilis* V583 looked at the toxic effect of Cu^{2+} among other metals on the transcriptome using a microarray study, but it did not find a common mechanism as that mentioned in the *P. aeruginosa* study. Instead, sub-lethal Cu repressed the transcription of a number of genes encoding proteins involved in DNA metabolism and cellular processes but up-regulated genes with a function involved in a cell envelope response and amino acid biosynthesis [175]. This result bears some similarity to our experiment under aerobic conditions regarding the majority of the metabolism transcripts being down-regulated and lack of Cu detoxification mechanism. In the *E. faecilis* study, the Cu concentration was much lower than the *Pseudomonas* study, and set to a similar level as ours, at 50 μM - a figure higher than the 16 μM Cu mark which is toxic to human serum [175] and which *E. faecilis* would normally encounter.

E. coli is an enteric bacterium with multiple Cu export systems in place that enables it to deal with Cu stress. A model was recently proposed that upon bacterial infection, the host uses a Cu intoxication strategy to reduce the intracellular survival of pathogens [176]. The main impacts on the cell from excessive Cu(I) would therefore be redox cycling, reacting with ROS and displacement of key metals such as solvent accessible Fe from Fe-S clusters, disrupting metabolism and eventually lead to cell death [162, 176]. Thus, Cu detoxification systems are likely to be an important factor in supporting pathogenic strains to establish infection and overcome a host attack. *P. denitrificans* is not a pathogen, and so it is perhaps expected that it does not contain Cu resistance mechanisms.

P. denitrificans may not encounter sufficiently high concentrations of Cu in the environment and , therefore, the survival advantage associated with these pathways in toxic Cu environments would not be necessary and evolutionarily not preferred.
We must first appreciate the environment in which *P. denitrificans,* a soil bacterium, is found, in order to understand how likely, it is to encounter Cu. 40 % of European agricultural soils are depleted in Cu and other trace metals due to aggressive farming practices with factors such as soil pH, organic matter and moisture affecting the availability of Cu [74]. Alternatively, some soils have excessive amounts of Cu, the primary source of which is the fertiliser used to improve crop yield. Soil treated with pig slurry can have 6 times the amount of free Cu compared to those treated with mineral fertiliser [177]. Using animal waste-based fertilisers increases the concentration of trace metals such as Cu and Zn in the soil. These metals are found in animal feed and once ingested are complexed by organic molecules then removed as waste [178]. Trace metals are not absorbed by plants to a great extent, and therefore the metals remain within the soil [177]. A study has also shown that metal stress within a soil can favour certain metal-resistant bacterial populations, providing them the capacity to make use of the metal and colonise extensively [179]. One example is Cu contaminated soil in wheat residue decomposition, which was dominated by β-proteobacteria that were capable of survival and degrading the soil organic matter [179], far more than α- and γ-proteobacteria. If PD1222 were in these Cu rich soils would they survive or succumb to the toxic effects of Cu? The latter is the most likely, with no system to support Cu resistance.

As mentioned, *P. denitrificans* may be present in Cu limited or rich soil, but no one complete mechanism for how it exploits, and imports Cu was shown here. Nevertheless, we know that Cu is vital for respiratory complexes within the cell, therefore, there must be a method to extract and import Cu from the soil and then direct it to the correct intracellular destination. Clearly the bacterium is amongst Cu in the soil as it needs it to survive, therefore it must have a method to reduce the impact of free Cu once internalised, i.e. chaperones, many of which have been identified in this work. The primary role would therefore be for the cell not to detoxify under such conditions, but to use the Cu chaperones efficiently to direct Cu to necessary destinations. Work in this thesis has identified a Cu binding, putative outer membrane chaperone, NosL, which is involved in maturing N_2OR under anaerobic conditions. If there is little Cu to import from the environment, then only a few Cu chaperones would be needed to prioritise and optimise the use of Cu in the periplasm,

for the purposes of respiration. The use of a Cu scavenger, a chalkophore, would also be an option for the direct import of Cu into the periplasm, where it may remain bound until it finds a protein in need of Cu. A porphyrin like molecule secreted by *P. denitrificans* has previously been identified in the growth media in a separate study. If Cu deficient cells are presented with this Cu bound chalkophore, then growth is restored to that under normal Cu concentrations [151]. Coproporphyrin III, the chalkophore of interest, is a by-product of heme synthesis though it is not understood how this system is regulated to sense Cu deficiency. *HemE,* Pden_3629, produces one of the precursors to the chalkophore mentioned but was not up-regulated in the Cu limited microarray experiment (data by Dr M Sullivan, not shown). In order to complement the phenotype of Cu limited growth using this metal bound chalkopore, an efficient uptake mechanism for this metal bound porphyrin, is necessary. *P. denitrificans* could have adapted this pathway in response to an environment undersupplied with Cu, though, no system was highlighted in the microarray experiment. We know *P. denitrificans* are excellent Cu scavengers as we mentioned in Chapter 4; they could extract residual Cu off the bottles if high Cu media had been previously used in them. A putative TonB outer membrane import protein could accrue Cu to the periplasm but there it would remain, most likely bound to Cu chaperones and may never be translocated across to the cytoplasm in substantial amounts. Any necessary number of atoms of Cu could be presented to the cytoplasm in a tightly regulated manner to mature any cupro-proteins, but if not, the periplasmic Cu chaperones mentioned could play the role in channelling Cu to its final respiratory enzymes in the periplasm but never to the cytoplasm. Yet, we have shown using a mutational study, *pden_0521* is important for transporting Cu from the cytoplasm to the periplasm, so there must be a dedicated system directing Cu to the cytoplasm. Essentially, we have identified parts of a common Cu regulatory systems. It may be that Cu detoxification systems are present, but that they are not regulated at a transcriptional level by Cu and thus they did not appear in our RNA sequencing dataset. The Cu detoxification genes may be constitutively expressed in *Paracoccus denitrificans*, and the regulation may take place post transcriptionally.

The final alternate explanation for how *P. denitrificans* treats an excess of Cu in the cell, could be a simple fact there is a novel Cu trafficking system present specific to this phylum. As mentioned, the full ATX1 like system was found in 2 other α-proteobacteria, the marine bacterium *D. shibae*, and the photosynthesising *R. capsulatus,* two bacteria found in very different environments to *P. denitrificans.* Yet, searches in β- and γ-proteobacteria searched unearthed the well- known Cu

trafficking systems, including *Pseudomonas* which was studied by RNA-Seq under sub-lethal Cu concentrations to further prove this. We did not find the same systems by hoping to observe induced transcripional changes in response to Cu excess, but as mentioned before, such a system could be constitutively expressed and would therefore not have appeared in our study.

In the anaerobic RNA-Seq experiment, the bacterium responded by up-regulating 4 transcripts which were of interest to us: *pden_0521*, *4443*, *4444* and *0926*. Each gene was removed from the genome in order to appreciate how important they are in the resistance to Cu excess. Notably, both *pden_4443* and *4444* (*scoB* and *pCuC*) mutants were not sensitive to excess Cu and therefore presented the same growth as WT PD1222. Even though these genes are up-regulated under both Cu limitation and excess, their role could be two-fold, in that during limitation these proteins work as high affinity chaperones, but under Cu excess they act as a Cu sink, thought it would seem, not an essential one. The two remaining genes were of interest due to their novelty. *pden_0521* was attractive after the recent publication describing how the *copA* gene in *E. coli* is transcribed and translated to generate both the Cu transporter and chaperone [134]. This made us ask whether *pden_0521* can do the same and produce the chaperone that is missing from the PD1222 genome, from this gene, in order to assist with Cu resistance in PD1222. We did not observe a significant enough phenotype in the mutant of *0521*$^{-}$ to respectfully say its removal was lethal to *P. denitrificans,* therefore it is unlikely to be the sole Cu trafficking centre in *P. denitrificans*, yet it still plays a role in transporting Cu from the cytoplasm to the periplasm (based on homology with other CopA, P-type ATPases). Investigation into the possibility of ribosomal frameshifting in this gene will be interesting and necessary. An alternative role for this P-type ATPase could be in the maturation of *Cc*O in particular, caa_3 and cbb_3. CtpA, a P-type ATPase in *Rhodobacter,* aquires and delivers Cu to Cu requiring enzymes in the membrane, and noticeably, mutants of this gene showed a decrease in caa_3 and cbb_3 activity [72]. It has been shown that the caa_3 oxidase is necessary for aerobic respiration in *Paracoccus* and that the high affinity cbb_3 oxidase is necessary for the switch from aerobic to anaerobic respiration[180]; both oxidases contain Cu. If indeed the role of Pden_0521 is to traffic Cu to these oxidases, their impaired activity could lead to the delayed growth, while an alternative, less efficient system is switched on, and hence, the slower exponential growth phase in the Δ*0521* mutant. It has also been mentioned that this form of ATPase may mature N_2OR [181] and we detected N_2O in the headspace of the mutant,

albeit a very small amount, therefore, could it be that this protein plays a subtle role in shuttling Cu from the cytoplasm to periplasmic chaperones that mature N_2OR. Based on the lack of a severe Nos^- phenotype, Pden_0521 it is not the sole route for Cu to access the periplasm but could be a route used to alleviate the cytoplasm of Cu, increasing the periplasmic Cu level and therefore fully maturing N_2OR. The analysis of the *0926* knock out also showed it was not lethal to *Paraoccus* under anaerobic conditions, but a noticeable phenotype was observed under aerobic conditions. In the presence of oxygen, the activity of free Cu would be enhanced through production of ROS, and therefore is a likely reason for such a phenotype. This CopM-like protein produced a minor phenotype under the remaining conditions, but again with one periplasmic chaperone missing, the effects of free Cu could be felt more readily by the cell and result in lower growth maximum. A discussion and summary to consolidate this new data to understand how Cu homeostasis in *P. denitrificans* is acheieved is in Chapter 7.

CHAPTER 7

Summary and Future Perspectives

In this thesis, various approaches were taken to understand how Cu is trafficked in *P. denitrificans*, with a particular emphasis on Cu centre biogenesis in N_2OR.

We have elucidated the role of NosL which is commonly found in the *nos* gene cluster: NosL binds and traffics Cu(I) to, and is therefore involved in the maturation of, the unique Cu_Z centre of N_2OR when Cu is sufficient. During Cu limitation, this protein is vital for trafficking Cu to both Cu centres.

The *nosL* gene is essential for whole cell N_2O reduction in *P. denitrificans* under Cu limited conditions (< 0.5 μM). The Nos^- phenotype, where N_2O reduction is abolished within the cell, is fully complemented both chemically (using Cu) and also biologically using full length *nosL in trans*. The sensitivity of the Δ*nosL* mutant to Cu led us to explore the state of N_2OR in this mutant, and to determine whether the Cu centres were occupied and, if so, to what extent. Surprisingly, N_2OR purified from the Δ*nosL* strain grown in Cu rich media contained significantly lower levels of Cu, with only 1 in 3 of the Cu_Z sites occupied with a cluster, as first described by a less intense Cu_Z signature in the absorbance spectrum. Further evidence from Cu assays showing fewer Cu ions per protein and activity assays, with ~50% of the activity of the wild type protein, verified these findings. This explains why no phenotype was observed under Cu replete conditions, as enough holo-protein is present in the cell under these conditions to turn over N_2O at a sufficiently rapid rate that we do not observe the gas. Under Cu limitation, the influence on N_2OR when the *nosL* gene is deleted is clear using the same analysis: N_2OR was purified as an apo-protein and there were no signs of Cu binding to the protein or N_2O reducing activity.

NosL may work in unison with other chaperones to mature N_2OR. In the absence of NosL, other periplamic Cu chaperones may functionally replace NosL but do so less efficiently, hence only partial occupation of the Cu_Z centre in N_2OR isolated from a Δ*nosL* strain grown in Cu replete media. In contrast, during Cu limitation, this alternative system either does not have a high enough affinity for Cu or have the ability to supply significant amounts of Cu to N_2OR, and so even partial population of either Cu centre is not possible. Therefore any alternative devivery system must be far less efficient in maturing N_2OR.

In establishing how *P. denitrificans* satisfies its requirement to produce holo-N_2OR, in which 12 Cu atoms are necessary, these alternative chaperones must be located within the periplasm. Cu is reactive and must be strictly limited within the intracellular environment to ensure it does not displace metals or produce reactive oxygen species. At present, little is known about how *P. denitrificans* imports Cu,

other than a potential Cu uptake system derived as a by-product during porphyrin synthesis, which is exported to recruit Cu and imported back into the cell once Cu is chelated [151]. Once inside the cell it is imperative that Cu is coordinated to reduce reactivity. One cannot say where the exact primary destination of Cu is upon entering the cell, whether Cu makes its way to the cytoplasm first and then into the periplasm, or whether it is directly imported into the periplasm. If the latter were the case then high affinity chaperones within the periplasm would be necessary to ensure Cu does not roam freely and to chaperone the metal to mature key respiratory enzymes. To date, four periplasmic chaperones have been investigated in the periplasm of PD1222 with regard to their role in maturation of oxidase enzymes during aerobic growth: *pCu1, scoA, pCu2* and *scoB*. Analysis of the cytochrome *c* oxidase in *P. denitrificans* strains deficient in each gene showed only the loss of *scoB* resulted in deminished oxidase acitivity and reduced Cu content, specifically at the Cu_A centre [146]. Both *scoB* and *pcu1* were up-regulated during Cu limitation, under anaerobic conditions in previous transcriptome work in the group, and both are putative chaperones of Cu to the Cu_A centre, especially in light of the *scoB* mutant which was important for Cu_A assembly in cytochrome *c* oxidase. In this work we define NosL as a Cu(I) binding chaperone with an affinity for Cu(I) in the atto-molar range (4.44×10^{-18} M) , determined using a BCS competition assay. In the oxidising periplasm the assumed oxidation state is Cu^{2+}. We have evidence that this metal ion can be reduced to Cu^{1+} by NosL without exogenous reductant, resulting in a bound cuprous ion. It is important to note at this point, the location of NosL has yet to be demonstrated, but it is predicted to be tethered to the outer membrane. The functional relevance of this is unclear. For example, it could imply that NosL is involved early in the Cu trafficking pathway, if Cu was imported directly into the periplasm. The purification of Strep-tag II N_2OR from wild type grown under Cu limited conditions showed that if all chaperones are present, then N_2OR is at least partially populated with Cu at both centres. Under Cu limitation in the absence of NosL but presence of PCuC and ScoB, N_2OR is purified in its apo-form. Thus, NosL is important for transporting Cu to the two Cu centres of N_2OR, implying that NosL functions at a late stage of the Cu trafficking pathway.

A study by Banci et al explains how Cu binding proteins exploit the increasing gradient of Cu binding affinity to allow Cu to transfer between proteins[182]. Thus it could be that Cu flows from weaker Cu(I)-binding chaperones to NosL before it populates the Cu centres of N_2OR or vice versa. A model has been drawn bearing in

mind what we know with regard to N_2OR maturation and how periplasmic proteins may interact during this process, Figure 7.1.

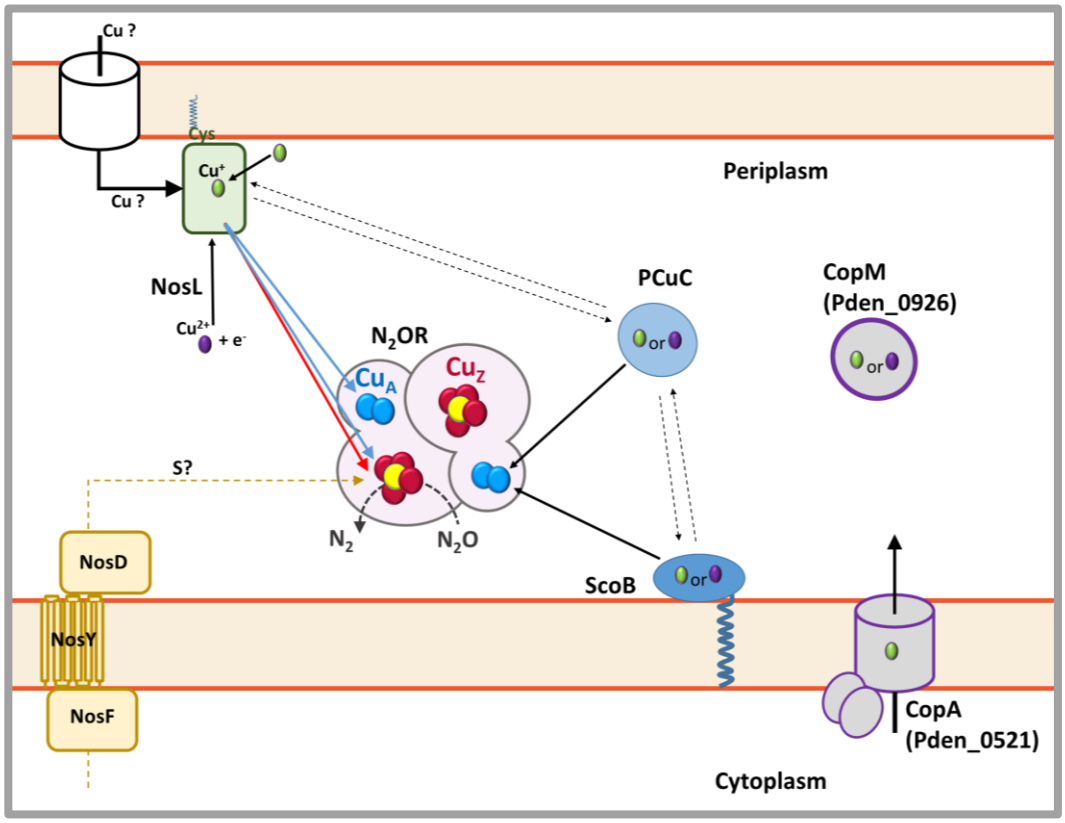

Figure 7.1. Scheme of Cu binding chaperones within the periplasm of *P. denitrificans*.. In this work, we show NosL is important for Cu_Z centre maturation when Cu is replete within the cell(red arrow), but also direct Cu to both centres during Cu limitation (blue arrow). PCuC and ScoB homologues have been shown to bind Cu and are also linked to Cu_A maturation and therefore likely involved in Cu_A maturation of N_2OR . How Cu may transfer between these chaperones is depicted by dashed lines. The *nosDFY* genes have been implicated in Cu_Z centre maturation and may provide the sulfur atom, working with NosL which provides the Cu to generate the Cu-S cluster. Included are the 2 Cu proteins identified from the transcriptome analysis, CopA (Pden_0521) and CopM (Pden_0926). CopA may be involved in populating Cu chaperones in the periplasm once Cu is passed from the cytoplasm.

The data presented here are able to answer at least in part, the question of which proteins are involved in the maturation of the Cu centres in N_2OR. It was shown that the Cu_A centre of N_2OR can be reconstituted by addition of Cu(II)/Cu(I) [99]. In

contrast, the same is not true of the Cu_Z centre. Therefore Cu must be supplied by specific chaperones and NosL is the first to be identified.

Our initial objective was not to find a Cu_Z centre specific chaperone, nonetheless we have. A short consideration of how the Cu-S cluster may be produced *in vivo* is given below.

An approach similar to the reconsitution of Fe-S clusters was used to attempt to build the Cu_Z centre, though no cluster was observed (data not shown). This method included a cysteine desulferase (NifS), Cu, L-cysteine as the sulfur source and a reductant. The main similarity between the Fe-S and this Cu-S cluster is the acid labile sulfide, which the crystal structures agree lies at the centre of the Cu ions in the cluster. The sulfur is not donated from a cysteine residue which is a part of the polypeptide chain. If NosL were to be the main source of Cu to the Cu_Z centre, then we would look to Fe-S biogenesis apparatus to provide the sulfur atom. PD1222 contains 1 of the 3 known Fe-S biogenesis systems: SUF, the sulfur mobilisation dependent Fe-S cluster synthesis system and only NifS of the Nif system, a cysteine desulferase. SUF is believed to generate Fe-S clusters under stress conditions which is likely to be the case as PD1222 undergoes stress to a point, adapting from oxic to anoxic environments in order to survive and using Fe-S clusters to switch these systems on (FnrP transcriptional regulator). The SUF system is more protective of the intermediates of Fe-S assembly against oxidative stress and reactive oxygen species [183] which could result in degredation of the cluster. All the components of Fe-S biogenesis apparatus mentioned are located in the cytoplasm of the cell and therefore are unlikely to take part in forming the Cu-S cluster. It is known that N_2OR is processed and transported through the Tat pathway to the periplasm where it then obtains its Cu cofactors [45]. So, the system must be strictly periplasmic. Homology has been recognised between NosDFY and ATM1 as ABC-type transporters (the latter is responsible for Fe-S maturation by exporting a sulfur species (a glutathione polysulfide) from the mitochondrion to the cytosol [184, 185]), could mean this is a route for the sulfur species to be trafficked before the sulfide is incorporated into the core of the Cu_Z centre. If NosDFY is indeed responsible for exporting a sulfur species, then there must be a pathway that directs this towards N_2OR. The nature of such a pathway is unknown and significant future work is needed to firstly verify the role of NosDFY in sulfur transfer and then to identify other partner proteins in trafficking the sulfur to N_2OR.

In terms of understanding the assembly of the Cu centres of N_2OR, exploring direct transfer of Cu from NosL to N_2OR is the most obvious next step. Ideally this would be tracked using absorbance spectrosocpy and also mass spectrometry to confirm the mass shift upon Cu transfer. This could then be incorporated into an analagous Fe-S cluster reconstitution method and from then an understanding of the other components necessary for building the Cu-S cluster can be developed.

We also investigated another gene in the NGS. An inadvertant double mutant (Δ*nosLX*) led us to investigate whether NosX is essential for N_2O reduction in *P. denitrificans*. A previous report describes a double *P. denitrificans* mutant, in both *nosX* and its homologue *nirX*, as having a Nos^- phenotype but that the single mutants were able to turn over N_2O, leading to the conclusion that the proteins are functional homologues [85]. The data presented here contradict this conclusion. We observed the Nos^- phenotype in the Δ*nosLX* mutant, producing N_2O at levels similar to the strain without *nosZ* and, more importantly in our case, independent to the total Cu in the cell. This led to the question of whether the nature of the Δ*nosLX* mutant was a result of the cumulative loss of *nosL* and *nosX* or simply from the loss of *nosX.* Analysis of the single mutant provided the evidence that the latter was the case; the loss of NosX dominates the phenotype. When N_2OR was purified from the Δ*nosX* background, the analysis, including the spectroscopic evidence, Cu content and activity of the protein, pointed towards full occupation of the 2 Cu centres. We are able to confirm, therefore, that NosX is not involved directly in trafficking Cu or sulfur to the Cu centres of N_2OR. It is likely, based on evidence recently published, that NosX is involved indirectly in activating the Cu_Z centre in N_2OR for catalytic purposes. Sequence homology between *Pd*NosX and the ApbE protein studied in *P. stutzeri* provides information on the strong possibility that *Pd*NosX is a FAD binding protein which can flavinylate NosR, which has a putative role in shuttling electrons to N_2OR for the reduction of N_2O. Therefore NosX is likely involved in maintaining the reaction cycle in conjuction with the product of another member of the NGC, *nosR.* Clearly, though, there is no significant redundancy between NosX and NirX and NirX alone cannot compensate for the absence of NosX.

Finally, the question of which detoxification systems are present in *P. denitrificans* that deal with high concentrations of Cu, was addressed. Bioinformatic anaylses indicated that there are no complete Cu detoxification or trafficking systems in the PD1222 genome that are closely related to the well studied and conserved systems found in eurkaryotes and prokaryotes. *P. denitrificans* clearly require Cu, especially

during anaerobic respiration, yet there were no obvious clues from the genome about how the bacterium deals with Cu when it is present at high concentration. One possibility is that these organisms do not encounter sufficiently high environmental concentrations of Cu to require the presence of a dedicated detoxification system. To establish whether other, unrecognised detoxification systems, might be present in *P. denitrificans*, we first defined the maximum sub toxic concentration of Cu in which the bacteria could survive without an obvious growth phenotype. Unsurprisingly, the upper limit was <100 μM Cu. This is much lower than those reported for other bacteria, such as *E. coli*, that can withstand 5 mM Cu and remain viable [106] .

We explored the transcriptome of PD1222 during growth under normal Cu and Cu excess and either anaerobic or aerobic conditions in an attempt to pinpoint any transcripts which changed significantly under Cu excess and could therefore be related to a Cu resistance function.

Under anaerobic conditions, 4 transcripts from the 79 most differentially expressed transcripts highlighted, could, once translated, potentially be related to Cu binding. These were *pden_4444*, *4443*, *0521* and *0926*. The first 2 encode PCuC and ScoB, as already discussed and explored in the literature [28]. We know they are up-regulated during Cu limitation, therefore acting in a Cu responsive fashion to assist in assembly of Cu-requiring proteins. The fact that they are also up-regulated under Cu excess could mean they play a key role in binding and storing Cu in the periplasm, which may help to reduce its reactivity/toxicity, though mutant analysis showed, under Cu excess, the strains reamined viable.

Pden_0521 is a P-type ATPase with 2 soluble N-terminal domains with strong similarity to CopA like proteins. Like *E. coli copA*, genes surrounding Pden_0521 are not the cognate chaperone or transcriptional regulators which one would expect based on the literature on these Cu export systems. Recent advances in understanding of CopA in *E. coli* have shown both the chaperone and transporter are translated from the single *copA* gene in *E. coli* due to ribosomal frameshifting [134]. A Δ*0521* mutant in *P. denitrificans* displayed a delayed growth phenotype when cultured aerobically and anaerobically under excess Cu. Therefore, we propose that this transporter plays a role in Cu detoxification in *P. denitrificans* by exporting the metal to the periplasm, as included in Figure 7.1. The Δ*0521* mutant also exhibited a (less severe) phenotype under normal Cu conditions, suggesting that it might also function in trafficking Cu to the periplasm of *P. denitrificans* for distribution to and maturation of Cu proteins, specifically respiratory enzymes.

The final gene of high interest was *pden_0926*, which encodes a protein which carries a DUF305 but more importantly this is a methionine rich periplasmic protein with similarity to the Cu metabolism protein CopM from *Synechocystis* [164] . Although this gene was found to be up-regulated under anaerobic Cu excess conditions, deletion of the gene did not result in a significantly Cu sensitive strain. However, aerobic growth of this mutant was severely limited, consistent with a role for this protein in detoxifying Cu in the periplasm under aerobic conditions, where the capacity of Cu to redox cycle through reaction with O_2 and reactive oxygen species would be enhanced. Thus, the transcriptomics data together with mutational studies of identified genes has revealed two important players in *P. denitrificans* Cu trafficking and detoxification: Pden_0521, a Cu-transporting P-type ATPase that we suggest is named *copA*/CopA; and, Pden_0926, a Met-rich periplasmic protein with similarity to CopM. Although these proteins clearly play roles in detoxification, the fact remains that *P. denitrificans* is remarkably sensitive to elevated environmental Cu and does not appear to be equipped at all to deal with the concentrations that many other bacteria can readily survive. This could be because the soil habitat of *P. denitrificans* is not a Cu rich environment and so elevated Cu levels are not encountered. It could also reflect that *P. denitrificans*, particulary under anaerobic conditions, requires significant amounts of Cu, principally for the denitrification enzyme N_2OR and so has efficient systems for Cu utilization rather than for detoxification.

There are many possible studies that could be carried out to exploit further the RNA transcript data collected. First, biochemical studies on Pden_0521 would establish whether it is indeed a Cu transporter. Also, oxidase activity assays of the Δ*0521* mutant would be essential to determine whether Pden_0521 supplies Cu to the caa_3 and cbb_3 oxidases. Biochemical studies of Pden_0926 would also be interesting. We predict Pden_0926, which is similar to CopM, a will be able to bind at least 1 Cu ion. It is intriguing that a periplasmic protein has so many methionine residues (10% of the total amino acids); this is most likely related to a Cu binding function. In answering these biochemical questions, the two proteins would provide significant further understanding of the Cu-related proteome within the periplasm of *P. denitrificans*.

In summary, this work has led to the identification of a Cu chaperone linked to the maturation of the only centre in nature known to reduce N_2O. Furthermore, a key gene, found in the NGC of α-proteobacteria at least, which is necessary for activating N_2OR and not maturing it was identified. These key findings will add to the

understanding of how N_2OR is matured and activated in the cell. The work also adds to our understanding of how Cu is dealt with in a bacterium which needs this crucial metal for respiration. Through the initial and unexpected observation of an apparent lack of Cu detoxification systems, two new genes involved in trafficking Cu in *P.denitrificans* have been identified. Together these findings add to the growing understanding of how the Cu centres of N_2OR are matured and will help develop strategies to assist in the future mitigation of N_2O emissions from the soil.

Bibliography

1. Gruber, N. and J.N. Galloway, (2008) An Earth-system perspective of the global nitrogen cycle. *Nature*. **451**(7176): p. 293-6.
2. Griffis, T.J., Z. Chen, J.M. Baker, J.D. Wood, D.B. Millet, X. Lee, R.T. Venterea, and P.A. Turner, (2017) Nitrous oxide emissions are enhanced in a warmer and wetter world. *Proceedings of the Natural Academy of Science U S A*. **114**(45): p. 12081-12085.
3. Fowler, D., M. Coyle, U. Skiba, M.A. Sutton, J.N. Cape, S. Reis, L.J. Sheppard, A. Jenkins, B. Grizzetti, J.N. Galloway, P. Vitousek, A. Leach, A.F. Bouwman, K. Butterbach-Bahl, F. Dentener, D. Stevenson, M. Amann, and M. Voss, (2013) The global nitrogen cycle in the twenty-first century. *Philosophical Transactions of the Royal Society B*. **368**(1621): p. 20130164.
4. Kim, J. and D.C. Rees, (1994) Nitrogenase and biological nitrogen fixation. *Biochemistry*. **33**(2): p. 389-397.
5. Kartal, B. and J.T. Keltjens, (2016) Anammox Biochemistry: a Tale of Heme c Proteins. *Trends Biochem Sci*. **41**(12): p. 998-1011.
6. Stein, L.Y. and M.G. Klotz, (2016) The nitrogen cycle. *Current Biology*. **26**(3): p. R94-R98.
7. Stein, L.Y., (2019) Insights into the physiology of ammonia-oxidizing microorganisms. *Current Opinion in Chemical Biology*. **49**: p. 9-15.
8. Ravishankara, A.R., J.S. Daniel, and R.W. Portmann, (2009) Nitrous Oxide (N_2O): The Dominant Ozone-Depleting Substance Emitted in the 21st Century. *Science*. **326**(5949): p. 123-125.
9. Stieglmeier, M., M. Mooshammer, B. Kitzler, W. Wanek, S. Zechmeister-Boltenstern, A. Richter, and C. Schleper, (2014) Aerobic nitrous oxide production through N-nitrosating hybrid formation in ammonia-oxidizing archaea. *The ISME journal*. **8**(5): p. 1135-1146.
10. Thomson, A.J., G. Giannopoulos, J. Pretty, E.M. Baggs, and D.J. Richardson, (2012) Biological sources and sinks of nitrous oxide and strategies to mitigate emissions. *Philosophical Transactions of the Royal Society B*. **367**: p. 1157-1168.
11. Hu, H.W., D. Chen, and J.Z. He, (2015) Microbial regulation of terrestrial nitrous oxide formation: understanding the biological pathways for prediction of emission rates. *FEMS Microbiology Rev*iew **39**(5): p. 729-49.
12. Erisman, J.W., M.A. Sutton, J. Galloway, Z. Klimont, and W. Winiwarter, (2008) How a century of ammonia synthesis changed the world. *Nature Geosciences* **1**(10): p. 636-639.
13. Kraft, B., H.E. Tegetmeyer, R. Sharma, M.G. Klotz, T.G. Ferdelman, R.L. Hettich, J.S. Geelhoed, and M. Strous, (2014) Nitrogen cycling. The environmental controls that govern the end product of bacterial nitrate respiration. *Science*. **345**(6197): p. 676-9.
14. Richardson, D., H. Felgate, N. Watmough, A.J. Thomson, and E. Baggs, (2009) Mitigating release of the potent greenhouse gas N_2O from the nitrogen cycle-could enzymic regulation hold the key? *Trends in Biotechnology*. **27**(7): p. 388-397.
15. Wunderlin, P., J. Mohn, A. Joss, L. Emmenegger, and H. Siegrist, (2012) Mechanisms of N2O production in biological wastewater treatment under nitrifying and denitrifying conditions. *Water Research* **46**(4): p. 1027-37.
16. Jones, C.M., D.R. Graf, D. Bru, L. Philippot, and S. Hallin, (2013) The unaccounted yet abundant nitrous oxide-reducing microbial community: a potential nitrous oxide sink. *ISME Journal* **7**(2): p. 417-26.

17. Serventi, F., Z.A. Youard, V. Murset, S. Huwiler, D. Buhler, M. Richter, R. Luchsinger, H.M. Fischer, R. Brogioli, M. Niederer, and H. Hennecke, (2012) Copper Starvation-inducible Protein for Cytochrome Oxidase Biogenesis in *Bradyrhizobium japonicum*. *Journal of Biological Chemistry*. **287**(46): p. 38812-38823.
18. Richardson, D.J., (2000) Bacterial respiration: a flexible process for a changing environment. *Microbiology*. **146 (Pt 3)**: p. 551-71.
19. Contreras, I., C.S. Toro, G. Troncoso, and G.C. Mora, (1997) Salmonella typhi mutants defective in anaerobic respiration are impaired in their ability to replicate within epithelial cells. *Microbiology*. **143 (Pt 8)**: p. 2665-72.
20. Bueno, E., S. Mesa, E.J. Bedmar, D.J. Richardson, and M.J. Delgado, (2012) Bacterial Adaptation of Respiration from Oxic to Microoxic and Anoxic Conditions: Redox Control. *Antioxidants & Redox Signaling*. **16**(8): p. 819-852.
21. Bouchal, P., I. Struharova, E. Budinska, O. Sedo, T. Vyhlidalova, Z. Zdrahal, R. van Spanning, and I. Kucera, (2010) Unraveling an FNR based regulatory circuit in *Paracoccus denitrificans* using a proteomics-based approach. *Biochimica Et Biophysica Acta-Proteins and Proteomics*. **1804**(6): p. 1350-1358.
22. Hutchings, M.I., J.C. Crack, N. Shearer, B.J. Thompson, A.J. Thomson, and S. Spiro, (2002) Transcription factor FnrP from *Paracoccus denitrificans* contains an iron-sulfur cluster and is activated by anoxia: identification of essential cysteine residues. *Journal of Bacteriology*. **184**(2): p. 503-508.
23. Van Spanning, R.J., E. Houben, W.N. Reijnders, S. Spiro, H.V. Westerhoff, and N. Saunders, (1999) Nitric oxide is a signal for NNR-mediated transcription activation in *Paracoccus denitrificans*. *Journal of Bacteriolology* **181**(13): p. 4129-32.
24. VanSpanning, R.J.M., A.P.N. DeBoer, W.N.M. Reijnders, H.V. Westerhoff, A.H. Stouthamer, and J. VanDerOost, (1997) FnrP and NNR of *Paracoccus denitrificans* are both members of the FNR family of transcriptional activators but have distinct roles in respiratory adaptation in response to oxygen limitation. *Molecular Microbiology*. **23**(5): p. 893-907.
25. Lee, Y.Y., N. Shearer, and S. Spiro, (2006) Transcription factor NNR from *Paracoccus denitrificans* is a sensor of both nitric oxide and oxygen: isolation of nnr* alleles encoding effector-independent proteins and evidence for a haem-based sensing mechanism. *Microbiology*. **152**(Pt 5): p. 1461-70.
26. Bergaust, L., R.J.M. van Spanning, A. Frostegard, and L.R. Bakken, (2012) Expression of nitrous oxide reductase in *Paracoccus denitrificans* is regulated by oxygen and nitric oxide through FnrP and NNR. *Microbiology-Sgm*. **158**: p. 826-834.
27. Qu, Z., L.R. Bakken, L. Molstad, A. Frostegard, and L.L. Bergaust, (2016) Transcriptional and metabolic regulation of denitrification in *Paracoccus denitrificans* allows low but significant activity of nitrous oxide reductase under oxic conditions. *Environmental Microbiology* **18**(9): p. 2951-63.
28. Sullivan, M.J., A.J. Gates, C. Appia-Ayme, G. Rowley, and D.J. Richardson, (2013) Copper control of bacterial nitrous oxide emission and its imact on vitamin B_{12}-dependent metabolism. *Proceedings of the Natural Academy of Science U S A* **110**(49): p. 19926-19931.
29. Zumft, W.G., (1997) Cell biology and molecular basis of denitrification. *Microbiology Molecular Biology Review*. **61**(4): p. 533-616.
30. Berks, B.C., D. Baratta, J. Richardson, and S.J. Ferguson, (1993) Purification and characterization of a nitrous oxide reductase from *Thiosphaera pantotropha*. Implications for the mechanism of aerobic nitrous oxide reduction. *European Journal Biochemistry* **212**(2): p. 467-76.

31. Berks, B.C., S.J. Ferguson, J.W.B. Moir, and D.J. Richardson, (1995) Enzymes and associated electron transport systems that catalyse the respiratory reduction of nitrogen oxides and oxyanions. *Biochimica et Biophysica Acta - Bioenergetics*. **1232**(3): p. 97-173.
32. Field, S.J., F.H. Thorndycroft, A.D. Matorin, D.J. Richardson, and N.J. Watmough, (2008) The respiratory nitric oxide reductase (NorBC) from *Paracoccus denitrificans*. *Methods in Enzymology* **437**: p. 79-101.
33. Rubino, J.T. and K.J. Franz, (2012) Coordination chemistry of copper proteins: How nature handles a toxic cargo for essential function. *Journal of Inorganic Biochemistry*. **107**(1): p. 129-143.
34. Williams, R.J., (1995) Energised (entatic) states of groups and of secondary structures in proteins and metalloproteins. *European Journal of Biochemistry* **234**(2): p. 363-81.
35. Pena, M.M., J. Lee, and D.J. Thiele, (1999) A delicate balance: homeostatic control of copper uptake and distribution. *Journal of Nutrition* **129**(7): p. 1251-60.
36. Valko, M., H. Morris, and M.T. Cronin, (2005) Metals, toxicity and oxidative stress. *Current Medicinal Chemistry* **12**(10): p. 1161-208.
37. Osman, D., C.J. Patterson, K. Bailey, K. Fisher, N.J. Robinson, S.E. Rigby, and J.S. Cavet, (2013) The copper supply pathway to a *Salmonella* Cu,Zn-superoxide dismutase (SodCII) involves P(1B)-type ATPase copper efflux and periplasmic CueP. *Molecular Microbiology* **87**(3): p. 466-77.
38. Coyle, C.L., W.G. Zumft, P.M. Kroneck, H. Korner, and W. Jakob, (1985) Nitrous oxide reductase from denitrifying *Pseudomonas perfectomarina*. Purification and properties of a novel multicopper enzyme. *European Journal of Biochemistry* **153**(3): p. 459-67.
39. Snyder, S.W. and T.C. Hollocher, (1987) Purification and some characteristics of nitrous oxide reductase from *Paracoccus denitrificans*. *Journal of Biological Chemistry* **262**(14): p. 6515-25.
40. SooHoo, C.K. and T.C. Hollocher, (1991) Purification and characterization of nitrous oxide reductase from *Pseudomonas aeruginosa* strain P2. *Journal of Biological Chemistry* **266**(4): p. 2203-9.
41. Hulse, C.L. and B.A. Averill, (1990) Isolation of a high specific activity pink, monomeric nitrous oxide reductase from *Achromobacter cycloclastes*. *Biochemical and Biophysical Research Communications*. **166**(2): p. 729-35.
42. Dell'Acqua, S., S.R. Pauleta, J.J. Moura, and I. Moura, (2012) Biochemical characterization of the purple form of *Marinobacter hydrocarbonoclasticus* nitrous oxide reductase. *Philosophical Transactions of the Royal Society-Biological Sciences* **367**(1593): p. 1204-12.
43. Brown, K., K. Djinovic-Carugo, T. Haltia, I. Cabrito, M. Saraste, J.J. Moura, I. Moura, M. Tegoni, and C. Cambillau, (2000) Revisiting the catalytic Cu_Z cluster of nitrous oxide (N_2O) reductase. Evidence of a bridging inorganic sulfur. *Journal of Biological Chemistry* **275**(52): p. 41133-6.
44. Heikkila, M.P., U. Honisch, P. Wunsch, and W.G. Zumft, (2001) Role of the Tat ransport system in nitrous oxide reductase translocation and cytochrome cd1 biosynthesis in *Pseudomonas stutzeri*. *Journal of Bacteriology* **183**(5): p. 1663-71.
45. Dreusch, A., D.M. Burgisser, C.W. Heizmann, and W.G. Zumft, (1997) Lack of copper insertion into unprocessed cytoplasmic nitrous oxide reductase generated by an R20D substitution in the arginine consensus motif of the signal peptide. *Biochimica et Biophysica Acta*. **1319**(2-3): p. 311-8.
46. Pomowski, A., W.G. Zumft, P.M. Kroneck, and O. Einsle, (2011) N_2O binding at a [4Cu:2S] copper-sulphur cluster in nitrous oxide reductase. *Nature*. **477**(7363): p. 234-7.

47. Richardson, D.J., L.C. Bell, A.G. McEwan, J.B. Jackson, and S.J. Ferguson, (1991) Cytochrome c2 is essential for electron transfer to nitrous oxide reductase from physiological substrates in *Rhodobacter capsulatus* and can act as an electron donor to the reductase in vitro. Correlation with photoinhibition studies. *European Journal of Biochemistry*. **199**(3): p. 677-83.
48. Vanspanning, R.J.M., C. Wansell, N. Harms, L.F. Oltmann, and A.H. Stouthamer, (1990) Mutagenesis of the gene encoding cytochrome c550 of *Paracoccus denitrificans* and analysis of the resultant physiological effects. *Journal of Bacteriology*. **172**(2): p. 986-996.
49. Moir, J.W.B. and S.J. Ferguson, (1994) Properties of a Paracoccus denitrificans mutant deleted in cytochrome c550 indicate that a copper protein can substitute for this cytochrome in electron transport to nitrite, nitric oxide and nitrous oxide. *Microbiology*. **140**(2): p. 389-397.
50. Dell'acqua, S., I. Moura, J.J. Moura, and S.R. Pauleta, (2011) The electron transfer complex between nitrous oxide reductase and its electron donors. *Journal of Biological Inorganic Chemistry* **16**(8): p. 1241-54.
51. Haltia, T., K. Brown, M. Tegoni, C. Cambillau, M. Saraste, K. Mattila, and K. Djinovic-Carugo, (2003) Crystal structure of nitrous oxide reductase from *Paracoccus denitrificans* at 1.6 A resolution. *Biochemical Journal* **369**(Pt 1): p. 77-88.
52. Kroneck, P.M., W.A. Antholine, J. Riester, and W.G. Zumft, (1988) The cupric site in nitrous oxide reductase contains a mixed-valence [Cu(II),Cu(I)] binuclear center: a multifrequency electron paramagnetic resonance investigation. *FEBS Letters.* **242**(1): p. 70-4.
53. Farrar, J.A., W.G. Zumft, and A.J. Thomson, (1998) CuA and CuZ are variants of the electron transfer center in nitrous oxide reductase. *Proceedings of the Natural Academy of Science U S A.* **95**(17): p. 9891-6.
54. Randall, D.W., D.R. Gamelin, L.B. LaCroix, and E.I. Solomon, (2000) Electronic structure contributions to electron transfer in blue Cu and CuA. *Journal of Biological Inorganic Chemistry*. **5**(1): p. 16-29.
55. Farrar, J.A., A.J. Thomson, M.R. Cheesman, D.M. Dooley, and W.G. Zumft, (1991) A model of the copper centres of nitrous oxide reductase (*Pseudomonas stutzeri*). Evidence from optical, EPR and MCD spectroscopy. *FEBS Letters*. **294**(1-2): p. 11-5.
56. Brown, K., M. Tegoni, M. Prudencio, A.S. Pereira, S. Besson, J.J. Moura, I. Moura, and C. Cambillau, (2000) A novel type of catalytic copper cluster in nitrous oxide reductase. *Nature Structural Biology*. **7**(3): p. 191-195.
57. Brown, K., K. Djinovic-Carugo, T. Haltia, I. Cabrito, M. Saraste, J.J.G. Moura, I. Moura, M. Tegoni, and C. Cambillau, (2000) Revisiting the catalytic CuZ cluster of nitrous oxide (N_2O) reductase - Evidence of a bridging inorganic sulfur. *Journal of Biological Chemistry*. **275**(52): p. 41133-41136.
58. Singh, S.K., S.A. Roberts, S.F. McDevitt, A. Weichsel, G.F. Wildner, G.B. Grass, C. Rensing, and W.R. Montfort, (2011) Crystal structures of multicopper oxidase CueO bound to copper(I) and silver(I): functional role of a methionine-rich sequence. *Journal of Biological Chemistry*. **286**(43): p. 37849-57.
59. Rasmussen, T., B.C. Berks, J. Sanders-Loehr, D.M. Dooley, W.G. Zumft, and A.J. Thomson, (2000) The catalytic center in nitrous oxide reductase, CuZ, is a copper-sulfide cluster. *Biochemistry*. **39**(42): p. 12753-6.
60. Dell'Acqua, S., S.R. Pauleta, I. Moura, and J.J. Moura, (2011) The tetranuclear copper active site of nitrous oxide reductase: the CuZ center. *Journal of Biological Inorganic Chemistry*. **16**(2): p. 183-94.
61. Carreira, C., S.R. Pauleta, and I. Moura, (2017) The catalytic cycle of nitrous oxide reductase - The enzyme that catalyzes the last step of denitrification. *Journal of Inorganic Biochemistry*. **177**: p. 423-434.

62. Johnston, E.M., C. Carreira, S. Dell'Acqua, S.G. Dey, S.R. Pauleta, I. Moura, and E.I. Solomon, (2017) Spectroscopic Definition of the CuZ degrees Intermediate in Turnover of Nitrous Oxide Reductase and Molecular Insight into the Catalytic Mechanism. *Journal of the American Chemical Society*. **139**(12): p. 4462-4476.
63. Ghosh, S., S.I. Gorelsky, P. Chen, I. Cabrito, J.J. Moura, I. Moura, and E.I. Solomon, (2003) Activation of N_2O reduction by the fully reduced μ4-sulfide bridged tetranuclear CuZ cluster in nitrous oxide reductase. *Journal of the American Chemical Society*. **125**(51): p. 15708-9.
64. Johnson, B.J., W.E. Antholine, S.V. Lindeman, M.J. Graham, and N.P. Mankad, (2016) A One-Hole Cu4S Cluster with N_2O Reductase Activity: A Structural and Functional Model for CuZ. *Journal of the American Chemical Society*.**138**:13107-13110.
65. Rasmussen, T., B.C. Berks, J.N. Butt, and A.J. Thomson, (2002) Multiple forms of the catalytic centre, CuZ, in the enzyme nitrous oxide reductase from *Paracoccus pantotrophus*. *Biochemical Journal*. **364**(Pt 3): p. 807-15.
66. Wust, A., L. Schneider, A. Pomowski, W.G. Zumft, P.M.H. Kroneck, and O. Einsle, (2012) Nature's way of handling a greenhouse gas: the copper-sulfur cluster of purple nitrous oxide reductase. *Biological Chemistry*. **393**.
67. Charnock, J.M., A. Dreusch, H. Korner, F. Neese, J. Nelson, A. Kannt, H. Michel, C.D. Garner, P.M. Kroneck, and W.G. Zumft, (2000) Structural investigations of the CuA centre of nitrous oxide reductase from *Pseudomonas stutzeri* by site-directed mutagenesis and X-ray absorption spectroscopy. *European Journal of Biochemistry*. **267**(5): p. 1368-81.
68. Johnson, B.J., W.E. Antholine, S.V. Lindeman, and N.P. Mankad, (2015) A Cu4S model for the nitrous oxide reductase active sites supported only by nitrogen ligands. *Chemical Communications (Camb)*. **51**(59): p. 11860-3.
69. Neupane, D.P., B. Jacquez, A. Sundararajan, T. Ramaraj, F.D. Schilkey, and E.T. Yukl, (2017) Zinc-Dependent Transcriptional Regulation in *Paracoccus denitrificans*. *Frontiers in Microbiology*. **8**: p. 569.
70. Wunsch, P. and W.G. Zumft, (2005) Functional domains of NosR, a novel transmembrane iron-sulfur flavoprotein necessary for nitrous oxide respiration. *Journal of Bacteriology*. **187**(6): p. 1992-2001.
71. Wunsch, P., H. Korner, F. Neese, R.J. van Spanning, P.M. Kroneck, and W.G. Zumft, (2005) NosX function connects to nitrous oxide (N_2O) reduction by affecting the Cu(Z) center of NosZ and its activity in vivo. *FEBS Letters*. **579**(21): p. 4605-9.
72. Honisch, U. and W.G. Zumft, (2003) Operon structure and regulation of the nos gene region of *Pseudomonas stutzeri*, encoding an ABC-Type ATPase for maturation of nitrous oxide reductase. *Journal of Bacteriology*. **185**(6): p. 1895-902.
73. Riester, J., W.G. Zumft, and P.M. Kroneck, (1989) Nitrous oxide reductase from *Pseudomonas stutzeri*. Redox properties and spectroscopic characterization of different forms of the multicopper enzyme. *European Journal of Biochemistry*. **178**(3): p. 751-62.
74. Srinivasan, V., A.J. Pierik, and R. Lill, (2014) Crystal structures of nucleotide-free and glutathione-bound mitochondrial ABC transporter Atm1. *Science*. **343**(6175): p. 1137-40.
75. Wunsch, P., M. Herb, H. Wieland, U.M. Schiek, and W.G. Zumft, (2003) Requirements for Cu-A and Cu-S center assembly of nitrous oxide reductase deduced from complete periplasmic enzyme maturation in the nondenitrifier *Pseudomonas putida*. *Journal of Bacteriology*. **185**(3): p. 887-896.
76. McGuirl, M.A., L.K. Nelson, J.A. Bollinger, Y.K. Chan, and D.M. Dooley, (1998) The nos (nitrous oxide reductase) gene cluster from the soil bacterium

Achromobacter cycloclastes: cloning, sequence analysis, and expression. *Journal of Inorganic Biochemistry*. **70**(3-4): p. 155-69.
77. McGuirl, M.A., J.A. Bollinger, N. Cosper, R.A. Scott, and D.M. Dooley, (2001) Expression, purification, and characterization of NosL, a novel Cu(I) protein of the nitrous oxide reductase (nos) gene cluster. *Journal of Biological Inorganic Chemistry*. **6**(2): p. 189-95.
78. Zhang, L., C. Trncik, S.L.A. Andrade, and O. Einsle, (2017) The flavinyl transferase ApbE of *Pseudomonas stutzeri* matures the NosR protein required for nitrous oxide reduction. *Biochimica et Biophysica Acta*. **1858**(2): p. 95-102.
79. Vishniac, W. and M. Santer, (1957) The thiobacilli. *Bacteriology Review*. **21**(3): p. 195-213.
80. Glover, M., ed, DNA Cloning I. 1985: IRL Press.
81. Pace, C.N., F. Vajdos, L. Fee, G. Grimsley, and T. Gray, (1995) How to measure and predict the molar absorption coefficient of a protein. *Protein Science : A Publication of the Protein Society*. **4**(11): p. 2411-2423.
82. Kristjansson, J.K. and T.C. Hollocher, (1980) First practical assay for soluble nitrous oxide reductase of denitrifying bacteria and a partial kinetic characterization. *Journal of Biological Chemistry*. **255**(2): p. 704-7.
83. Banerjee, S. and S. Mazumdar, (2012) Electrospray ionization mass spectrometry: a technique to access the information beyond the molecular weight of the analyte. *International Journal of Analytical Chemistry*. **2012**: p. 282574.
84. Crack, J.C., A.J. Thomson, and N.E. Le Brun, (2017) Mass spectrometric identification of intermediates in the O_2-driven [4Fe-4S] to [2Fe-2S] cluster conversion in FNR. *Proceedings of the National Academy of Sciences*. **114**(16): p. E3215.
85. Saunders, N.F., J.J. Hornberg, W.N. Reijnders, H.V. Westerhoff, S. de Vries, and R.J. van Spanning, (2000) The NosX and NirX proteins of *Paracoccus denitrificans* are functional homologues: their role in maturation of nitrous oxide reductase. *Journal of Bacteriology*. **182**(18): p. 5211-7.
86. Hallin, S., L. Philippot, F.E. Löffler, R.A. Sanford, and C.M. Jones, Genomics and Ecology of Novel N_2O-Reducing Microorganisms. *Trends in Microbiology*. **26**(1): p. 43-55.
87. Schafer, A., A. Tauch, W. Jager, J. Kalinowski, G. Thierbach, and A. Puhler, (1994) Small mobilizable multi-purpose cloning vectors derived from the *Escherichia coli* plasmids pK18 and pK19: selection of defined deletions in the chromosome of Corynebacterium glutamicum. *Gene*. **145**(1): p. 69-73.
88. Tett, A.J., S.J. Rudder, A. Bourdès, R. Karunakaran, and P.S. Poole, (2012) Regulatable Vectors for Environmental Gene Expression in Alphaproteobacteria. *Applied and Environmental Microbiology*. **78**(19): p. 7137-7140.
89. Dreusch, A., J. Riester, P.M. Kroneck, and W.G. Zumft, (1996) Mutation of the conserved Cys165 outside of the CuA domain destabilizes nitrous oxide reductase but maintains its catalytic activity. Evidence for disulfide bridges and a putative protein disulfide isomerase gene. *European Journal of Biochemistry*. **237**(2): p. 447-53.
90. Chan, Y.K., W.A. McCormick, and R.J. Watson, (1997) A new nos gene downstream from nosDFY is essential for dissimilatory reduction of nitrous oxide by *Rhizobium* (*Sinorhizobium*) *meliloti*. *Microbiology*. **143**(8): p. 2817-24.
91. Boyd, J.M., J.A. Endrizzi, T.L. Hamilton, M.R. Christopherson, D.W. Mulder, D.M. Downs, and J.W. Peters, (2011) FAD Binding by ApbE Protein from Salmonella

enterica: a New Class of FAD-Binding Proteins. *Journal of Bacteriology*. **193**(4): p. 887-895.
92. Hayashi, M., Y. Nakayama, M. Yasui, M. Maeda, K. Furuishi, and T. Unemoto, (2001) FMN is covalently attached to a threonine residue in the NqrB and NqrC subunits of Na+-translocating NADH-quinone reductase from *Vibrio alginolyticus*. *FEBS Letters*. **488**(1): p. 5-8.
93. Pomowski, A., W.G. Zumft, P.M. Kroneck, and O. Einsle, (2010) Crystallization of purple nitrous oxide reductase from *Pseudomonas stutzeri*. *Acta Crystallography Sector F Structural Biology Crystallography Communication*. **66**(Pt 11): p. 1541-3.
94. Schneider, L.K. and O. Einsle, (2016) Role of calcium in secondary structure stabilization during maturation of Nitrous Oxide Reductase. *Biochemistry*. **55**(10): p. 1433-1440.
95. Kroneck, P.M., W.A. Antholine, J. Riester, and W.G. Zumft, (1989) The nature of the cupric site in nitrous oxide reductase and of CuA in cytochrome c oxidase. *FEBS Letters*. **248**(1-2): p. 212-3.
96. Felgate, H., G. Giannopoulos, M.J. Sullivan, A.J. Gates, T.A. Clarke, E. Baggs, G. Rowley, and D.J. Richardson, (2012) The impact of copper, nitrate and carbon status on the emission of nitrous oxide by two species of bacteria with biochemically distinct denitrification pathways. *Environmental Microbiology*. **14**(7): p. 1788-800.
97. Prudencio, M., A.S. Pereira, P. Tavares, S. Besson, I. Cabrito, K. Brown, B. Samyn, B. Devreese, J. Van Beeumen, F. Rusnak, G. Fauque, J.J. Moura, M. Tegoni, C. Cambillau, and I. Moura, (2000) Purification, characterization, and preliminary crystallographic study of copper-containing nitrous oxide reductase from *Pseudomonas nautica* 617. *Biochemistry*. **39**(14): p. 3899-907.
98. Paraskevopoulos, K., S.V. Antonyuk, R.G. Sawers, R.R. Eady, and S.S. Hasnain, (2006) Insight into catalysis of nitrous oxide reductase from high-resolution structures of resting and inhibitor-bound enzyme from *Achromobacter cycloclastes*. *Journal of Molecular Biology*. **362**(1): p. 55-65.
99. Savelieff, M.G., T.D. Wilson, Y. Elias, M.J. Nilges, D.K. Garner, and Y. Lu, (2008) Experimental evidence for a link among cupredoxins: red, blue, and purple copper transformations in nitrous oxide reductase. *Proceedings of the Natural Academy of Sciences U S A*. **105**(23): p. 7919-24.
100. Okuda, S. and H. Tokuda, (2011) Lipoprotein sorting in bacteria. *Annual Reviews of Microbiology*. **65**: p. 239-59.
101. Taubner, L.M., M.A. McGuirl, D.M. Dooley, and V. Copie, (2006) Structural studies of Apo NosI, an accessory protein of the nitrous oxide reductase system: Insights from structural homology with MerB, a mercury resistance protein. *Biochemistry*. **45**(40): p. 12240-12252.
102. Ellman, G.L., (1959) Tissue sulfhydryl groups. *Archives of Biochemistry and Biophysics*. **82**(1): p. 70-77.
103. Pountney, D.L., I. Schauwecker, J. Zarn, and M. Vasak, (1994) Formation of Mammalian Cu8-Metallothionein in vitro: Evidence for the Existence of Two Cu(I)4-Thiolate Clusters. *Biochemistry*. **33**(32): p. 9699-9705.
104. Blair, D. and H. Diehl, (1961) Bathophenanthrolinedisulphonic acid and bathocuproinedisulphonic acid, water soluble reagents for iron and copper. *Talanta*. **7**(3): p. 163-174.
105. Xiao, Z., F. Loughlin, G.N. George, G.J. Howlett, and A.G. Wedd, (2004) C-Terminal domain of the membrane copper transporter Ctr1 from *Saccharomyces cerevisiae* binds four Cu(I) ions as a cuprous-thiolate polynuclear cluster: sub-femtomolar Cu(I) affinity of three proteins involved in copper trafficking. *Journal of the American Chemical Society*. **126**(10): p. 3081-3090.

106. Grey, B. and T.R. Steck, (2001) Concentrations of copper thought to be toxic to *Escherichia coli* can induce the viable but nonculturable condition. *Applied and Environmental Microbiology*. **67**(11): p. 5325-5327.
107. Lowry, O.H., N.J. Rosebrough, A.L. Farr, and R.J. Randall, (1951) Protein measurement with the Folin phenol reagent. *Journal of Biological Chemistry*. **193**(1): p. 265-75.
108. Siluvai, G.S., M. Nakano, M. Mayfield, and N.J. Blackburn, (2011) The essential role of the Cu(II) state of Sco in the maturation of the Cu(A) center of cytochrome oxidase: evidence from H135Met and H135SeM variants of the Bacillus subtilis Sco. *Journal of Biological Inorganic Chemistry*. **16**(2): p. 285-97.
109. Trasnea, P.-I., A. Andrei, D. Marckmann, M. Utz, B. Khalfaoui-Hassani, N. Selamoglu, F. Daldal, and H.-G. Koch, (2018) A copper relay system involving two periplasmic chaperones drives cbb_3-type Cytochrome c Oxidase biogenesis in *Rhodobacter capsulatus*. *ACS Chemical Biology*.
110. Blundell, K.L., M.A. Hough, E. Vijgenboom, and J.A. Worrall, (2014) Structural and mechanistic insights into an extracytoplasmic copper trafficking pathway in *Streptomyces lividans*. *Biochemical Journal*. **459**(3): p. 525-38.
111. Koay, M., L. Zhang, B. Yang, M.J. Maher, Z. Xiao, and A.G. Wedd, (2005) CopC protein from *Pseudomonas syringae*: intermolecular transfer of copper from both the copper(I) and copper(II) sites. *Inorganic Chemistry*. **44**(15): p. 5203-5205.
112. Chong, L.X., M.R. Ash, M.J. Maher, M.G. Hinds, Z. Xiao, and A.G. Wedd, (2009) Unprecedented binding cooperativity between Cu(I) and Cu(II) in the copper resistance protein CopK from *Cupriavidus metallidurans* CH34: implications from structural studies by NMR spectroscopy and X-ray crystallography. *Journal of the Americal Chemical Society*. **131**(10): p. 3549-64.
113. Zumft, W.G., (2005) Biogenesis of the bacterial respiratory Cu-A, Cu-S enzyme nitrous oxide reductase. *Journal of Molecular Microbiology and Biotechnology*. **10**(2-4): p. 154-166.
114. Altschul, S.F., T.L. Madden, A.A. Schaffer, J. Zhang, Z. Zhang, W. Miller, and D.J. Lipman, (1997) Gapped BLAST and PSI-BLAST: a new generation of protein database search programs. *Nucleic Acids Res*. **25**(17): p. 3389-402.
115. Rosenzweig, A.C., D.L. Huffman, M.Y. Hou, A.K. Wernimont, R.A. Pufahl, and T.V. O'Halloran, (1999) Crystal structure of the Atx1 metallochaperone protein at 1.02 A resolution. *Structure*. **7**(6): p. 605-17.
116. Rosenzweig, A.C. and T.V. O'Halloran, (2000) Structure and chemistry of the copper chaperone proteins. *Current Opinion in Chemical Biology*. **4**(2): p. 140-147.
117. Arguello, J.M., E. Eren, and M. Gonzalez-Guerrero, (2007) The structure and function of heavy metal transport P1B-ATPases. *Biometals*. **20**(3-4): p. 233-48.
118. Banci, L., I. Bertini, S. Ciofi-Baffoni, L. Gonnelli, and X.C. Su, (2003) Structural basis for the function of the N-terminal domain of the ATPase CopA from Bacillus subtilis. *Journal of Biological Chemistry*. **278**(50): p. 50506-13.
119. Cobine, P.A., G.N. George, C.E. Jones, W.A. Wickramasinghe, M. Solioz, and C.T. Dameron, (2002) Copper transfer from the Cu(I) chaperone, CopZ, to the repressor, Zn(II)CopY: metal coordination environments and protein interactions. *Biochemistry*. **41**(18): p. 5822-9.
120. Ma, Z., D.M. Cowart, R.A. Scott, and D.P. Giedroc, (2009) Molecular insights into the metal selectivity of the copper(I)-sensing repressor CsoR from *Bacillus subtilis*. *Biochemistry*. **48**(15): p. 3325-34.

121. Peuser, V., J. Glaeser, and G. Klug, (2011) The RSP_2889 gene product of *Rhodobacter sphaeroides* is a CueR homologue controlling copper-responsive genes. *Microbiology*. **157**(Pt 12): p. 3306-13.
122. Changela, A., K. Chen, Y. Xue, J. Holschen, C.E. Outten, T.V. O'Halloran, and A. Mondragon, (2003) Molecular basis of metal-ion selectivity and zeptomolar sensitivity by CueR. *Science*. **301**(5638): p. 1383-7.
123. Gaballa, A., M. Cao, and J.D. Helmann, (2003) Two MerR homologues that affect copper induction of the *Bacillus subtilis* copZA operon. *Microbiology*. **149**(Pt 12): p. 3413-21.
124. Rensing, C. and G. Grass, (2003) *Escherichia coli* mechanisms of copper homeostasis in a changing environment. *FEMS Microbiology Review*. **27**(2-3): p. 197-213.
125. Djoko, K.Y., L.X. Chong, A.G. Wedd, and Z. Xiao, (2010) Reaction mechanisms of the multicopper oxidase CueO from *Escherichia coli* support its functional role as a cuprous oxidase. *Journal of the American Chemical Society*. **132**(6): p. 2005-15.
126. Roberts, S.A., A. Weichsel, G. Grass, K. Thakali, J.T. Hazzard, G. Tollin, C. Rensing, and W.R. Montfort, (2002) Crystal structure and electron transfer kinetics of CueO, a multicopper oxidase required for copper homeostasis in *Escherichia coli*. *Proceedings of the National Academy of Sciences*. **99**(5): p. 2766-2771.
127. Outten, F.W., D.L. Huffman, J.A. Hale, and T.V. O'Halloran, (2001) The independent cue and cus systems confer copper tolerance during aerobic and anaerobic growth in *Escherichia coli*. *Journal of Biological Chemistry*. **276**(33): p. 30670-7.
128. Chacon, K.N., T.D. Mealman, M.M. McEvoy, and N.J. Blackburn, (2014) Tracking metal ions through a Cu/Ag efflux pump assigns the functional roles of the periplasmic proteins. *Proceedings of the Natural Academy of Science U S A*. **111**(43): p. 15373-8.
129. Loftin, I.R., S. Franke, S.A. Roberts, A. Weichsel, A. Heroux, W.R. Montfort, C. Rensing, and M.M. McEvoy, (2005) A novel copper-binding fold for the periplasmic copper resistance protein CusF. *Biochemistry*. **44**(31): p. 10533-40.
130. Pontel, L.B. and F.C. Soncini, (2009) Alternative periplasmic copper-resistance mechanisms in Gram negative bacteria. *Molecular Microbiology*. **73**(2): p. 212-25.
131. Yoon, B.Y., Y.H. Kim, N. Kim, B.Y. Yun, J.S. Kim, J.H. Lee, H.S. Cho, K. Lee, and N.C. Ha, (2013) Structure of the periplasmic copper-binding protein CueP from *Salmonella enterica serovar Typhimurium. Acta Crystallography D Biological Crystallography*. **69**(Pt 10): p. 1867-75.
132. Larkin, M.A., G. Blackshields, N.P. Brown, R. Chenna, P.A. McGettigan, H. McWilliam, F. Valentin, I.M. Wallace, A. Wilm, R. Lopez, J.D. Thompson, T.J. Gibson, and D.G. Higgins, (2007) Clustal W and Clustal X version 2.0. *Bioinformatics*. **23**(21): p. 2947-2948.
133. Nicholas, K.B. and H.B.J. Nicholas, (1997) GeneDoc: a tool for editing and annotating multiple sequence alignments. *Distributed by the author. http://www.psc.edu/biomed/genedoc*.
134. Meydan, S., D. Klepacki, S. Karthikeyan, T. Margus, P. Thomas, J.E. Jones, Y. Khan, J. Briggs, J.D. Dinman, N. Vazquez-Laslop, and A.S. Mankin, (2017) Programmed Ribosomal Frameshifting Generates a Copper Transporter and a Copper Chaperone from the Same Gene. *Molecular Cell*. **65**(2): p. 207-219.
135. Preisig, O., R. Zufferey, and H. Hennecke, (1996) The *Bradyrhizobium japonicum* fixGHIS genes are required for the formation of the high-affinity cbb_3-type cytochrome oxidase. *Archives of Microbiology*. **165**(5): p. 297-305.

136. Koch, H.G., C. Winterstein, A.S. Saribas, J.O. Alben, and F. Daldal, (2000) Roles of the ccoGHIS gene products in the biogenesis of the *cbb*$_3$-type cytochrome c oxidase. *Journal of Molecular Biology*. **297**(1): p. 49-65.
137. de Gier, J.W., M. Schepper, W.N. Reijnders, S.J. van Dyck, D.J. Slotboom, A. Warne, M. Saraste, K. Krab, M. Finel, A.H. Stouthamer, R.J. van Spanning, and J. van der Oost, (1996) Structural and functional analysis of *aa*$_3$-type and *cbb*$_3$-type cytochrome c oxidases of *Paracoccus denitrificans* reveals significant differences in proton-pump design. *Molecular Microbiology*. **20**(6): p. 1247-60.
138. Horng, Y.C., P.A. Cobine, A.B. Maxfield, H.S. Carr, and D.R. Winge, (2004) Specific copper transfer from the Cox17 metallochaperone to both Sco1 and Cox11 in the assembly of yeast cytochrome C oxidase. *Journal of Biological Chemistry*. **279**(34): p. 35334-40.
139. Banci, L., I. Bertini, S. Ciofi-Baffoni, T. Hadjiloi, M. Martinelli, and P. Palumaa, (2008) Mitochondrial copper(I) transfer from Cox17 to Sco1 is coupled to electron transfer. *Proceedings of the Natral Academy of Science U S A*. **105**(19): p. 6803-8.
140. Robinson, N.J. and D.R. Winge, (2010) Copper Metallochaperones. *Annual Review Biochemistry.* . **79**.
141. Abriata, L.A., L. Banci, I. Bertini, S. Ciofi-Baffoni, P. Gkazonis, G.A. Spyroulias, A.J. Vila, and S. Wang, (2008) Mechanism of Cu(A) assembly. *Nature Chemical Biology*. **4**(10): p. 599-601.
142. Thompson, A.K., J. Gray, A. Liu, and J.P. Hosler, (2012) The roles of *Rhodobacter sphaeroides* copper chaperones PCu(A)C and Sco (PrrC) in the assembly of the copper centers of the *aa*$_3$-type and the *cbb*$_3$-type cytochrome c oxidases. *Biochimica et Biophysica Acta*. **1817**(6): p. 955-64.
143. Banci, L., I. Bertini, S. Ciofi-Baffoni, T. Kozyreva, M. Mori, and S. Wang, (2011) Sco proteins are involved in electron transfer processes. *Journal of Biological Inorganic Chemistry*. **16**(3): p. 391-403.
144. Mattatall, N.R., J. Jazairi, and B.C. Hill, (2000) Characterization of YpmQ, an accessory protein required for the expression of cytochrome c oxidase in *Bacillus subtilis*. *Journal of Biological Chemistry*. **275**(37): p. 28802-9.
145. Ekici, S., G. Pawlik, E. Lohmeyer, H.-G. Koch, and F. Daldal, (2012) Biogenesis of *cbb*$_3$-type cytochrome c oxidase in *Rhodobacter capsulatus*. *Biochimica et Biophysica Acta - Bioenergetics*. **1817**(6): p. 898-910.
146. Dash, B.P., M. Alles, F.A. Bundschuh, O.-M.H. Richter, and B. Ludwig, (2015) Protein chaperones mediating copper insertion into the CuA site of the aa3-type cytochrome c oxidase of *Paracoccus denitrificans*. *Biochimica et Biophysica Acta - Bioenergetics*. **1847**(2): p. 202-211.
147. Djoko, K.Y., Z. Xiao, D.L. Huffman, and A.G. Wedd, (2007) Conserved mechanism of copper binding and transfer. A comparison of the copper-resistance proteins PcoC from *Escherichia coli* and CopC from *Pseudomonas syringae*. *Inorganic Chemistry*. **46**(11): p. 4560-8.
148. Djoko, K.Y., Z. Xiao, and A.G. Wedd, (2008) Copper resistance in *E. coli*: the multicopper oxidase PcoA catalyzes oxidation of copper(I) in Cu(I)Cu(II)-PcoC. *Chembiochem*. **9**(10): p. 1579-82.
149. Chillappagari, S., M. Miethke, H. Trip, O.P. Kuipers, and M.A. Marahiel, (2009) Copper acquisition is mediated by YcnJ and regulated by YcnK and CsoR in *Bacillus subtilis. Journal of Bacteriology*. **191**(7): p. 2362-70.
150. Bergeron, R.J., W.R. Weimar, and J.B. Dionis, (1988) Demonstration of ferric L-parabactin-binding activity in the outer membrane of *Paracoccus denitrificans*. *Journal of Bacteriology*. **170**(8): p. 3711-7.
151. Anttila, J., P. Heinonen, T. Nenonen, A. Pino, H. Iwai, E. Kauppi, R. Soliymani, M. Baumann, J. Saksi, N. Suni, and T. Haltia, (2011) Is coproporphyrin III a

copper-acquisition compound in *Paracoccus denitrificans*? *Biochimica et Biophysica Acta*. **1807**(3): p. 311-8.
152. Kim, H.J., D.W. Graham, A.A. DiSpirito, M.A. Alterman, N. Galeva, C.K. Larive, D. Asunskis, and P.M.A. Sherwood, (2004) Methanobactin, a Copper-Acquisition Compound from Methane-Oxidizing Bacteria. *Science*. **305**(5690): p. 1612-1615.
153. Koh, E.I. and J.P. Henderson, (2015) Microbial Copper-binding Siderophores at the Host-Pathogen Interface. *Journal of Biological Chemistry*. **290**(31): p. 18967-74.
154. Bray, N.L., H. Pimentel, P. Melsted, and L. Pachter, (2016) Near-optimal probabilistic RNA-seq quantification. *Nature Biotechnoogyl*. **34**(5): p. 525-7.
155. Smith, S.G., V. Mahon, M.A. Lambert, and R.P. Fagan, (2007) A molecular Swiss army knife: OmpA structure, function and expression. *FEMS Microbiology Letters*. **273**(1): p. 1-11.
156. Pautsch, A. and G.E. Schulz, (2000) High-resolution structure of the OmpA membrane domain. *Journal of Molecular Biology*. **298**(2): p. 273-82.
157. Lazzaroni, J.C., J.F. Dubuisson, and A. Vianney, (2002) The Tol proteins of *Escherichia coli* and their involvement in the translocation of group A colicins. *Biochimie*. **84**(5-6): p. 391-7.
158. Lloubes, R., A. Bernadac, L. Houot, and S. Pommier, (2013) Non classical secretion systems. *Research in Microbiology*. **164**(6): p. 655-63.
159. Landeta, C., D. Boyd, and J. Beckwith, (2018) Disulfide bond formation in prokaryotes. *Nature Microbiology*. **3**(3): p. 270-280.
160. Wessler, S., G. Schneider, and S. Backert, (2017) Bacterial serine protease HtrA as a promising new target for antimicrobial therapy? *Cell Communication and Signaling*. **15**: p. 4.
161. Barr, I., J.A. Latham, A.T. Iavarone, T. Chantarojsiri, J.D. Hwang, and J.P. Klinman, (2016) The pyrroloquinoline quinone (PQQ) biosynthetic pathway: Demonstration of de novo carbon-carbon cross-linking within the peptide substrate (PqqA) in the presence of the Radical SAM enzyme (PqqE) and its peptide chaperone (PqqD). *Journal of Biological Chemistry*.**291**(17):p.8877-8884.
162. Chillappagari, S., A. Seubert, H. Trip, O.P. Kuipers, M.A. Marahiel, and M. Miethke, (2010) Copper stress affects iron homeostasis by destabilizing iron-sulfur cluster formation in *Bacillus subtilis*. *Journal of Bacteriology* **192**(10): p. 2512-2524.
163. Asard, H., R. Barbaro, P. Trost, and A. Berczi, (2013) Cytochromes b561: ascorbate-mediated trans-membrane electron transport. *Antioxidant Redox Signalling*. **19**(9): p. 1026-35.
164. Giner-Lamia, J., L. López-Maury, and F.J. Florencio, (2015) CopM is a novel copper-binding protein involved in copper resistance in Synechocystis sp. PCC 6803. *MicrobiologyOpen*. **4**(1): p. 167-185.
165. Warner, D.F., S. Savvi, V. Mizrahi, and S.S. Dawes, (2007) A riboswitch regulates expression of the coenzyme B12-independent methionine synthase in *Mycobacterium tuberculosis*: implications for differential methionine synthase function in strains H37Rv and CDC1551. *Journal of Bacteriology*. **189**(9): p. 3655-3659.
166. Hondorp, E.R. and R.G. Matthews, (2004) Oxidative stress inactivates cobalamin-independent methionine synthase (MetE) in *Escherichia coli*. *PLOS Biology*. **2**(11): p. e336.
167. Brondijk, T.H., A. Nilavongse, N. Filenko, D.J. Richardson, and J.A. Cole, (2004) NapGH components of the periplasmic nitrate reductase of *Escherichia coli* K-12: location, topology and physiological roles in quinol oxidation and redox balancing. *Biochemical Journal*. **379**(Pt 1): p. 47-55.

168. Feliciello, I., D. Zahradka, K. Zahradka, S. Ivanković, N. Puc, and D. Đermić, (2018) RecF, UvrD, RecX and RecN proteins suppress DNA degradation at DNA double-strand breaks in *Escherichia coli*. *Biochimie*. **148**: p. 116-126.
169. Cuthbertson, L. and J.R. Nodwell, (2013) The TetR Family of Regulators. *Microbiology and Molecular Biology Reviews : MMBR*. **77**(3): p. 440-475.
170. Lu, Z., M. Takeuchi, and T. Sato, (2007) The LysR-Type Transcriptional Regulator YofA Controls Cell Division through the Regulation of Expression of ftsW in *Bacillus subtilis*. *Journal of Bacteriology*. **189**(15): p. 5642-5651.
171. Sperandio, B., C. Gautier, S. McGovern, D.S. Ehrlich, P. Renault, I. Martin-Verstraete, and E. Guédon, (2007) Control of methionine synthesis and uptake by MetR and homocysteine in *Streptococcus mutans*. *Journal of Bacteriology*. **189**(19): p. 7032-7044.
172. Braz, V.S., J.F. da Silva Neto, V.C.S. Italiani, and M.V. Marques, (2010) CztR, a LysR-Type Transcriptional regulator involved in zinc homeostasis and oxidative stress defense in *Caulobacter crescentus*. *Journal of Bacteriology*. **192**(20): p. 5480-5488.
173. Ohshima, T., R. Kawakami, Y. Kanai, S. Goda, and H. Sakuraba, (2007) Gene expression and characterization of 2-keto-3-deoxygluconate kinase, a key enzyme in the modified Entner-Doudoroff pathway of the aerobic and acidophilic hyperthermophile *Sulfolobus tokodaii*. *Protein Expression and Purification*. **54**(1): p. 73-8.
174. Quintana, J., L. Novoa-Aponte, and J.M. Argüello, (2017) Copper homeostasis networks in the bacterium *Pseudomonas aeruginosa*. *Journal of Biological Chemistry*. **292**(38): p. 15691-15704.
175. Coelho Abrantes, M., M.d.F. Lopes, and J. Kok, (2011) Impact of manganese, copper and zinc ions on the transcriptome of the nosocomial pathogen *Enterococcus faecalis* V583. *PLoS ONE*. **6**(10): p. e26519r
176. Djoko, K.Y., C.-l.Y. Ong, M.J. Walker, and A.G. McEwan, (2015) The role of copper and zinc toxicity in innate immune defense against bacterial pathogens. *The Journal of Biological Chemistry*. **290**(31): p. 18954-18961.
177. da Rosa Couto, R., J. Faversani, C.A. Ceretta, P.A.A. Ferreira, C. Marchezan, D. Basso Facco, L.P. Garlet, J.S. Silva, J.J. Comin, C.A. Bizzi, E.M.M. Flores, and G. Brunetto, (2018) Health risk assessment and soil and plant heavy metal and bromine contents in field plots after ten years of organic and mineral fertilization. *Ecotoxicology and Environmental Safety*. **153**: p. 142-150.
178. Jensen, J., M.M. Larsen, and J. Bak, (2016) National monitoring study in Denmark finds increased and critical levels of copper and zinc in arable soils fertilized with pig slurry. *Environmental Pollution*. **214**: p. 334-340.
179. Bernard, L., P.A. Maron, C. Mougel, V. Nowak, J. Lévêque, C. Marol, J. Balesdent, F. Gibiat, and L. Ranjard, (2009) Contamination of soil by copper sffects the dynamics, diversity, and activity of soil bacterial communities involved in wheat decomposition and carbon storage. *Applied and Environmental Microbiology*. **75**(23): p. 7565-7569.
180. Giannopoulos, G., M.J. Sullivan, K.R. Hartop, G. Rowley, A.J. Gates, N.J. Watmough, and D.J. Richardson, (2017) Tuning the modular *Paracoccus denitrificans* respirome to adapt from aerobic respiration to anaerobic denitrification. *Environmental Microbiology*. **19**(12): p. 4953-4964.
181. Hassani, B.K., C. Astier, W. Nitschke, and S. Ouchane, (2010) CtpA, a copper-translocating P-type ATPase involved in the biogenesis of multiple copper-requiring enzymes. *Journal of Biological Chemistry*. **285**(25): p. 19330-7.
182. Banci, L., I. Bertini, S. Ciofi-Baffoni, T. Kozyreva, K. Zovo, and P. Palumaa, (2010) Affinity gradients drive copper to cellular destinations. *Nature*. **465**: p. 645-648.

183. Outten, F.W., (2015) Recent advances in the Suf Fe-S cluster biogenesis pathway: Beyond the Proteobacteria. *Biochimica et biophysica acta*. **1853**(6): p. 1464-1469.
184. Lee, J.Y., J.G. Yang, D. Zhitnitsky, O. Lewinson, and D.C. Rees, (2014) Structural basis for heavy metal detoxification by an Atm1-type ABC exporter. *Science*. **343**(6175): p. 1133-1136.
185. Schaedler, T.A., J.D. Thornton, I. Kruse, M. Schwarzlander, A.J. Meyer, H.W. van Veen, and J. Balk, (2014) A conserved mitochondrial ATP-binding cassette transporter exports glutathione polysulfide for cytosolic metal cofactor assembly. *Journal of Biological Chemistry*. **289**(34): p. 23264-74.

Appendix A

A.1 Anaerobic data set

Fold change based on *b* values (log_2), is colour coded as follows:

-2.0 to -3.0	-1.51 to -2.0	-1.01 to -1.5	-0.5 to -1.0	0.5 to 1.0	1.01 to 1.5	1.51 to 2.0	2.01 to 2.5

Transporters

Locus	Gene	Predicted function	Fold change (b value, log_2)	TPM Cu-Replete	TPM Cu-Excess	Fold change
Pden_0521		heavy metal translocating P-type ATPase	0.93	7.33	18.26	2.49
Pden_0683		Cell division and transport-associated protein TolQ	1.08	211.18	620.36	2.93
Pden_0684		Cell division and transport-associated protein TolR	1.11	96.2	290.57	3.02
Pden_0686		TolB, N-terminal domain protein	0.68	126.20	250.92	1.98
Pden_0687		OmpA domain protein	0.96	273.24	706.34	2.58
Pden_0688		conserved hypothetical protein	0.98	173.72	457.42	3.51
Pden_0849		Putative outer membrane protein	2.49	642.33	8053.43	12.53
Pden_1807		Extracellular solute-binding protein, family 5	0.65	70.12	135.12	1.93
Pden_1840	LOLC/E	Lipoprotein releasing system, transmembrane protein	0.68	72.23	142.67	1.97
Pden_2034		Phospholipid transport, toluene tolerance family protein	0.56	70.88	123.82	1.75
Pden_2875		OmpA/MotB domain protein	1.15	318.81	1013.17	3.18
Pden_4324		OmpA/MotB domain protein	1.10	3.47	10.72	3.09

Metabolism

Locus	Gene	Predicted function	Fold change (b value, log_2)	TPM Cu-High	TPM Cu-Excess	Fold change
Pden_0206		Shot-chain dehydrogenase/reductase SDR	1.04	21.18	59.06	2.79
Pden_0515		Sarcosine oxidase, alpha subunit family	0.56	12.99	22.84	1.75
Pden_0566		L-erythro-3-methylmalyl-CoA dehydratase	0.56	38.58	67.15	1.74
Pden_1355		Methionine synthase (B12 independent)	-0.89	670.37	270.53	0.403
Pden_4207		Poly-beta-hydroxybutyrate polymerase domain protein	0.69	4.13	8.30	2.01

Oxidoreductase/reductase

Locus	Gene	Predicted function	Fold change (b value, log_2)	TPM Cu-High	TPM Cu-Excess	Fold change
Pden_0063		Oxidoreductase, molybdopterin binding protein	0.97	25.15	66.8	2.65
Pden_0064		Ferric reductase Domain protein transmembrane component	1.06	5.87	17.22	2.93
Pden_0658		Ferredoxin-NADP(+) reductase	0.75	312.98	658.75	2.10
Pden_0720		NADH:flavin oxidoreductase/NADH oxidase	0.73	34.21	70.22	2.05
Pden_1819		DSBA oxidoreductase	0.79	192.23	424.65	2.21
Pden_2095		DSBA oxidoreductase	1.21	310.84	1043.69	3.36
Pden_3792		DSBA oxidoreductase	0.83	84.08	19.12	2.26

Biosynthesis

Locus	Gene	Predicted function	Fold change (b value, log_2)	TPM Cu-High	TPM Cu-Excess	Fold change
Pden_0423		4-diphosphocytidyl-2-C-methyl-D-erythritol kinase	0.81	25.78	56.52	2.19
Pden_0892		YceI family protein	1.21	903.8	2690.1	3.2
Pden_2033		Penicillin-binding protein, 1A family	0.58	132.77	238.19	1.79
Pden_2359		Coenzyme PQQ biosynthesis protein E	1.20	1.77	5.64	3.19
Pden_2360		Coenzyme PQQ synthesis D	0.87	3.53	8.50	2.4
Pden_2361		PQQ biosynthesis	1.12	1.83	5.67	3.08
Pden_2659		Murein endopeptidase, Metallo peptidase, MEROPS family M74	0.60	101.81	183.74	1.80
Pden_3637		Propionyl-CoA carboxylase	0.65	6.25	12.08	1.93
Pden_3978		Cytochrome c biogenesis protein	0.56	162.36	283.43	1.74
Pden_4043		ErfK/YbiS/YcfS/YnhG family protein	0.79	57.45	126.25	2.20

Phage control and drug resistance/antimicrobial

Locus	Gene	Predicted function	Fold change (b value, log_2)	TPM Cu-High	TPM Cu-Excess	Fold change
Pden_1381		Invasion associated locus B family protein	0.67	870.53	1717.19	1.97
Pden_1382		Serine protease Do	1.64	91.88	477.11	5.19
Pden_2721		Efflux transporter, RND family, MFP subunit	1.12	30.47	90.33	2.96
Pden_2722		Transporter, hydrophose/amiphile efflux-1 (HAE1) family.	1.05	23.56	67.39	2.86
Pden_3449		RND efflux system, outer membrane lipoprotein, NodT family	0.73	4.29	8.90	20.7

Transcription regulators/DNA related

Locus	Gene	Predicted function	Fold change (b value, log_2)	TPM Cu-High	TPM Cu-Excess	Fold change
Pden_2216	RpoH	RNA polymerase, sigma 32 subunit	0.84	111.27	257.78	2.32
Pden_2713	MutL	DNA mismatch repair	0.57	16.21	28.68	1.77
Pden_2964		Sigma 54specific, transcriptional regulators, Fis family	0.71	132.94	270.81	20.3
Pden_2979		RNA polymerase, sigma 24 subunit, ECF subfamily	-0.85	14.31	5.96	0.42

Maturation/miscellaneous

Locus	Gene	Predicted function	Fold change (b value, log_2)	TPM Cu-Replete	TPM Cu-Excess	Fold change
Pden_0424		Tetratricopeptide TPR_2 repeat protein (mediates P-P interactions)	0.97	41.54	106.3	2.56
Pden_1848		Cytochrome c oxidase, cbb3-type, subunit I	-0.55	395.66	229.94	0.58
Pden_1937		Cytochrome c, class I		2453.2	4934.74	2.01
Pden_2023		Redoxin domain protein	0.7	117.15	362.81	2.79
Pden_2490	NirF	Cytochrome d_1, heme region	1	223.53	394.92	1.77
Pden_2545		Cytochrome B561	0.57	73.28	169.86	2.31
Pden_2669		Outer membrane lipoprotein carrier protein LolA	0.84	140.18	344.96	2.46
Pden_2714		Peptidase M16 domain/ zinc protease (pfam)	0.9	45.64	143.26	3.14

Pden_2715		Peptidase M16 domain/ zinc protease (pfam)	0.95	42.37	109.63	2.59
Pden_2803		Beta-lactamase domain protein	1.1	21.05	65.32	3.10
Pden_2822		Response regulator receiver protein	0.49	298.13	484.41	1.62
Pden_3866		Disulfide bond formation protein DsbB	0.98	131.25	344.16	2.62
Pden_3901		ATPase associated with various cellular activities, AAA_3	0.98	41.8	100.61	2.41
Pden_3904		N-terminal double-transmembrane domain protein	0.89	28.76	80.78	2.8
Pden_4318	CtaG/ Cox11	Cytochrome c oxidase assembly protein CtaG/Cox11	-0.67	359.56	180.57	0.5
Pden_4443	ScoB	Electron transport protein, SCO1/SenC	0.78	181.61	394.17	2.17
Pden_4444	PCu1	Protein of unknown function DUF461	1.2	105.26	338.77	3.21
Pden_4738	NapH	Periplasmic nitrate reductase	-0.73	42.87	20.30	0.47

Hypothetical Proteins / Domains of unknown function (DUF)

Locus	Gene	Predicted function	Fold change (b value, log_2)	TPM Cu-High	TPM Cu-Excess	Fold change
Pden_0091		Hypothetical protein	-0.6	68.46	38.59	0.56
Pden_0319		Conserved hypothetical protein	-1.0	132.1	46.29	0.350

Pden_0437		Conserved hypothetical protein	0.9	61.25	151.26	2.46
Pden_0439		Hypothetical protein	1.1	122.79	370.5	3.01
Pden_0926		Protein of unknown function DUF305	1.5	203.61	882.9	4.34
Pden_1407		Hypothetical protein	0.9	35.79	8275	2.31
Pden_1932		Protein of unknown function	1.3	25.36	91.70	3.61
Pden_2011		Hypothetical protein	1.4	29.33	124.92	4.26
Pden_2096		Protein of known function DUF1159	1.1	70.09	206.86	2.91
Pden_2181		Protein of known function DUF1501	0.6	12.12	23.05	1.90
Pden_2260		Hypothetical protein	0.6	84.57	158.6	1.875
Pden_2519		Hypothetical protein	1.6	73.28	169.86	2.32
Pden_2776		Conserved hypothetical protein	0.8	61.42	410.23	2.28
Pden_3905		Conserved hypothetical protein	0.9	34.33	82.05	2.39
Pden_4093		Hypothetical protein	-0.7	16.5	8.09	0.49
Pden_4300		Protein of unknown function DUF1223	1.1	69.66	216.55	3.10
Pden_4524		Hypothetical protein	1.5	4.41	19.48	4.41
Pden_5015		Hypothetical protein	-0.7	12.18	6.34	0.52

A.2 Aerobic data set

Fold change based on *b* values (log_2), is colour coded as follows:

-1.51 to -2.0	-1.01 to -1.5	-0.5 to -1.0	0.5 to 1.0	1.01 to 1.5	1.51 to 2.0	2.01 to 2.5

Transporters

Locus	Gene	Predicted function	Fold change (b value, log_2)	TPM Cu-High	TPM Cu-Excess	Fold change
Pden_0864		ABC transporter related	-1.20	33.4	14.52	0.43
Pden_1671		Extracellular solute binding protein, family 5	1.38	213.3	558.46	2.6
Pden_2576		ABC transporter	-1.11	35.9	16.74	0.46
Pden_3209		TRAP dicarboxylate transporter, DctP subunit	-1.49	61.87	22.12	0.35
Pden_4039		ABC-type nitrate/sulfate/bicarbonate transporter, periplasmic component TauA	-1.49	20.70	6.70	0.32
Pden_4181		Mannitol/Sorbital binding protein	-1.45	43.11	15.81	0.36
Pden_4308		Lipoprotein, YaeC family	1.14	270.09	594.64	2.2
Pden_5081		Amino acid ABC transporter substrate-binding protein, PAAT familY	-1.51	8.50	2.98	0.35

Biosynthesis

locus	Gene	Predicted function	Fold change (b value, log_2)	TPM Cu-High	TPM Cu-Excess	Fold change
Pden_0534		tRNA pseudouridine synthase A	-1.41	34.50	13.01	0.37
Pden_2033		penicillin-binding protein, 1A family	-1.05	225.72	110.61	0.48
Pden_2361		Coenzyme PQQ biosynthesis C	-1.51	5.26	1.82	0.34
Pden_2671		Amidase	-1.34	44.03	17.48	0.39
Pden_3631		Adenosylcobamine-phosphate-synthase	-1.17	33.67	15.04	0.45

Pden_3997		1-deoxy-D-xyluose 5-phospho reductoisomerase	-1.09	97.87	44.90	0.45
Pden_4055		Glutamate 5-kinase	-1.00	132.99	66.61	0.50
Pden_4253		ATP: Cob(I)alamin adenosyltransferase	-1.00	7.16	1.63	0.22

DNA/RNA/chromosome or transcription

locus	Gene	Predicted function	Fold change (b value, log_2)	TPM Cu-High	TPM Cu-Excess	Fold change
Pden_0689		tRNA-lysidine synthetase	-2.43	69.73	12.84	0.18
Pden_0723		Transcriptional regulator, LysR family	-1.04	141.80	69.58	0.49
Pden_0944		Transcriptional regulator, TetR	-2.42	20.77	3.83	0.1844
Pden_1279		Phage integrase family protein	-1.14	34.61	15.80	0.46
Pden_1545		Histone family protein nucleoid-structuring	1.23	111.75	257.78	2.3
Pden_1784		Transcriptional regulator, LuxR family	-1.67	8.79	2.72	0.31
Pden_1954		SAM-dependant methyltransferase	-1.23	47.91	20.57	0.44
Pden_2577		23S rRNA Uracil-trimethyltransferase	-1.79	27.94	8.11	0.30
Pden_2795		Putative helicase/exonuclease	-1.13	37.59	17.44	0.47
Pden_2835		RecF DNA replication and repair	-1.22	86.43	37.388	0.40
Pden_2940		Transcriptional regulator, TetR family	-1.32	86.97	34.27	0.39
Pden_3991		Transcriptional regulator, AraC family	-1.17	22.12	9.85	0.45
Pden_4484		DNA replication and repair RecN	-1.11	84.06	39.31	0.46
Pden_4724		GreA/B family transcription elongation factor	-1.17	318.81	139.70	0.44

Metabolism

Locus	Gene	Predicted function	Fold change (b value, log_2)	TPM Cu-High	TPM Cu-Excess	Fold change
Pden_0546		Monooxygenase, FAD binding	-1.44	87.71	32.66	0.37
Pden_0798		Aminotransferase, class IV	1.06	233.36	488.43	2.09
Pden_1952		Glucose-6-phospho-1-dehydrogenase	-1.03	54.56	26.97	0.49
Pden_2223		Cytidine diaminase, Zn binding	-1.43	71.45	26.18	0.48
Pden_2474		ATPase BadF/G and BcrA/F	-1.51	19.98	7.09	0.35
Pden_2537		Precorrin-6A reductase	-1.20	48.03	20.94	0.44
Pden_2539		Precorrine methylase	-1.76	21.11	6.08	0.29
Pden_2540		Precorrin-4 C11-methyltransferase	-1.22	55.32	23.88	0.43
Pden_2541		Cobyrinate a-c-diamide synthase	-1.10	57.48	27.06	0.47
Pden_2617		Fe-containing alcohol dehydrogenase	-1.98	12.87	3.26	0.25
Pden_2688		Inositol monophosphatase	-1.67	61.33	19.41	0.32
Pden_4298	MetZ	O-succinylhemoserine sulfhydrylase	1.00	142.32	287.30	2.02
Pden_4811		Beta-ketodiphyl CoA Thiolase	-1.56	8.37	2.86	0.34
Pden_5084		2-keto-3-deoxygluconate kinase	-2.74	3.69	0.55	0.15

Miscellaneous

Locus	Gene	Predicted function	Fold change (b value, log_2)	TPM Cu-High	TPM Cu-Excess	Fold change
Pden_0428		GCNS-related N-acyltransferase	-1.74	55.15	16.33	0.29
Pden_0435		translation factor SUA5	-2.23	59.82	12.96	0.22
Pden_0530		Peptidase M22-glycoprotease	-1.51	45.98	16.14	0.36

Pden_0738		Transferase hexapeptide repeat	-1.08	247.41	116.59	0.47
Pden_0873		Ribonuclease P protein component	-2.35	440.01	86.88	0.19
Pden_1310		Integral membrane sensor signal transduction histidine kinase	-1.39	22.07	8.53	0.39
Pden_1377		Redoxin domain protein	1.46	641.98	1751.27	2.73
Pden_1702		PimS2 protein	-1.64	7.75	2.49	0.33
Pden_2044		NDIX hydrolase	-1.50	114.51	40.09	0.35
Pden_2215		Pseodouridine synthase RluA family	-1.19	87.98	38.75	0.44
Pden_2352		Histidine kinase , ATP binding response regulator/receiver	-1.97	38.67	9.92	0.26
Pden_2903		Aminodeoxychorismate lyase	-1.48	300.98	108.6	0.36
Pden_3879		GCN5-related N-acyl transferase	-1.3	230.98	93.86	0.40
Pden_4176		HAD-superfamily hydrolase, superfamily IA, variant 3	-2.49	7.18	1.24	0.17
Pden_4743		Peptigoglycan binding domain 1 protein	-1.34	55.05	22.02	0.4
Pden_5085		Hydratase/decarboxylase family	-1.94	3.44	0.88	0.26

Hypothetical Proteins / Domains of unknown function (DUF)

Locus	Gene	Predicted function	Fold change (b value, log_2)	TPM Cu- High	TPM Cu- Excess	Fold change
Pden_0090		Hypothetical Protein	1.20	579.52	1335.41	4.06
Pden_0367		Hypothetical Protein	1.55	16.23	47.10	2.90
Pden_0577		Hypothetical Protein	-1.21	294.43	126.39	0.43
Pden_1524		Putative chromosome segregation protein,SMC	1.23	5.62	13.37	2.38
Pden_1953		Hypothetical Protein	-1.8	27.27	7.56	0.28
Pden_2090		Conserved Hypothetical Protein	1.04	34.81	72.27	2.12

Pden_3352		DUF-close to cation transporter (Pden_3353)	1.40	28.73	74.45	2.66
Pden_3602		Hypothetical protein	1.13	16.73	37.20	2.22
Pden_3685		Hypothetical protein	-1.87	5518.19	1475.19	0.27
Pden_3902		Hypothetical protein	-1.52	24.30	8.42	0.35
Pden_4642		Hypothetical protein	1.40	2.24	6.00	2.68
Pden_5121		Hypothetical protein	-1.36	105.54	40.50	0.38
Pden_5124		Hypothetical protein	-1.99	24.28	6.03	0.25